UNIVERSITÉ DE MONTRÉAL

PRÉDICTION DU COMPORTEMENT GÉOCHIMIQUE DES REJETS MINIERS PORTEURS DE TERRES RARES

MOHAMED EDAHBI

DÉPARTEMENT DES GENIES CIVIL, GÉOLOGIQUE ET DES MINES

ÉCOLE POLYTECHNIQUE DE MONTRÉAL

THÈSE PRÉSENTÉE EN VUE DE L'OBTENTION

DU DIPLÔME DE PHILOSOPHIAE DOCTOR

(GÉNIE MINÉRAL)

AVRIL 2018

UNIVERSITÉ DE MONTRÉAL

ÉCOLE POLYTECHNIQUE DE MONTRÉAL

UNIVERSITÉ DU QUÉBEC EN ABITIBI-TÉMISCAMINGUE

Cette thèse intitulée :

PRÉDICTION DU COMPORTEMENT GÉOCHIMIQUE DES REJETS MINIERS PORTEURS DE TERRES RARES

présentée par : EDAHBI Mohamed

en vue de l'obtention du diplôme de : Philosophiae Doctor

a été dûment acceptée par le jury d'examen constitué de :

M. ZAGURY Gérald, Ph. D., président

M. PLANTE Benoît, Ph. D., membre et directeur de recherche

M. BENZAAZOUA Mostafa, Ph. D., membre et codirecteur de recherche

M. JAMIESON Heather, Ph. D., membre

M. JÉBRAK Michel, D. Sc. A., membre externe

DÉDICACE

À mes chers parents, ma grande mère, mes frères et mes sœurs !!

REMERCIEMENTS

Je tiens avant tout à remercier mon directeur de thèse, le professeur Benoît Plante, et mon co-directeur, le professeur Mostafa Benzaazoua, pour leur soutien, leur motivation, leur encadrement, leurs conseils précieux, et leur implication durant toute la période de la thèse. Le travail sous vos directions m'a ouvert un champ de possibilité énorme et je leur en suis très reconnaissant. Merci de m'avoir donné cette opportunité pour grandir professionnellement et personnellement.

Je tiens à remercier nos partenaires financiers industriels et gouvernementaux, en particulier le conseil de recherches en sciences naturelles et en génie (CRSNG) qui a financé une majeure partie du projet dans le cadre d'une subvention de recherche et développement coopératif (RDC) et d'une subvention d'engagement partenarial (SEP). Mes vifs remerciements vont aux compagnies GéoMega Ressources Inc. et Matamec Inc., représentées respectivement par madame Mia Plettier, géochimiste de l'environnement et Monsieur Sylvain Doire, directeur de l'environnement pour leur contribution pertinente tout le long de cette thèse; en particulier durant la phase d'échantillonnage. Je remercie aussi Raphaël Mermillod-Blondin, métallurgiste sénior travaillant pour la compagnie minière Agnico-Eagle, de m'accueillir dans son laboratoire pour réaliser mon stage Mitacs.

Un immense merci est dédié à mes parents, ma source d'inspiration et ma passion de vivre, sans eux mes rêves seront irréalisables. A mes sœurs, Fatima, Latifa, Samira, Souhaila, et à mes deux frères Mostafa et Abdelatif, je dis merci pour le soutien et les encouragements constants durant mes études.

Je remercie chaleureusement toutes les personnes qui ont collaboré de près ou de loin à la réalisation de ce projet, plus particulièrement la famille Benzaazoua, Hassan Bouzahzah et Yassine Taha. Merci pour les encouragements et les bons moments passés ensemble.

Je tiens à addresser mes remerciements à toute l'équipe de l'URSTM de l'UQAT pour leur bonne humeur et leur aide judicieuse dans la réalisation des essais de laboratoire: Mathieu, Bruno Bossé, Alain, Mélinda, Patrick, Joël, Yvan, Mélanie, Marc, Janie, Louise, Sylvie, Nancy. Merci à Denis Bois ancien directeur administratif de l'IRME-UQAT, et à Jovette Godbout directrice administrative actuelle de l'IRME-UQAT de m'avoir offert l'occasion de travailler comme agent de recherche durant le projet. Un grand merci est dedié encore une fois à Mostafa Benzaazoua pour m'avoir permis d'enseigner avec lui le cours de la minéralogie appliquée comme auxiliaire d'enseignement.

Je remercie chaleureusement tous les professeurs de l'IRME UQAT-Polytechnique qui ont contribué à ma formation, pour leur disponibilité et leur collaboration précieuse tout le long du processus de cette thése: Bruno Bussière, Tikou Belem, Mamert Mbonimpa, Isabelle Demers et Carmen Mihaela Neculita.

Je remercie aussi mes collègues et amis étudiants, en particulier Cécile, Céline, Jihane, Babacar, Ibrahima, Hamza, Abdeljalil, Abdellatif, Nour, Nathalie, Koly, Vincent, Marie-Pier, Denis, Christelle, Bissé, Aicha, Touria, Chloé, Ibrahim, Hicham, Houssem, Takoua, Aurèlie Tamkssaoute etc.

Finalement, je tiens à adresser mes remerciements aux évaluateurs de ma thèse, Dr. Jamieson Heather et Dr. Jébrak Michel, pour leur disponibilité afin d'évaluer ma thése, et Dr. Zagury Gérald, pour présider le jury.

RÉSUMÉ

Les éléments de terres rares (REE), appelés aussi lanthanides, désignent un groupe de 17 éléments chimiques (lanthane (La) jusqu'au lutétium (Lu), plus scandium (Sc) et l'yttrium (Y). Ils sont associés essentiellement à des phases minérales de types carbonates, silicates, et/ou phosphates. Les REE sont devenus de nos jours des matières premières hautement stratégiques et indispensables à certaines industries (i.e., véhicules électriques et hybrides, systèmes de radar, batteries rechargeables, téléphones cellulaires, écrans LCD, produits électroniques, etc.). Ils sont contrairement à ce que suggère leur appellation, ils ne sont pas des « terres » mais plutôt des métaux et ils ne sont pas « rares » car ils sont assez répandus dans l'écorce terrestre. Ils sont présentsdans la nature sous forme de minéraux d'aspects terreux. Ils s'y retrouvent en quantité plus abondante que le plomb, et que l'argent mais ils sont rarement trouvés dans des concentrations rentables à exploiter (ils demeurent dilués dans la croûte terrestre). Le qualificatif « rare » signifie la rareté des technologies pour les extraire et les séparer. Parmi leurs particularités, on peut mentionner leur association fréquente avec d'autres éléments (i.e., Zr, Th, U, Ba, F, etc.), et ils sont difficiles à séparer les uns des autres. Pour l'instant, la Chine est le premier producteur mondial des REE (environ 97 % de la production mondiale). Face à ce constat, plusieurs compagnies minières à travers le monde ont renforcé leurs activités d'exploration pour répondre aux besoins mondiaux qui ne cessent d'augmenter et, par conséquent, atténuer les effets du monopole chinois.

Les gisements des REE font partie des gisements dits à faible teneur et fort tonnage, ce qui génère beaucoup de rejets solides et liquides (roches stériles, rejets de concentrateur, autres effluents miniers). Les rejets solides, sans valeur commerciale, sont souvent entreposés en surface dans les sites miniers. L'eau de pluie et de fonte des neiges percolant à travers ces rejets miniers est susceptible d'être contaminée via les réactions géochimiques ayant lieu naturellement au contact de l'eau et de l'oxygène. À l'échelle du Québec, la législation minière en vigueur oblige les entreprises à engager des garanties financières pour couvrir l'ensemble des coûts liés à la phase d'après-mine afin de réhabiliter les sites exploités en respectant l'environnement. À l'égard de toutes ces contraintes, le développement d'un projet minier nécessite la prédiction du comportement géochimique des rejets miniers qui seront produits durant les exploitations minières, entreposés en surface et exposés aux conditions atmosphériques. En plus de favoriser l'acceptabilité sociale des projets miniers, la prédiction permet, d'une part, d'anticiper le potentiel de génération de contaminants à partir des futurs empilements de rejets miniers et, d'autre part,

d'élaborer des stratégies saines de gestion et d'entreposage des rejets miniers. C'est dans ce cadre que s'inscrit le présent projet.

Présentement, des lacunes importantes sur les impacts environnementaux des rejets miniers porteurs des REE ont été notées dans la littérature, en particulier en ce qui concerne : (i) la réactivité des phases porteuses des REE, (ii) les processus géochimiques contrôlant la mobilité et le fractionnement des REE lors des interactions eaux-roches (l'adsorption, la précipitation et/ou coprécipitation, etc.), (iii) la spéciation des REE dans les gisement naturels les plus communs, (iv) la séparation minéralurgique et métallurgique des REE, et (v) la toxicité des REE. L'objectif de cette thèse est d'étudier le comportement géochimique des rejets miniers issus de deux types de gisements porteurs de terres rares (carbonates et silicates) afin de mieux comprendre les processus géochimiques qui seront responsables d'une contamination éventuelle des eaux de drainage. L'atteinte de cet objectif passe par la prédiction de la qualité des eaux de drainage à partir de l'étude d'échantillons d'exploration pour les projets Montviel, de la compagnie Ressources Géoméga, et Kipawa, de la compagnie Matamec explorations.

Le projet Montviel (Lebel-sur-Quévillon, Canada) vise une mine à ciel ouvert pour exploiter un gisement de terres rares légères estimé à 250 millions de tonnes (Mt) de carbonatites de REE-Nb avec une teneur en terres rares de 1.47 % d'oxydes de terres rares (OTR). Les dépôts du gisement sont associés à une intrusion alcaline protérozoïque datée de 1894 Ma. Quant au projet Kipawa, Témiscamingue, Canada, il vise l'exploitation d'un gisement de terres rares lourdes de 19 Mt avec une teneur moyenne de 0.41 % de OTR sur une période de 15 ans sous forme d'une mine à ciel ouvert.

Le travail concernant ces deux gisements de terres rares a été fait sur des échantillons issus des carottes d'exploration en guise de stériles à Montviel, et sur des échantillons en vrac représentant différentes lithologies de la fraction stérile du gisement Kipawa. Pour mieux caractériser les minéraux porteurs de terres rares et augmenter les réponses géochimiques durant les essais cinétiques sur les échantillons des deux gisements, les phases porteuses de terres rares ont été concentrées via une combinaison de techniques gravimétriques, séparation magnétique, flottation, et par liqueur dense. Ces échantillons préconcentrés ont été soumis à des essais en mini-cellules d'altération afin d'évaluer la mobilité des terres rares et autres contaminants associés. Les échantillons post démantèlements issus des différents essais cinétiques ont été caractérisés pour :

(i) établir les bilans géochimiques, (ii) élucider les mécanismes d'altération des minéraux porteurs de REE, et (iii) déterminer les minéraux secondaires précipités et la spéciation des REE une fois lixiviés.

L'atteinte de ces objectifs s'effectue via une approche méthodologique en plusieurs phases, consistant d'abord en une caractérisation physique, physico-chimique et minéralogique détaillée d'échantillons représentatifs des futurs stériles miniers. Ces échantillons ont été soumis à des essais cinétiques de percolation et de lixiviation en batch (SPLP, TCLP, et CTEU-9). La détermination de la teneur solide en REE a été effectuée via une digestion suivie de l'analyse par ICP-MS pour une vingtaine d'éléments chimiques, ainsi que le soufre par analyse ICP-AES. L'analyse de roche totale (éléments majeurs et mineurs) a été effectuée par XRF. La teneur en soufre total et en carbone total a été déterminée au four à induction dans l'objectif de déterminer le potentiel de neutralisation et le bilan acide-base. La composition minéralogique des échantillons a été évaluée par une combinaison d'observations de sections polies au microscope optique (MO), au microscope électronique à balayage (MEB), par QEMSCAN, ainsi que par analyse par diffraction des rayons X (réconciliée aux analyses chimiques). Afin de préciser la composition de certains minéraux (éléments en trace), des échantillons ont été analysés par microsonde électronique en WDS (wavelength dispersive spectroscopy), permettant d'analyser les compositions minérales avec une limite de détection de l'ordre de 20 à 100 ppm à l'échelle du grain.

Le traitement et l'interprétation des résultats obtenus à partir des différents essais cinétiques et de lixiviation de laboratoire indiquent que les eaux percolant à travers les lithologies du projet Montviel sont alcalines, avec des pH respectant en général les limites exigées par les législations en vigueur. Les éléments F et Ba peuvent présenter des préoccupations environnementales dans le cas d'absence d'une atténuation naturelle (sorption ou précipitation). Or, le Ba précipite vraisemblablement *in situ* sous forme des sels insolubles (i.e. barytine) et le pH demeure inférieur aux limites réglementaires grâce à l'effet des pluies acides de la région de Lebel-sur-Quévillon (teneur en sulfates inférieure à 10 mg/l) et la dissolution du CO_2 dans les eaux de drainage minier.

La comparaison des résultats géochimiques issus des différents essais (cellules humides, mini-cellules, essais de lixiviation TCLP, SPLP, et CTEU-9) montre des différences significatives entre les essais cinétiques et les essais de lixiviation. Le type d'essai a un impact direct sur les taux de lixiviation des terres rares et les métaux associés. La différence entre les différents essais est due principalement aux paramètres suivants : la granulométrie, le ratio solide-liquide, la durée des

essais, et le type de solution de lixiviation. Les essais CTEU-9 demeurent les seuls essais qui génèrent des résultats plus proches de ceux des essais en cellules humides. Par ailleurs, la comparaison des résultats du laboratoire avec ceux des essais de terrain indique la présence d'un effet d'échelle supérieur pour les essais *in situ*. Cet effet d'échelle est causé principalement par les effets de température, la dissolution de CO_2, la granulométrie, le ratio-solide/liquide.

Les résultats des essais cinétiques de laboratoire montrent une faible lixiviation des REE avec une mobilité élevée des terres rares lourdes versus les terres rares légères. Les calculs thermodynamiques effectués par Vminteq et Phreeqc, ainsi que les caractérisations post-démantèlement, indiquent que le faible taux de relargage des REE est dû essentiellement aux phénomènes de sorption, de précipitation sous forme de minéraux secondaires (i.e., $REEPO_4$) et/ou de coprécipétation par d'autres minéraux secondaires de Fe, SO_4, Ca, F, et PO_4^{3-}. Ces processus géochimiques réduiraient significativement la mobilité des REE en favorisant leur fractionnement à l'intérieur des rejets miniers. Les phosphates de terres rares ($REEPO_4$) sont les principaux minéraux secondaires impliqués dans le fractionnement des REE.

La comparaison entre les essais de laboratoire et les barils du terrain indique une augmentation significative de la dissolution des carbonates dans les essais *in situ*. Malgré l'augmentation de la dissolution des carbonates *in situ*, les concentrations élémentaires associées aux carbonates (Ca, Ba, Sr, REE, Th, U) restent sous les limites permises au Québec. Cette réactivité importante des carbonates *in situ* pourrait assurer un important potentiel de neutralisation à long terme des futurs stériles de Montviel. La comparaison de la réactivité des carbonates et celle des silicates des terres rares montre une différence d'un à 2 ordres de grandeur supérieure pour les carbonates de REE. Comme les deux échantillons ont les mêmes caractéristiques (i.e. la granulométrie, le rapport liquide/solide, le degré de libération, etc.), les différences pourraient être dues principalement à la différence de réactivité entre les deux matériaux.

Pour assurer une gestion intégrée des stériles pour les futures mines en question dans cette thèse, un modèle conceptuel de la future halde à stérile pour Montviel est proposé. La base de la halde à stérile devrait être compactée et inclinée pour favoriser les écoulements latéraux des eaux, et sera composée de matériaux de la lithologie la moins problématique, appelée silicocarbonatites. Une fois cette base construite, le reste des stériles pourrait être déposé par-dessus. Les effluents liquides récoltés autour de la halde devraient passer à travers un drain calcaire constitué par les matériaux les plus carbonatés, appelés calciocarbonatites, pour assurer un traitement passif efficace. Cette

méthode d'entreposage permettrait d'assurer une meilleure stabilité géochimique des rejets miniers porteurs des REE.

Les résultats de ce présent projet, parmi les premiers à combler la lacune de données scientifiques au sujet du comportement géochimique de minéraux porteurs des terres rares, permettra de contribuer à l'essor de l'industrie des terres rares du Canada en fournissant des réponses nécessaires à une gestion saine des rejets miniers de ces types d'exploitations. Les connaissances développées dans cette thèse sur la prédiction du comportement géochimique de rejets miniers de terres rares pourraient contribuer à faciliter l'exploitation des gisements des terres au Canada, faisant actuellement face à une réticence sociale et environnementale.

Mots-clés : gisements de terres rares; stériles miniers porteurs des terres rares; fractionnement et mobilité des terres rares; minéraux secondaires de REE; carbonates et silicates de REE; prédiction de la qualité des eaux de drainage; essais cinétiques de laboratoire; essais de lixiviation; essais de terrain; effet d'échelle; approche d'entreposage des rejets miniers porteurs de REE.

ABSTRACT

The rare earth elements (REE) consist of seventeen chemical elements (fifteen lanthanides, La to Lu, as well as Y and Sc). In ore deposits, REE are primarily associated with carbonate, silicate, and phosphate minerals. REE are currently considered as strategic metals for modern industrial requirements largely due to their wide range of applications, which include uses in: hybrid vehicles, radar systems, rechargeable batteries, mobile phones, flat screen display panels, compact fluorescent light bulbs, and other electronic products. Contrary to what their name suggests, the REE are no particularly rare. In fact, they are more abundant in the Earth's crust than lead (Pb) and are several orders of magnitude more abundant than silver (Ag); their abundance is also similar to chromium (Cr) and nickel (Ni). However, the term "rare" is apt for describing the scarcity of economically viable deposits of REE, and the difficulty inherent to physically separating the REE from one another because of their similar chemical properties. Additionally, REE-bearing minerals are often contaminated with actinides such as thorium and uranium, and other elements (e.g., F, Zr, Ba). At present (2017), China controls 97 % of the global REE market, and, as a circumvention strategy, other countries try to find and mine their own REE reserves with high economic potentials.

Rare earth element deposits are characteristically large-tonnage, low-grade operations which could generate significant quantities of liquid and solid wastes (e.g., waste rocks, tailings, and effluents) as a result of both mining and refining activities. Solid wastes, which have no commercial value, are often stored at the surface and, therefore, exposed to ambient environmental conditions. Meteoric and ground waters can be contaminated via the geochemical reactions that occur naturally during mine waste-water interactions. Since legislation in Québec (Canada; where this study takes place) requires mining companies to provide financial guarantees to cover all costs associated with the site reclamation prior to the start of operations, the development of a project requires the ability to predict the geochemical behavior of mine wastes and their associated effluents in advance. These predictions also promote the social acceptability of mining projects by allowing for the identification of potential contaminants of concern and the development of suitable and specific environmental management and waste disposal strategies.

Presently, several REE mining projects are in development in Canada, particularly in Québec (e.g., Montviel, Matamec, Strange Lake). Most publications found in the current literature focus on the

geology of REE deposits, models for their formation, and the concentrations of REE found in surface waters and sediments downstream of REE-bearing geological formations. However, the geochemical behavior of REE-bearing mine wastes has not been studied to date. This has led to significant knowledge gaps, particularly with respect to: (i) the reactivity of REE-bearing minerals; (ii) the geochemical processes, such as adsorption, precipitation, and co-precipitation, which can control the mobility and fractionation of REE during water-rock interactions; (iii) the speciation of REE within ores; (iv) the mineralurgical and metallurgical separation of REE; and (v) REE toxicity. The purpose of this thesis was to study the geochemical behavior of mine wastes from two types of REE bearing ore deposits (i.e., carbonatites and silicates) in order to understand the geochemical processes which control the contamination of mine drainage waters. This was carried out using predictive tests to assess the long-term drainage quality coming from REE-bearing mine wastes at Montviel mine (Ressources GéoMégA) and Kipawa mine (Matamec explorations, Inc.).

The Montviel project (Lebel-sur-Quévillon, Canada) will be involve the open-pit extraction of 250 million tonnes (Mt) of REE-Nb carbonatites with a REE content estimated at 1.47 % of rare earth oxides (REO). Rare earth element mineralization in this deposit is hosted primarily in the carbonatites of the Montviel alkaline proterozoic intrusion, which consists of a series of mafic/ultramafic rocks that are younger (1894 ± 3.5 million years) than the surrounding rocks, weakly metamorphosed, and undeformed. The Kipawa project (Témiscamingue, Québec) will extract 19 Mt of material with an average grade of 0.41 % REO over a 15-year period using an open-pit method.

The study of these two REE-bearing ores was performed using samples from drill cores for the Montviel deposit and bulk samples representing different lithologies for the Kipawa deposit. In order to better characterize REE-bearing minerals and to enhance the geochemical responses, a REE concentrate sample was prepared using gravity and magnetic separation. This work aims to understand the geochemical behavior of the Montviel (carbonatite orebody) and the Kipawa mine wastes including waste rocks and REE concentrate to predict the quality of the drainage waters. Weathering cells were used to evaluate the leachability and mobility of REE and other associated contaminants (e.g., F, Sr, Ba). At the end of these tests, the solids were characterized in order to: (i) establish the geochemical mass balances, (ii) determine the alteration mechanisms of REE-bearing minerals, and (iii) identify secondary minerals and the leached speciation of the REE.

These objectives were accomplished using a multi-step approach. First, physical, chemical, and mineralogical characterizations of representative samples were performed for the future mine wastes from Montviel (carbonatites) and Kipawa (silicates). These samples were submitted to percolation kinetic and leaching tests (TCLP, SPLP, and CTEU-9). Chemical analyses were performed using ICP-AES and -MS after a multi-acid digestion (HCl, HNO_3, and HF). Whole-rock analyses were performed using X-ray fluorescence on a powdered aliquot of each sample. The total sulfur (S) and carbon (C) contents were measured using an induction furnace analyzer. The mineralogical composition of the studied materials was determined using optical microscopy, quantitative scanning electron microscopy, and X-Ray diffraction reconciled with chemical data. In order to accurately determine the mineralogical composition of REE-bearing minerals, electron microprobe analyses (EMPA)/wavelength dispersive spectroscopy were used. EPMA was performed on selected minerals in order to define their REE contents with higher accuracy due to the low detection limits of the technique (0.14-0.35 %).

The treatment and the interpretation of the data obtained from the kinetic and leaching tests, indicated that the water percolating through the lithologies of the Montviel deposit are alkaline and pH values were generally within regulatory limits. Fluorine and barium could present environmental concerns without natural attenuation by sorption or precipitation. However, Ba could precipitate *in situ* as an insoluble salt (i.e., barite) and the pH could remain below the regulatory limits because of acidic rain waters in the Lebel-sur-Quévillon region (sulphate content < 10 mg/l) and the dissolution of CO_2 in mine drainage waters.

Comparison of the geochemical data from the different tests (humidity cells, TCLP, SPLP, and CTEU-9 tests) showed significant differences between the kinetic and leaching tests. The type of test had a direct impact on the leaching rates of the REE and associated metals. The differences between the tests were mainly due to variations in: grain size distribution, solid/liquid ratio, duration of the test, and the type of the leaching solution. The CTEU-9 test presented similar results with those of humidity cells. Comparison of the laboratory results with those of the field tests indicates the presence of a significant scale effect. This is likely due to the effects of temperature, CO_2 dissolution, grain size distribution, and solid/liquid ratio.

The results of the kinetic tests show a low leachability of REE with a high mobility of the heavy rare earth elements (HREE) compared to the light rare earth elements (LREE). Thermodynamic

equilibrium calculations performed using Visual MINTEQ indicate the possibility of secondary mineral precipitation of Fe, SO_4, Ca, F, and PO_4^{3-} (i.e., $REEPO_4$, iron oxides, and clays), which could sorb and/or co-precipitated the leached REE. This geochemical behavior could significantly reduce the mobility of REE by promoting their partitioning within mine wastes. Rare earth phosphates ($REEPO_4$) are the main secondary minerals which are involved into the REE partitioning.

The comparison between laboratory and field tests indicates a significant increase in carbonate dissolution during the field tests. Despite this increase, the concentrations of elements associated with carbonate dissolution (Ca, Ba, Sr, REE, Th, U) remained below the regulatory limits. The high reactivity of carbonates *in situ* could ensure a significant long-term neutralization potential in the future Montviel waste rocks. In order to implement an integrated management strategy for the waste rocks that will be produced by sites discussed in this thesis, a conceptual model of the future waste rocks pile is proposed. The base of the waste rocks pile should be compacted and tilted to promote lateral water flow, and it should be composed of materials from the least problematic lithology (silicocarbonatites). The remaining portion of the waste rocks could be placed on the top of the silicocarbonatites. The liquid effluents, collected around the pile, should be passed through a limestone drain (calciocarbonatites) for passive treatment. This method of storage could ensure a better geochemical stability of REE-bearing mine wastes.

The results of this project have contributed to filling important knowledge gaps related to the reactivity of REE-bearing phases, as well as REE leaching behavior and toxicity. This study also contributes to the development of Canada's rare earth mining industry by providing information necessary to design suitable management strategies for the two types of studied REE-bearing mine wastes. The knowledge developed in this thesis relating to the prediction of the geochemical behavior of wastes from REE deposits can also help to facilitate the social acceptability of REE mining projects.

Keywords : rare earth elements ores; REE-bearing mine wastes; carbonates and silicates of REE; QEMSCAN analysis, degree of liberation, REE leachability, REE speciation, fractionation and mobility of rare earth elements; REE secondary minerals; water quality prediction; kinetic tests; leaching tests; field tests; scale effect; approach to the storage of REE-bearing mine waste.

TABLE DES MATIÈRES

LISTE DES TABLEAUX

LISTE DES FIGURES

LISTE DES SIGLES ET ABRÉVIATIONS

ABA	Acid-Base Accounting
ACP	Analyse par composante principale
AMD	Acid-mine drainage
AP	Acid-potential
ASTM	American Society for Testing and Materials, : American Society for Testing and Materials
B.E.T	Brunaer, Emmet et Teller, auteurs d'une méthode de caractérisation de la surface spécifique
Be	Béryllium
BRGM	Bureau de recherches géologiques et minières
BSE	Back Scattered Electrons
Ca	Calcium
$CaCl_2$	Chlorure de calcium
CaO	Oxyde de calcium
Ce	Cérium
Ce	Concentration à l'équilibre (mg/l)
CEAEQ	Centre d'expertise en analyse environnementale du Québec
Cf	Concentration finale (mg/l)
CND	Contaminated neutral drainage
CRSNG	Conseil de Recherches en Sciences Naturelles et en Génie du Canada
CTEU-9	Centre technologique des eaux usées – méthode 9
Cu	Cuivre
D_{10}	The value ofthe particle diameter at 10 % in the cumulative distribution
D_{50}	The value of the particle diameter at 50 % in the cumulative distribution
D_{80}	The value of the particle diameter at 80 % in the cumulative distribution
D_{90}	The value of the particle diameter at 90 % in the cumulative distribution
DAC	Drain anoxique calcaire
DMA	Drainage minier acide
DNC	Drainage neutre contaminé
DOC	Drain oxique calcaire
Dy	Dysprosium

Ea	Énergie d'activation (kJ/mol)
EDS	Energy dispersive spectroscopy
EDTA	Éthylène Diamine Tétra-Acétique
Eh	Potentiel d'oxydo-réduction (V /ENH) 1 Redox potential
EPMA	Electron probe micro-analyzer
Er	Erbium
ETR	Elément de terres rares
Eu	Europium
Fe	Fer
Gd	Gadolinium
Gs	Densité relative (g.cm-3)
H^+	Proton
H_2SO_4	Acide sulfurique
HCl	Acide chlorhydrique
HEDTA	N-hydroxyethyl-ethylenediamine-triacetic acid
HF	Acide fluorhydrique
HFSE	High field strenght elements
HNO_3	Acide nitrique
Ho	Holmium
HREE	Terres rares lourdes
I	Force ionique (mol/l)
I.S.	Indice de saturation
ICP-AES	Inductively Coupled Plasma Atomic Emission Spectroscopy
ICP-MS	Inductively Coupled Plasma Mass Spectrometry
IMCOA	Compagnie des minéraux industriels de l'Australie
L	Litre
La	Lanthane
LILE	Large ion Lithophile
LREE	Terres rares légères
Lu	Lutétium
M	Concentration molaire (mol/l)
MEB	Microscope Électronique à Balayage

MREE	Terres rares moyennes
Na_2CO_3	Carbonate de sodium
NaCl	Chlorure de sodium
NaOH	Soude
NASC	North American Shale Composite
Nb	Niobium
Nd	Néodyme
Ng	Nanogramme
NNP	Net Neutralization potential
NP	Neutralization potential
NTA	Acide nitrilotriacétique
O_2	Oxygène
P	Phosphore
PA	Potentiel d'acidification
PCA	Principal component analysis
PCB	Polychlorobiphényle
PCO_2	Pression partielle de dioxyde de carbone
PDC	Pyridinium dichromate
pH	Potentiel d'hydrogène
pHpzc	pH at the point of zero charge
Pm	Prométhium
PM10	Particule de diamètre aérodynamique inférieur à 10µm
PM2.5	Particule de diamètre aérodynamique inférieur à 2.5µm
PN	Potentiel de neutralisation
PNN	Pouvoir net de neutralisation
Ppm	Partie par million
Pr	Praséodyme
q_e	Quantité sorbée à l'équilibre (mg/g ou mg/l)
QEMSCAN	Quantitative Evaluation of Minerais by Scanning Electron Microscopy
R	Constante des gaz parfaits (8,3144 J/mol/K)
R^2	Coefficient de détermination / Determination coefficient
RE	Terres rares

REE	Éléments de terres rares
REMM	Règlement sur les effluents des mines de métaux
REN	Mononitrides de terres rares
RIME	Research institute of mining and environment
S/C	Sulfur/ carbon
Sc	Scandium
SEM	Scanning electron microscope
Sm	Samarium
SPLP	Synthetic precipitation leaching procedure
SSA	Specifie surface area (m2.g-l)
T	Température (K)
Ta	Thallium
Tb	Terbium
TCLP	Toxicity characteristic leaching procedure
Th	Thorium
TIMA	TESCAN Integrated Mineral Analyzer
Tm	Thulium
TOC	Tranche oxique calcaire
TREO	Oxydes de terres rares
U	Uranium
UAQT	Université du Québec en Abitibi-Témiscamingue
UO_2	Thorianite
USA	Etats-Unis d'Amérique
USGS	United States Geological Survey
USGS	United States Geological Survey
V	Volume (L)
wt. %	Percentage by weight
XRD	XRD
XRF	X-ray fluorescence
Y	Yttrium
Yb	Ytterbium
Z	Charge ionique

LISTE DES ANNEXES

CHAPITRE 1 INTRODUCTION GÉNÉRALE

1.1 Contexte de l'étude

L'industrie minière contribue de manière significative au développement socioéconomique des pays miniers. Les compagnies minières sont de réelles partenaires des milieux où elles s'implantent. Par exemple, au Canada, l'industrie minière (minéraux et métaux) contribue à hauteur de 2,7 % à 4,5 % du PIB du Canada (Association minière du Canada, 2015). Cependant, avec l'épuisement des gisements à forte teneur, la tendance actuelle est d'exploiter les gisements à faible teneur et fort tonnage, ce qui génère beaucoup de rejets solides et liquides (roches stérile, rejets de concentrateur, effluents miniers). Ces rejets, le plus souvent sans valeur commerciale, sont entreposés en surface ou retournés sous terre sous forme de remblai pour le soutènement. L'eau de pluie et de fonte des neiges percolant sur et au travers des rejets miniers, appelée eau de drainage minier, est susceptible d'être contaminée via les réactions géochimiques ayant cours naturellement dans les rejets au contact de l'eau et de l'oxygène. C'est ce qui oblige les gouvernements à légiférer contre le potentiel de pollution minière. La loi sur les mines oblige les entreprises à engager des garanties financières pour couvrir l'ensemble des coûts liés à la phase d'après mine (Aubertin et al., 2002; Vérificateur général du Québec, 2012). La législation minière devient de plus en plus sévère et contraignante pour obliger les entreprises exerçant des activités minières à respecter l'environnement.

Sachant toutes ces contraintes, le développement d'un projet minier nécessite la prédiction du comportement géochimique des rejets miniers en vue de prédire la qualité des eaux de drainage. Ceci permet aux entreprises minières non seulement de statuer sur le potentiel de génération des contaminants dans les eaux de drainage des futurs empilements de rejets, mais aussi d'élaborer des stratégies de gestion et d'en connaître les coûts relatifs. C'est dans ce cadre que s'inscrit le présent projet.

Présentement, plusieurs projets de mines de terres rares sont en développement au Canada (Montviel, Matamec, Strange Lake etc.). Cependant, le comportement géochimique des rejets miniers de REE n'a fait l'objet d'aucune étude jusqu'à maintenant. Par conséquent, on trouve des lacunes dans la littérature sur : (i) la réactivité des phases porteuses des REE, (ii) la spéciation des REE, (iii) les processus géochimiques contrôlant la mobilité et le fractionnement des REE lors des

interactions eaux-roches (l'adsorption, la précipitation et/ou la coprécipétation, etc.). L'objectif du projet proposé est de prédire le comportement géochimique de rejets miniers porteurs de terres rares, à partir de l'étude des matériaux du projet Montviel, de la compagnie Ressources Géoméga, et du projet Kipawa, de la compagnie Matamec Explorations.

Le site Montviel est une future mine à ciel ouvert visant à exploiter un gisement de terres rares estimé à 250 millions de tonnes (Mt) de carbonatites de REE-Nb. Les dépôts du gisement sont associés à une intrusion alcaline protérozoïque datée de 1894 Ma. Le gisement Montviel est situé à 97 km au nord de la ville de Lebel-sur-Quevillon (Québec, Canada). Il est étalé sur une surface de 32 km^2 (Desharnais and Duplessis, 2011). La zone minéralisée en REE comprend cinq lithologies : des silicocarbonatites, des calciocarbonatites, des magnesiocarbonatites, des ferrocarbonatites et des brèches polygéniques de carbonatites. Ces lithologies sont composées essentiellement de carbonates (calcite, ankérite, sidérite, barytocalcite, strontianite, et carbonates de REE tels que burbankite et kukharenkoite), des silicates (albite, diopside, biotite, chlorite), des phosphates (apatite et monazite), et des sulfures sous forme de trace (pyrite, pyrrhotite, chalcopyrite, sphalérite, et galène) (Edahbi et al., 2015; Goutier, 2006; Nadeau et al., 2015).

Le projet Kipawa est un projet de mine à ciel ouvert visant à exploiter un gisement de terres rares de 19 Mt sur une période de 15 ans. La minéralisation est située à 140 km au sud de la ville Rouyn-Noranda (Québec, Canada). Le gisement est composé essentiellement de trois types de minéraux : eudyalite, mosandrite et britholite. Les phosphates (apatite) sont aussi présents sous forme de trace. Trois zones portant les noms des trois minéraux porteurs de terres rares sont à distinguer : zone eudyalite, zone mosandrite et zone britholite. Ils contiennent essentiellement : La, Ce, Pr, Nd et Sm comme terres rares légères et Eu, Gd, Tb, Dy, Ho, Er, Tm, Yb and Lu, et Y comme terres rares lourdes (tiré du rapport technique préparé par Roche en collaboration avec SGS, Golder et Genivar; Roche et al., 2012). Le Complexe Kipawa est un complexe alcalin-intrusif de syénite et de granite d'une épaisseur de 200 mètres.

1.2 Problématique générale

L'exploitation minière génère de grandes quantités de rejets stockés en surface. Une fois entreposés en surface, les minéraux peuvent devenir instables suite à leur interaction avec l'eau et l'oxygène (exemple des sulfures : pyrite, pyrrhotite). La réactivité de ces rejets dépend de nombreux

paramètres tels que : leur nature (carbonates, silicates, sulfures), les conditions géochimiques (pH, Eh), la cinétique d'altération, présence ou non d'impuretés minérales, la granulométrie et la surface spécifique. Ainsi, l'oxydation des sulfures exposés aux conditions du terrain pourrait conduire à la génération du drainage minier acide (DMA). Ce type de drainage minier est caractérisé par des eaux acides avec des concentrations en métaux dépassant, parfois de plusieurs ordres de grandeur, les normes environnementales. Au cours de ces processus d'oxydation et de neutralisation, lorsque les minéraux neutralisants sont présents en quantité suffisantes, ils neutralisent avec des cinétiques différentes l'acide sulfurique généré par l'oxydation des sulfures. Plusieurs minéraux secondaires peuvent précipiter comme le gypse, la barite, les oxyhydroxydes de fer, d'aluminium, et de manganèse, pouvant piéger certains contaminants (Duzgoren et al., 2009; Fernández-Caliani et al., 2009; Medas et al., 2013; Wang et al., 2016). De plus, certains métaux comme le Fe, l'Al et le Mn peuvent s'hydrolyser et génèrent ainsi plus d'acidité.

Dans le cas où le pH des lixiviats est compris entre 6,5 et 9,5, on parle d'un drainage neutre contaminé (DNC). Dans ces conditions, les métaux à forte mobilité tels qe le zinc, le nickel, et l'arsenic peuvent se trouver dans les eaux de drainage et leurs concentrations peuvent dépasser les normes mentionnées par la Directive 019 (Bussière et al., 2005; Pepin, 2009; Plante et al., 2014).

Les gisements de terres rares se retrouvent typiquement dans des formations géologiques n'étant pas potentiellement génératrices de DMA, de par leur faible teneur en minéraux sulfurés et leur faible réactivité. Cependant, très peu de littérature est disponible sur la lixiviation de terres rares et des contaminants qui leur sont associés tels que l'uranium et le thorium (Singh et Hendry, 2013 ; Hierro et al., 2012; Sapsford et al., 2012; Wang et al., 2012; Arnold et al., 2011). On note aussi un manque de documentation traitant des rejets miniers et leur comportement environnemental issus de l'exploitation de mines des REE. En outre, le développement de projets de lithium et de terres rares au Canada, pour lesquels peu de connaissances sont disponibles quant à leur comportement géochimique, soulève de nouveaux défis pour l'industrie minière et les instances réglementaires (NRCan, 2012), sans compter l'acceptabilité sociale.

La présence de REE en solution est généralement attribuable à la dissolution naturelle des phases porteuses et/ou sous l'action de l'acidité générée par l'oxydation de minéraux sulfurés. Dans les stériles du projet Montviel, par exemple, on trouve au moins deux types de minéraux porteurs des REE, soit les carbonates et l'apatite, qui aussi liées à un mélange de carbonates de Ba-Sr-REE. De

plus, les minéraux porteurs des terres rares sont souvent contaminés par quelques actinides comme le thorium et l'uranium. La dissolution de ces phases pourrait se faire suivant les réactions données par les équations 1.1 et 1.2 :

$$(REE,Ba,Ca,Sr,F)\text{-}CO_3 + H_2O + CO_2 \rightarrow REE^{3+} + Ba^{+} + Ca^{2+} + Sr^{2+} + F^{-} + Th^{4+} + U^{6+} + 2HCO_3 \quad [1.1]$$

$$(REE,Ba,Ca,Sr,F)\text{-}CO_3 + H_2SO_4 \rightarrow REE^{3+} + SO_4^{2-} + Ba^{+} + Ca^{2+} + Sr^{2+} + F^{-} + Th^{4+} + U^{6+} + H_2CO_3 \quad [1.2]$$

Les équations 1.1 et 1.2 montrent que la dissolution des carbonates de terres rares génère des ions calcium, baryum, strontium et des REE en solution, de même que les éléments radioactifs tels que le thorium et l'uranium. En présence de carbonates de REE, l'acidité produite par l'oxydation des sulfures (présents en faible quantité) ou celle des eaux météoriques (pluies acides), est consommé par les REE-carbonates neutralisants présents dans les rejets. À des pH alcalins, les terres rares pourraient précipiter sous forme de fluorures ($REEF_3$), de chlorures ($REECl_3$), et/ou de sels comme les phosphates ($REEPO_4$) et les sulfates ($REESO_4$) de terres rares. La figure 1-1 montre l'effet de la variation du pH d'une solution contenant des REE trivalents à des concentrations typiques de celles rencontrées dans les essais cinétiques du présent projet sur le fractionnement des terres rares.

.

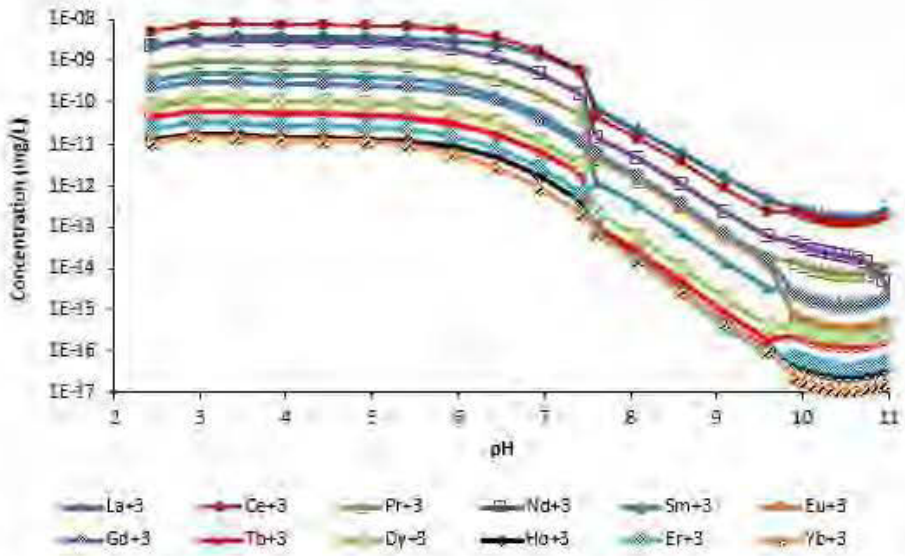

Figure 1-1 : Effet du pH sur la distribution des terres rares issues des cellules humides des matériaux de Géomega (Edahbi et al., 2015).

La figure 1-1 montre que les REE demeurent solubles jusqu'à des pH aux alentours de 7,5. Au-delà de ce pH, les concentrations chutent pour atteindre des niveaux minimums à pH 10. Pour cette raison, il est fort possible de retrouver une quantité non négligeable de ces métaux en solution dans des conditions de drainage neutre contaminé. En outre, les processus de sorption peuvent engendrer un délai avant le relargage des REE à des concentrations problématiques.

Les essais cinétiques sont des outils qui ont été développés surtout pour prédire la génération de DMA. Leur utilisation pour prédire le comportement géochimique de rejets potentiellement générateurs de DMA est d'ailleurs largement documentée dans la littérature scientifique (e .g. (Anawar, 2015; Aubertin et al., 2002; Benzaazoua et al., 2004; Bouzahzah et al., 2013, 2014; Demers et al., 2015; Erguler and Kalyoncu, 2015; Tang et al., 2016; Villeneuve et al., 2004, 2009). Cependant, l'utilisation des outils cinétiques de prédiction dans le cas de rejets miniers faiblement réactifs et/ou faiblement sulfureux peut s'avérer inadaptée (Plante et al., 2011, 2014). Malgré cela, leur utilisation demeure inévitable en raison de l'absence d'outils plus appropriés à ces conditions. Plus de détails sur les essais cinétiques peuvent être trouvés dans Bouzahzah, 2013 et Villeneuve, 2004, 2009.

1.3 Objectifs de la thèse

1.3.1 Objectif général

L'objectif principal du projet est de développer une approche méthodologique pour la caractérisation et la prédiction du comportement géochimique de rejets miniers porteurs de terres rares, à partir de l'étude de lithologies issues deux types de gisements : la carbonatite de Montviel (Ressources Géoméga) et l'intrusion peralcaline silicatée de Kipawa (Matamec Explorations). Cela nous permettra de mieux approfondir les connaissances sur la géochimie des terres rares dans des conditions de DNC.

1.3.2 Objectifs spécifiques

Pour atteindre l'objectif principal, différents objectifs spécifiques sont définis :

1. Caractériser les stériles porteurs de terres rares dans les lithologies des deux gisements (Montviel et Kipawa) à l'aide de techniques de caractérisations avancées incluant celles qui

permettent d'investiguer la spéciation minéralogique (par exemple, DRX, MEB-EDS et WDS; QEMSCAN, XANES);

2. Évaluer le comportement géochimique des différentes lithologies composant les stériles des gisements à l'échelle du laboratoire et du terrain (*in situ*) et de mettre en évidence l'effet d'échelle;
3. Élucider les mécanismes d'altération des minéraux porteurs des REE dans chaque gisement;
4. Évaluer les effets des carbonates, des oxyhydroxydes de fer et des phosphates sur la mobilité des REE;
5. Développer un outil de prédiction du comportement géochimique des terres rares;
6. Évaluer le potentiel de sorption des REE de ces matériaux;
7. Proposer des avenues préliminaires de gestion intégrée des futurs stériles des deux projets permettant d'atténuer un éventuel drainage contaminé en REE.

1.4 Hypothèses de recherche

Lors de l'entreposage des rejets miniers en surface, les eaux de drainage minier sont susceptibles d'être contaminée via plusieurs processus géochimiques ayant cours naturellement dans les rejets en interaction avec de l'eau et de l'oxygène. Cependant, lorsque les rejets miniers sont faiblement réactifs et/ou contiennent très peu de sulfures comme dans le cas des deux gisements Montviel et Kipawa, les réponses géochimiques sont moins prononcées et par conséquent le potentiel contaminant de ces rejets miniers demeure encore méconnu. Par ailleurs, le comportement géochimique des contaminants potentiels associées à ces minerais, tels que les REE résiduels, est très peu étudié. Ainsi, les hypothèses de recherche pour aborder cette problématique s'énoncent comme suit :

1. Le processus de dissolution des phases porteuses des REE pourrait favoriser l'établissement des conditions d'un drainage minier contaminé;
2. L'oxydation des sulfures, même à faibles teneurs, peut accentuer le relargage des REE;
3. Dans des conditions d'un pH neutre à alcalin, les phénomènes de sorption induisent des délais avant l'apparition du drainage contaminé en REE, qu'il conviendrait dans ce cas de quantifier;

4. La mobilité des REE peut, dans certaines conditions, être contrôlée par les minéraux secondaires qui précipitent;
5. La stabilité et la réactivité des minéraux porteurs de terres rares pourraient être liées à plusieurs facteurs d'ordre minéralogique et textural ainsi que géochimiques;

1.5 Originalité du projet

Cette thèse de doctorat est originale et novatrice en raison des lacunes importantes observées dans la littérature au niveau de : (i) la caractérisation environnementale de rejets miniers porteurs de REE, (ii) les taux de réaction de certaines phases de terre rare, et (iii) la gestion qui pourrait être suggérée pour les rejets miniers issus des exploitations des gisements des REE. Les données trouvées dans la littérature sont souvent associées à la détermination des concentrations des REE dans les eaux de mer, et à des eaux interstitielles des sédiments dans des bassins sédimentaires terrestres (en milieux oxique ou anoxique). D'autres travaux d'exploration géochimiques se sont attardés à la signature géochimique des REE dans les cours d'eau et leurs sédiments en aval d'une formation géologique contenant des REE (Franchi et al., 2015; Lisboa et al., 2015; Liu et al., 2016; Mackay et al., 2016; Zhang and Gao, 2015). Malgré que ces données ne soient pas directement appliquées à des rejets miniers, elles pourraient aider à interpréter et à comprendre le comportement géochimique des matériaux géologiques issus des deux projets miniers de REE étudiés dans cette thèse. Des études de cas ont mis en évidence: (i) la genèse et la typologie des gisements des REE, (ii) les conditions contrôlant la distribution des REE dans ces gisements, et (iii) les risques ainsi que la toxicité associée aux REE dissouts (voir chapitre 2- Environmental challenges and identification of the knowledge gaps associated to ree mine wastes management). De plus, aucune étude n'a été faite jusqu'à présent sur le comportement géochimique des REE issus des roches stériles et de minerais de gisements de REE, d'où la pertinence de ce travail de doctorat.

1.6 Structure de la thèse

L'atteinte des objectifs de la thése s'effectue via une approche en plusieurs phases. Ainsi, après le chapitre d'introduction où on présente le contexte et la problématique de l'étude, le chapitre II de la thèse présente une revue critique de la littérature, notamment celle qui porte sur les REE le long du cycle minier. Dans ce chapitre, il sera notamment question de récolter des données sur le comportement géochimique de lithologies porteuses de REE, particulièrement en ce qui à trait aux

intrusions de types alcalines et aux carbonatites (telles que celles correspondant aux contextes géologiques des projets Kipawa et Montviel). Cette revue de littérature critique fait l'objet d'un article de revue soumis à la revue *Journal of Cleaner production* avec comité de lecture (en cours de révision).

Le chapitre III présente une étude fondamentale ayant permis de mieux comprendre le comportement géochimique des REE en solution en interaction avec des phases minérales synthétisées. Ce chapitre a été rédigé et présenté sous forme d'un article scientifique accepté dans la revue scientifique *Chemosphere*.

Les chapitres IV et V du manuscrit traitent quant à eux des principaux résultats de caractérisations minéralogiques, géochimiques, et les calculs d'équilibre thermodynamiques obtenus pour des échantillons de roches stériles et un concentré de REE de Montviel soumis respectivement à des essais en cellule humide et en mini-cellules d'altération. Ces deux chapitres ont été présentés en deux articles scientifiques acceptés respectivement dans les revues scientifiques *Environmental Science and Pollution Research* et *Minerals*.

Le chapitre VI de la thèse présente les résultats de minéralogie en spectrométrie en dispersion des énergies (EDS) automatisée (QEMSCAN®) d'échantillons de roches stériles et d'un concentré de REE de Kipawa soumis à des essais en mini-cellules d'altération. Ces résultats ont été rédigés sous forme d'un article de revue accepté au *Journal of Geochemical Exploration*.

Le chapitre VII présente une discussion générale revenant sur certains aspects traités partiellement dans les chapitres précédents et qui feront l'objet de :

- la comparaison entre les résultats géochimiques issus des essais cinétiques percolés (les cellules humides et les mini-cellules d'altération) et ceux issus des essais de lixiviation en batch (TCLP, SPLP, et CTUE-9),
- l'effet d'échelle entre les essais de laboratoire et les barils du terrain, une approche d'entreposage des rejets miniers porteurs de REE et un guide d'évaluation environnementale basé essentiellement sur les résultats de cette thèse dans le but d'obtenir des résultats fiables permettant de mieux prédire le comportement géochimique des matériaux porteurs de REE.

Enfin, le chapitre VIII présente les principales conclusions tirées de ce travail de thèse ainsi que les recommandations à suivre lors du développement d'un projet minier de REE. Enfin, les

différentes annexes apportent des informations et des résultats complémentaires à ceux présentés dans les différents chapitres de la thèse.

1.7 Retombées

Peu de travaux de recherche ont été consacrés à la problématique de la prédiction de la qualité des eaux de drainage des rejets miniers contenant des teneurs résiduelles en REE, sachant que celles-ci peuvent avoir des impacts considérables aux niveaux environnemental et financier. Ce projet permettra de développer une expertise novatrice au sujet de la prédiction du comportement géochimique de rejets miniers de terres rares. Ce projet permettra ainsi d'apporter plusieurs éléments de réponses et des données d'intérêt pouvant combler les lacunes sur le comportement géochimique des REE. Il permettra d'apporter plusieurs informations capitales quant au comportement géochimique de rejets de mines de terres rares nécessaires aux projets présentement en développement dans le pays (par exemple, Montviel, Kipawa, Lac Strange et Lac Misery, au Québec). Cela permettrait aussi de combler des lacunes d'ordre législatif dans les règlements et directives qui encadrent l'industrie minière au Canada. Une meilleure connaissance du comportement géochimique des REE permettra de contribuer à une meilleure gestion des rejets de miniers de REE, ce qui peut conférer au Canada des avantages économiques certains afin de développer des projets de REE à moindre coût, tout en minimisant les impacts environnementaux et sociaux.

1.8 Contribution scientifique de la thèse

Cette thèse est composée de huit chapitres dont cinq sont sous forme d'articles de revue déjà soumis ou publiés dans des revues scientifiques internationales. Cette thèse a fait l'objet de cinq articles de revue, trois articles de conférences (annexe A, B et C) et quatre posters. Un autre article de revue a été publié dans le cadre d'un stage MITACS parallèle aux travaux de cette thèse, en collaboration avec la compagnie minière Agnico-Eagle (annexe D). Je suis l'auteur principal des différents articles publiés dans le cadre de ce projet de mémoire. Le travail réalisé depuis la collecte des données jusqu'à la rédaction a été éffectué par moi-même sous la supervision de mon directeur Benoît Plante et mon co-directeur Mostafa Benzaazoua.

1.8.1 Les articles de revues

1- Environmental challenges and identification of the knowledge gaps associated to REE mine wastes management (*Journal of Cleaner Production* – under review).
Edahbi. M.; Plante. B.; Benzaazoua. M.

2- Mobility of rare earth elements in mine drainage: influence of iron oxides, carbonates, and phosphates (*Chemosphere*, On-line https://doi.org/10.1016/j.chemosphere.2018.02.054).
Edahbi. M.; Plante. B.; Benzaazoua. M.; Ward. M.; Pelletier.M.

3- Geochemistry of rare earth elements within waste rocks from the montviel carbonatite deposit, Québec, Canada (*Environmental science and pollution research*, On-line https://doi.org/10.1007/s11356-018-1309-7).
Edahbi. M.; Plante. B.; Benzaazoua. M.; Kormos. L.; Pelletier. M.

4- Rare earth elements (La, Ce, Pr, Nd, and Sm) from a carbonatite deposit: Enrichment process, mineralogical characterization and geochemical behavior (*Minerals*, On-line https://doi:10.3390/min8020055).
Edahbi. M.; Plante. B.; Benzaazoua. M.; Kormos. L.; Pelletier. M.

5- Mineralogical characterization using QEMSCAN® and leaching potential study of REE within silicate ores: A case study of the Matamec project, Québec, Canada (*Journal of Geochemical Exploration*, On-line https://doi: 10.1016/j.gexplo.2017.11.007)
Edahbi. M.; Benzaazoua. M; Plante. B; Kormos. L.; Doire. S.

6- CIL gold losses characterization in a double refractory ore: Creating a synergistic approach between mineralogical characterization, diagnostic leach tests and preg-robbing tests. Process Mineralogy of critical metals (*Hydrometallurgy journal*- accepted with minor corrections).
Edahbi. M.; Mermillod-Blondin. R.; Plante.B.; Benzaazoua. M.

1.8.2 Articles de conférences avec comité de lecture

1- Mineralogical and geochemical study of rare earth elements from carbonatites deposit. 13th SGA Biennial meeting at Nancy, France.
Edahbi. M.; Plante. B.; Benzaazoua. M.; Kormos. L.; Pelletier. M.

2- Mineralogical and geochemical study of rare earth element from a silicate deposit. Process Mineralogy '17. Cape Town, South Africa.
Edahbi. M.; Plante. B.; Benzaazoua. M.; Kormos.L.; Doire.S.

3- Mineralogical characterization and geochemical behavior of rare earth elements (REE) from a carbonatite deposit: Montviel deposit. Process Mineralogy '17. Cape Town, South Africa.
Edahbi. M.; Plante. B.; Benzaazoua. M.; Kormos.L.; Pelletier, M.

1.8.3 Posters

1- Mineralogical and geochemical study of rare earth elements from carbonatites deposit. 13th SGA Biennial meeting at Nancy, France.
Edahbi. M.; Plante. B.; Benzaazoua. M.; Kormos.L.; Pelletier. M.

2- Mineralogical and geochemical study of rare earth element from a silicate deposit. Process Mineralogy '17. Cape Town, South Africa.
Edahbi. M.; Plante. B.; Benzaazoua. M.; Kormos.L.; Doire.S.

3- Recovery and characterization of REE -bearing phosphates. International Symposium on Innovation and Technology in the Phosphate Industry (SYMPHOS 2017).
Edahbi. M.; Plante. B.; Benzaazoua. M.; Taha. Y.; Hakkou. R.

4- Mineralogical Characterization, Geochemical Behavior and XFAS Study of Rare Earth Elements in Carbonatites. Driving discovery 2017 APS/CNM users meeting A-19.
Edahbi. M.; Plante. B.; Bouzahzah. H.; Benzaazoua. M.; Finfrock. Z.; 2017.

CHAPITRE 2 REVUE CRITIQUE DE LA LITTÉRATURE : ARTICLE 1 : ENVIRONMENTAL CHALLENGES AND IDENTIFICATION OF THE KNOWLEDGE GAPS ASSOCIATED WITH REE MINE WASTES MANAGEMENT

Cet article est soumis à la revue Journal of Cleaner production en décembre 2017

Edahbi, M.[a]; Plante, B.[a] ; Benzaazoua, M.[a]

[a] Université du Québec en Abitibi-Témiscamingue (UQAT), 445 boul de l'Université, Rouyn-Noranda J9X 5E4, QC, Canada.

2.1 Abstract

In the last decade, the rare earth elements (REE) industry (from exploration, treatment to environmental impacts) has attracted tremendous attention from the scientific and industrial communities. In fact, in the framework of sustainable development, social acceptability, and environmental regulations, it is now necessary to integrate environmental studies as early as possible in the design and development of mining projects. However, the scarcity in REE release from mine wastes publications led to significant knowledge gaps in understanding the environmental impact of REE mine wastes. This critical review addresses the environmental challenges and identify the knowledge gaps associated to REE mining. It discusses: (i) the typology of REE deposits, (ii) the REE-bearing minerals reactivity, (iii) the ore processing and characterization of the associated REE waste, (iv) the industrial leaching of REE, and (v) the REE behavior in natural environments and proposes an investigation approach "REE leaching studies" to predict the REE impacts on the exposed environments.

Keywords: REE geochemistry; REE deposits; REE bearing minerals reactivity; REE ore processing; factors controlling the REE leachability; REE environmental impacts.

2.2 Introduction

The rare earth elements (REE) are composed of seventeen chemical elements with atomic numbers from 57 to 71 (La to Lu), along with scandium (Sc), and yttrium (Y) (atomic numbers 21 and 39 respectively). Promethium (Pm) is not included because of its little abundance in natural deposits (unstable isotopes, the only natural isotope ^{147}Pm having a half-life of less than three years). The REE are neither rare nor earth; they are, contrary to what their name suggests,

fairly common in the Earth's crust. They are more abundant than lead, and are several orders of magnitude more abundant than silver (Gibert, 2012). Their abundance is similar to that of chromium and nickel (Calas, 2012). Therefore, the term "rare" would rather apply to the scarcity of economically exploitable deposits of REE, and the difficulty to separate them from one another because of their similar properties (Feng et al., 2014; Jaireth et al., 2014; Jiang et al., 2004; Knutson et al., 2014; Li et al., 2009).

Geochemists generally distinguish two groups of REE: light rare earth elements (LREE) (La to Sm) and heavy rare earth elements (HREE) (Eu to Lu). All REE possess similar chemical and physical properties, e.g., the same external electronic configuration: [Xe] $6s^2$ $5d^1$ $4f^x$, « x » varying from 0 to14. REE are present as trivalent cations (M^{3+} charge) except Eu and Ce which can have charges of +2 and +4 depending on the redox conditions. The main difference between each REE is in their ionic size, which decrease with increasing atomic number (from 1.2 to 0.7Å as the atomic number increases from 57 to 71). REE are endowed with unique spectroscopic and magnetic properties. Furthermore, the REE size distribution allows their substitution with other metallic elements (e.g., Ca, Na, and U) which present similar ionic radius. REE can combine with anions (e.g. halogen ions and oxyanions) to give soluble (e.g., chlorides, nitrates) and insoluble (e.g., sulfides, fluorides, carbonates, oxalates, phosphates) salts, in addition to their abilities to form stable complexes with organic molecules (e.g., fulvic acid and organic matter). REE find their applications in hybrid vehicles, rechargeable batteries, wind turbines (renewable energy), mobile phones, flat screen display panels, compact fluorescent light bulbs, laptop computers, disk drives, catalytic converters, etc.

In the framework of sustainable development, social acceptability, and environmental regulations, nowadays the integration of environmental studies in the design and development of REE mining projects, which has not been done until now, becomes an urgent necessity.

At present, China holds 94 % of the global REE market (Schlinkert and Boogaart, 2015). As a circumvention strategy, other countries try to find and mine their own REE reserves that constitute a high economic potential. REE are currently considered strategic metals according to the mining industry (Chen, 2011; Jaireth et al., 2014; Lee et al. , 2012; McLellan et al., 2014; Nieto et al., 2013; Wübbeke, 2013). Moreover, as shown in Figure 2-1 the REE demand is always greater than the REE supply. This will lead to a competition for REE resources between the world's leading industrial powers, especially the United States of America, the European Union, and China.

Figure 2-1 : Supply and Demand of REE (2010 to 2015) (Standing Committee of Natural Resources-Canada, 2014).

Based on the geological context (magmatic and metamorphic processes) the REE mineral deposits can be divided mainly into six categories (Goutier, 2006; Nadeau et al., 2015; Orris and Grauch, 2002) (i) alkaline (ii) hyperalkaline magmatism, (iii) carbonatites, (iv) placer deposits, and (v) clay minerals ("ion adsorption" in laterites) (Orris and Grauch, 2002). The recycling of REE from end-products could be another important source of REE such as magnets, compact fluorescent light bulbs, and other electronic products (Jowitt et al., 2018; Schulze et al., 2017). During water-rock interactions, REE-bearing phases exhibit significant reactivity under leaching conditions (Ali, 2014; Edahbi et al., 2017, 2018a, 2018b, 2018c).

During mining and refining, REE industry generates significant quantities of solid and liquid wastes like any kind of mine (e.g., 9600 to 1200 tons of mining waste per ton of REE; Hurst, 2010). The main waste generated by REE mining industry are waste rocks (coarse-grained) with no commercial value, and tailings (finely ground ore from which the economic minerals were removed), derived from mineralurgical and hydrometallurgical treatments (Filho et al., 2016). The interaction of these wastes with water and oxygen upon exposure to environmental conditions induce the oxidation of sulfide minerals, a process that is generally acid-generating that will promote the dissolution of the other minerals (Nordstrom et al. 2012; Blowes et al., 2003, Plante et al., 2011a) and could significantly affects the surrounding environment.

In natural environments, weathering/leaching of REE deposits and industrial wastes (such as mine wastes rocks and tailings, municipal wastes, etc.) are the main source of REE. Depending on the nature of REE bearing minerals, their degree of dissolution order is as follows: REE

carbonates > REE iron oxides/hydroxides > REE silicates (Linnen et al., 2014; Zhang et al., 2015). REE-bearing minerals release their REE content in leachates when they are dissolved, and that is why REE have been used as tracers in natural environments (e.g. REE signature of ground waters; Delgado et al., 2012). Upon chemical weathering, the most mobile elements are found in natural waters, while the less soluble elements might precipitate or co-precipitate in secondary minerals (e.g., iron, manganese and aluminum oxy-hydroxides). The aqueous REE solubility depends mainly on pH, temperature, ionic strength, organic matter content, redox potential, and solution chemistry (Ding et al., 2002; Inguaggiato et al., 2015; Linnen et al., 2014).

An intensive exploitation of REE resources and uncontrolled leakage from REE-bearing tailings can pose a serious environmental threat, increasing REE concentrations in soil, water, and air, especially in the perimeter of the mining area (e.g., around the Bayan Obo and Mountain Pass mines in China and USA, respectively) (Coussy, 2004; Huang et al., 2016; Schreiber et al., 2016; Wang et al., 2014). Regarding the hydrometallurgical treatment process, HCl, HNO_3, and H_2SO_4 acids are widely used to leach REE. Leaching the ore with sulfuric acid could lead to REE fractionation by gypsum formation (Peelman et al., 2014)). At the time of REE apatite dissolution using sulfuric acid, 80 % of the REE in solution is fractionated due to the precipitation of $CaSO_4$. Moreover, organic acids (e.g., humic and fulvic) could increase the REE-bearing minerals dissolution by the acidity effects (Goyne et al., 2010; Barman et al., 1992).

This paper presents a critical review on the environmental challenges related to REE mining, with an emphasis on: (i) the typology of REE deposits, (ii) the REE-bearing minerals reactivity, (iii) the ore processing and characterization of their associated REE waste, (iv) the industrial leaching of REE, and (v) the REE behavior in natural environments.

2.3 Typology of REE deposits

Numerous studies have been conducted worldwide on REE mineralization indices covering several types of REE deposits (Chen, 2011; Jaireth et al., 2014; Jiang et al., 2004; Kanazawa and Kamitani, 2006; Orris and Grauch, 2002; Pingitore et al., 2014; Yang et al., 2011; Zaitsev et al., 2014). The main REE-bearing mineral phases are: (i) carbonates, (ii) silicates, (iii) iron oxyhydroxides, and (iv) phosphates (Table 2-1). Depending on their origins, REE deposits are associated with delamination of the lithosphere, mantle upwelling, and metasomatism

(Chakhmouradian and Wall, 2012). The purpose of this chapter is to describe the main REE deposits and their characteristics.

2.3.1 Deposits associated with pegmatites

The pegmatites complexes may contain REE as economic substances, often in combination with other elements such as niobium, tantalum, zinc, yttrium and beryllium (e.g., Chaffee County, Colorada, Strange Lake alkali complex, Québec) (Hanson et al., 1992; Miller et al., 1997). The Motzfeldt Centre deposit (Greenland) of tantalum, niobium, and REE is a typical case of hyperalkaline magmatism. The Nb (52 %) and Ta (6-7 %) are mostly concentrated in the pyrochlore $(Na,Ca,Ce)_2(Nb,Ti,Ta)_2(O,OH,F)$ compared to other REE minerals (Table 2-1)(Rocha et al., 2001). REE (from 3000 to 5000 ppm) are present mainly in bastnaesite $(Ce,La)(CO_3)F$, zircon $(Zr,REE)SiO_4$, and monazite $(Ce,La,Nd,Th)PO_4$ (Table 2-1). Furthermore, according to the USGS, more than 350 deposits of this type are identified worldwide (Orris and Grauch, 2002).

2.3.2 Deposits associated with carbonatites

Carbonatites are igneous rocks containing more than 50 % primary carbonates. However, most carbonatites are polygenic and show hydrothermal and metasomatic signatures. The most abundant carbonates in these rocks are calcite and dolomite, whereas ankerite, siderite, rhodochrosite, and magnesite are relatively rare (Chakhmouradian et al., 2012). Carbonates, as well as their alterative products, are the main sources of REE in the world (Verplanck and Gosen, 2011). Carbonatites are known to have an enrichment of LREE in comparison to HREE due to fractional crystallization of the carbonates and remobilization by hydrothermal fluids (Nadeau et al., 2015). The REE mineralization may be at the heart and/or outside of the carbonatite (e.g., in veins).

The main REE-bearing minerals associated with carbonates are fluorocarbonates (bastnaesite, parasite, and synchysite), hydrated carbonates (ancylite), and phosphates (apatite and monazite). Other REE-bearing phases are less common, such as britholite or burbankite, which are considered products of metasomatic processes; processes involving chemical composition changes of a rock during rock-fluids interactions and/or substitution of minerals without melting (Zaitsev et al., 1998). In the literature, several REE deposits are known to be associated to carbonatites (e.g., Mt Weld carbonatite, Australia; St-Honoré, Dolodeau, Creveir township, Short Lake, Grevet, Oka, and Montviel in Canada). The Mt Weld deposit, called Central

Lanthanide Deposit (LCD), is considered a rare earth elements rich ore (an average grade of 7.5 % rare earth oxides). REE mineralization of this deposit is hosted mainly in a volcanic plug, which consists of a series of volcanic rocks. REE bearing minerals are mainly phosphate minerals which contain 70 % of rare earth oxides and disseminated within goethite and limonite (Humphries, 2012; Lottermoser, 1990). Mt Weld concentrator, based on flotation, is a process designed to produce 26, 500 tons of rare earth oxides (Walker, 2010). Considered one the Other REE deposits hosted in carbonatite exist in the world, e.g., Mountain Pass and Bear Lodge (United States), Bayan Obo (China), Palabora (South Africa), Barra do Itapirapua (Brazil), and Khibina (Kola Peninsula, Russia) (Orris et Grauch, 2002).

Tableau 2-1 : Classification of REE-bearing minerals (data obtained from webmineral).

Mineral class	**REE bearing minerals[(1)]**	**$LREE_2O_3$ (%)**	**$HREE_2O_3$ (%)**	**REE**	**Associated contaminants**
Carbonates	Bastnaesite $(La,Ce)(CO_3)F$	74.90	-	Ce, La	-
	Parasite $Ca(Ce,La)_2(CO_3)_3F_2$	41.96	-	-	-
	Synchysite $Ca(La,Ce)(CO_3)_2F$	51.41	-	Ce, La	-
	Burbankite $(Na,Ca)_3(Sr,Ba,La,Ce)_3(CO_3)_5$	6.97	-	Ce, La	-
	Kukharenkoite $Ba_2(La,Ce)(CO_3)_3F$	18.36	-	Ce, La, Pr, Nd	-
Phosphates	Apatite $(Ca,La,Ce)_5(PO_4)_3F$	12	-	Ce, La	U, Th
	Monazite $(Ce,Sm,Gd,Nd)PO_4$	50.87	-	Ce, Sm, Gd, Nd	Th
	Xenotime $YbPO_4$	-	73.52	Yb	-
Silicates	Mosandrite $Na(Na,Ca)_2(Ca,Ce,Y)_4(Ti,Nb,Zr)(Si_2O_7)_2(O,F)_2F_3$	26.95	6.18	Ce, Y	Nb, Zr
	Britholite $(Ce,Ca,Th,La,Nd)_5(SiO_4,PO_4)_3(OH,F)$	32.32	-	Ce, La, Nd, Y	Th
	Eudialyte $Na4(Ca,Ce)_2(Fe,Mn,Y)ZrSi_8O_{22}(OH,Cl)_2$	8.27	1.14	Ce, Y	Zr
	Zircon $ZrSiO_4$	4.41	-	La, Ce, Pr, Nd	Zr

Oxides	Samarskite $(La,Ce,Fe,U)(Nb,Ta)_5O_4$	24.34	-	La, Ce	U, Nb
	Pyrochlore $(Na,Ca)_2Nb_2O_6(OH,F)$	11.5	-	La, Ce	Nb
	Cerianite $(Ce,Th)O_2$	63.09	-	Ce	Th
	Fergusonite $YNbO_4$	-	45.93	Y	Nb

(1)Noted that REE contents could vary widely from deposit to deposit.

2.3.3 REE Deposits associated with paleoplacers

Placers are detrital deposits derived from the degradation of a wide range of rocks (granitic, metamorphic, and/or sedimentary). The older placers, called also paleoplacers, are often enriched by high value minerals after their initial deposition (e.g., Elliot Lake deposits, Canada). In this case, the Elliot Lake deposits contained mostly brannerite, monazite, uraninite, uranothorite, and uranothorianite (Robertson and Gould, 1983).These types of deposits can reach economically exploitable concentrations of LREE (Orris and Grauch, 2002) due to metasomatism and alteration phenomena. However, the placers may also contain high levels of Th and U (≤8.4 wt. % ThO2, and ≤5.8 wt. % UO2) (Chakhmouradian et al., 2012). Moreover, the feasibility of utilizing these deposits depends mainly on the ability to manage the radioactive wastes resulting from the ore processing. For example, the main REE-bearing minerals found in placers and paleoplacers are xenotime, monazite, and zircon. These deposits are distributed all over the world, such as in Oak Grove (Idaho, USA), Hilton Head Island (South Carolina, USA), Elliot Lake (Ontario, Canada), Bald Mountain (Ontario, Canada), Kerala (India), Queesland State (Australia), and Richards Bay (South Africa) (Kanazawa and Kamitani, 2006; Orris and Grauch, 2002). The current trend is to explore these rich REE placers taking the advantage of their proximity to waterways (coastal placer) and low production and treatment costs (reduced grinding).

2.3.4 Mineral clays "ion adsorption"

Laterites (red, yellow, or brown rocks) are formed by physical expansion and geochemical weathering of geological substrate in tropical and subtropical climates. Lateritic soils are mainly composed of clay minerals. In general, they are loose and indurated materials rich in iron (e.g., goethite, lepidocrocite, and hematite) and aluminum hydroxides, which are especially prone to adsorption phenomena at their surface. The alteration products, including REE, are concentrated in the laterites by adsorption. These lateritic clays are important type of surface

deposits, found in southern China since the 1970's, as well as in Madagascar, Laos, and other tropical countries. Anionic clays generally have REE levels ≤ 0.3 % by rare earth oxides (REO) weight (Sappin and Beadoin, 2015). However, their extraction and treatment are relatively easy. This type of deposit alone ensures 35 % of Chinese REE production (Chakhmouradian et al., 2012). Nevertheless, the exploitation of REE laterites caused serious environmental damage in China such as deforestation and atmospheric pollution (Yang et al., 2013). In fact, in order to access to the REE laterites deposits, removal of the overburden (soil and trees located above) results in large scale deforestation, in addition to the mine tailings ponds and waste rock piles. Today, the HREE demand is increasing (Chen, 2011; Zhang et al., 2017) faster than what the cationic clays are capable of providing to satisfy the needs of the industrial development. Many scientists and researchers are looking into other potential sources of REE, such as deep-sea mud which could be a significant REE resource (up to 500ppm REE), because of their strong adsorption on iron oxy-hydroxides and Phillipsite (Kato et al., 2011). Other sources of REE are exist, such as iron-titanium oxides (ilmenite) and phosphates (apatite, monazite, and xenotime). In most cases, these deposits are not economically exploitable for REE, in most cases, these deposits are not economically for REE, but they may be exploitable for ilmenite, phosphates, and zircon. (Chakhmouradian and Zaitsev, 2012).

2.3.5 Other sources of REE: Recycling

Given the fact that the REE demand exceeds its supply from the geological resources, recycling techniques for REE are an alternative solution to reduce supply risks and to mitigate the environmental problems associated with mining and refining of REE. For example, in China, each ton of REE produced generates approximately 8.5 kg of fluorite, 13 kg of dust, 9600 to 1200 tons of mining waste, 75 cubic meters of acidic water, and one ton of radioactive waste (Hurst, 2010). However, the supply of REE from secondary sources will always be small relative to ore production because of the great difficulties in collecting the REE present in small amounts in a multitude of products.

The need for REE recycling technology is justified by: (i) the global demand to replace a highly polluting economy with an environmentally friendly green economy, (ii) the scarcity of economically exploitable REE mines, (iii) the fact that recycling can be a promising REE resource especially for countries with insufficient natural resources within their borders, (iv) the fact that recycling can contribute to keep the REE prices relatively stable, and (v) Reducing the cost of the REE production. However, REE recovery technologies from electrical waste and

electronic equipment (WEEE) require advanced processes which have not reached industrial levels yet (Tsamis and Coyne 2015). Extractive metallurgical techniques are well known but the main challenge lies in the treatment of impurities associated with certain typical recyclats (Liu et al., 2014; Quinn et al., 2017). Table 2-2 covers the materials to be recycled as well as the techniques used to recover the REE contents.

Recycled materials mainly include compact fluorescent lamps, permanent magnets, rechargeable batteries, electric vehicles, as well as end-of-life electronic products (computers, television screens, printers, photocopiers, television screens, etc.; Alonso et al., 2012, Binnemans et al., 2013). However, despite the research done on REE recycling, less than 5 % of REE have been recycled (Free, 2014). To extract the REE from the various end-of-life products, several processes have been developed and applied. All these processes are hydrometallurgical-based such as the sequential leaching, total dissolution, and selective dissolution. The recovery efficiency depends essentially on the nature of object containing the REE, the REE to be extracted, the extraction technology used, and the extraction conditions (Table 2-2).

Tableau 2-2 : Summary of some technologies used in recycling of the rare earths.

Substance recycled	REE (%)	Extraction technology	Extraction Conditions	Extraction efficiency (%)	Remarks	References
Fluorescent lamps	10-20	Sequential leaching Autoclave	HCl 30-150°C	-	Greater consumption of Chemical products	Tunsu et al., 2014 Yang et al., 2013
SmCo magnet	23-33	Total dissolution	3M HCl, HNO_3 or H_2SO_4	100	Decreased yield with increased temperature	Tanaka et al., 2013
FeNdB magnet	26.7	Total dissolution Selective dissolution	HCl H_2SO_4 Low temp.	100 96-99	Decreased yield with increased temperature	Lee et al., 2012 Tanaka et al., 2013

2.4 REE-bearing minerals reactivity

REE deposits are classified as low-grade deposits (in the order of ppm; Chakhmouradian et al., 2012; Nadeau et al., 2015). The acidity produced by the oxidation of sulfides within the REE mine tailings could lead to dissolution of various mineralogical phases, including the REE

bearing minerals (Lim et al., 2016). In fact, the dissolution of these minerals can generate mine drainage water contaminated with heavy metals, REE, and other toxic elements (e.g., Cd, Ni, As, etc.). The concentrations of the released elements may exceed the environmental norms. Unfortunately, knowledge on REE release from mine wastes is very limited. In order to predict the quality of future mining drainage waters, a better understanding of the reactivity of REE-bearing minerals is required.

REE are integrated into the crystalline structure of silicates, carbonates, and phosphates by substitution of other elements, depending on the ionic radius and charge of the ions. For example, Ca^{2+}, Na^{+}, Th^{2+}, and U^{3+} cations will be replaced by the REE^{3+} cations (Figure 2-2). The most studied cases in the literature are the exchange between Ca and REE in apatite and calcite (see the review by Lipin and Mackay, 1989).

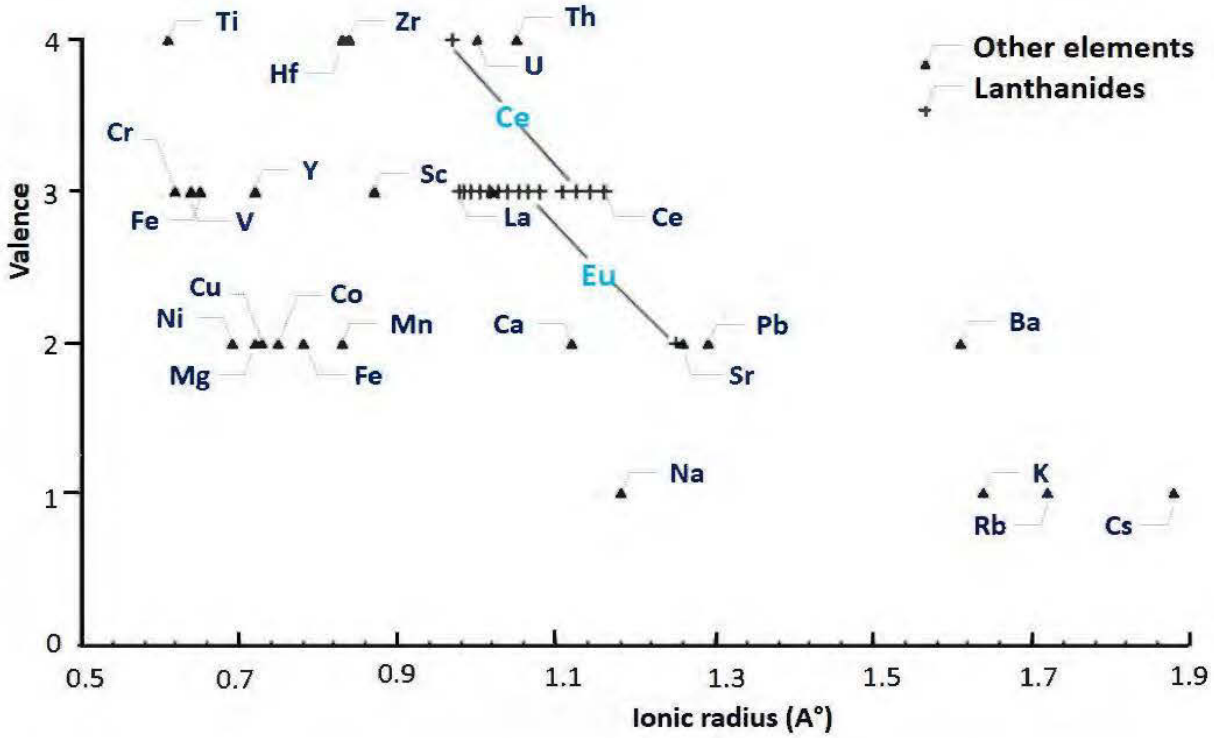

Figure 2-2 : Relationship between ionic radius and valence of REE and other metallic elements (inspired from Lipin and McKay, 1989).

The REE geochemistry is determined by their host minerals. The REE leached into solution are found in three forms: (i) associated with suspended particles, (ii) associated with colloidal-like micro-particles, and (iii) free and/or dissolved ions (Sholkovitz, 1995). Therefore, the fine particulates will play a key role in the REE transport. Before getting to this point, a better understanding of REE geochemistry requires (1) an understanding of the geochemistry of their

bearing minerals, (2) identification of the factors controlling their reactivity, and (3) identification of the main processes governing the mobility of REE.

2.4.1 REE Carbonate reactivity

During their formation process, carbonates can be associated with different REE. These carbonates are characterized by a high porosity and high sorption capacities (Einsele, 2013). It has been recognized that the carbonate minerals are more reactive than silicates, phosphates, or oxy-hydroxides. Blowes and Ptacek (1994) proposed the following hierarchy for carbonates reactivity: calcite > dolomite > Mg-ankerite > ankerite > siderite. Moreover, there are many types of carbonate systems: (i) homogeneous closed system, (ii) open homogeneous system, (iii) heterogeneous closed system, and (iv) open heterogeneous system (Appelo and Postma, 2004). The partial pressure of CO_2 above a carbonate solution, its pH, temperature, and the presence of organic matter are the main factors controlling the dissolution of carbonates in the field conditions (e.g., Prigiobbe and Mazzotti, 2013). The acidity generated during the oxidation of sulfide minerals can increase the REE release from carbonate minerals. For example, carbonatite deposits contain at least three types of REE-bearing minerals, namely carbonates, apatite, and a Ba-Sr-REE mixture (Edahbi et al., 2015). In addition, these REE minerals are often contaminated with a few actinides such as thorium and uranium. The dissolution of these phases could be carried out according to the reactions given by equations 1 and 2:

$$(REE,Ba,Ca,Sr,Th,U,F)CO_3 + H_2O + CO_2 \rightarrow REE^{3+} + Ba^{+} + Ca^{2+} + Sr^{2+} + F^{-} + Th^{4+} + U^{6+} + 2\ HCO_3^{-} \quad [2.1]$$

$$(REE,Ba,Ca,Sr,Th,U,F)CO_3 + H_2SO_4 \rightarrow REE^{3+} + SO_4^{2-} + Ba^{+} + Ca^{2+} + Sr^{2+} + F^{-} + Th^{4+} + U^{6+} + 2\ HCO_3^{-} \quad [2.2]$$

Both equations 2.1 and 2.2 show that the dissolution of REE carbonates can generate calcium, barium, strontium, and REE ions in solution, as well as their thorium and uranium trace contaminants. The acid produced by the oxidation of sulfides will most likely be consumed by the carbonates, including the REE-bearing ones, maintaining near-neutral to slightly alkaline pH levels. Under these conditions, REE can precipitate as fluorides ($REEF_3$), chlorides ($REECl_3$), and oxy-salts such as phosphates ($REEPO_4$) and sulfates ($REESO_4$) which are characterized by low solubility under such alakaline conditions (pH ~ 8) (Table 2-3).

Tableau 2-3 : Solubility product constants of REE compounds.

Compound	Formula	K_{sp} (25°C)	References
REE carbonate	$REE_2(CO_3)_3$	$10^{-28.25}$ to $10^{-35.77}$	Firsching et al., 1986
Yttrium fluoride	YF_3	8.62 X 10^{-21}	David et al., 2000
Yttrium hydroxide	$Y(OH)_3$	10^{-22}	David et al., 2000
REE phosphate	$REEPO_4$	10^{-24}	Firsching et al., 1993

The main factors controlling REE carbonates reactivity are summarized in Table 2-4.

Tableau 2-4 : Main factors controlling carbonates reactivity.

Parameter	Impact on carbonates	References
CO_2 partial Pressurein the case of closed system	increasing P_{CO2} promotes dissolution of carbonates and therefore a significant generation of alkalinity	Prigiobbe et Mazzotti, 2013 Tavares et al.,2015
pH	the rate of carbonates dissolution is inversely proportional to pH	Arvidson et al., 2003; Alkattan et al., 1998
Temperature	Carbonates solubility decreases as the temperature increases	Coto et al., 2012; Li and Duan, 2011; Morse and Arvidson, 2002; Peng et al., 2015; Zendah et al., 2013
Organic matter	The CO_2 presence, fulvic and humic acids can significantly increase the carbonates dissolution	Bennett et al., 1988; Buckau et al., 2000; Kodama and Schnitzer, 1973; Koriko et al., 2007; Tamir et al., 2013

2.4.2 Reactivity of silicates

In comparison with the carbonates, the dissolution of silicates is negligible at near neutral pH but becomes significant when the pH decreases (e.g., Gruber et al., 2016; Lammers et al., 2017; Moncur et al., 2005). The dissolution of silicate minerals is often incongruent and depends on pH, mineral structure, mineralogical composition, external environmental factors, and temperature. For example, the dissolution of the plagioclase feldspar anorthite can be congruent (Equation 2.3) or incongruent (Equation 2.4) (Sherlock et al., 1995):

$$(Ca, REE)\ A1_2Si_2O_8 + 2\ H^+ + 6\ H_2O \rightarrow Ca^{2+} + 2A1^{3+} + 2\ H_4SiO_4 + REE^{3+} + 6OH^- \quad [2.3]$$

$$(Ca, REE)\ Al_{12}Si_2O_8 + 2\ H^+ + H_2O \rightarrow Ca^{2+} + REE^{3+} + Al_2Si_2O_5(OH)_4 \quad [2.4]$$

In addition, White and Brantley. (2003) observed that the silicate weathering rates R ($mol.m^{-2}s^{-1}$) can be measured as follows: R = 3.1* 10-13 $t^{0,61}$ with t being the weathering time. It is

important to note that weathering processes can lead to concentrate and/or fractionate the REE. The main factors affecting the dissolution of REE silicates are summarized in Table 2-5.

Tableau 2-5 : Main factors controlling silicate reactivity.

	Impact on silicates	**References**
Redox conditions	Any change in pH-Eh conditions causes a change in precipitation, co-precipitation and adsorption of REE.	Saldi et al., 2013 ; Edahbi et al., 2017
pH	the rate of silicates dissolution is inversely proportional to pH	Benzaazoua et al., 2004; Megan et Susan, 2016; Plante et al., 2010
Temperature	Silicates solubility increases as the temperature increases	Lammers et al., 2017 ; Megan et Susan, 2016; _Ptáček et al., 2015
Impurities	Many silicates contain impurities ➔ their crystal lattices are weakened ➔ dissolution is relatively easy	Le Bouffant et al., 1982

2.4.3 Reactivity of phosphates

Apatite, monazite, and xenotime are examples of phosphate minerals that may contain significant levels of REE, especially La, Ce, Pr, and Nd. Additionally, apatite is also considered as a major source of phosphorus and fluorine in the earth's crust. Their dissolution in natural systems release fluorine, REE, calcium, and phosphorus (Bilal et al., 1998; Cherifa et al., 2000). Phosphates are characterized by low solubility in dilute acids in comparison with strong acids (Cherifa et al., 2000). The chemical process of apatite dissolution is shown in reactions (2.5) and (2.6):

$$(Ca,REE)_5(PO_4)_3F + 5H_2SO_4 \rightarrow 5(Ca,REE)SO_4 + 3H_3PO_4^- + HF \quad [2.5]$$

$$2(Ca,REE)_5(PO_4)_3F + 15H_2O \rightarrow 10Ca^{2+} + 10REE^{3+} + 6PO_4^{3-} + 2F^- + 30OH^- \quad [2.6]$$

In favourable pH-Eh conditions, the REE precipitate and/or co-precipitate as $REEPO_4$ and $REEF_3$. The main parameters that govern the dissolution process are acid concentration and nature (either organic acids like humic and fulvic acids, or inorganic acids), temperature, chemical composition of the solution, and the presence of bacteria. Furthermore, the dissolution of apatite may be inhibited by the presence of lead because of the rapid precipitation of a lead phosphate phase at the apatite surface (passivation mechanism) (Dorozhkin, 2002; Miretzky et al., 2008). Adsorbed cations such as zinc may also block the dissolution sites of hydroxyapatite ($Ca_5(PO_4)_3OH$) (Lingawi et al., 2011).

2.5 Ore processing and the associated REE waste

The first step in REE production is to prepare a concentrate using different methods based on physical, mineralogical, chemical, and magnetic properties of the REE bearing minerals. The most common methods for the concentrate preparation are gravimetric methods, magnetic separation, and flotation (Dehaine et al., 2015; Jordens et al., 2016). Before leaching step, the REE concentrate is submitted to the sulphuric acid baking that is widely used in the REE industry. The baked product is dissolved in water or dilute acid, and often gives better extractions than those obtained by direct leaching. The structural and chemical properties of REE bearing minerals do not facilitate their separation from gangue minerals (e.g., in solid solution with other minerals, in inclusions) (Zheng et al., 2017). The processes for obtaining REE in the form of pure products are long, delicate, and expensive (Figure 2-3).

The REE processing operations begin with a mechanical pre-concentration taking the advantage of their magnetic properties (Jordens et al., 2016; Dehaine et al., 2015). The mechanical pre-concentration is carried out by:

- Magnetic separation using high magnetic separators;
- Gravimetric techniques (Mozley Table, Falcon concentrators, Knelson, etc.).
    - Acid or alkaline leaching
    - Hydrometallurgical treatment

The second step aims to decrease the proportions of the gangue minerals by trying to float the REE-bearing minerals. This step is decisive for removing harmful elements before the extraction stage (hydrometallurgy / pyrometallurgy). The third step consists of acid or alkaline leaching to dissolve and leach the REE out of the solids. Acid leaching is generally carried out using a strong acid (e.g., sulfuric, hydrochloric, or nitric acid), whereas a basic solution (e.g. soda or carbonate) is used in the alkaline leaching (Xie et al., 2014). The fourth step is the hydrometallurgical treatment to separate the dissolved REE through selective precipitation, ion exchange on resins, solvent extraction, etc (Zhang et al., 2015).

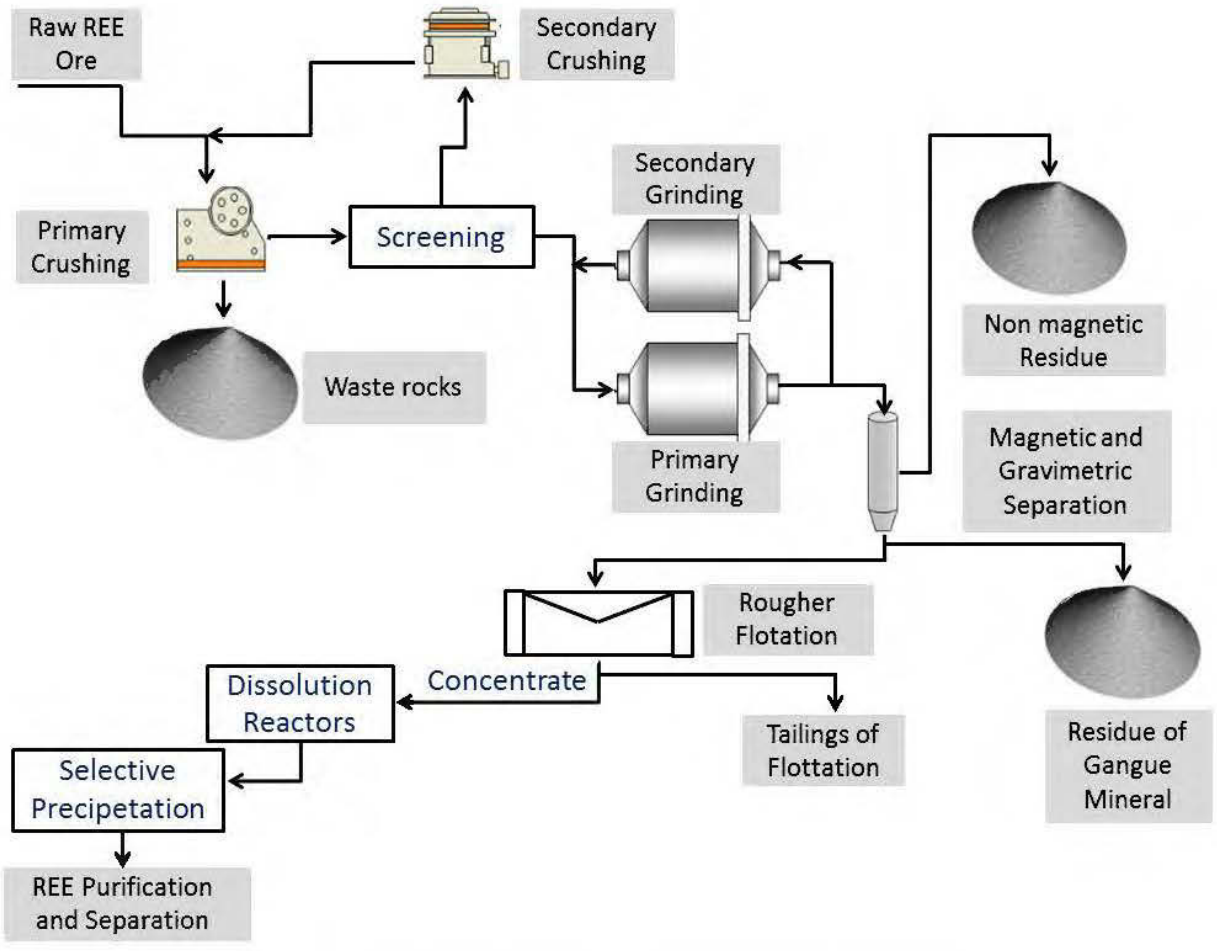

Figure 2-3 : Conventional REE ore processing flowsheet.

At the end of each step of the treatment process, a REE concentrate and the associated tailings are generated. These tailings are often in pulp and characterized by a very fine grain size, whose chemical and mineralogical composition varies greatly from one tailings to another depending on the ore and the processes applied.

For gravimetric separation, the wastes are mostly composed of gangue minerals such as quartz, micas (muscovite, biotite, phlogopite), carbonates (calcite, dolomite), and clays, with low concentrations of the denser minerals such as sulfides, iron oxides, magnetite, hematite, and ilmenite, which are concentrated with the REE during the process. For magnetic separation wastes, the dense fraction from the gravity separation feeds the magnetic separation process to recover REE bearing minerals. The diamagnetic minerals (such as pyrite, barytocalcite, and gangue minerals), are concentrated in the magnetic separation wastes. For flotation wastes, the mineralogical composition will be essentially composed of the gangue minerals left out of the flotation concentrate. Their chemical composition will vary depending on the flotation reagents

used, which are selected based upon the REE-bearing minerals. The flotation reagents in the tailings may have harmful effects to the environment.

2.5.1 Industrial leaching of REE

In order to improve REE leaching efficiency, the REE-bearing minerals are concentrated using different processes briefly described in the previous section, then thermally treated and leached in the presence of acidic or caustic reagents. Various parameters of the REE leaching can be adjusted depending on the materials (e.g., leaching agent, solvent concentration, temperature, time of leaching, particle size, stirring speed, etc.) (Baral et al., 2014 ; Bian et al., 2011, Das et al., 2013) (Table 2-6).

2.5.1.1 REE leaching by mineral acids (HCl, H_2SO_4, or HNO_3)

The choice of leaching agent (nitric acid, sulfuric acid, or hydrochloric acid) depends on the desired selectivity of the REE separation process, types of gangue minerals as well as the types of reactants used in other extraction procedures (Table 2-6) (Deqian et al., 2017). The use of sulfuric acid (H_2SO_4) promotes both leaching of the REE contents from phosphates (e.g., apatite), and precipitation of gypsum ($CaSO_4 \cdot 2H_2O$) which has adverse effects on the process efficiency. Gypsum precipitation can be minimized by using nitric acid (HNO_3) instead of sulfuric acid, as illustrated by the following reactions (Peelman et al., 2014):

$$(Ca,REE)_{10}(PO_4)_6F_2 + 10\ H_2SO_4 \rightarrow 6\ H_3PO_4 + 10\ CaSO_4.x\ H_2O + 2\ HF + 10\ REE^{3+} \quad [2.7]$$

$$2\ REEPO_4 + 3\ H_2SO_4 \rightarrow REE_2(SO_4)_3 + 6\ H^+ + 2\ PO_4^{3-} \quad [2.8]$$

$$(Ca,REE)_{10}(PO_4)_6F_2 + 20\ HNO_3 \rightarrow 6\ H_3PO_4 + 10\ Ca(NO_3)_2 + 2\ HF + 10\ REE^{3+} \quad [2.9]$$

The leaching time, acid concentration, solid/liquid ratio, stirring speed, and temperature are the main factors that control the apatite leaching efficiency (Xie et al., 2014)Jorjani et al., 2008) have noticed that the REE recovery increases with increasing acid concentration and decreases when the solid/liquid ratio increased (Table 2-6). HCl usually leaches faster than sulphuric acid at any temperature, but its industrial applications are limited by its higher cost and its accelerated corrosion of metallic structures (Baral et al., 2014).

2.5.1.2 Leaching by organic acids

In this section, the proposed lixiviants have been tested only in the laboratory. These laboratory studies are important to find alternative means to reduce the environmental impacts associated to the REE mine wastes (Table 2-6). The organic acids which are used in REE leaching from

phosphate minerals are citric, oxalic, phthalic, and salicylic acids. The amount of REE released increases linearly with increasing concentration of oxalic, citric, and phthalic acids (Goyne et al., 2010). While, REE leaching is minimal in the presence of salicylic acid, because of the low acidity of aromatic acids (Goyne et al., 2010). The importance of the organic acids in the REE leaching process from monazite follows the order: citric acid > oxalic acid > salicylic acid (Goyne et al., 2010).

2.5.1.3 Other REE enrichment methods

Other REE leaching methods (e.g., chlorination, carbothermal reduction, digestion with hydrofluoric acid) are cited in the literature (Gupta and Krishnamurthy, 1992). In industry, alkaline leaching is preferred to extract REE from the minerals with a high REE content (e.g., xenotime, monazite). At a temperature of 140°C and NaOH concentration of 50 % v/v, the REE extraction yield can reach 99.9 % (Alex et al., 1998). The resulting leachates are treated with ammonia or sodium pyrophosphates in order to remove thorium. The precipitation by ammonia is the most appropriate method because it facilitates the preferential precipitation of LREE and thorium, which leads to a HREE enrichment in the filtrate (Vijayalakshmi et al., 2001). The microwave-assisted leaching (MAL) is also used in industry to increase the extraction efficiency of metals. This technique allows the reduction of leaching time, increases the metal recovery, and is environmentally benign (no emission of hazardous gases) (Al-Harahsheh and Kingman, 2004). However, the microwave-assisted leaching suffers from many drawbacks such as low recovery of extracted metal, difficulties in solid/liquid separation, and a deleterious effect of impurities on the ease of purification (Al-Harahsheh and Kingman 2003).

Tableau 2-6 : Summary of the leaching conditions of REE-bearing minerals.

Mineral	Leaching agent	Concentration (mol/l, unless otherwise noted)	Leaching time (min)	Stirring speed (rpm)	Temperature (°C)	References
Bastnaesite	HCl	2.5	30 to 240	200 to 300	55	(Baral et al., 2014)
	H_2SO_4	15	30 to 240	200 to 300	25	
	HNO_3	8	30 to 240	200 to 300	70	
	HCl	6	90	-	90	(Bian et al., 2011)
	H_2SO_4+thiourea	1 to 3	360	-	25	(Yörükoğlu et al.,2003)
						(Jorjani et al., 2008)
Apatite	HNO_3	20 to 60 vol%	10 to 140	100 to 200	60	(Goyne et al., 2010)
	Oxalate	$6.72x10^{-3}$	1680	8	25	
	Phtalate	$5.12x10^{-3}$	1680	8	25	
	Citrate	$5.46x10^{-3}$	1680	8	25	
	Salicylate	$6.63x10^{-3}$	1680	8	25	(Goyne et al., 2010)
Monazite	Oxalate	$6.48x10^{-3}$	1680	8	25	
	Phtalate	$5.14x10^{-3}$	1680	8	25	
	Citrate	5.16 to $5.44x10^{-3}$	1680	8	25	
	Salicylate	$6.02x10^{-3}$	1680	8	25	(Oelkers and Poitrasson, 2002)
	No ligand	-	-	-	50 to 230	
						(Panda et al., 2014)
	HCl	6	120	-	90	
						(Alex et al., 1998)
	NaOH	50 % w/v	240	-	170	
						(Vijayalakshmi et al., 2001)
Xenotime	NaOH	50 % w/v	240	-	100 to 140	(Moldoveanu and Papangelakis,
	H_2SO_4	concentrated	360	-	250	2013)
Clay minerals	$(NH_4)_2SO_4$	0.05 to 2.5	60	-	< 50	

2.6 REE behavior in natural environments

2.6.1 Environmental impacts of REE exploitation

In the past, the exploitation of REE deposits have produced harmful environmental impacts. The year 1998 was the worst in the history of REE in terms of pollution (Ali, 2014). In that year the USA closed the last American REE mine (Moutain Pass in California) because of a spill of a hundred thousand liters of radioactive water. As will be described below, devastating environmental impacts were recorded in China, especially near its main REE mining areas (e.g. the Bayan Obo mine region).

2.6.1.1 Effect of REE on air quality

The REE emissions to the atmosphere in the gaseous form or as atmospheric aerosols (particles in suspension) causes disturbances in the air quality (Stille et al., 2009; Wang et al., 2004). These disturbances lead to changes in the chemical composition of the air from the local to the global scale. Of course, the risks associated with these disturbances are not of the same magnitude and nature according to the spatial and temporal scales concerned (areas near the mining zones are more problematic). The atmospheric aerosols include any particles or suspended matter having an aerodynamic diameter ranging from some nanometers to 10 µm. The most studied cases in the literature are for fine (PM2.5) and coarse (PM10) particles, which have an aerodynamic diameter of 2.5 and 10 µm, respectively. The study of these particles essentially allows analyzing atmospheric aerosols and the levels and distributions of REE as suspended particles (Wang and Liang, 2014a; Wang et al., 2014). In the vicinity of the Bayan Obo mine in China, REE suspended in particulate matter (PM10) range from 149.8 to 239.6 ng/m^3 in total particulates (particles + material), and 42.8 to 68.9 ng/m^3 in August 2012 and March 2013, respectively. Moreover, a strong concentration gradient is observed in the main wind direction (Wang et al., 2014). These fine particulates can cause respiratory and cardiovascular diseases, severe intestinal disorders, keratosis, and skin cancer (Cheng et al., 2013).

2.6.1.2 Effect REE on soil and plant growth

Currently, there are no data showing that plants need REE to grow. However, the use of REE as fertilizer can cause adverse effects on the quality of tsoil and growth of plants by indirect means (Sneller et al.,2000), such as (i) Fe substitution by Sc, (ii) Ca/Mg replacement, and (iii)

phosphate deficiency due to its precipitation as REE phosphates. Furthermore, the presence of high concentrations of REE in soils affects the bioavailability of some elements which are necessary for the plant growth. The REE effect on adsorption of phosphorus in five different types of Chinese agricultural soils was studied through batch adsorption and desorption experiments in the presence and absence of REE. The study indicated that the amount of P adsorbed tends to decrease when the soil contains lower concentrations of REE (Wang and Liang, 2014b). Thomas et al. (2014) tested the effects of lanthanum (4.96 mg/l), cerium (3.85 mg/l), and yttrium (10.29 mg/l) on the growth of the following plants: Asclepias syriaca L., Desmodium canadense, Panicum virgatum L., Raphanus sativus, and Solanum lycopersicum. Their study showed that the La, Ce, and Y have harmful impacts on the plants growth. A. syriaca and D. canadense lost 10 to 20 % of their biomass. Moreover, the slow accumulation of these elements in the environment could become problematic (Thomas et al., 2014).

2.7 Closing remarks

The results of this study demonstrate that REE mining and refining are known to generate high amounts of liquid and solid wastes, with potential deleterious effects on the environment. In the near future, the REE consumption is expected to continue increasing because they are irreplaceable in many technological sectors. As a result, many REE projects will be developed around the world in the next decades. For example, in Canada more than 200 projects are being developed. In the framework of sustainable development, social acceptability obligations, and environmental regulations, it is nowadays necessity for mining projects to evaluate all environmental impacts that may occur from REE deposit exploitation. The feasibility of a REE project depends intimately on the ability to face the environmental challenges and issues (e.g. waste management, site rehabilitation, water treatment). Despite this, few studies aimed at the REE mining operations impacts on air, water, soil, plants, and health. Finally, further research is necessary in order to fill important knowledge gaps on REE, especially regarding their environmental impacts, the reactivity of REE-bearing phases, as well as REE leaching and toxicity.

Finally, REE leaching studies are one of the most important keys which can be used in order to understand and predict the geochemical behavior of REE-bearing minerals upon exposure to environmental conditions. The mineralogy and leachability of REE from different deposits (HREE and/or LREE mine projects) must be investigated to predict their geochemical behavior

and to evaluate the factors controlling REE mobility in ambient conditions. All deposit lithologies including ore and waste rocks must be sampled, characterized using a multi-technique mineralogical approach (e.g., automated SEM-EDS, EPMA-WDS, XRD, EXAFS), and then submitted to laboratory and field kinetic testing to investigate their REE release potential. When possible and relevant, each lithology must be managed separately in order to ensure an integrated risk management framework policy and encourage the valorization and reuse of these waste into eco-friendly products.

REFERENCES

Al-Harahsheh, M., and Kingman, S. (2004). Microwave-assisted leaching—a review. Hydrometallurgy, 73(3), 189-203.

Alex, P., Suri, A. K., and Gupta, C. K. (1998). Processing of xenotime concentrate. Hydrometallurgy, 50(3), 331-338.

Ali, S. H. (2014). Social and environmental impact of the rare earth industries. Resources, 3(1), 123-134.

Alkattan, M., Oelkers, E. H., Dandurand, J.-L., and Schott, J. (1998). An experimental study of calcite and limestone dissolution rates as a function of pH from −1 to 3 and temperature from 25 to 80°C. Chemical Geology, 151(1–4), 199-214.

Appelo, C. A. J., and Postma, D. (2004). Geochemistry, groundwater and pollution: CRC press.

Arvidson, R. S., Ertan, I. E., Amonette, J. E., and Luttge, A. (2003). Variation in calcite dissolution rates:: A fundamental problem? Geochimica et Cosmochimica Acta, 67(9), 1623-1634.

Baral, S. S., Shekar, K. R., Sharma, M., and Rao, P. V. (2014). Optimization of leaching parameters for the extraction of rare earth metal using decision making method. Hydrometallurgy, 143, 60-67. doi:10.1016/j.hydromet.2014.01.006

Barman, A. K., Varadachari, C., and Ghosh, K. (1992). Weathering of silicate minerals by organic acids. I. Nature of cation solubilisation. Geoderma, 53(1-2), 45-63.

Bennett, P. C., Melcer, M. E., Siegel, D. I., and Hassett, J. P. (1988). The dissolution of quartz in dilute aqueous solutions of organic acids at 25°C. Geochimica et Cosmochimica Acta, 52(6), 1521-1530.

Bian, X., Yin, S.-h., Luo, Y., and Wu, W.-y. (2011). Leaching kinetics of bastnaesite concentrate in HCl solution. Transactions of Nonferrous Metals Society of China, 21(10), 2306-2310.

Bilal, E., Marciano, V., Marques, Correia Neves, J., Fuzikawa, K., Riffel, B. F., . Nasraoui, M. (1998). Altération hydrothermale des monazites-(Ce) des pegmatites du district de Santa Maria de Itabira (Minas Gerais, Brésil). Comptes Rendus de l'Académie des Sciences - Series IIA - Earth and Planetary Science, 326(10), 693-700.

Binnemans, K., Jones, P. T., Blanpain, B., Van Gerven, T., Yang, Y., Walton, A., and Buchert, M. (2013). Recycling of rare earths: a critical review. Journal of Cleaner Production, 51, 1-22.

Blowes, D. W., Ptacek, C. J., Jambor, J. L., and Weisener, C. G. (2003). 9.05 - The Geochemistry of Acid Mine Drainage A2 - Turekian, Heinrich D. HollandKarl K Treatise on Geochemistry (pp. 149-204). Oxford: Pergamon.

Blowes, D., and Ptacek, C. (1994). Acid-neutralization mechanisms in inactive mine tailings. National Water Research Institute.

Buckau, G., Artinger, R., Geyer, S., Wolf, M., Fritz, P., and Kim, J. I. (2000). Groundwater in-situ generation of aquatic humic and fulvic acids and the mineralization of sedimentary organic carbon. Applied Geochemistry, 15(6), 819-832.

Calas, G. (2012). Elements International Magazine of Mineralogy, Geochemistry, and Petrology, 8(ISSN: 1811-5209).

Chakhmouradian, A. R., and Wall, F. (2012). Rare Earth Elements: Minerals, Mines, Magnets (and More). Elements, 8(5), 333-340. doi:10.2113/gselements.8.5.333

Chen, L., Ma, T., Du, Y., and Xiao, C. (2017). Dissolved Rare Earth Elements of Different Waters in Qaidam Basin, Northwestern China. Procedia Earth and Planetary Science, 17, 61-64.

Chen, Y., Tian, Q., Chen, B., Shi, X., and Liao, T. (2011). Preparation of lithium carbonate from spodumene by a sodium carbonate autoclave process. Hydrometallurgy, 109(1–2), 43-46.

Cheng, Z., Jiang, J., Fajardo, O., Wang, S., and Hao, J. (2013). Characteristics and health impacts of particulate matter pollution in China (2001–2011). Atmospheric Environment, 65(0), 186-194.

Cherifa, A. B., Rogez, J., Jemal, M., and CMathieu, J. (2000). Dissolution de l'hydroxyapatite et du phosphate tricalcique β dans les solutions d'acide nitrique. Journal of Thermal Analysis and Calorimetry, 63, 689–697.

Coto, B., Martos, C., Peña, J. L., Rodríguez, R., and Pastor, G. (2012). Effects in the solubility of CaCO3: Experimental study and model description. Fluid Phase Equilibria, 324(0), 1-7.

County, S.B. (2004). Final Environmental Impact Report for Molycorp, Inc. Mountain Pass Mine 30-year Plan, ENSR International, Department, S.B.C.L.U.S., Molycorp, I., Development, S.B.C.E. and Group, P.S.

Das, N., and Das, D. (2013). Recovery of rare earth metals through biosorption: An overview. Journal of Rare Earths, 31(10), 933-943.

David, R. (2000). LIDE (ed.),"CRC Handbook of Chemistry and Physics": CRC Press LLC, Inc. USA.

Davris, P., Stopic, S., Balomenos, E., Panias, D., Paspaliaris, I., and Friedrich, B. (2017). Leaching of rare earth elements from eudialyte concentrate by suppressing silica gel formation. Minerals Engineering, 108, 115-122.

Dehaine, Q., and Filippov, L. O. (2015). Rare earth (La, Ce, Nd) and rare metals (Sn, Nb, W) as by-product of kaolin production, Cornwall: Part1: Selection and characterisation of the valuable stream. Minerals Engineering, 76, 141-153.

Delgado, J., Pérez-López, R., Galván, L., Nieto, J. M., and Boski, T. (2012). Enrichment of rare earth elements as environmental tracers of contamination by acid mine drainage in salt marshes: A new perspective. Marine Pollution Bulletin, 64(9), 1799-1808.

Ding, R., and WooD, S. A. (2002). The aqueous geochemistry of the rare earth elements and yttrium. Part X. Potentiometric determination of stability constants of acetate complexes of La3+, Nd3+, Gd3+and Yb3+ at 25–70 C and 1 bar. Water-Rock Interactions, Ore Deposits, and Environmental Geochemistry: A Tribute to David A. Crerar, The Geochemical Society Special Publication No, 7.

Dorozhkin, S. V. (2002). A review on the dissolution models of calcium apatites. Progress in Crystal Growth and Characterization of Materials, 44(1), 45-61.

Edahbi, M., Plante, B., Benzaazoua, M., Ward, M., & Pelletier, M. (2018a). Mobility of rare earth elements in mine drainage: Influence of iron oxides, carbonates, and phosphates. Chemosphere, 199, 647-654.

Edahbi, M., Plante, B., Benzaazoua, M., Kormos, L., & Pelletier, M. (2018b). Rare Earth Elements (La, Ce, Pr, Nd, and Sm) from a Carbonatite Deposit: Mineralogical Characterization and Geochemical Behavior. Minerals, 8(2), 55.

Edahbi, M., Plante. B., Benzaazoua. M., and Pelletier. M. (2018c). Geochemistry of rare earth elements within waste rocks from the Montviel carbonatite deposit, Québec, Canada. Environmental Science and Pollution Research DOI: 10.1007/s11356-018-1309-7.

Edahbi, M., Benzaazoua, M., Plante, B., Doire, S., and Kormos, L. (2017). Mineralogical characterization using QEMSCAN® and leaching potential study of REE within silicate ores: A case study of the Matamec project, Québec, Canada. Journal of Geochemical Exploration, https://doi.org/10.1016/j.gexplo.2017.11.007.

Einsele, G. (2013). Sedimentary basins: evolution, facies, and sediment budget: Springer Science and Business Media.

Feng, C., Bi, X., Liu, S., and Hu, R. (2014). Fluid inclusion, rare earth element geochemistry, and isotopic characteristics of the eastern ore zone of the Baiyangping polymetallic Ore

district, northwestern Yunnan Province, China. Journal of Asian Earth Sciences, 85(0), 140-153.

Firsching, F. H., and Kell, J. C. (1993). The solubility of the rare-earth-metal phosphates in sea water. Journal of Chemical and Engineering Data, 38(1), 132-133.

Firsching, F. H., and Mohammadzadei, J. (1986). Solubility products of the rare-earth carbonates. Journal of Chemical and Engineering Data, 31(1), 40-42.

Free, M. L. (2014). Chapter 2.8 - Biohydrometallurgy A2 - Seetharaman, Seshadri Treatise on Process Metallurgy (pp. 983-993). Boston: Elsevier.

Gibert, B. (2012). Ressources minérales et matériaux pour l'énergie. Laboratoire Géosciences Montpellier-Bât.22 - 2eme étage, France.

Goutier, J. (2006). Géologie de la région du lac au Goéland (32F/15): Ressources naturelles et Faune, Québec.

Goyne, K. W., Brantley, S. L., and Chorover, J. (2010). Rare earth element release from phosphate minerals in the presence of organic acids. Chemical Geology, 278(1–2), 1-14.

Gruber, C., Kutuzov, I., and Ganor, J. (2016). The combined effect of temperature and pH on albite dissolution rate under far-from-equilibrium conditions. Geochimica et Cosmochimica Acta, 186, 154-167.

Gupta, C. K., and Krishnamurthy, N. (1992). Extractive metallurgy of rare earths. International Materials Review, 37(5), 197–248.

Hanson, S. L., Simmons, W. B., Webber, K. L., and Falster, A. U. (1992). Rare-earth-element mineralogy of granitic pegmatites in the Trout Creek Pass District, Chaffee County, Colorado. The Canadian Mineralogist, 30(3), 673-686.

Herrmann, H., Nolde, J., Berger, S., and Heise, S. (2016). Aquatic ecotoxicity of lanthanum – A review and an attempt to derive water and sediment quality criteria. Ecotoxicology and Environmental Safety, 124, 213-238.

Huang, X., Deng, H., Zheng, C., and Cao, G. (2016). Hydrogeochemical signatures and evolution of groundwater impacted by the Bayan Obo tailing pond in northwest China. Science of The Total Environment, 543, 357-372.

Humphries, M. (2013). Rare Earth Elements: The Global Supply Chain. Congressional Research Service, 7-5700 (http://www.fas. org/sgp/crs/natsec/R41347.pdf) (accessed on August 12th, 2017).

Hurst, C. (2010). China's rare earth elements industry: What can the west learn?. Institute for the Analysis of Global Security Washington DC.

Inguaggiato, C., Censi, P., Zuddas, P., Londoño, J. M., Chacón, Z., Alzate, D., . . . D'Alessandro, W. (2015). Geochemistry of REE, Zr and Hf in a wide range of pH and water composition: The Nevado del Ruiz volcano-hydrothermal system (Colombia). Chemical Geology, 417, 125-133.

Ippolito, N. M., Innocenzi, V., De Michelis, I., Medici, F., and Vegliò, F. (2017). Rare earth elements recovery from fluorescent lamps: A new thermal pretreatment to improve the efficiency of the hydrometallurgical process. Journal of Cleaner Production, 153, 287-298.

Jaireth, S., Hoatson, D. M., and Miezitis, Y. (2014). Geological setting and resources of the major rare-earth-element deposits in Australia. Ore Geology Reviews, 62(0), 72-128.

Jiang, S.-Y., Yu, J.-M., and Lu, J.-J. (2004). Trace and rare-earth element geochemistry in tourmaline and cassiterite from the Yunlong tin deposit, Yunnan, China: implication for migmatitic–hydrothermal fluid evolution and ore genesis. Chemical Geology, 209(3–4), 193-213.

Jordens, A., Marion, C., Grammatikopoulos, T., and Waters, K. E. (2016). Understanding the effect of mineralogy on muscovite flotation using QEMSCAN. International Journal of Mineral Processing, 155, 6-12.

Jorjani, E., Bagherieh, A. H., Mesroghli, S., and Chelgani, S. C. (2008). Prediction of yttrium, lanthanum, cerium, and neodymium leaching recovery from apatite concentrate using artificial neural networks. Journal of University of Science and Technology Beijing, Mineral, Metallurgy, Material, 15(4), 367-374.

Jowitt, S. M., Werner, T. T., Weng, Z., & Mudd, G. M. (2018). Recycling of the Rare Earth Elements. Current Opinion in Green and Sustainable Chemistry.

Kanazawa, Y., and Kamitani, M. (2006). Rare earth minerals and resources in the world. Journal of Alloys and Compounds, 408–412, 1339-1343.

Kato, Y., Fujinaga, K., Nakamura, K., Takaya, Y., Kitamura, K., Ohta, J., Iwamori, H. (2011). Deep-sea mud in the Pacific Ocean as a potential resource for rare-earth elements. Nature Geosci, 4(8), 535-539.

Nordstrom, D. (2012). Models, validation, and applied geochemistry: Issues in science, communication, and philosophy. Applied Geochemistry, 27(10), 1899-1919.

Knutson, H.-K., Max-Hansen, M., Jönsson, C., Borg, N., and Nilsson, B. (2014). Experimental productivity rate optimization of rare earth element separation through preparative solid phase extraction chromatography. Journal of Chromatography A, 1348(0), 47-51.

Kodama, H., and Schnitzer, M. (1973). Dissolution of chlorite minerals by fulvic acid. Canadian Journal of Soil Science, 53(2), 240-243.

Koriko, M., Tchangbedji, G., Baba, G., Kili, A. K., and Gnandi, K. (2007). Effets de l'acidité et de la nature de l'acide sur la dissolution du phosphate naturel de Hahotoé-Kpogamé (Togo) par quelques acides conventionnels. Comptes Rendus Chimie, 10(6), 529-534.

Lammers, K., Smith, M. M., and Carroll, S. A. (2017). Muscovite dissolution kinetics as a function of pH at elevated temperature. Chemical Geology.

Le Bouffant, L., Daniel, H., Martin, J. C., and BruyÈRe, S. (1982). Effect of impurities and associated minerals on quartz toxicity. The Annals of Occupational Hygiene, 26(5), 625-634.

Leal Filho, W. (2016). Chapter 17 - An Analysis of the Environmental Impacts of the Exploitation of Rare Earth Metals Rare Earths Industry (pp. 269-277). Boston: Elsevier.

Lee, J., Kim, D., Lee, S., and Kim, H. (2012). Effect of rare-earth elements on the plasma etching behavior of the RE–Si–Al–O glasses. Journal of Non-Crystalline Solids, 358(5), 898-902.

Li, D. (2017). A review on yttrium solvent extraction chemistry and separation process. Journal of Rare Earths, 35(2), 107-119.

Li, J., and Duan, Z. (2011). A thermodynamic model for the prediction of phase equilibria and speciation in the H2O–CO2–NaCl–CaCO3–CaSO4 system from 0 to 250°C, 1 to 1000 bar with NaCl concentrations up to halite saturation. Geochimica et Cosmochimica Acta, 75(15), 4351-4376.

Li, L., Li, H., Wang, D., and Zhang, C. (2009). Trace Elements and Rare Earth Elements Geochemistry and Its Metallogenic Significance for Cu-Zn Ore Deposits in Tongbai Area, Henan Province, China. Earth Science Frontiers, 16(6), 325-336.

Li, X., Chen, Z., Chen, Z., and Zhang, Y. (2013). A human health risk assessment of rare earth elements in soil and vegetables from a mining area in Fujian Province, Southeast China. Chemosphere, 93(6), 1240-1246.

Lim, H., Ibana, D., and Eksteen, J. (2016). Leaching of rare earths from fine-grained zirconosilicate ore. Journal of Rare Earths, 34(9), 908-916.

Lingawi, H., Barbour, M., Lynch, R., and Anderson, P. (2011). Effect of Zinc Ions (zn2+) on Hydroxyapatite Dissolution Kinetics Studied Using Scanning Microradiography. Caries Research, 45(2), 195.

Linnen, R. L., Samson, I. M., Williams-Jones, A. E., and Chakhmouradian, A. R. (2014). 13.21 - Geochemistry of the Rare-Earth Element, Nb, Ta, Hf, and Zr Deposits. In H. D.

Holland and K. K. Turekian (Eds.), Treatise on Geochemistry (Second Edition) (pp. 543-568). Oxford: Elsevier.

Liu, H., Zhang, S., Pan, D., Tian, J., Yang, M., Wu, M., and Volinsky, A. A. (2014). Rare earth elements recycling from waste phosphor by dual hydrochloric acid dissolution. Journal of Hazardous Materials, 272, 96-101.

Manuela Vinha G. Silva, M., M.S. Cabral Pinto, M., and Carvalho, P. C. S. (2016). Major, trace and REE geochemistry of recent sediments from lower Catumbela River (Angola). Journal of African Earth Sciences, 115, 203-217.

Mayfield, D. B., and Fairbrother, A. (2014). Examination of rare earth element concentration patterns in freshwater fish tissues. Chemosphere, 120(0), 68-74.

McLellan, B. C., Corder, G. D., Golev, A., and Ali, S. H. (2014). Sustainability of the Rare Earths Industry. Procedia Environmental Sciences, 20(0), 280-287.

Miretzky, P., and Fernandez-Cirelli, A. (2008). Phosphates for Pb immobilization in soils: a review. Environmental Chemistry Letters, 6(3), 121-133.

Moldoveanu, G. A., and Papangelakis, V. G. (2013). Recovery of rare earth elements adsorbed on clay minerals: II. Leaching with ammonium sulfate. Hydrometallurgy, 131–132(0), 158-166.

Moncur, M. C., Ptacek, C. J., Blowes, D. W., and Jambor, J. L. (2005). Release, transport and attenuation of metals from an old tailings impoundment. Applied Geochemistry, 20(3), 639-659.

Morse, J. W., and Arvidson, R. S. (2002). The dissolution kinetics of major sedimentary carbonate minerals. Earth-Science Reviews, 58(1–2), 51-84.

Nadeau, O., Cayer, A., Pelletier, M., Stevenson, R., and Jébrak, M. (2015). The Paleoproterozoic Montviel carbonatite-hosted REE–Nb deposit, Abitibi, Canada: Geology, mineralogy, geochemistry and genesis. Ore Geology Reviews, 67, 314-335.

Nadeau, O., Stevenson, R., and Jébrak, M. (2014). The Archean magmatic-hydrothermal system of Lac Shortt (Au-REE), Abitibi, Canada: Insights from carbonate fingerprinting. Chemical Geology, 387, 144-156.

Nadeau, O., Stevenson, R., and Jébrak, M. (2016). Evolution of Montviel alkaline-carbonatite complex by coupled fractional crystallization, fluid mixing and metasomatism — Part II: Trace element and Sm–Nd isotope geochemistry of metasomatic rocks: implications for REE-Nb mineralization. Ore Geology Reviews, 72, Part 1, 1163-1173.

Nicolas-Alonso, L. F., and Gomez-Gil, J. (2012). Brain computer interfaces, a review. Sensors, 12(2), 1211-1279.

Nieto, A., Guelly, K., and Kleit, A. (2013). Addressing criticality for rare earth elements in petroleum refining: The key supply factors approach. Resources Policy, 38(4), 496-503.

Oelkers, E. H., and Poitrasson, F. (2002). An experimental study of the dissolution stoichiometry and rates of a natural monazite as a function of temperature from 50 to 230 °C and pH from 1.5 to 10. Chemical Geology, 191, 73 – 87.

Oral, R., Pagano, G., Siciliano, A., Gravina, M., Palumbo, A., Castellano, I., Trifuoggi, M. (2017). Heavy rare earth elements affect early life stages in Paracentrotus lividus and Arbacia lixula sea urchins. Environmental Research, 154, 240-246.

Orris, G. J., and Grauch, R. I. (2002). Rare Earth Element Mine,Deposits, and Occurences. USGC (Science for a changing world).

Panda, R., Kumari, A., Jha, M. K., Hait, J., Kumar, V., Rajesh Kumar, J., and Lee, J. Y. (2014). Leaching of rare earth metals (REMs) from Korean monazite concentrate. Journal of Industrial and Engineering Chemistry, 20(4), 2035-2042.

Peelman, S., Sun, Z. H. I., Sietsma, J., and Yang, Y. (2016). Chapter 21 - Leaching of Rare Earth Elements: Review of Past and Present Technologies A2 - Lima, Ismar Borges De. In W. L. Filho (Ed.), Rare Earths Industry (pp. 319-334). Boston: Elsevier.

Peng, C., Crawshaw, J. P., Maitland, G. C., & Trusler, J. M. (2015). Kinetics of calcite dissolution in CO_2-saturated water at temperatures between (323 and 373) K and pressures up to 13.8 MPa. Chemical Geology, 403, 74-85.

Pingitore, N., Clague, J., and Gorski, D. (2014). Round Top Mountain rhyolite (Texas, USA), a massive, unique Y-bearing-fluorite-hosted heavy rare earth element (HREE) deposit. Journal of Rare Earths, 32(1), 90-96.

Plante, B., Benzaazoua, M., and Bussière, B. (2010). Predicting Geochemical Behaviour of Waste Rock with Low Acid Generating Potential Using Laboratory Kinetic Tests. Mine Water and the Environment, 30(1), 2-21. doi:10.1007/s10230-010-0127-z

Prigiobbe, V., and Mazzotti, M. (2013). Precipitation of Mg-carbonates at elevated temperature and partial pressure of CO2. Chemical Engineering Journal, 223, 755-763.

Prudêncio, M. I., Valente, T., Marques, R., Braga, M. A. S., and Pamplona, J. (2017). Rare Earth Elements, Iron and Manganese in Ochre-precipitates and Wetland Soils of a Passive Treatment System for Acid Mine Drainage. Procedia Earth and Planetary Science, 17(Supplement C), 932-935.

Ptáček, P., Bartoníčková, E., Švec, J., Opravil, T., Šoukal, F., Wasserbauer, J., and Másilko, J. (2015). Preparation, kinetics of sinter-crystallization and properties of hexagonal

strontium-yttrate-silicate apatite phase: SrY4[SiO4]3O. Ceramics International, 41(1, Part B), 1779-1795.

Quinn, J. E., Soldenhoff, K. H., and Stevens, G. W. (2017). Solvent extraction of rare earth elements using a bifunctional ionic liquid. Part 2: Separation of rare earth elements. Hydrometallurgy, 169, 621-628.

Robertson, J. A., and Gould, K. L. (1983). Gould. Uranium and thorium deposits of northern Ontario. No. 25. Ontario Ministry of Natural Resources.

Rocha, E., Nasraoui, M., Soubiès, F., Bilal, E., and de Parseval, P. (2001). Évolution géochimique du pyrochlore au cours de l'altération météorique du gisement de Catalão II (Goiás, Brésil). Comptes Rendus de l'Académie des Sciences - Series IIA - Earth and Planetary Science, 332(2), 91-98.

Saldi, G. D., Daval, D., Morvan, G., and Knauss, K. G. (2013). The role of Fe and redox conditions in olivine carbonation rates: an experimental study of the rate limiting reactions at 90 and 150 C in open and closed systems. Geochimica et Cosmochimica Acta, 118, 157-183.

Schlinkert, D., and van den Boogaart, K. G. (2015). The development of the market for rare earth elements: Insights from economic theory. Resources Policy, 46, Part 2, 272-280.

Schreiber, A., Marx, J., Zapp, P., Hake, J.-F., Voßenkaul, D., and Friedrich, B. (2016). Environmental impacts of rare earth mining and separation based on eudialyte: A new European way. Resources, 5(4), 32.

Schulze, R., Weidema, B. P., Schebek, L., & Buchert, M. (2017). Recycling and its effects on joint production systems and the environment–the case of rare earth magnet recycling–Part I—Production model. Resources, Conservation and Recycling.

Sherlock, E., Lawrence, R., and Poulin, R. (1995). On the neutralization of acid rock drainage by carbonate and silicate minerals. Environmental Geology, 25(1), 43-54.

Sholkovitz, E. R. (1995). The aquatic chemistry of rare earth elements in rivers and estuaries. Aquatic Geochemistry, 1(1), 1-34.

Smith, M. M., and Carroll, S. A. (2016). Chlorite dissolution kinetics at pH3–10 and temperature to 275°C. Chemical Geology, 421, 55-64.

Sneller, F. E. C., Kalf, F. D., Weltje, L., and Wezel, A. P. V. (2000). Maximum Permissible Concentrations and Negligible Concentrations for Rare Earth Elements (REEs). Research for man and environnement, RIVM report 601501011.

Tamir, G., Shenker, M., Heller, H., Bloom, P. R., Fine, P., and Bar-Tal, A. (2013). Organic N mineralization and transformations in soils treated with animal waste in relation to carbonate dissolution and precipitation. Geoderma, 209–210(0), 50-56.

Tatarko, P., and Kašiarová, M. (2015). 2 - Silicon nitride based ceramic composites toughened by rare-earth oxide additives A2 - Qin, Qinghua. In J. Ye (Ed.), Toughening Mechanisms in Composite Materials (pp. 35-71): Woodhead Publishing.

Tavares, L. M., Costa, E. M. d., Andrade, J. J. d. O., Hubler, R., and Huet, B. Effect of calcium carbonate on low carbon steel corrosion behavior in Saline co2 high pressure environmentals. Applied Surface Science.

Thomas, P. J., Carpenter, D., Boutin, C., and Allison, J. E. (2014). Rare earth elements (REEs): Effects on germination and growth of selected crop and native plant species. Chemosphere, 96, 57-66.

Tsamis, A., and Coyne, M. (2015). Recovery of rare earths from electronic wastes: An opportunity for High-Tech SMEs. Directorate general for internal policies policy department a: economic and scientific policy.

Tunsu, C., Ekberg, C., and Retegan, T. (2014). Characterization and leaching of real fluorescent lamp waste for the recovery of rare earth metals and mercury. Hydrometallurgy, 144, 91-98.

Turetta, C., Barbaro, E., Capodaglio, G., and Barbante, C. (2017). Dissolved rare earth elements in the central-western sector of the Ross Sea, Southern Ocean: Geochemical tracing of seawater masses. Chemosphere, 183, 444-453.

Tyler, G., and Olsson, T. (2001). Plant uptake of major and minor mineral elements as influenced by soil acidity and liming. Plant and Soil, 230(2), 307-321.

Verplanck, P. L., and Gosen, B. S. V. (2011). Carbonatite and alkaline intrusion-related rare earth element deposits-a deposit model USGS.

Verplanck, P. L., Nordstrom, D. K., Taylor, H. E., and Kimball, B. A. (2004). Rare earth element partitioning between hydrous ferric oxides and acid mine water during iron oxidation. Applied Geochemistry, 19(8), 1339-1354.

Vijayalakshmi, R., Mishra, S. L., Singh, H., and Gupta, C. K. (2001). Processing of xenotime concentrate by sulphuric acid digestion and selective thorium precipitation for separation of rare earths. Hydrometallurgy, 61(2), 75-80.

Walker, S. (2010). Breaking the rare-earth monopoly. Engineering and Mining Journal, 211(10), 46.

Wang, C., Liang, Y., and Xu, W. (2015). On the significance of temperatures derived from major element and REE based two-pyroxene thermometers for mantle xenoliths from the North China Craton. Lithos, 224–225, 101-113.

Wang, L., and Liang, T. (2014a). Accumulation and fractionation of rare earth elements in atmospheric particulates around a mine tailing in Baotou, China. Atmospheric Environment, 88(0), 23-29.

Wang, L., and Liang, T. (2014b). Effects of exogenous rare earth elements on phosphorus adsorption and desorption in different types of soils. Chemosphere, 103(0), 148-155.

Wang, L., Liang, T., Zhang, Q., and Li, K. (2014). Rare earth element components in atmospheric particulates in the Bayan Obo mine region. Environmental Research, 131(0), 64-70.

Weltje, L., Verhoof, L. R., Verweij, W., and Hamers, T. (2004). Lutetium speciation and toxicity in a microbial bioassay: testing the free-ion model for lanthanides. Environ Sci Technol, 38(24), 6597-6604.

White, A. F., and Brantley, S. L. (2003). The effect of time on the weathering of silicate minerals: why do weathering rates differ in the laboratory and field? Chemical Geology, 202(3–4), 479-506.

Wübbeke, J. (2013). Rare earth elements in China: Policies and narratives of reinventing an industry. Resources Policy, 38(3), 384-394.

Xie, F., Zhang, T. A., Dreisinger, D., and Doyle, F. (2014). A critical review on solvent extraction of rare earths from aqueous solutions. Minerals Engineering, 56, 10-28.

Yang, K.-F., Fan, H.-R., Santosh, M., Hu, F.-F., and Wang, K.-Y. (2011). Mesoproterozoic carbonatitic magmatism in the Bayan Obo deposit, Inner Mongolia, North China: Constraints for the mechanism of super accumulation of rare earth elements. Ore Geology Reviews, 40(1), 122-131.

Yang, X. J., Lin, A., Li, X.-L., Wu, Y., Zhou, W., and Chen, Z. (2013). China's ion-adsorption rare earth resources, mining consequences and preservation. Environmental Development, 8, 131-136.

Yong, R., and Zheng, L. (1993). Adsorption and desorption of rare earth elements on soils and synthetic oxides. Acta Scientiae Circumstantiae, 13, 288.

Yörükoğlu, A., Obut, A., and Girgin, İ. (2003). Effect of thiourea on sulphuric acid leaching of bastnaesite. Hydrometallurgy, 68(1–3), 195-202.

Yoshida, S., Muramatsu, Y., Tagami, K., and Uchida, S. (1998). Concentrations of lanthanide elements, Th, and U in 77 Japanese surface soils. Environment International, 24(3), 275-286.

Zaitsev, A. N., Terry Williams, C., Jeffries, T. E., Strekopytov, S., Moutte, J., Ivashchenkova, O. V.,Borozdin, A. P. (2014). Rare earth elements in phoscorites and carbonatites of the Devonian Kola Alkaline Province, Russia: Examples from Kovdor, Khibina, Vuoriyarvi and Turiy Mys complexes. Ore Geology Reviews, 61, 204-225.

Zaitsev, A. N., Wall, F., and Bas, M. J. L. (1998). REE-Sr-Ba minerals from the Khibina carbonatites, Kola Peninsula, Russia: their mineralogy, paragenesis and evolution. Mineralogical Magazine, 62(2), 225-250.

Zendah, H., Khattech, I., and Jemal, M. (2013). Thermochemical and kinetic studies of the acid attack of "B" type carbonate fluorapatites at different temperatures (25–55)°C. Thermochimica Acta, 565(0), 46-51.

Zhang, K., Zhu, X.-K., and Yan, B. (2015). A refined dissolution method for rare earth element studies of bulk carbonate rocks. Chemical Geology, 412, 82-91.

Zhang, S., Ding, Y., Liu, B., and Chang, C.-c. (2017). Supply and demand of some critical metals and present status of their recycling in WEEE. Waste Management, 65, 113-127.

Zhao, Y., Yu, R., Hu, G., Lin, X., and Liu, X. (2017). Characteristics and environmental significance of rare earth elements in PM2.5 of Nanchang, China. Journal of Rare Earths, 35(1), 98-106.

Zheng, Q., Wu, W., and Bian, X. (2017). Investigations on mineralogical characteristics of rare earth minerals in Bayan Obo tailings during the roasting process. Journal of Rare Earths, 35(3), 300-308.

CHAPITRE 3 ARTICLE 2 : MOBILITY OF RARE EARTH ELEMENTS IN MINE DRAINAGE: INFLUENCE OF IRON OXIDES, CARBONATES, AND PHOSPHATES

Cet article est accepté dans la revue Chemosphere, 2018

Edahbi, M.[a]; Plante, B.[a]; Benzaazoua, M.[a]; Ward, M.[b]; Pelletier, M.[c]

[a] Université du Québec en Abitibi-Témiscamingue (UQAT), 445 boul de l'Université, Rouyn-Noranda J9X 5E4, QC, Canada.

[b]University of Western Ontario, Surface Science Western, 999 Collip Circle, P.O. Box 12, London, Ontario N6G 0J3 Canada.

[b]Advanced Photon Source - Argonne National Laboratory; Chicago, USA.

[c]Ressources Géoméga, St-Lambert, Canada.

3.1 Abstract

The geochemical behavior of rare earth elements (REE) was investigated using weathering cells. The influence of sorption and precipitation on dissolved REE mobility and fractionation is evaluated using synthetic iron-oxides, carbonates, and phosphates. Sorption cell tests are conducted on the main lithologies of the expected waste rocks from the Montviel deposit. The sorbed materials are characterized using a scanning electron microscope (SEM) equipped with a microanalysis system (energy dispersive spectroscopy EDS) (SEM-EDS), X-ray diffraction (XRD), and X-ray absorption near edge structure (XANES) in order to understand the effect of the synthetic minerals on REE mobility. The results confirm that sorption and precipitation control the mobility and fractionation of REE. The main sorbent phases are the carbonates, phosphates (present as accessory minerals in the Montviel waste rocks), and iron oxides (main secondary minerals generated upon weathering of the Montviel lithologies). The XANES results show that REE are present as trivalent species after weathering. Thermodynamic equilibrium calculations results using Visual Minteq suggest that REE could precipitate as secondary phosphates ($REEPO_4$).

Keywords: weathering cell tests, contaminated mine drainage, waste rocks, REEs, sorption cells, thermodynamic equilibrium calculations, XANES

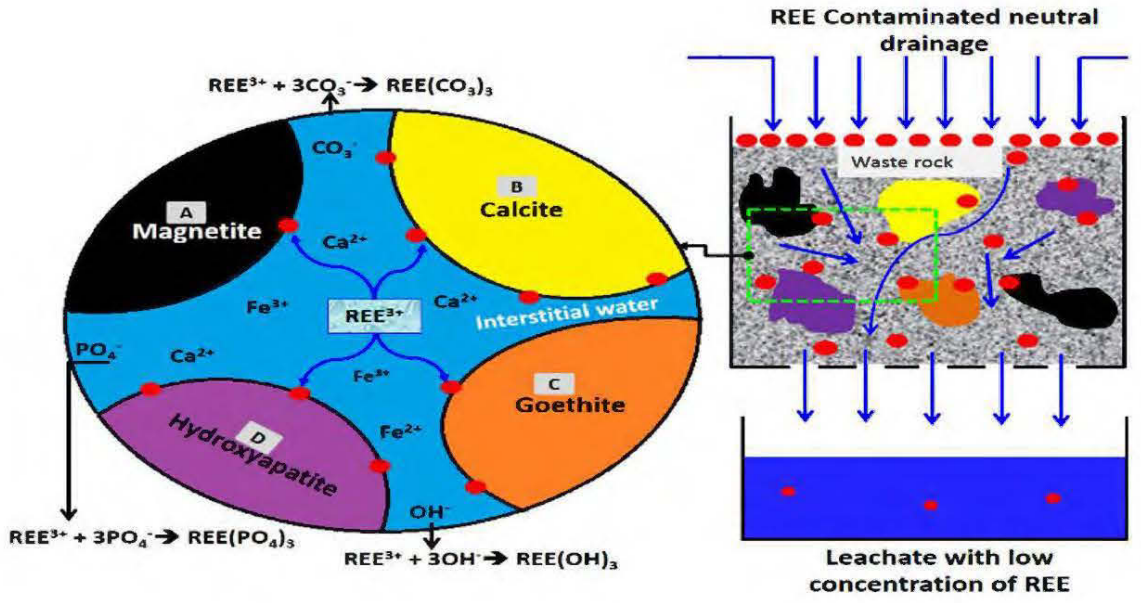

Graphical abstract

3.2 Introduction

Mine waste rocks and tailings may generate acid mine drainage and/or contaminated neutral drainage (e.g., Benzaazoua et al., 2004; Plante et al., 2014) containing contaminants such as REE and transition metals (e.g., Fe, Pb, Cu, and Zn). The oxidation of sulfides within mining materials can accelerate the dissolution of REE-bearing minerals (e.g. carbonates, silicates, and phosphates) and favor the leaching of REE and other associated contaminants such as uranium, thorium, and niobium (Ayora et al., 2016; Balboni et al., 2017; Carron et al., 1955; Liu et al., 2016; Rim et al., 2013; Roth et al. 2017, Zhu et al., 2015). Sorption phenomena, precipitation, and coprecipitation can play a significant role in reducing the transport of REE and other metals into the environment (Blowes et al., 2003, Plante, Benzaazoua and Bussière, 2010b, Bouzahzah et al., 2013, Prudêncio et al., 2017), depending on the redox potential, the pH, and the elemental concentrations (Burrows et al., 2017, Cravotta and Watzlaf, 2003). The secondary minerals formed during leaching can re-dissolve and release their constituents in the leachate, especially when the pH becomes more acidic (Ayora et al., 2016).

Presently, several REE mining projects are in development in Canada, particularly in Québec (e.g., Montviel, Matamec, Strange Lake). For the Montviel carbonatite deposit, Nadeau et al. (2016) showed that the main lithological units of the complex were calciocarbonatites, ferrocarbonatites, silicocarbonatites, and polygenic breccia, with REE concentrations ranging

from 100 ppm to 3.54 wt.% mainly associated to carbonates and fluorocarbonates. The REE in the Montviel deposit were concentrated by coupled fractional crystallization, fluid mixing, and metasomatism (Nadeau et al., 2016).

Unfortunately, knowledge on REE release from mine wastes is very sparse, despite the development of several REE mine projects around the world. The geochemical behavior of REE depends mainly on the type and the amount of minerals (i.e., carbonates, phosphates, oxyhydroxides, clays minerals, etc.) in contact with mine drainage. The sorption capacity for each mineral is a function of its zeta potential, its cation exchange capacity, the pH of the solution, and its specific surface area (Middlesworth and Wood, 1998, Liu et al., 2017). The geological materials found in mine wastes (i.e., iron oxides, carbonates, etc.) can contribute to contaminant removal from drainage waters (Benzaazoua et al., 2004, Bouzahzah et al., 2013, Blowes et al., 2003). To the best of our knowledge, no previous study has explored the influence of iron oxides, calcite, and apatite on controlling the leaching of REE using kinetic tests. Thus, the purpose of this work is: (1) to study the potential effect of iron oxides, calcite, and hydroxyapatite on the fractionation and mobility of REE, and (2) to evaluate the sorption potential of REE onto waste rocks from a potential REE carbonatite deposit (Montviel carbonatite, Québec, Canada). The achievement of these objectives can address knowledge gaps associated to REE mining to better manage the REE residue and to contribute to minimizing their potential environmental impacts.

3.3 Materials and methods

In this study, the geochemical behavior of REE were assessed using two different tests: (1) evaluation of the effect of synthetic minerals (e.g. iron oxides, calcite, and hydroxyapatite) on REE mobility upon leaching in weathering cells, and (2) evaluation of sorption capacity using sorption cells for five waste rock samples coming from the Montviel carbonatite deposit.

3.3.1 Chemical, and mineralogical characterizations

The chemical composition of the Montviel samples was determined using Inductively Coupled Plasma (ICP-AES/MS) (Perkin Elmer Optima 3100-RL ICP-AES and Agilent 7700 ICP-MS) analysis after a multi-acid digestion (HCl, HNO_3, Br_2, and HF). The leachates issued from weathering cells were analyzed with ICP-AES/ MS. The ICP-AES is used to analyze trace and major elements, while ICP-MS is used to analyze REE. Also, the pH, Eh, and electrical

conductivity of leachates were determined immediately after sampling with a pH/mV meter and an electrical conductivity meter.

The mineralogical composition of the samples was determined by the Bruker A.X.S. D8 Advance X-Ray diffraction (XRD) instrument with a copper anode (Cu-Kα radiation). The DiffracPlus EVA software was used to identify the detected minerals and the TOPAS software was used to quantify their abundance using Rietveld refinement, allowing a detection limit and precision of up to 0.5-1 wt.% (Young, 1993).

A Hitachi S-3500N scanning electron microscope (SEM), equipped with a microanalysis system (energy dispersive spectroscopy, or EDS) was used to: (1) detect and analyze minerals in low concentrations (less than the detection limit of the XRD), (2) confirm the presence of the minerals detected by XRD, and (3) analyze the elemental composition of the REE-bearing minerals present in samples.

3.3.2 Preparation of synthetic minerals

The methodology used for mineral synthesis is summarized in Figure 3-1. All minerals were synthesized using the chemical route (precipitation/coprecipitation) (Babou-Kammoe et al., 2012, Jaiswal et al., 2013, Britel, 2007). Hematite (Fe_2O_3), magnetite (Fe_3O_4), and calcite ($CaCO_3$) were prepared in a single step, while hydroxyapatite required two steps (synthesized and calcined at 900°C for two hours; (Britel, 2007). The purity of the synthetic minerals was confirmed by XRD.

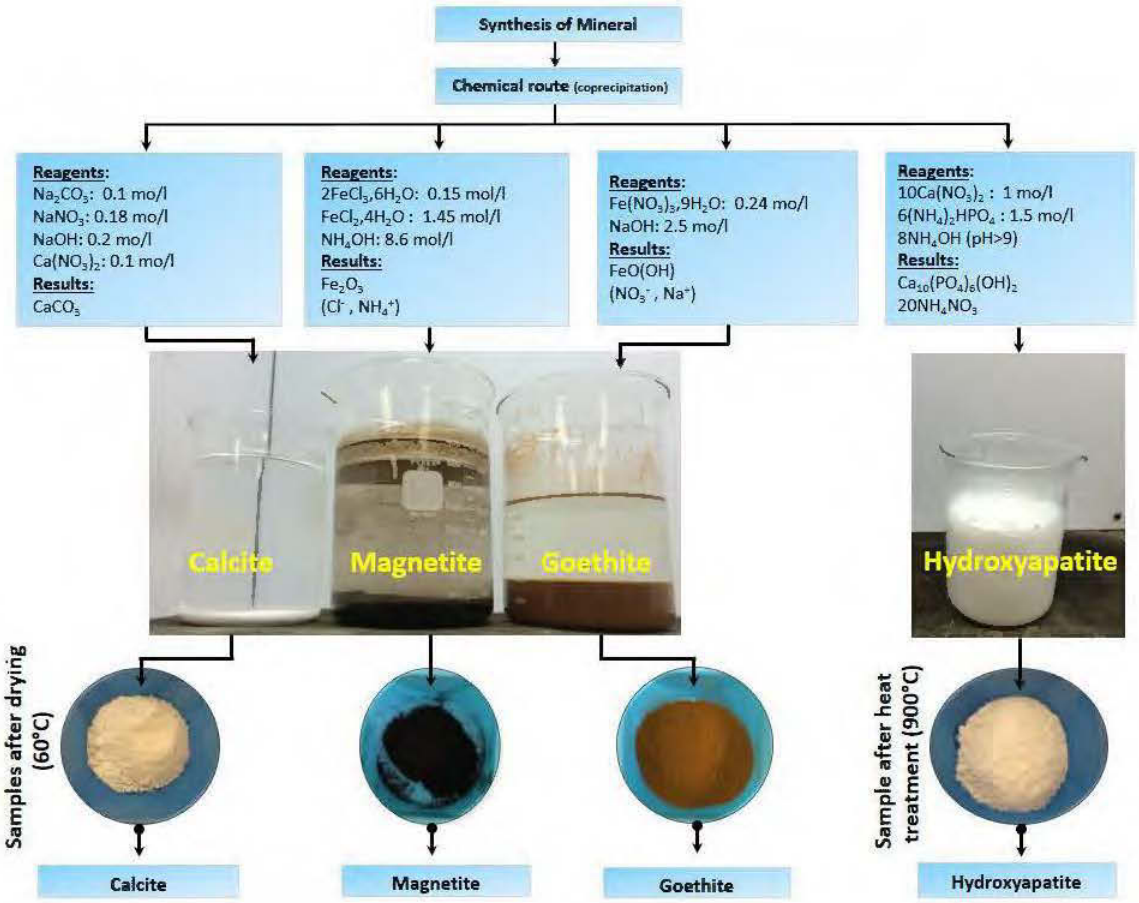

Figure 3-1 : Mineral synthesis methods.

3.3.3 Design of mineral mixtures

The carbonatites of Montviel are composed mainly of carbonates (e.g., calcite), iron oxyhydroxides (e.g., goethite and magnetite), phosphates (apatite), traces of sulfides (mainly pyrite), and REE-bearing minerals such as REE-carbonates (Nadeau et al., 2015). During REE leaching in kinetic tests, the mineral phases can retain leached REE^{3+} through surface reaction mechanisms. To gain an understanding of the effects of each mineral on REE mobility, different mineralogical possibilities were simulated using pure mineral mixtures. A total of five mixtures composed of goethite, magnetite, calcite, hydroxyapatite, and pyrite, were used in this study. These mixtures were subjected to weathering cell tests to study the extent of REE carbonate weathering in response to pyrite oxidation, and the effect of calcite, magnetite, goethite, and hydroxyapatite on the mobility of Ce and La coming from $Ce_2(CO_3)_3$ and/or $La_2(CO_3)_3$ dissolution. In order to accelerate the weathering of the Ce- and La-carbonates, 5 % of pyrite is added to each of the mixtures (Figure 3-2).

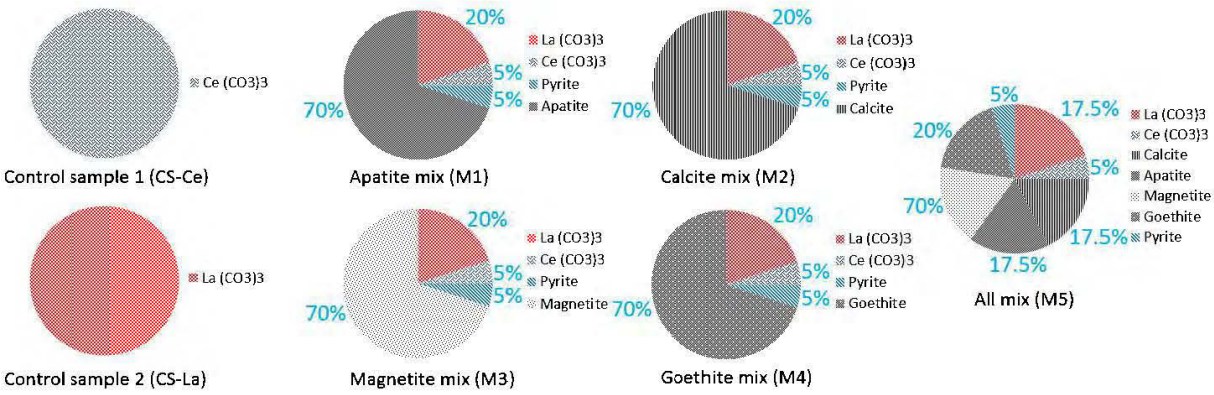

Figure 3-2 : Composition of the weathering cell mixtures.

3.3.4 Montviel lithologies study

3.3.4.1 Sampling of lithologies

The waste rocks were sampled from drill cores of the Montviel deposit located 97 km north of Lebel-sur-Quévillon, Quebec province, Canada. Approximately 5 kg of three waste rock lithologies Brec, CaC, and SiC (described as breccia, calciocarbonatite, and silico-carbonatite) and two ore grades FeC-LG and FeC-HG (ferrocarbonatites low-grade LG, and high-grade HG) were pulverized to less than 300 µm, homogenized, and prepared separately for physical, chemical, and mineralogical characterizations and sorption cell tests.

3.3.5 Testing methods

3.3.5.1 Weathering cells and sorption cells

The geochemical behavior of the five synthetic mixtures was evaluated using weathering cells (small-scale of humidity cells), while the sorption potential of waste rock lithologies was evaluated using sorption cells (modified weathering cells) (Plante et al., 2010a). The seven weathering cells (described in Figure 3-2) and the five sorption cells (Montviel lithologies; Figure 3-3) consisted of 10 cm-wide Buchner funnels filled with 67 g of each sample placed over a 0.45 µm filter. The cells were rinsed bi-weekly for 175 days with 50 ml of deionized water for the weathering cells and 50 ml of 1 mg/l Ce adjusted to pH 8 to simulate the field conditions (in deionized water) for the sorption cells, and left to dry under ambient air between flushes. The choice of Ce is mainly related to its high abundance within the Montviel lithologies (up to approximately 14000 mg/kg) and the fact that it is the REE leached in the highest concentrations in humidity cells (Edahbi et al., 2018). The sorbed quantities were calculated by the comparison between the Ce concentrations in the leachates with those of the leaching water.

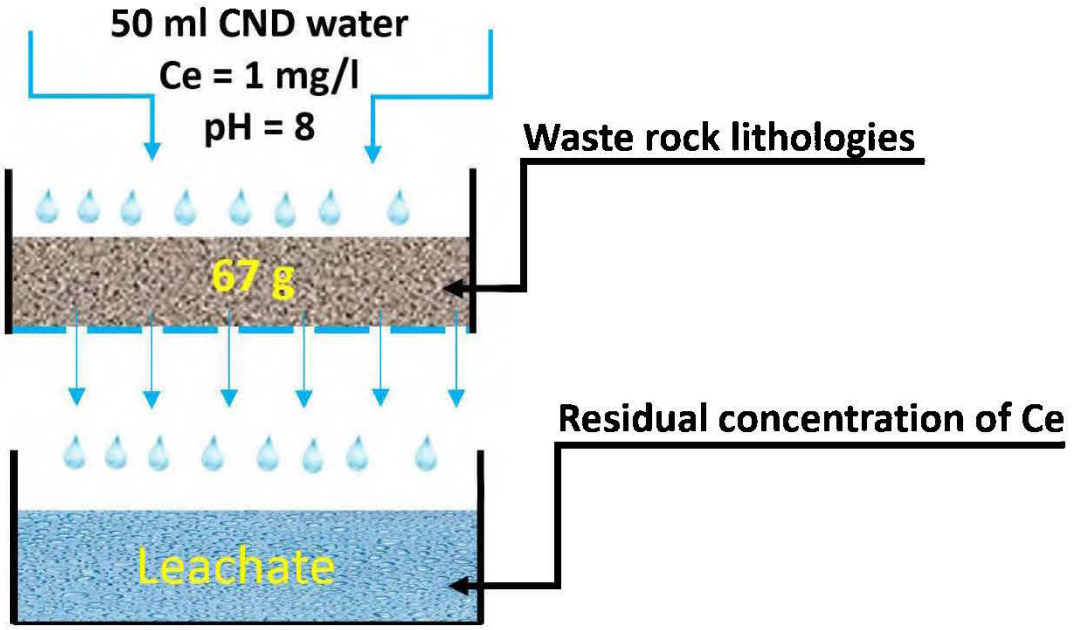

Figure 3-3 : Schematics of the sorption cells used in this present study.

3.3.5.2 Cation exchange capacity (CEC) and zeta potential measurements

The CEC enables to estimate the capacity of materials to retain cations during leaching conditions. The CEC was determined according to the method suggest by Pelloux et al., (1971) using the following formula:

$$CEC = \frac{a}{10} \times \frac{1}{23} \times \frac{100}{b} \; [meq/100\ g\ of\ dry\ sample]$$

a = concentration of sodium (mg/l);

b = mass of the dry residue (g).

The zeta potential was determined based on the electrophoretic mobility of particles in a suspension measured using a ZetaCompact Zeta Meter, where the displacement speed of the particles in suspension recorded in real time with a high resolution digital camera (Dibbs, 1972; Gence and Ozbay, 2006). For all measurements but for calcite, the pH was varied from 1 to 8 at a fixed ionic strength ($NaNO_3$ 0.1 M). This enables to determine the point of zero charge (pH_{pzc}) which describes the condition when the electrical charge density on a surface is zero, which in turn enables to deduce how the surface charge of minerals affects Ce sorption.

3.3.6 Crystal-chemical analyses

3.3.6.1 XANES analysis

X-ray absorption near edge structure (XANES) spectroscopy provides elementally specific information about the local chemical environment around an absorbing atom (e.g. Ce in $Ce_2(CO_3)_3$), such as the oxidation state of the absorber and coordination symmetry (eg. tetrahedral vs. octahedral). The XANES spectrum represents the x-ray absorption of the sample as a function of energy (Ward, 2013). XANES is highly sensitive to the oxidation state and/or local symmetry of the absorbing atom. XANES measurements were performed at beamline 20BM of the Advanced Photon Source (APS), Argonne National Laboratory, USA. XANES measurements were performed at the cerium L3-edge (5723 eV) in fluorescence yield (FY) detection mode using a 12-element Canberra solid-state Ge detector. A mixture of 70/30 sccm (standard cubic centimeters per minute) of He/N_2 gases were used in I_0 (incident beam intensity), and 100 % N_2 in I_t (transmitted beam intensity) and I_{ref} (post-reference beam intensity) ion chambers. These gasses were selected to improve the signal/noise ratio. The XANES spectra were collected on aliquots of the dismantled weathering cells samples of the pure mineral mixtures. Pure mineral grains were manually picked in order to avoid having Ce- and La-carbonates in the analyzed samples: apatite grains from M1, calcite grains from M2, magnetite grains from M3, goethite grains from M4, and a mixture of apatite, calcite, magnetite and goethite grains from M5.

3.4 Results and discussion

3.4.1 Synthetic mineral characterization

Zeta potential

The zeta potential values of synthetic minerals enabled to determine their pH_{pzc}. Sorption of cationic (i.e., REE^{3+}, metals) species over a given mineral surface will take place mainly at pH values higher than its pHpzc. The pH_{pzc} of goethite is 6.1, while that of magnetite and hydroxyapatite are 3.18 and 4.9, respectively. For calcite, only the zeta potential at its natural pH is measured because of its dissolution under acidic pH; the calcite pH_{pzc} ranges between 8 and 9.5 (Al Mahrouqi et al., 2017; Quast, 2016; Somasundaran, 1968; Erdemoğlu and Sarıkaya, 2006). At its natural pH (6.2), its zeta potential is negative and, consequently, the sorption of

cations is probable in the weathering cell conditions, as is the case for goethite, magnetite, and hydroxyapatite.

3.4.2 Waste rock characterization

3.4.2.1 Mineralogical characterization

The mineralogical characterization of the waste rock samples determined by XRD shows that all samples except CaC, are composed of the same chemical phases in different proportions (Table 3-1). Carbonates make up 48-94 % of the composition, and the remaining phases are mainly phosphates (2-22.6 %), REE-bearing minerals (5-9 %), and silicate minerals (5-30 %). These carbonate-dominated materials may enable a significant sorption potential for REE. The optical microscopy observations enabled the identification of sulfide minerals such as pyrite (FeS_2) (most abundant), sphalerite (ZnS), galena (PbS), pyrrhotite ($Fe_{(1-X)}S$), chalcopyrite ($CuFeS_2$), and pentlandite $(Fe,Ni)_9S_8$ at trace levels (<1 %).

The scanning electron microscope (SEM) investigations demonstrate that the samples are mainly composed of two types of REE-bearing minerals: (i) REE carbonates and phosphates (i.e., burbankite, carbocernaite, apatite, and REE-Ca-Mg carbonates), (ii) REE-Ba-Sr carbonate. (iii) REE are present as liberated minerals and/or as inclusions within carbonate and phosphate minerals, (iv) all analyzed minerals mainly contain LREE (La, Ce, Pr, Nd, and Sm) compared to HREE (Dy, Tb, Ho, Lu), (v) three groups of REE minerals were detected with variable concentrations of REE, (vi) some sulfides (pyrite, pyrrhotite, galena, and sphalerite) and iron oxides were also identified.

3.4.2.2 Chemical characterisation

The chemical results show that all samples are richer in LREE (412-6,117 mg/kg) compared to HREE (106-5595 mg/kg), which is consistent with previous findings (Nadeau et al., 2015). The lithologies FeC-HG and FeC-LG have the highest concentrations of LREE, while SiC exhibits the lowest concentration. Cerium is the most abundant REE element in all samples, with a maximum concentration observed in FeC-HG (14000 mg/kg) and a minimum concentration in SiC (2200 mg/kg). Ba (2240-10000 mg/kg), Sr (6790-10000 mg/kg), F (150-673 mg/kg), and Ca (95000-150000 mg/kg) show a good correlation with REE in samples. Barytocalcite, a Ba-REE-Sr mixture, apatite, carbonates (calcite, ankerite, REE carbonates), and strontianite minerals are the main sources of these elements in the Montviel lithologies as demonstrated by the mineralogical characterization (Table 3-1).

3.4.2.3 Cation Exchange Capacity (CEC)

The CEC for all waste rock samples ranged from 6 to 12.36 meq/100g. The FeC-HG sample exhibits the highest value (12.36 meq/100g), SiC and BreC samples have similar values of CEC (10.83-10.95 meq/100g), while CaC and FeC-LG exhibit the lowest values of CEC (6-9.83 meq/100g) (Table 3-1). These results are consistent with the mineralogical compositions, as the highest values are associated to samples with the highest carbonate content. Samples with greater CEC, such as FeC-HG, SiC, and BreC, can retain more positively charged ions (i.e., Na^{+}, Mg^{2+}, Ca^{2+}, and REE^{3+}).

Tableau 3-1 . Chemical and mineralogical characterization of the waste rocks

Parameters	Units	BreC	CaC	FeC-LG	FeC-HG	SiC
pH		10.2	10	9.6	10	10.4
CEC	meq/100 g	10.82±0.07	9.87±0.05	6.06±0.04	12.36±0.09	10.95±0.02
Elemental concentration						
REE	%	0.64	0.12	0.84	3	0.47
Mn	%	0.55	1.3	2.1	1.7	1.3
Ca	%	19	19	11	9.2	11
Na	%	0.32	0.45	0.12	0.9	0.46
Mg	%	2.6	2.3	4.2	3.3	3.8
K	%	1.5	0.9	0.75	0.96	1.6
Fe	%	6.8	12	20	16	12
Pb	%	0.03	0.012	0.008	0.008	0.008
F	%	0.07	0.015	0.03	0.032	0.033
Ba	%	0.51	1.8	1.4	1.9	2.6
Sr	%	1.3	1.4	0.95	2.8	0.6
Mineralogical composition						
Sulfides	%	1.7	0.8	0.4	1.6	0.7
Carbonates	%	48.1	82.1	92.5	74.8	67.5
Phosphates	%	22.6	2.7	-	2.0	2.0
REE bearing minerals	%	-	-	-	13.8	-
Silicates	%	27.5	14.5	5.1	7.9	29.9

3.5 Geochemical behavior

3.5.1 Synthetic mineral mixes

The pH, acidity, electrical conductivity, and alkalinity values of the weathering cell leachates on the synthetic minerals mixes are shown in Figure 3-4. The magnetite mix (M4) leachates shows the most acidic pH (average of 5.32) and the lowest electrical conductivity (average of 325.83 µS.cm^{-1}). The calcite mix (M2) exhibits the highest pH (average of 8.34) compared to the others, which is due to its calcite background. The goethite mix (M4) leachates show a mean pH of 6.07, whereas the apatite mix (M1) and all minerals mix (M5) leachates have mean pH values of 5.81 and 7.81, respectively. The redox potentials varied from 194 to 500 mV and they are of the same order of magnitude for all mixtures. The alkalinity values stabilized below 120 mg $CaCO_3$/l for all leachates; the calcite mix (M2) and the all minerals mix (M5) exhibited the highest values (average of 84 mg $CaCO_3$/l) due to the dissolution of calcite. The electrical conductivity values of all samples stabilized below 460 µS/cm after 175 days of testing.

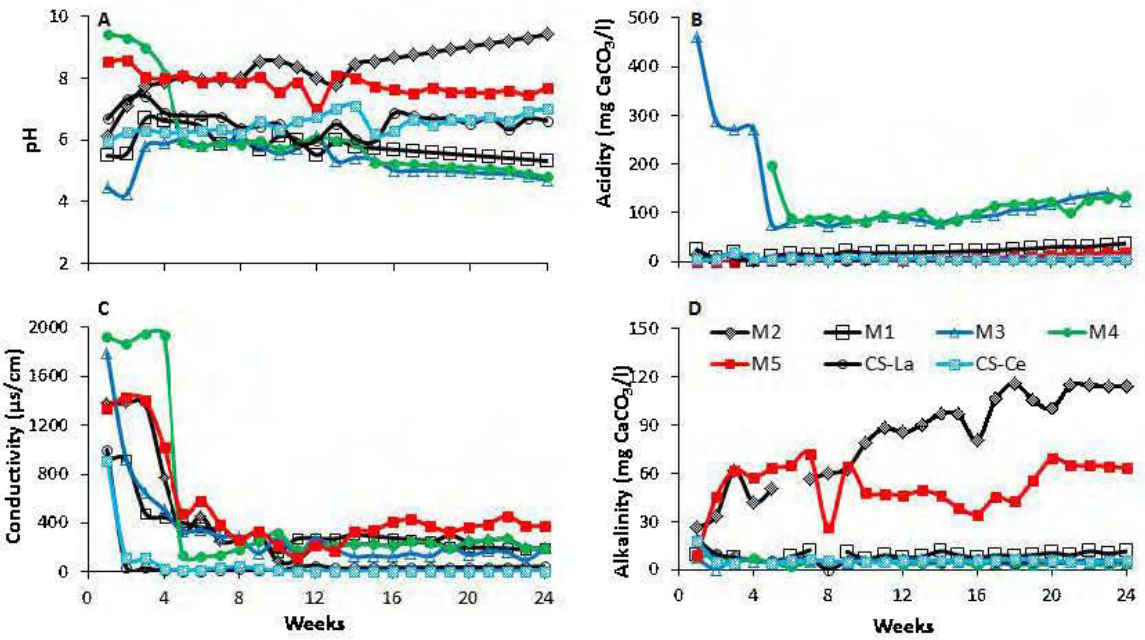

Figure 3-4 : pH (A), acidity (B), electrical conductivity values (µS cm^{-1}) (C), and alkalinity (D) of the weathering cell leachates of the apatite mix (M1), calcite mix (M2), magnetite mix (M3), goethite mix (M4), all minerals mix (M5), control sample Ce (CS-Ce), and control sample La (CS-La) samples.

The Ca concentration in leachates of the calcite (M2; 176 mg/l) and all minerals mix (M5; 149 mg/l) is higher compared to those from the apatite mix (M1; 129 mg/l) due to their higher calcite contents (Figure 3-5A). The sulfur concentrations in the leachates tend to be higher for lower pH values, as sulfide oxidation accelerates at lower pH values (Figure 3-5B). All leachates have low iron concentration (under 0.2 mg/l, therefore is not shown), probably due to its precipitation under leaching conditions as suggested by thermodynamical equilibrium calculations.

The cumulative Ca vs S curves (or oxidation-neutralization curves) of the apatite (M1), calcite mix, and all mix show a linear relationship (determination coefficient R^2 of 0.99), reflecting the reaction of calcite (neutralization) in response to pyrite oxidation during the tests (Figure 3-5C). Moreover, Figures 3-5D, E, and F show that the REE release is related to that of SO_4. The REE release seems to be closely related to the pH; the lower pH values within the M3 and M4 leachates enable greater REE releases, while the higher pH values of the M2 and M5 generate the lower REE releases. Moreover, the REE release in some materials significantly increases when the pH values decrease below a threshold, most probably because of a significant reduction of sorption phenomena. These results suggest that REE are released from the Ce- and La-carbonates in response to sulfide oxidation, and that the release is controlled by sorption phenomena when the conditions are favourable.

The Ce+La concentrations (Figure 3-6) are low for the all minerals mix (M5; <0.01 mg/l) and the calcite mix (M2; <0.36 mg/l), although they contain similar proportions of cerium and lanthanum carbonates as the other mixtures (the only exception being M5 with 17.5 % Ce-carbonate instead of 20 %). These results are due to the presence of calcite that competes with the Ce- and La-carbonates to neutralize the acid generated by pyrite oxidation. The apatite (M1) mix leachates exhibit an average Ce+La concentration of 12 mg/l, which is lower than for the magnetite (M3) and goethite (M4) mixes.

The Ce+La concentrations from the weathering cells of the mineral mixes and the pure Ce- and La-carbonates are shown in Figure 3-6. During 175 days of testing, the La concentrations from the CS-La cell remained below 2 mg/l with a slight increasing trend, while the Ce concentrations from the CS-Ce cell decreased rapidly from 80 mg/l at the beginning to less than 10 mg/l after 5 weeks (Figure 3-6). For the mineral mixes, the Ce+La concentrations are lower in leachates of the apatite (M1) and calcite (M2) mixtures than in those of magnetite (M3) and goethite (M4) mixes. Thermodynamical equilibrium calculations (not shown) suggest that Ce and La in all leachates are far from equilibrium and should not precipitate. These results suggest

that the presence of calcite and apatite seem to exert a greater control on the release of Ce+La than magnetite and goethite.

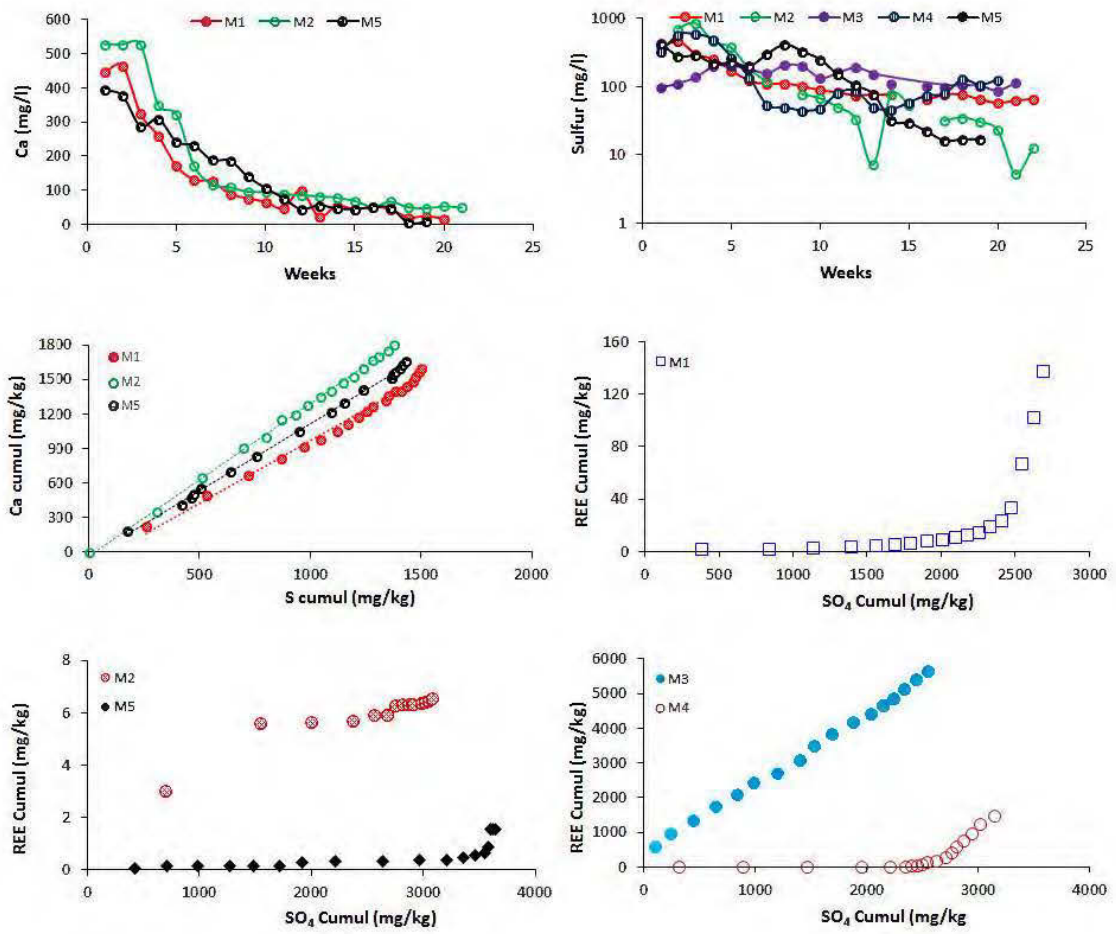

Figure 3-5 : Partial weathering cell results: Ca concentrations (A), sulfur concentrations (B), oxidation neutralization curves (C); cumulative REE vs SO4 of apatite mix M1 (D), calcite mix M2 and all minerals mix M5 (E); magnetite mix M3 and goethite mix M4 (F).

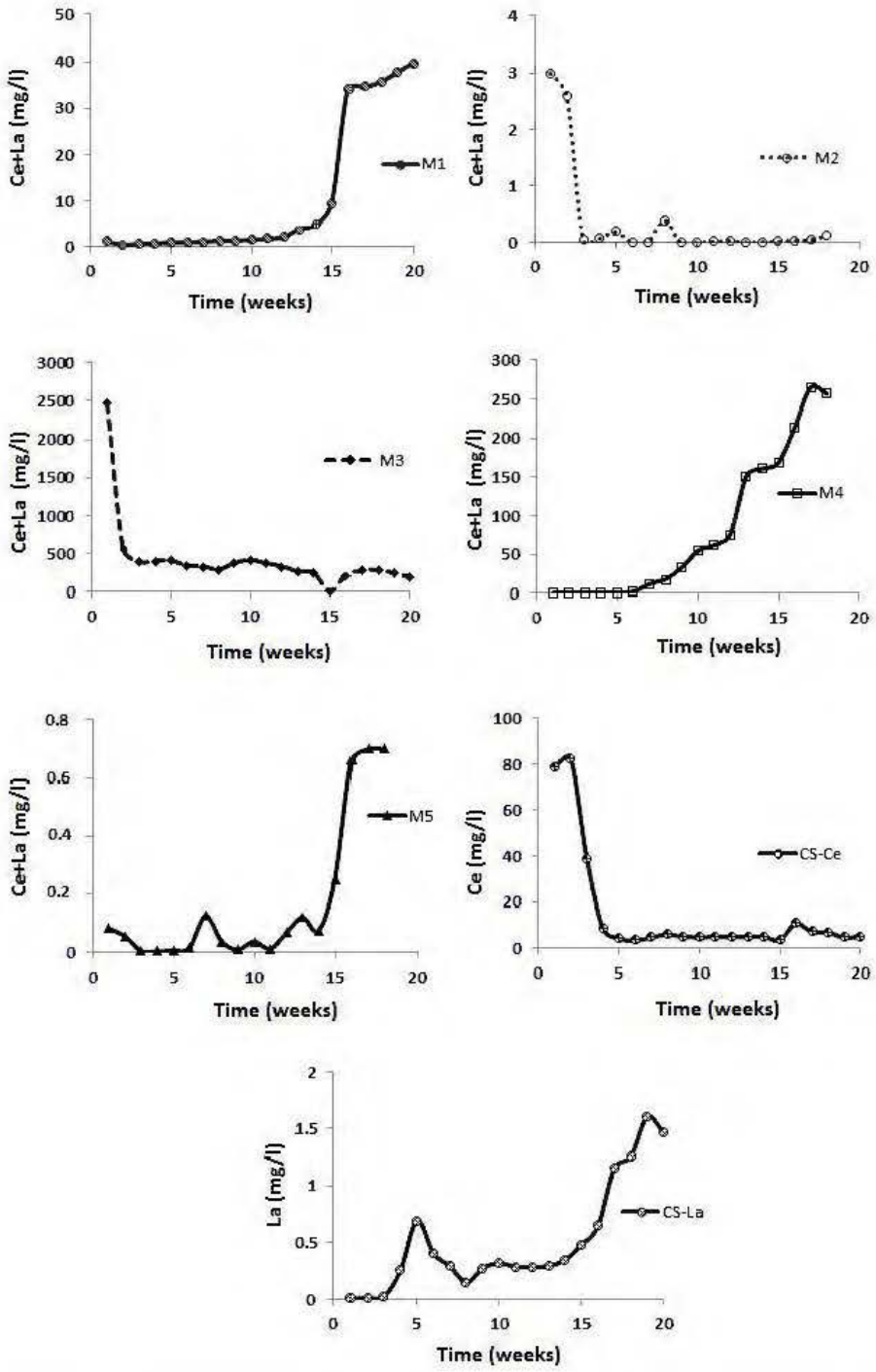

Figure 3-6 : Concentration of Ce+La from mixtures M1 (apatite mix), M2 (calcite mix), M3 (goethite mix), M4 (magnetite mix), and M5 (all minerals mix) and control samples CS-Ce and CS-La.

3.5.2 Sorption cells

3.2.1. Sorption cells

The Ce sorption in Montviel waste rocks was evaluated using modified weathering cells (sorption cells) rinsed with 1 mg/l Ce solutions adjusted to pH 8. The pH values of the leachates issued from sorption cells remain near-neutral throughout the tests, with the FeC-LG sample pH values (average of 7.80) being slightly lower than the others (8-8.2). The electrical conductivity values show the same trend in all samples and vary between 350 and 470 µS/cm after 175 days of testing. The Ca, Mg, Mn, and Si concentrations are higher in the leachates issued from the FeC-LG waste rocks (Ca: around 17 mg/l; Mg: up to 11 mg/l; Mn: up to 0.1 mg/l; and Si: around 72 mg/l) than those of the other samples (Ca: 10- 12 mg/l; Mg: 4-7 mg/l; Mn: 0.3-0.4 mg/l; and Si: 42-61 mg/l). The Al, Ba, and S concentrations generated by the FeC-HG waste rocks are greater (Al: 0.2 mg/l; Ba: 0.5-1.8 mg/l; and S: 10-25 mg/l) than those of other samples (Al: 0.2 mg/l; Ba: 0.5-1.8 mg/l; and S: 10-25 mg/l). The higher Sr concentrations are found in leachates of CaC waste rock samples (around 7 mg/l).

All sorption cells leached between 0.11 and 164.92 µg/l Ce (not shown). Note that the Ce concentrations leached from these samples in humidity cell tests were less than 2 µg/l (Edahbi et al., 2018), which suggests a high sorption of Ce within samples under humidity cell conditions. The quantity of Ce retained (q, in mg/kg) is calculated using the following equation:

$$q = \frac{(C_i - C_f)V}{m}$$

C_i: Initial metal concentration of Ce (mg/l)

C_f: Final metal concentration of Ce (mg/l)

V: Volume of solution (l)

m: Mass of sample (kg)

The profiles of the cumulative q values are shown in Figure 7. All materials show similar profiles due to the similar residual Ce concentrations measured in the leachates. The fact that the cumulative Ce retention profiles do not show a plateau (and that the leached Ce remained low throughout the sorption cell tests) suggests that the sorption potential was not fully saturated during the tests.

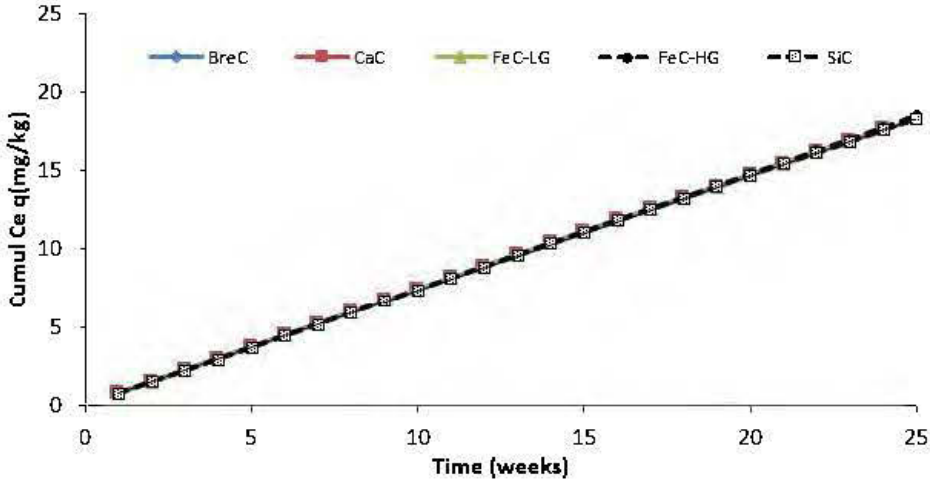

Figure 3-7 : Sorbed metal quantities (q) in sorption cells.

3.5.2.1 Post-testing analyses

Thermodynamic equilibrium calculations of the leachate compositions of weathering cells using Visual Minteq suggest that various secondary oxyhydroxides (i.e., ferrihydrite, lepidocrocite, goethite, and hematite) are oversaturated. On the other hand, these calculations suggest that Ce and La secondary minerals remain far from equilibrium. Therefore, the Ce and La concentrations in the leachates are not controlled by secondary precipitations, but most probably by sorption phenomena.

Hand sorted grains were chosen for XANES analyses on the post-dismantlement samples of the weathering cells on pure mineral mixes in order to avoid Ca- and La-carbonates: apatite grains from M1, calcite grains from M2, magnetite grains from M3, goethite grains from M4, and a mixture of apatite, calcite, magnetite, and goethite grains from M5. The Ce L3-edge XANES spectra of these hand sorted grains are shown in Figure 8. Presence of Ce^{3+} in all the samples was determined by comparing the spectra in the XANES region with a reference Ce-carbonate, because of its similarity to the Ce carbonates found in the samples. The XANES spectra from all samples exhibit a strong white line peak at 5723 eV, which confirms the Ce^{3+} retention (Figure 3-8) most probably by sorption phenomena.

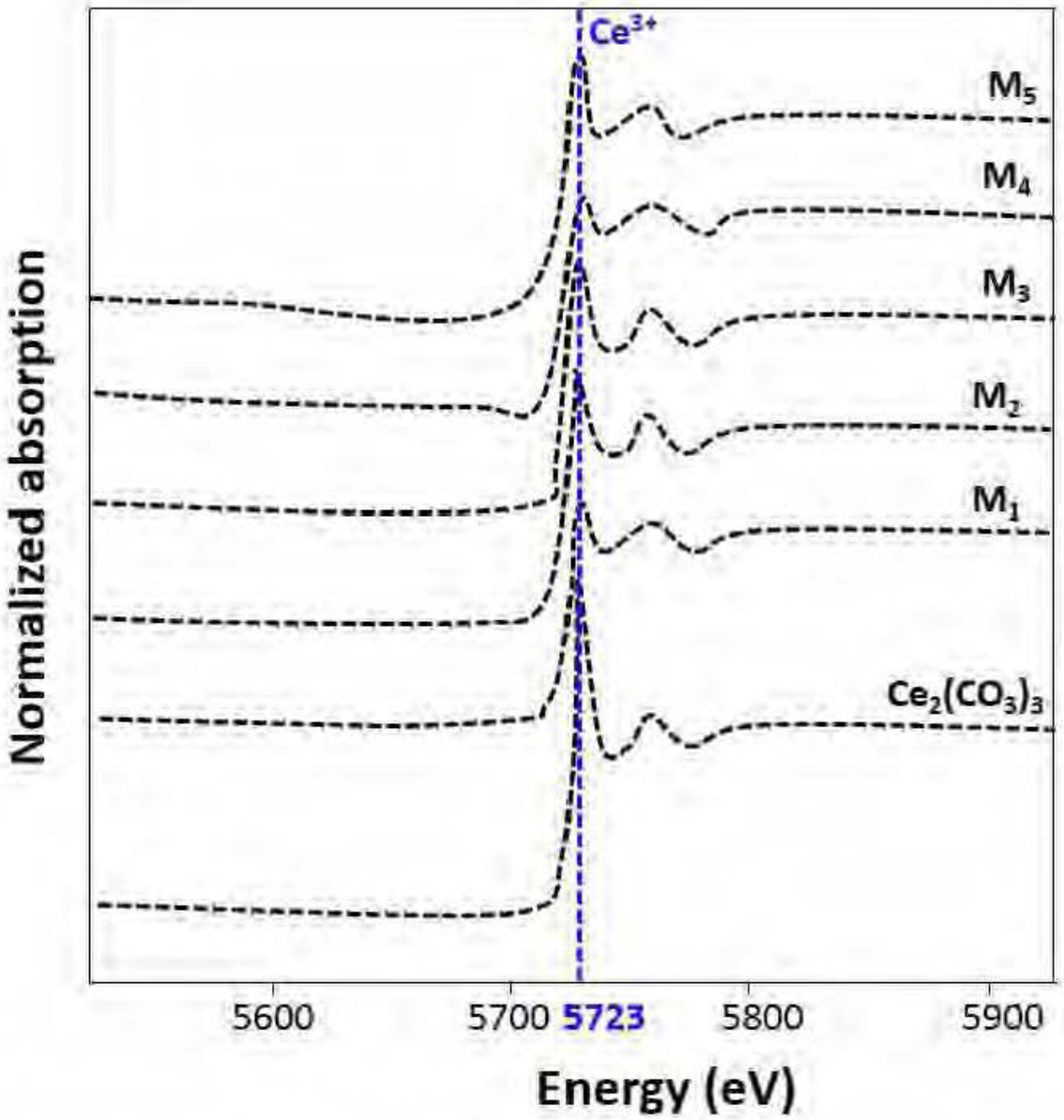

Figure 3-8 : Cerium L3-edge XANES spectra of the hydroxyapatite mixture (M1), the calcite mixture (M2), the goethite mixture (M3), the magnetite mixture (M4), the calcite-hydroxyapatite mixture (M5), and a $Ce_2(CO_3)_3 \cdot xH_2O$ reference standard.

After 175 days, the weathering cells were dismantled. Weathered waste rocks from the weathering cells were collected, prepared in polished sections, and investigated using secondary electron imagery with a SEM. SEM observations show the formation of secondary iron oxyhydroxides such as $Fe(OH)_3$ and mixtures of REE-Fe-Al. These minerals also have a significant Ce content, which suggest the co-precipitation of Ce by Fe and Al secondary precipitates.

3.6 Implications for the environmental geochemistry of REE-bearing waste rock

The graphical abstract summarizes a conceptual approach for understanding the geochemical behavior of REE-bearing waste rocks, which can then be used to predict the water quality issued from mining drainage. This conceptual approach is described below.

Carbonates (REE-bearing or not) are the most abundant minerals in REE carbonatites and can be naturally dissolved under the effects of CO_2 dissolution (generating carbonic acid) and/or by the acidity produced by sulfide oxidation. These reactions generate metals (Ba, Sr, Fe etc.), REE, and other associated contaminants which are released in leachates and pore waters. Upon percolation of the leachate through the waste rocks, the different contaminant concentrations can be controlled by precipitation, coprecipitation, and sorption phenomena. Environmental factors such as pH, ionic strength, redox potential, temperature could have a significant impact on REE mobility. Mihajlovic et al., (2017) showed that REE fractionation is promoted by a decrease of Eh and an increase of Al, Mn, and Fe concentrations. Moreover, a decrease of pH (from 6.6 to 4.6), increases the release of REE in the leachates. This finding is coherent with the work of Edahbi et al., (2018), in which an inverse relationship between REE and Fe, Al, and Mn was observed. However, it is challenging to discern which of these processes exert the most significant control of the REE concentrations released by REE-bearing mine wastes. To better understand which geochemical mechanisms govern the environmental behavior of REE, further research is needed. Other techniques, such as Nd isotope analysis, may allow for a more definitive understanding of the trends observed during REE fractionation.

3.7 Conclusions and recommendations

The major findings through this study are summarized in the following ideas:

- The study based on synthetic minerals shows that calcite, apatite, and iron oxyhydroxides (goethite and magnetite) could significantly reduce the mobility of REE. These minerals possess different sorption capacities, with the calcite and apatite minerals being the major sorbing phases;
- The XANES study suggests that Ce is within the materials as Ce^{3+} ;

- The SEM observations demonstrate that iron oxyhydroxides can coprecipitate Ce under leaching conditions;
- A strong relationship was observed between the total S and REE (Ce+La) leached in weathering cells, which suggest that sulfide oxidation increase the leaching of REE;
- The minerals composing the Montviel waste rocks possess significant sorption capacities for Ce.

3.8 Acknowledgements

The authors thank the URSTM staff for their technical and analytical supports and NSERC for funding of this study. The authors also thank gratefully the mining company Geomega Resources for the great help, especially in the sampling steps. This research used resources of the Advanced Photon Source, an Office of Science User Facility operated for the U.S. beamline, sector 20. Department of Energy (DOE) Office of Science by Argonne National Laboratory, and was supported by the U.S. DOE under Contract No. DE-AC02-06CH11357, and the Canadian Light Source and its funding partners.

REFERENCES

Al Mahrouqi, D., Vinogradov, J. and Jackson, M.D. (2017). Zeta potential of artificial and natural calcite in aqueous solution. Advances in Colloid and Interface Science 240(Supplement C), 60-76.

Ayora, C., Macías, F., Torres, E., Lozano, A., Carrero, S., Nieto, J.-M., Pérez-López, R., Fernández-Martínez, A. and Castillo-Michel, H. (2016). Recovery of rare earth elements and yttrium from passive-remediation systems of acid mine drainage. Environ Sci Technol 50(15), 8255-8262.

Babou-Kammoe, R., Hamoudi, S., Larachi, F. and Belkacemi, K. (2012). Synthesis of CaCO3 nanoparticles by controlled precipitation of saturated carbonate and calcium nitrate aqueous solutions. The Canadian journal of chemical engineering 90(1), 26-33.

Balboni, E., Simonetti, A., Spano, T., Cook, N.D. and Burns, P.C. (2017). Rare-earth element fractionation in uranium ore and its U(VI) alteration minerals. Applied Geochemistry 87(Supplement C), 84-92.

Benzaazoua, M., Bussiére, B., Dagenais, A.M. and Archambault, M. (2004). Kinetic tests comparison and interpretation for prediction of the Joutel tailings acid generation potential. Environmental Geology 46(8), 1086-1101.

Blowes, D.W., Ptacek, C.J., Jambor, J.L. and Weisener, C.G. (2003). Treatise on Geochemistry, pp. 149-204, Pergamon, Oxford.

Bouzahzah, H., Benzaazoua, M., Bussiere, B. and Plante, B. (2013). Prediction of Acid Mine Drainage: Importance of Mineralogy and the Test Protocols for Static and Kinetic Tests. Mine Water and the Environment 33(1), 54-65.

Britel, O. (2007). Modélisation et optimisation par la méthodologie des plans d'expériences de la synthèse: De l'hydroxyapatite phosphocalcique, du phosphate tricalcique apatitique, du phosphate de calcium apatitique carbonate.

Burrows, J.E., Cravotta, C.A. and Peters, S.C. (2017). Enhanced Al and Zn removal from coal-mine drainage during rapid oxidation and precipitation of Fe oxides at near-neutral pH. Applied Geochemistry 78(Supplement C), 194-210.

Carron, M., Skinner, D. and Stevens, R. (1955). Determination of Thorium and of Rare Earth Elements in Cerium Earth (Minerals) and Ores. Analytical Chemistry 27(7), 1058-1061.

Cravotta, C.A. and Watzlaf, G.R. (2003). Handbook of Groundwater Remediation using Permeable Reactive Barriers, pp. 19-66, Academic Press, San Diego.

Davris, P., Stopic, S., Balomenos, E., Panias, D., Paspaliaris, I. and Friedrich, B. (2017). Leaching of rare earth elements from eudialyte concentrate by suppressing silica gel formation. Minerals Engineering 108, 115-122.

Dibbs, H. P. (1972). The determination of the zeta potential of minerals. Information Canada.

Edahbi, M., Benzaazoua, M., Plante, B., Doire, S. and Kormos, L. (2017). Mineralogical characterization using QEMSCAN® and leaching potential study of REE within silicate ores: A case study of the Matamec project, Québec, Canada. Journal of Geochemical Exploration 185, 64–73.

Edahbi, M., Plante, B., Benzaazoua, M. and Pelletier, M. (2018). Geochemistry of rare earth elements within waste rocks from the Montviel carbonatite deposit, Québec, Canada. Environmental Science and Pollution Research DOI: 10.1007/s11356-018-1309-7.

Erdemoğlu, M. and Sarıkaya, M. (2006). Effects of heavy metals and oxalate on the zeta potential of magnetite. Journal of Colloid and Interface Science 300(2), 795-804.

Frostad, S., Klein, B. and Lawrence, R.W. (2002). Evaluation of laboratory kinetic test methods for measuring rates of weathering. Mine Water and the Environment 21(4), 183-192.

Gence, N., and Ozbay, N. (2006). pH dependence of electrokinetic behavior of dolomite and magnesite in aqueous electrolyte solutions. Applied surface science, 252(23), 8057-8061.

Inguaggiato, C., Burbano, V., Rouwet, D. and Garzón, G. (2017). Geochemical processes assessed by Rare Earth Elements fractionation at "Laguna Verde" acidic-sulphate crater lake (Azufral volcano, Colombia). Applied Geochemistry 79, 65-74.

Jaiswal, A., Banerjee, S., Mani, R. and Chattopadhyaya, M. (2013). Synthesis, characterization and application of goethite mineral as an adsorbent. Journal of Environmental Chemical Engineering 1(3), 281-289.

Liu, H., Guo, H., Xing, L., Zhan, Y., Li, F., Shao, J., Niu, H., Liang, X. and Li, C. (2016). Geochemical behaviors of rare earth elements in groundwater along a flow path in the North China Plain. Journal of Asian Earth Sciences 117, 33-51.

Liu, H., Pourret, O., Guo, H. and Bonhoure, J. (2017). Rare earth elements sorption to iron oxyhydroxide: Model development and application to groundwater. Applied Geochemistry 87(Supplement C), 158-166.

Mihajlovic, J., Stärk, H.-J. and Rinklebe, J. (2017). Rare earth elements and their release dynamics under pre-definite redox conditions in a floodplain soil. Chemosphere 181, 313-319.

Nadeau, O., Cayer, A., Pelletier, M., Stevenson, R. and Jébrak, M. (2015). The Paleoproterozoic Montviel carbonatite-hosted REE–Nb deposit, Abitibi, Canada: Geology, mineralogy, geochemistry and genesis. Ore Geology Reviews 67, 314-335.

Nadeau, O., Stevenson, R. and Jébrak, M. (2016a). Evolution of Montviel alkaline-carbonatite complex by coupled fractional crystallization, fluid mixing and metasomatism — Part II: Trace element and Sm–Nd isotope geochemistry of metasomatic rocks: implications for REE-Nb mineralization. Ore Geology Reviews 72, Part 1, 1163-1173.

Nadeau, O., Stevenson, R., and Jébrak, M. (2016b). Evolution of Montviel alkaline-carbonatite complex by coupled fractional crystallization, fluid mixing and metasomatism — Part II: Trace element and Sm–Nd isotope geochemistry of metasomatic rocks: implications for REE-Nb mineralization. Ore Geology Reviews 72, 1163-1173.

Pelloux, P., Dabin, B., Fillmann, G., and Gómez, P. (1971). Méthodes de détermination des cations échangeables et de la capacité d'échange dans les sols.

Plante, B., Bussière, B., and Benzaazoua, M. (2014). Lab to field scale effects on contaminated neutral drainage prediction from the Tio mine waste rocks. Journal of Geochemical Exploration, 137, 37--47. http://doi.org/10.1016/j.gexplo.2013.11.004.

Plante, B., Benzaazoua, M. and Bussière, B. (2010a). Kinetic Testing and Sorption Studies by Modified Weathering Cells to Characterize the Potential to Generate Contaminated Neutral Drainage. Mine Water and the Environment 30(1), 22-37.

Plante, B., Benzaazoua, M. and Bussière, B. (2010b). Predicting Geochemical Behaviour of Waste Rock with Low Acid Generating Potential Using Laboratory Kinetic Tests. Mine Water and the Environment 30(1), 2-21.

Prudêncio, M.I., Valente, T., Marques, R., Braga, M.A.S. and Pamplona, J. (2017). Rare Earth Elements, Iron and Manganese in Ochre-precipitates and Wetland Soils of a Passive Treatment System for Acid Mine Drainage. Procedia Earth and Planetary Science 17(Supplement C), 932-935.

Quast, K. (2016). The use of zeta potential to investigate the interaction of oleate on hematite. Minerals Engineering 85(Supplement C), 130-137.

Rim, K.T., Koo, K.H. and Park, J.S. (2013). Toxicological Evaluations of Rare Earths and Their Health Impacts to Workers: A Literature Review. Safety and Health at Work 4(1), 12-26.

Roth, E., Bank, T., Howard, B. and Granite, E. (2017). Rare Earth Elements in Alberta Oil Sand Process Streams. Energy & Fuels 31(5), 4714-4720.

Somasundaran, P. (1968). Zeta potential of apatite in aqueous solutions and its change during equilibration. Journal of Colloid and Interface Science 27(4), 659-666.

van Middlesworth, P.E. and Wood, S.A. (1998). The aqueous geochemistry of the rare earth elements and yttrium. Part 7. REE, Th and U contents in thermal springs associated with the Idaho batholith. Applied Geochemistry 13(7), 861-884.

Ward, M., J. (2013). X-ray Absorption Fine Structure and X-ray Excited Optical Luminescence Studies of Gallium Nitride - Zinc Oxide Solid Solution Nanostructures. University of Western Ontario, Electronic Thesis and Dissertation Repository, 2013, .

Young, R.A. (1993). The rietveld method, International union of crystallography.

Zhu, Z., Pranolo, Y. and Cheng, C.Y. (2015) Separation of uranium and thorium from rare earths for rare earth production – A review. Minerals Engineering 77(Supplement C), 185-196.

CHAPITRE 4 ARTICLE 3 : GEOCHEMISTRY OF RARE EARTH ELEMENTS WITHIN WASTE ROCKS FROM THE MONTVIEL CARBONATITE DEPOSIT, QUÉBEC, CANADA

Cet article est accepté dans la revue Environmental Science and Pollution Research, 2018

Edahbi, M.[a]; Plante, B.[a]; Benzaazoua, M.[a]; Pelletier, M.[b]

[a]IRME-UQAT, Research Institute - Mines and Environment, University of Quebec in Abitibi Témiscamingue, Rouyn-Noranda, Canada J9X 5E4

[b]Ressources Géoméga, St-Lambert, Canada

4.1 Abstract

Several rare earth elements (REE) mine projects around the world are currently at the feasibility stage. Unfortunately, few studies have evaluated the contamination potential of REE and their effects on the environment. In this project, the waste rocks from the carbonatites within the Montviel proterozoic alkaline intrusion (near Lebel-sur-Quévillon, Quebec, Canada) are assessed in this research. The mineralization is mainly constituted by light REE (LREE) fluorocarbonates (qaqarssukite-Ce, kukharenkoite-Ce), LREE carbonates (burbankite, Sr-Ba-Ca-REE, barytocalcite, strontianite, Ba-REE-carbonates), and phosphates (apatite, monazite). The gangue minerals are biotites, chlorite, albite, ankerite, siderite, and calcite. The SEM-EDS analyses show that: (i) the majority of REE are associated with the fine fraction (<106 µm), (ii) REE are mainly associated with carbonates, (iii) all analyzed minerals preferably contain LREE (La, Ce, Pr, Nd, Sm, Eu), (iv) the sum of LREE in each analyzed mineral varies between ~ 3 and 10 wt.%, (v) the heavy REE (HREE) identified are Gd and Yb at < 0.4 wt.%, and (vi) three groups of carbonate minerals were observed containing variable concentrations of Ca, Na, and F. Furthermore, the mineralogical composition of REE-bearing minerals, REE mobility, and REE speciation were investigated. The leachability and geochemical behavior of these REE-bearing mine wastes were tested using normalized kinetic testing (humidity cells). Leachates results displayed higher LREE concentrations than HREE, with decreasing shale-normalized patterns. Thermodynamical equilibrium calculations suggest that the precipitation of secondary REE minerals may control the REE mobility.

Keywords: Montviel carbonatites (Quebec, Canada), rare earth elements (REE), Mineralogical characterisation, geochemical behavior, speciation, Humidity cells, modelling.

4.2 Introduction

Rare earth elements (REE) are composed of seventeen chemical elements grouped together in the periodic table, specifically the fifteen (La to Lu), as well as scandium (Sc) and yttrium (Y). Scandium and yttrium are considered REE because their occurrences in the same geological formations as the lanthanides and exhibit similar chemical properties. REE are often classified into light REE (LREE, La to Gd) and heavy REE (HREE, Tb to Lu, and Y). The main reported differences between the geochemical behaviors of LREE and HREE lays on the electron configuration of each element. Indeed, the size of the REE ions decreases with increasing atomic number (due to the increased nuclear charge that is shielded by the 4f electrons), and many geochemical processes (cationic exchange, adsorption, precipitation, co-precipitation) are influenced by the ionic size and charge (Lipin 1989). REE resources are now considered as strategic metals because of their use in modern technologies and industries (Jaireth et al., 2014; McLellan et al., 2014) . Currently, China supplies 94 % of the global REE market. However, REE mining and refining are known to generate negative impacts on the environment, as seen in China, USA, Malaysia (Gonzalez et al., 2014; Sneller et al., 2000; Wang and Liang 2014; Yang et al., 2013). REE are often found as substitutions within the crystal lattice of carbonates, sulfides, fluorides, chlorides, phosphates, and oxyhydroxides (Kato et al., 2011; Lipin 1989; Miekeley et al., 1992; Steinmann and Stille 2008) . Release rates could be controlled by secondary mineral precipitation and/or co- precipitation (iron oxide and clays).

In the framework of sustainable development, social acceptability, and environmental regulations, it is nowadays necessary to integrate the environmental aspects as early as possible in the development of mining projects. Unfortunately, knowledge on REE release from mine wastes is very sparse, despite several REE mine projects in development. The objective of the geochemical prediction is to anticipate the mine drainage quality and to optimize the mine waste management strategies.

The purpose of this paper is to improve knowledge on REE leaching from mine wastes in order to predict their geochemical behavior.

4.3 Materials and methods

Mineralogical techniques, namely X-ray diffraction (XRD), scanning electron microscopy (SEM-EDS) as well as humidity cell tests were used to characterize and study the REE leaching potential of five lithologies from the Montviel deposit.

4.3.1 Montviel site

Montviel deposit is located in the heart of the Canadian shield, approximately 97 km north of the Lebel-sur-Quevillon city, Quebec province, Canada (Desharnais and Duplessis 2011) (Figure 4-1). REE mineralization of this deposit is hosted mainly in carbonatites within the Montviel alkaline proterozoic intrusion (David et al., 2006; Nadeau et al., 2014), which consists of a series of mafic/ultramafic rocks that are younger than the old (1894 ± 3.5 million years) surrounding rocks, weakly metamorphosed and undeformed (Goutier 2006). GéoMéga estimates the indicated resources to be approximately 183.9 Mt at 1.45 % total rare earth oxide (TREO) and 66.7 Mt at 1.46 % TREO in the inferred resources category. TREO refers to the sum total of rare earth elements present in a deposit. The sill is composed of ferrocarbonatites, apatite-ferrocarbonatite, silicocarbonatite, breccia, and calciocarbonatite containing mostly LREE. This site has been the subject of several geological and metallogenic order studies (Goutier 2006; Nadeau et al., 2014, 2015, 2016).

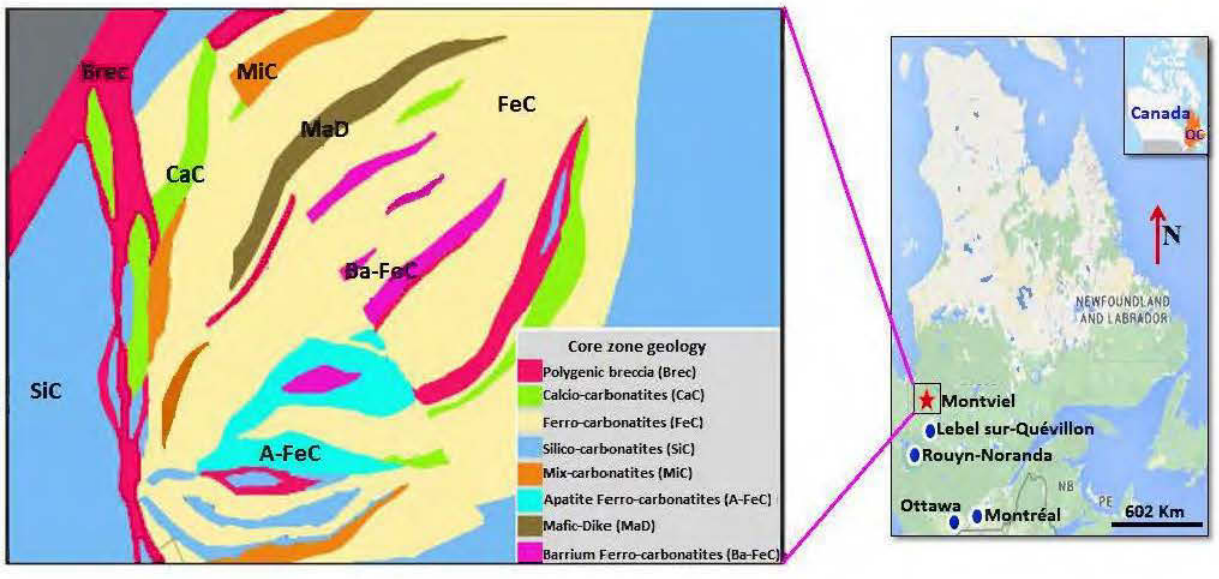

Figure 4-1 : Geographic location and core zone geology of the Montviel site (adopted from Ressources GéoMéga and modified from Edahbi et al., 2015).

4.3.2 Sampling

Different lithologies were sampled (approximately 5 kg) from drill cores: three waste rock samples, namely Breccia (Brec), calciocarbonatite (CaC-LG), and silicocarbonatite (SiC-LG), as well as two ore samples, low-grade ferrocarbonatite (FeC-LG) and high-grade ferrocarbonatite (FeC-HG) (Figure 4-1). The samples were crushed, sieved to < 6.9 mm, and homogenized before mineralogical and geochemical characterizations.

4.3.3 Characterization methods

The particle size distribution was determined by sieving. The specific gravity (SG) of the waste rocks was determined on powdered samples (pulverization at less than 300 µm) with a Micromeritics Helium Pycnometer (Micromeritics Accupyc 1330) (Merkus 2009). The chemical compositions were determined by a combination of methods on a pulverized aliquot of the samples. The whole rock analysis was conducted by X-ray fluorescence (XRF, Bruker Tiger series) in order to determine major elements, especially silicon oxides which the content is not accurate using Inductively Coupled Plasma (ICP). Total sulfur and carbon contents were determined using an induction furnace (ELTRA CS-2000). Sulfide sulfur was calculated by subtracting the acid-soluble sulfate sulfur determined by ICP-AES (Perkin Elmer Optima 3100-RL) following a 40 % HCl extraction (Sobek 1978) from the total sulfur. Major and minor elements were analyzed by Inductively Coupled Plasma (Perkin Elmer Optima 3100-RL ICP-AES and Agilent 7700 ICP-MS) analysis after a multi-acid digestion (HCl, HNO_3, Br_2, HF) of a 500 mg aliquot.

The mineralogy was determined on polished sections made of the five samples using an optical microscope (Zeiss Axio imager.M2m) and a scanning electron microscope (SEM–Hitachi S-3500N) equipped with an EDS INCA XMass 20 mm^2 SDD). The polished sections were prepared using a method developed for samples containing heavy minerals in order to avoid their preferential sedimentation (Kwitko-Ribeiro 2012). The optical microscope (OM) observations mainly focused on sulfide minerals, while the stoichiometry of the REE-bearing minerals was measured with analyses of the grains using the SEM-EDS system. The mineralogical modal composition was also performed with a Bruker A.X.S. D8 Advance X-Ray diffraction (XRD) instrument equipped with a copper anticathode (detection limit of 0.5 to 1 wt. %). The mineralogical quantification was performed with a Rietveld (1993) fitting of the XRD data with the TOPAS software. In order to reconcile the final mineralogical results, chemical and mineralogical results are collected, compared, and adjusted to determine with high precision the percentages of mineral phases present within samples.

All leachates obtained from for humidity cells were analyzed with the ICP-AES and ICP-MS after acidification of a filtered (0.45 µm) aliquot to about 2 % HNO_3. Pore water pH and Eh measurements were done using a pH/mV meter (Orion triode electrode/ Orion 920A controller) immediately after leaching. Acidity and alkalinity were determined by titration with sodium hydroxide and sulfuric acid, respectively (MA. 315 - Alc-Aci 1.0).

The modified Sobek procedure of Lawrence and Wang (1996) is used to determine the acid-base accounting (ABA). The acid-generation potential (AP) was calculated by multiplying the sulfide sulfur (total sulfur content obtained from an induction furnace - sulfate sulfur content) by a factor of 31.25; while the neutralization potential (NP) was determined by HCl additions followed by back-titration of the excess acid to an endpoint pH of 8.3. The Carbonate NP (CNP) was calculated by multiplying the carbon content (induction furnace) by a factor of 83.3. The net neutralization potential (NNP) is obtained by the difference between the AP and NP (NNP=NP-AP), and the NP/AP ratio was calculated. Interpretations of the results are based on the Price (2009) criteria.

Humidity cell tests were performed in a Plexiglass chamber that provided air input and output. Five cells were filled with 1 kg of each sample (grain size less than 6.3 mm) placed on a geotextile lying on a perforated grid. The experiments lasted 234 weekly cycles. Dry air was passed through the sample container for the first three days, followed by humidified air for the next three days, and leaching on the 7th day with 500 ml of deionized water (pH ≈6) (Benzaazoua et al., 2004). Dry and humid air flows as well as the temperature were maintained stable for the length of the test. The leached solutions were analyzed for pH and REE contents. A more detailed description of the humidity cells is found in (Benzaazoua et al., 2004; Plante et al., 2012; Villeneuve et al., 2003, 2009).

4.3.4 Thermodynamic equilibrium calculations

Geochemical speciation models are widely used to describe the chemistry of mining drainage water (Bussière 2007; Nordstrom, 2011; Plante et al., 2010). Such models allow calculating ion activities and metal speciation in a wide range of conditions and can be used to calculate the saturation indices of a wide variety of minerals. Geochemical equilibrium calculation code; PHREEQC Interactive3.1.2-8538 using a database provided by BRGM (Parkhurst and Appelo 2013), was used to assess these aspects.

4.4 Results and discussion

4.4.1 Physical and chemical characterization

Physical and chemical characterization results of the Montviel waste rock samples are summarized in Table 4-1. The specific gravity (G_S) is similar for all samples. The samples show

comparable particle size distributions, except CaC-LG which is slightly finer (D_{10} =95 µm) than the other materials (D_{10} =175 µm).

The whole rock analyses of the waste rocks samples are shown in Table 4-1. The Brec shows the highest contents of P_2O_5 in comparison to the other samples, because of its higher phosphates content. The CaC-LG, FeC-LG, and FeC-HG samples show similar contents of CaO, MgO, and Fe_2O_3. The higher Fe_2O_3 content in these materials are mainly attributed to the presence of Fe, and Mg carbonates (dolomite, ankerite, siderite), as well as chlorite and biotite. The CaO is higher in the CaC-LG sample because of its higher carbonates content (dolomite, calcite). The remaining composition is represented by silicates and aluminosilicates, as shown by the SiO_2, Al_2O_3, K_2O, and Na_2O contents (Table 4-1). The SiO_2 is most abundant in the SiC-LG as expected based on its higher silicate minerals content (i.e., biotite, chlorite, diopside). The TiO_2, Cr_2O_3, and V_2O_5 contents are only present as traces in all samples (less than 0.7 %). The REE concentrations are lower in SiC-LG and higher in the FeC-HG. Moreover, the quantities of total LREE are higher relative to total HREE to in all materials, as could be seen in Table 4-1 and Figure 4-2.

Tableau 4-1 : Physical and chemical characterization of the Montviel samples; breccia (Brec), calciocarbonatite (CaC-LG), silicocarbonatite (SiC-LG), low-grade ferrocarbonatite (FeC-LG) and high-grade ferrocarbonatite (FeC-HG).

	Brec	**CaC-LG**	**FeC- LG**	**FeC-HG**	**SiC- LG**
Specific density (Gs)	3	3,1	3,36	3,3	3,26
Paste pH	10.16	10.05	9.58	10.07	10.35
D_{10} (µm)	175	95	175	175	175
D_{50} (µm)	2250	2075	2775	2250	2250
D_{90} (µm)	5000	5000	5500	5000	5000
Major oxides (%)					
Total sulfur	0.89	0.41	0.22	0.84	0.35
Total carbon	5.69	9.31	9.77	8.73	6.79
SiO_2	11.4	5.9	4.3	5.8	16.9
Al_2O_3	2.3	0.9	0.7	1.1	3.5
Fe_2O_3	11.5	17.7	23.5	22.1	19.4
MgO	4.9	3.8	8.5	6.3	7.4
CaO	30.2	27.6	19.2	15.7	17
Na_2O	0.9	1	0.4	1.5	1.8
K_2O	1.7	0.6	0.5	0.7	2.5
TiO_2	0.5	0.1	0.1	0.4	0.7
P_2O_5	6.7	0.3	0.3	0.07	0.3
MnO	0.8	1.6	2.6	2.1	1.5
Cr_2O_3	< 0.01	< 0.01	< 0.01	< 0.01	< 0.01
V_2O_5	0.02	0.01	< 0.01	< 0.01	0.03
LOI	20.9	32.7	34.3	29.6	21.5
Elemental concentrations (mg/l)					
Zn	807	1230	834	548	528
Pb	232	147	120	94.9	89.1
Cu	58.8	22.8	25	27.6	65.7
Ni	124	46	70.3	44	136
La	500	2 500	2 100	8 900	1 100
Ce	3 200	5 400	4 200	14 000	2 200
Pr	400	680	450	1400	250
Nd	1 500	2 200	1 300	4 100	850
Sm	270	330	150	390	110
Eu	75	77	31	78	28
Gd	200	270	99	290	66
Tb	24	20	6.2	15	5.5
Dy	110	74	16	31	18
Ho	18	11	2	3.3	2.5
Er	42	18	3.7	5.5	5.1
Tm	4,3	1.5	0.39	0.49	0.56
Yb	21	6.9	2.3	2.9	3.1
Lu	2.3	0.75	0.29	0.35	0.38
ΣLREE	6145	11457	8330	29158	4604
ΣHREE	221.6	132.15	30.88	58.54	35.14
LREE/HREE	28	82	270	498	131
ΣREE	6 367	11 589	8 361	29 216	4 639
EF	36	65	47	163	26
$[La/Gd]_N$	0.42	1.57	3.60	5.22	2.83
$[Gd/Yb]_N$	5.35	22	24.22	56.27	11.98
$[La/Yb]_N$	2.279	34.686	87.408	293.799	33.970
$[Ce/Ce^*]_N$	1.76	1.02	1.06	0.97	1.03
$[Eu/Eu^*]_N$	1.41	1.13	1.11	1.01	1.44

ΣLREE: total LREE (La to Gd); ΣHREE: total HREE (Tb to Lu); D_{10}, D_{50}, and D_{90} are the intercepts for 10 %, 50 % and 90 % of the cumulative mass respectively; LOI is the loss on ignition; EF: enrichment factor of REE, $EF=\Sigma REE_{Sample}/\Sigma REE_{NASC}$; $(La/Gd)_N$, $(La/Yb)_N$ and $(Gd/Yb)_N$ are normalized concentration ratios in the samples; Ce/Ce* is the value of the Ce anomaly calculated by $Ce/Ce^*=[(Ce_N)/(\sqrt{(La_N*Pr_N)})]$, $Eu/Eu^*=[(Eu_N)/(\sqrt{(Sm_N*Gd_N)})]$; Ce_N, Eu_N, La_N, Pr_N, Sm_N, and Gd_N are shale-normalized values against NASC.

A high variation in the ∑REE and LREE/HREE is observed in the studied samples. The enrichment factor (EF), which is superior to 1, indicate that the REE were enriched in these samples relative to the NASC (North American Shale Composite). All samples, except FeC-HG, are characterized by slight positive Ce and Eu anomalies. The positive anomalies of Ce ((Ce/Ce*)N >1) and Eu ((Eu/Eu*)N >1) mean that both of them are presented entirely as Ce3+ and Eu3+ (Leybourne et al., 2000; Purdy 2014).The NASC-normalized REE patterns of the Montviel samples are shown in Figure 4-2. The patterns have an asymmetrical decreasing shape indicating an enrichment of LREE compared to HREE (Figure 4-2).

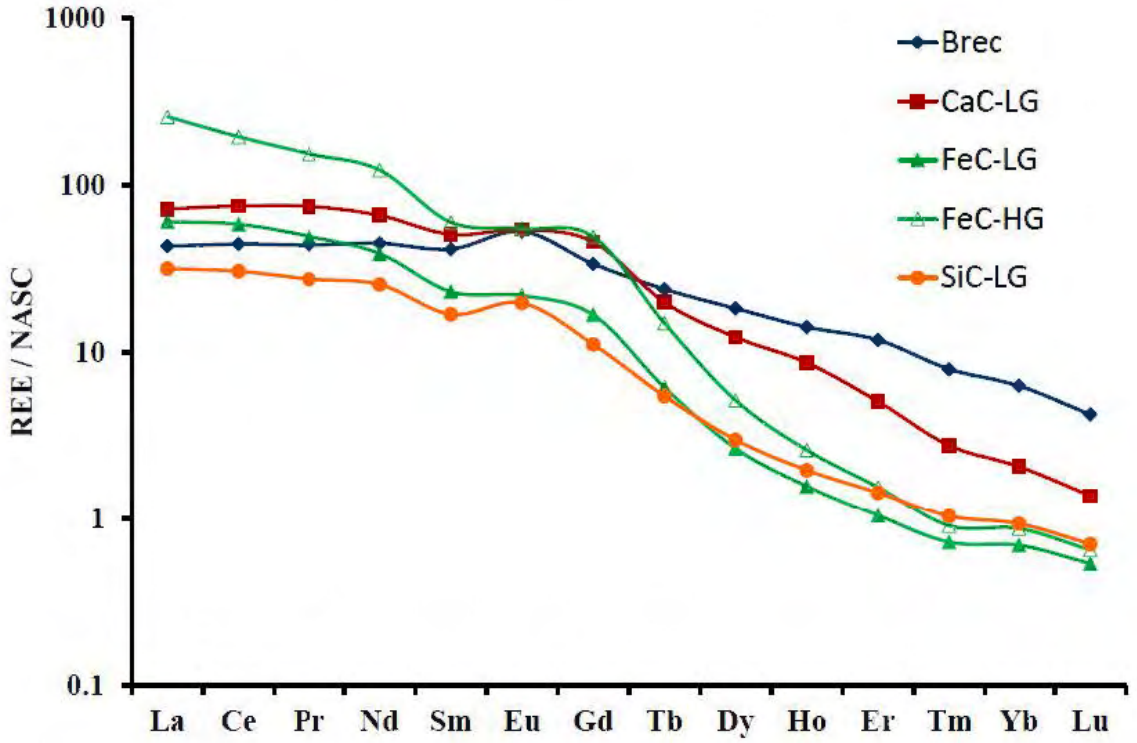

Figure 4-2 : NASC-normalized REE patterns of the studied lithologies.

4.4.2 Mineralogical composition of the Montviel lithogies

Optical microscopy observations show that pyrite is the most abundant sulfide mineral in the five samples, whereas sphalerite, galena, pyrrhotite, chalcopyrite, and pentlandite occur as traces (Table 4-2). The weight proportion of the various sulfides observed were estimated using chemical analyses, assuming all Zn within sphalerite, all Pb within galena, all Cu within chalcopyrite, and all Ni within pentlandite (Table 4-1). XRD results show also that the Montviel samples are mainly composed of carbonates (ankerite, calcite, barytocalcite, strontianite, and siderite). Ankerite is the main mineral detected, particularly in Fe-carbonatites and Si-carbonatites while cristobalite occurs in trace amounts. Sulfides were not detected by XRD in

the studied samples. The main REE-bearing minerals detected were monazite, except in FeC-LG. Burbankite and kukharenkoite only occur in FeC-HG sample, while apatite was only detected in the breccia sample. Other important gangue minerals, like biotite, were detected in all the studied samples. Chlorite occur in breccia and Ca-C, while albite and diopside only occur in SiC-LG. Celestine was only found in the FeC-LG sample (Table 4-2). These results are consistent with those found by other studies (Nadeau et al., 2015). All XRD quantification results are shown in Table 4-2.

Tableau 4-2 : Mineralogical characterization of the kinetic cells materials by XRD and Rietveld quantification (all results in wt. %)

Mineral	**Formulae**	**Brec**	**CaC**	**FeC-LG**	**FeC-HG**	**SiC**
Pyrite**	FeS_2	1.5	0.6	0.3	1.5	0.6
Pyrrhotite**	$Fe_{(1-x)}S$	0.04	0.02	0.01	0.04	0.02
Chalcopyrite**	$CuFeS_2$	0.02	0.01	0.01	0.01	0.02
Sphalerite**	ZnS	0.1	0.13	0.1	0.09	0.08
Galena**	PbS	0.03	0.02	0.01	0.01	0.01
Celestine	$SrSO_4$	-	-	2.0	-	-
Calcite	$CaCO_3$	27.5	36.7	4.7	5.9	14.4
Ankerite	$Ca(Fe^{++}, Mg, Mn)(CO_3)_2$	20.6	27.8	60.7	49.2	44.7
Siderite	$Fe^{++}CO_3$	-	17.6	21.9	16.7	8.4
Barytocalcite	$BaCa(CO_3)_2$	-	-	2.5	-	-
Strontianite	$SrCO_3$	-	-	2.7	3	-
Apatite	$(Ca_5(PO_4)_3F$	20.6	-	-	-	-
Monazite	$(Ce, La, Nd, Th)PO_4$	2	2.7	-	2	2
Burbankite	$(Na, Ca)_3(Sr, Ba, Ce)_3(CO_3)_5$	-	-	-	8.9	-
Kukharenkoite	$(Ce)\ (Ba_2Ce(CO_3)_3F$	-	-	-	4.9	
Cristobalite	SiO_2	1	-	-	-	-
Chlorite	$(Fe, Mg, Al)_6(Si, Al)_4O_{10}(OH)_8$	11.8	3	-	-	-
Biotite	$K(Mg, Fe^{++})_3AlSi_3O_{10}(OH, F)_2$	14.7	11.5	5.1	7.9	16.9
Diopside	$CaMgSi_2O_6$	-	-	-	-	7
Albite	$NaAlSi_3O_8$	-	-	-	-	6

**Proportions of sulfide minerals (wt %) are obtained by mineralogical calculations.

As shown in Table 4-3, the Montviel waste rocks have low total sulfur and sulfate contents. The neutralization potential of studied samples (NP) vary between 442 and 602 kg $CaCO_3$/t, while the acidity potential (AP) vary from 4 to 20 kg $CaCO_3$/t. Consequently, the net neutralization potentials (NNP, NP-AP) and CNP are all higher than 20 kg $CaCO_3$/t, and the NP/AP ratios are all above 24. These results suggest that the Montviel materials are non-acid generating (Adam et al., 1997).

Tableau 4-3 : Results of the ABA testing and carbon sulfur analysis

Static tests	Parameters	Unit	Brec	CaC-LG	FeC-LG	FeC-HG	SiC-LG
	C total	wt. %	5.69	9.31	9.77	8.73	6.79
	S_{total}	wt. %	0.89	0.41	0.22	0.84	0.35
	S in SO_4 state	wt. %	0.4	0.2	0.1	0.2	0.2
	AP	kg $CaCO_3$/t	16.2	7.8	4.1	20.3	4.4
	NP	kg $CaCO_3$/t	472	602	542	493	442
	NNP	kg $CaCO_3$/t	455.8	594.2	537.9	472.7	437.6
	NP/AP	-	29.1	77.1	133.5	24.3	100.9
Inorganic carbon corrected	C total	wt. %	7.5	9.8	12.9	11.8	10.5
	CNP	kg $CaCO_3$/t	622	819.2	1073.8	982.4	873.5
	NNP	kg $CaCO_3$/t	605.9	811.4	1069.66	962	869.1
	NP/AP	-	38.4	105	261.9	48.4	198.5

In Figure 4-3 the correlation between ΣLREE and Ba+Sr+F is shown. A positive correlation between these elements seems to exist in FeC-LG and FeC-HG samples (Figure 4-3 b), as well as in the Brec (Figure 4-3 c). This correlation suggests that the REE are contained essentially in Ba-Sr-F-carbonates. The minerals in the FeC-LG and FeC-HG samples can be classified into three groups (Figure 4-3 b): (i) group 1 is rich in LREE and poor in Ba+Sr+F; (ii) group 2 is rich in Ba+Sr+F and poor in LREE; and (iii) group 3 does not contain LREE (Figure 3b). However, this trend is not found for the CaC-LG and SiC-LG samples. Similar tendencies were found in the work of Nadeau et al., (2015).

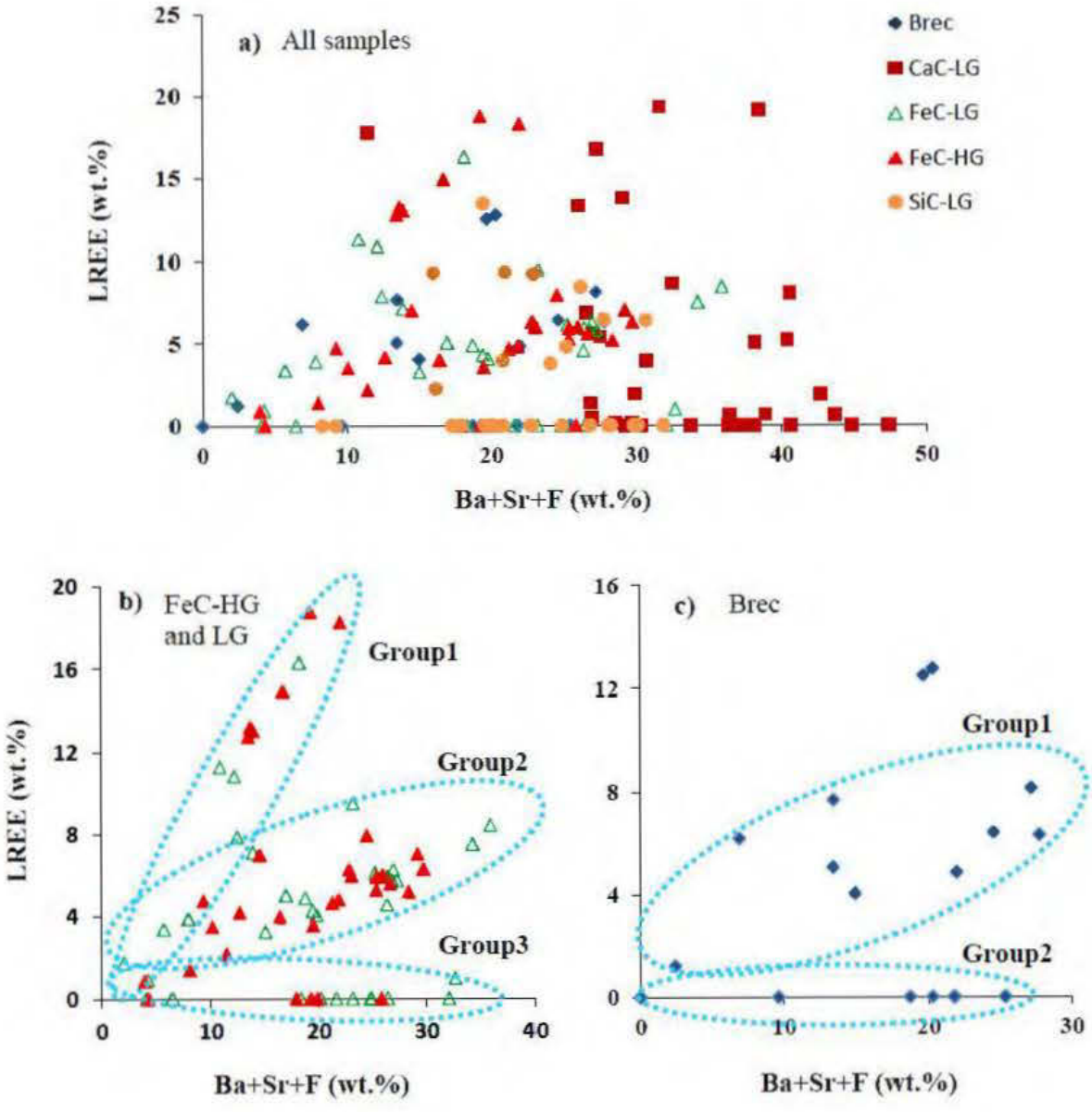

Figure 4-3 : SEM-EDS results correlation of total REE content with Ba, Sr, and F; a) LREE variation within all lithologies; b) LREE variation within FeC-HG and LG; C) LREE variation within Brec.

For further mineralogy investigation, Oxford Cameo® application has been used in order to locate regions of similar composition over large area of polished sections made off REE concentrate. This type of image is obtained by offsetting the X-ray spectrum into the visible range. The fine details of the BSE image are shown together with a full color overlay showing variations in elemental composition, indicating compositional changes. Individual X-ray photons are assigned a color, which depends on their energy. While conventional mapping applications may entail simultaneously viewing a number of elemental maps making it difficult to identify areas of similar composition, the cameo scatter plot shows the differences in spectral

content over all regions of the field (Princič et al., 2013). A typical cameo shot of the Montviel REE magnetic concentrate is shown in Figure 4-4, which shows the relationship between LREE and Ba+Sr+F in each analyzed mineral in all samples.

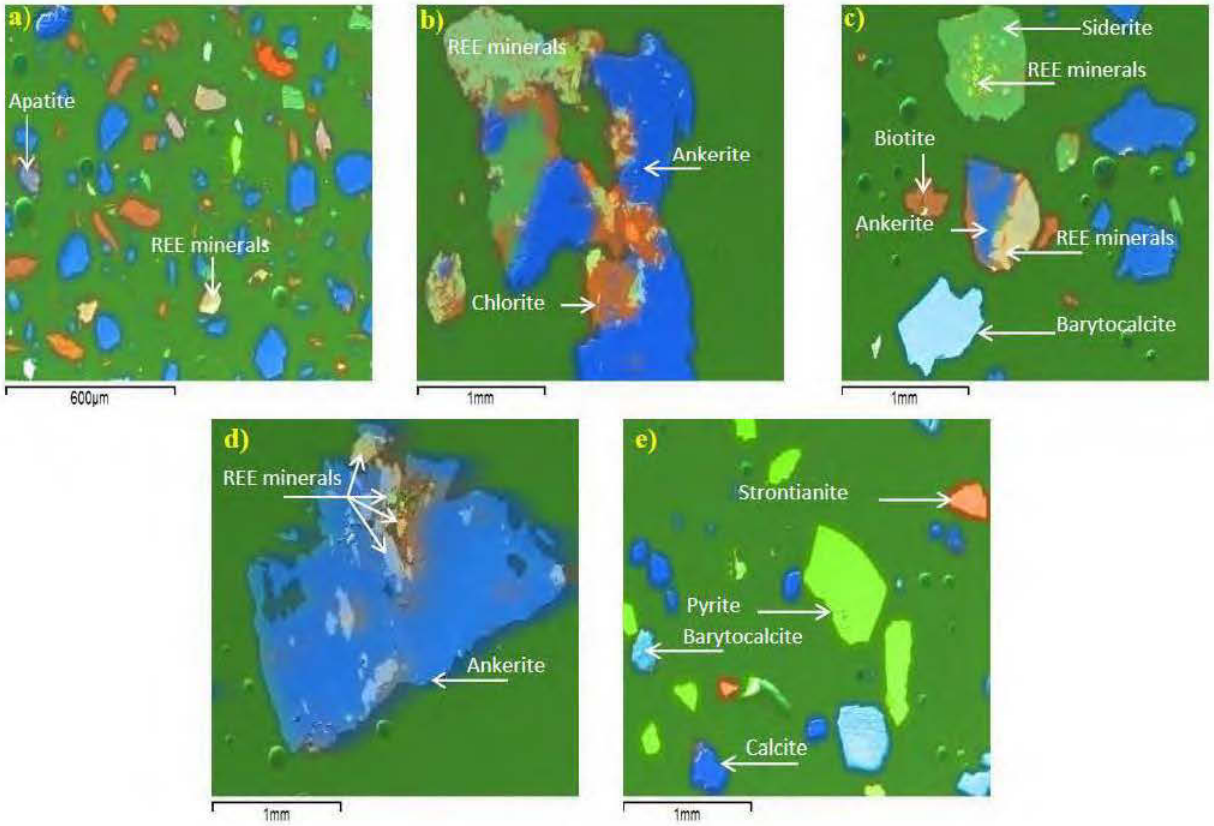

Figure 4-4 : Back-scattered electron images showing the different mineral phases associated to REE for Montviel samples; a) magnetic fine fraction (<106 µm); b) magnetic coarse fraction (>2 mm); c) inclusion and/or association of REE-bearing minerals with ankerite and siderite (106 µm – 2 mm); d) low magnetic coarse fraction (>2 mm); e) non- magnetic fraction (106 µm – 2 mm).

In summary, the Montviel mineralogical waste rock characterizations show that:

- REE-bearing minerals are found in two forms: free or included in carbonates (ankerite, siderite, barytocalcite, and slightly with calcite) (Figure 4-4);
- all analyzed minerals (REE carbonates, Ba-Sr-F-REE mixture) contain mostly LREE (La, Ce, Pr, Nd, Sm, and Eu);
- the sum of LREE in each analyzed mineral varies between ~ 0 and 19 wt %;
- the HREE identified are Gd and Yb with less than 0.4 % in all REE-bearing minerals;

- three groups of REE-bearing carbonate minerals were observed with variable concentrations of Ba, Sr, and F (Figure 4-3b);
- REE are more concentrated in the fine fraction (< 106 µm) (Figure 4-4a).

4.4.3 Leachate quality from Humidity cell tests

The leachate quality of the humidity cell tests is shown in Figure 4-5 and 4-6. The pH of all leachates remained near-neutral to slightly alkaline (7-10) over 819 testing days, without significant differences between materials. The alkalinity (Figure 4-5c) values decreased during the first 150 days of the testing duration, and remained stable afterwards between values of 20 to 50 mg CaCO3/l. The acidity remained <2 mg CaCO3/l for all materials throughout the tests. The electrical conductivities of the leachates stabilized between 30 and 430 µS/cm, and remained so until the last leaching cycle, the FeC-LG waste rocks generally showed lower conductivity values (29.7-146.8 µS/cm) than other materials. The F concentrations (0.015-3.18 mg/l) from all cells gradually decreased and stabilized close to 0.015 mg/l. Barium and Sr shows a similar trend and increased from 0.0352 to 2.71 mg/l. FeC-LG released lower concentrations of Sr (0.203-1.72 mg/l) while Brec, FeC-HG, CaC-LG, and SiC-LG released higher ones (up to 2.71, 2.37, 1.92 and 2.52 mg/l respectively). Barium concentrations in all samples increased continuously during the tests. The FeC-HG waste rock cells generated higher Ba concentrations (0.073-0.861 mg/l), while the Brec generated lower ones (0.0519-0.529 mg/l). The Brec sample generated higher Ca and Na levels than other cells (Ca: up to 10.1 mg/l; Na: up to 89.5 mg/l). For FeC-LG, Ca is up to 4.88 mg/l, while SiC-LG and CaC-LG the Ca is up to 8.59 and 5.05 mg/l respectively. Sodium values ranged from 0.08-80.1 mg/l, and FeC-LG lithology generated the lowest concentrations (up to 24.8 mg/l). As shown in Table 4-3, a part of the analyzed sulfur is in the sulfates form (i.e. celestine). The sulfur (considered as sulfates) concentrations showed significant differences between the five samples. The highest values (0.8-43 mg/l) were observed in Brec, while the lowest were observed in CaC-LG (0.5-10 mg/l) (Figure 4-6). Rare earth elements released concentrations corresponding to the five samples stabilized between 0.15 and 9 µg/l after the first 63 days except SiC-LG, for which REE concentrations stabilized after first 147 days. The gradual increase in concentration of Ca, Ba, and Sr in all samples could

explained by : (i) high reactivity of Ba-Sr-F-CO3 in comparison to other minerals (i.e. silicates), and/or (ii) the gradual dissolution is relied to the gradual S reaction rates (0.124-0.951 mg/l/d).

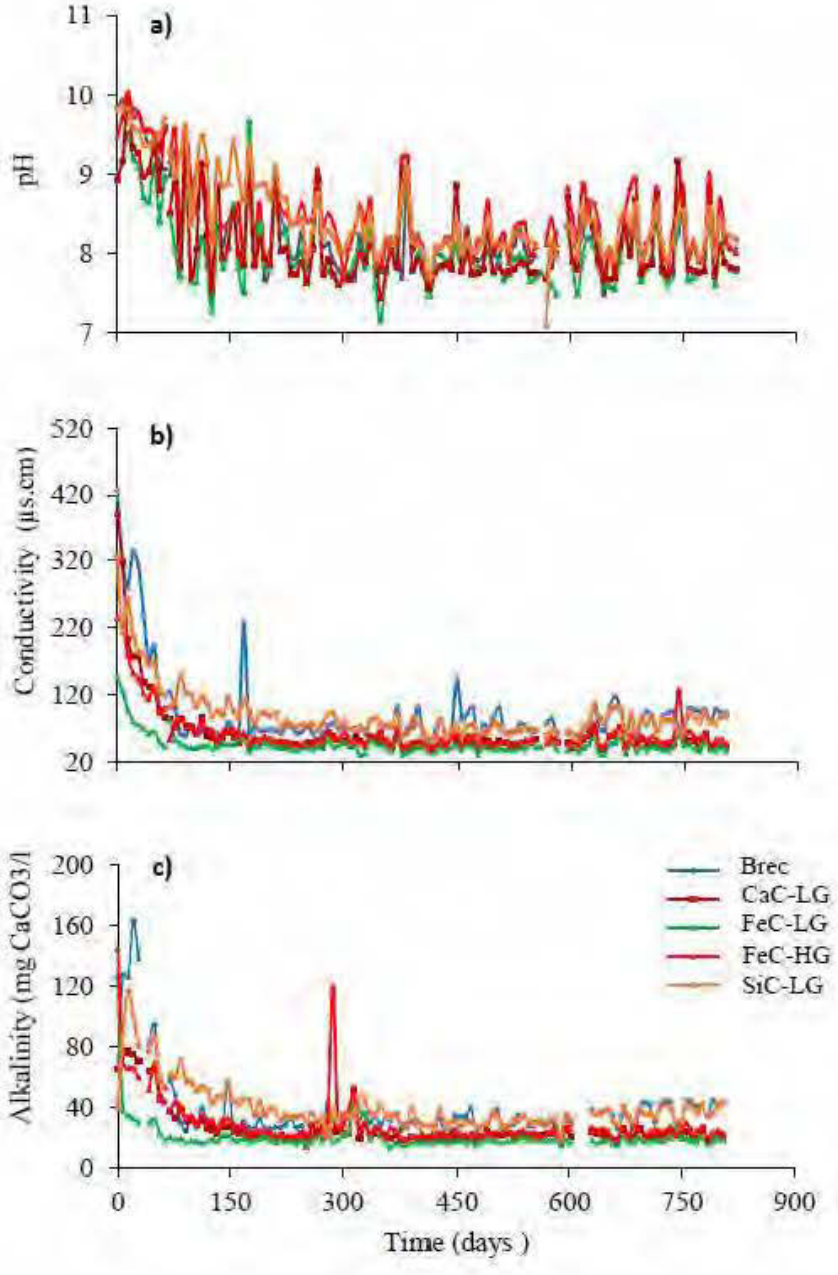

Figure 4-5 : Water quality evolution during humidity cell tests: a) pH, b) conductivity and c) alkalinity.

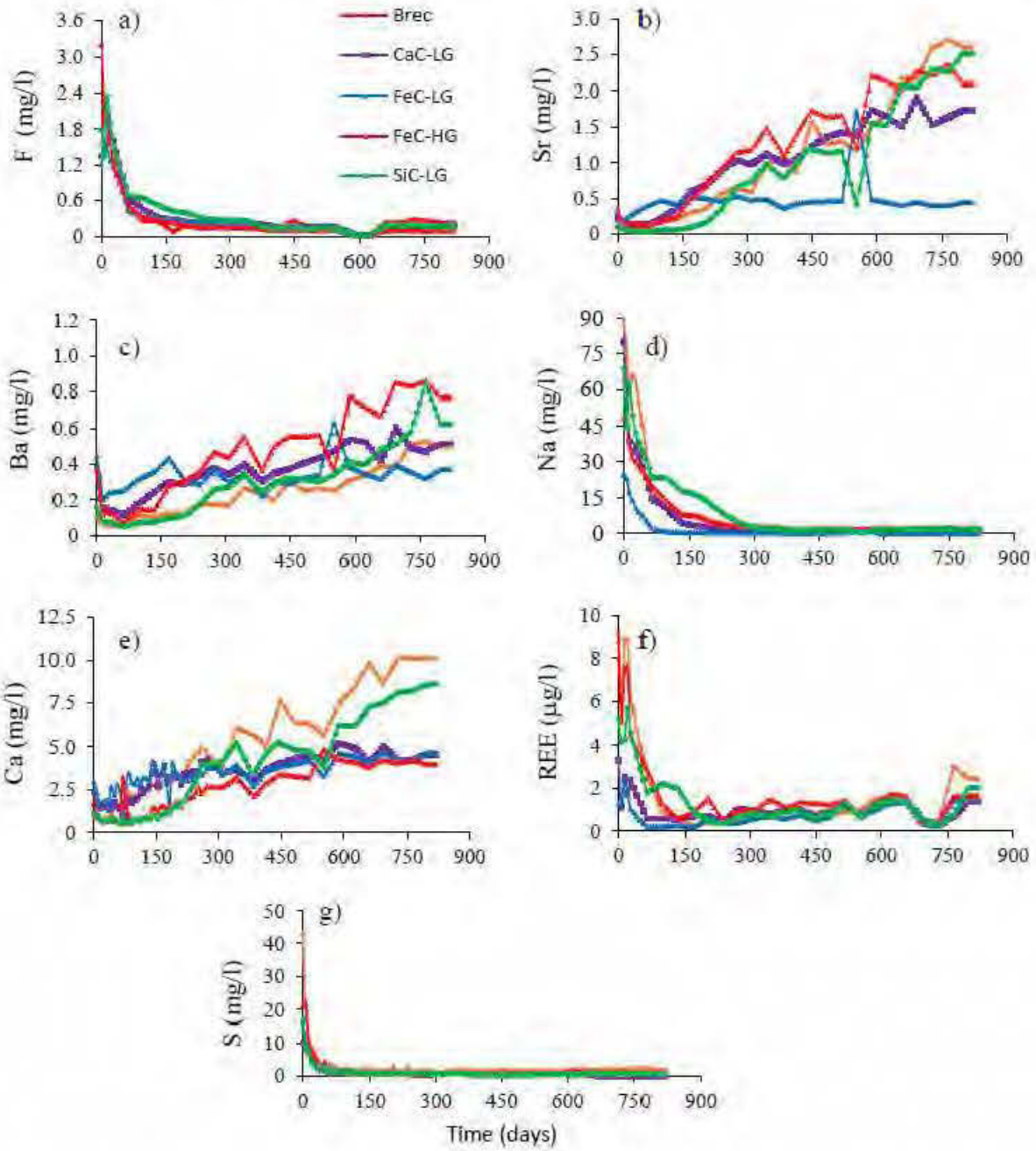

Figure 4-6 : Water quality evolution during humidity cell tests of Montviel waste rocks: a) F, b) Sr, c) Ba, d) Na, e) Ca, and f) REE.

4.4.4 Mineralogical evolution during Montviel waste rock weathering

The evolution of the main elements (Ca, Mg, Mn, Ba, Sr, F, and REE) associated to the neutralization-oxidation processes are represented in Figure 4-7. The neutralization processes are mainly associated to carbonate dissolution (REE and non-REE carbonates) as proven by the high Ca, Mg, Mn, Ba, Sr, F, and REE concentrations within the leachates. Figure 4-7a and 7b represent the evolution of the cumulative Ca+Mg+Mn+Ba+Sr+F versus SO_4. After 35 days of

testing, correlation indices vary between 0.81 to 0.99 and indicate linear tendencies in all samples. This geochemical behavior suggests that REE and Ca, Mg, Mn, Ba, Sr, and F have the same sources as demonstrated by the SEM-EDS. The results are expressed as cumulative masses of SO_4 (Figure 4-7c) and REE leached out of the kinetic tests (Figure 4-7d); representing respectively the oxidation of sulfide minerals, and REE-bearing minerals (mostly carbonates) dissolution. Results are cumulated after normalization by the dry weight (kg) of waste rocks tested in each humidity cell. For all the humidity cell tests, SO_4 and REE release rates (inflexion point in the cumulative curves) are observed after approximately 35 to 150 days, depending on the materials, and remain increase gradually through the remaining test duration. Figure 4-7e shows that REE leaching is proportional to the sulfide content of the waste rocks, as REE-bearing carbonates dissolve in response to the acid generated from sulfide oxidation. For example, after 535 days, approximately 0.10 mg/l of REE were produced by Brec (the most sulphide-rich material), compared to less than 0.04 mg/l for the FeC-LG (the less sulphidic). Furthermore, because of REE precipitation as suggested by thermodynamical calculations, it is clear that SO_4 vs REE does not give a correlation coefficient equal to 0.99 (Figure 4-7e).

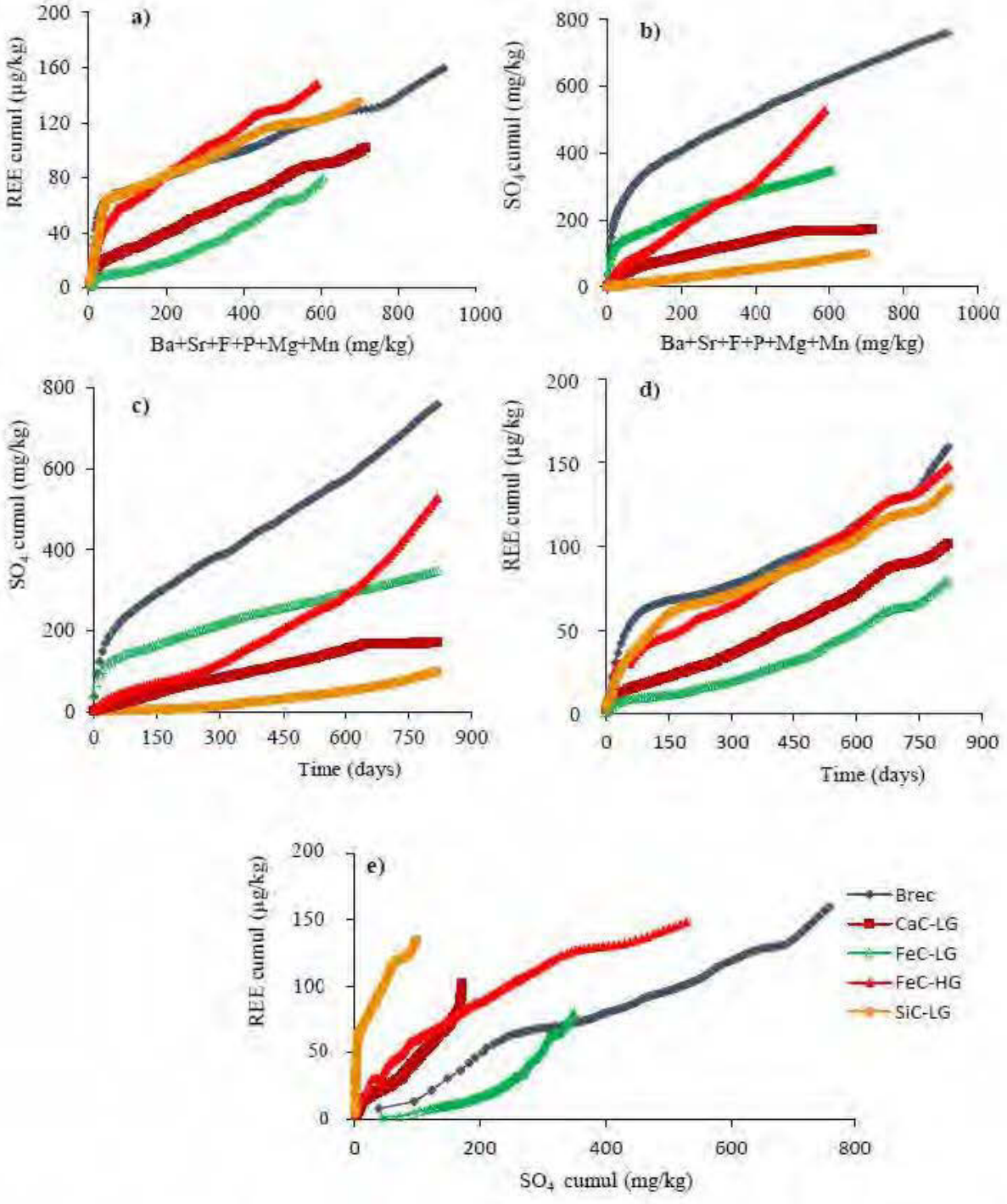

Figure 4-7 : Cumulative loads from the humidity cell tests on the Montviel sample: a) REE vs Ca+Mg+Mn+Ba+Sr+F, b) SO_4 vs Ca+Mg+Mn+Ba+Sr+F, c) cumulative sulfate loads, d) cumulative REE loads and e) REE vs SO_4.

The depletion curves of Ca, REE, Ba, Sr, and F (carbonates dissolution) and S (sulfide oxidation) are shown in Figure 4-8. The depletion curves show two types of depletion: (i) a first one for Na and F, characterized by a rapid elemental decrease, followed by stabilization after 105-245 days depending on the sample, and (ii) a second one for Ba, Sr, and Ca, characterized

by a very low depletion all through the tests (the rate depletion does not exceed 5 % for 819 days). REE depletions are negligible (less than 0.003 %). The Ba, Sr, and Ca release rates, related to barytocalcite, calcite, ankerite, strontianite, Celestine dissolution, while the F and Na, related mainly to burbankite and apatite dissolution respectively.

As for SO_4^{2-} and the elements related to carbonate dissolution, the rapid Na and F depletions observed in the first depletion stage and their subsequent decreases may be explained by three mechanisms: (i) dissolution of readily soluble phases, (ii) dissolution of fine particles, and (iii) surface passivation due to secondary minerals precipitation (Villeneuve et al., 2003; Benzaazoua et al., 2004; Plante et al., 2010). Furthermore, the Na and F depletion slopes of samples are steeper than those of the other elements (REE, Ca, Sr, Ba) while the S depletion slopes of the all samples are low and similar. The low slopes of depletion may be explained as following: (i) elements are leached and precipitated as suggested by Vminteq and PHREEQC, and/or (ii) REE-Ca-Sr-Ba bearing minerals are less reactive. The S reaction rates for all samples studied vary between 0.124 and 0.951 mg/l/d. The reaction rates obtained from the waste rocks are the same order. Moreover, the S reaction rates are significantly higher in the Brec samples (0.951 mg/l/d) and lowest in SiC-LG samples (0.124 and 0.951 mg/l/d). These results explain that the carbonate minerals seem to dissolve faster in Brec in comparison with other samples. In the basic conditions encountered in this study, REE could precipitate mainly as $REEPO_4$ as suggest by thermodynamic simulations and/or co-precipitate with other iron oxides- hydroxides (i.e. hematite, goethite, ferrihydrite, magnetite, etc.) (Valente et al., 2012).

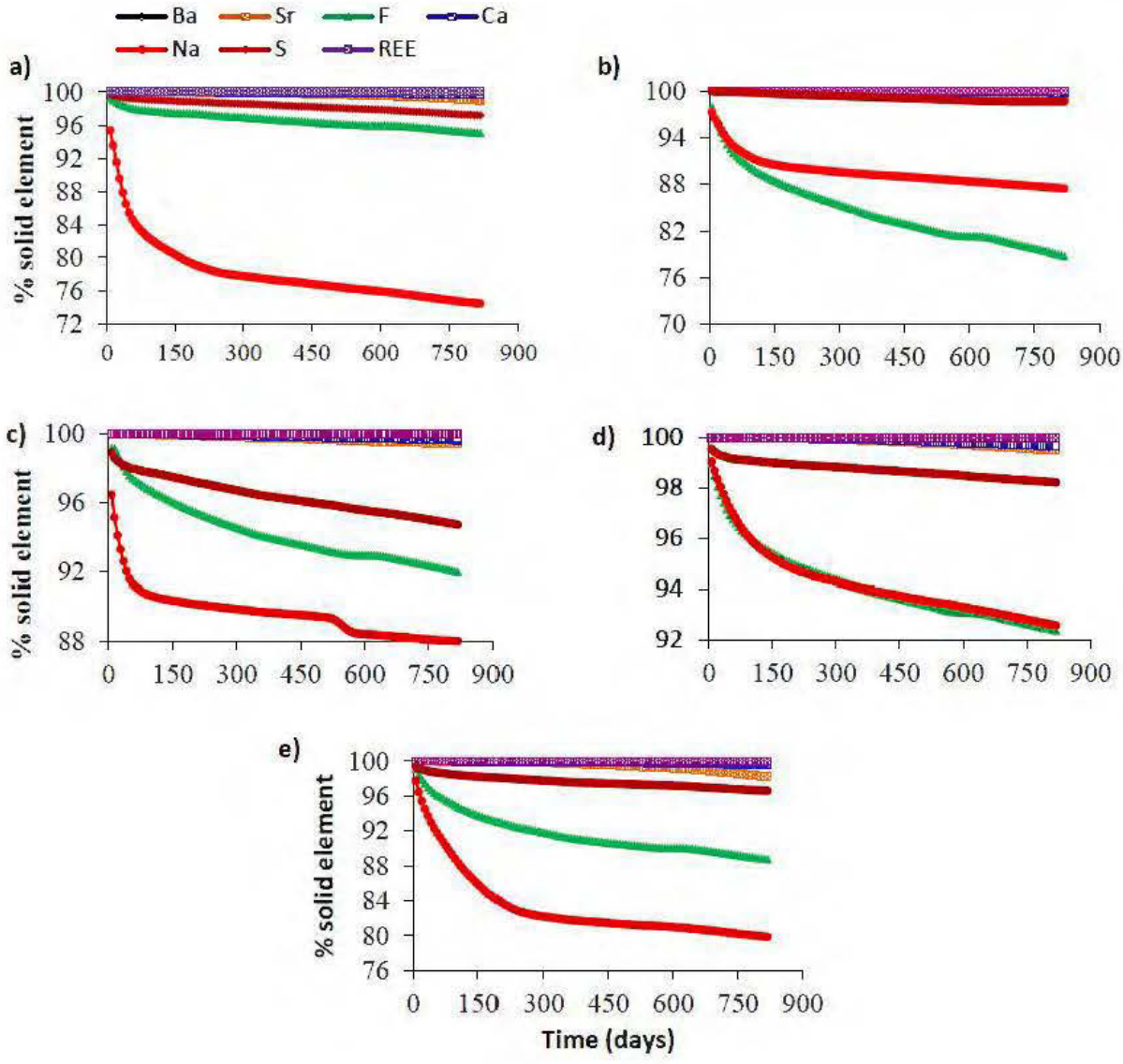

Figure 4-8 : Depletion curves of Ca, REE, Ba, Sr, and F within Brec (a), CaC (b), FeC-LG (c), FeC-HG (d), and SiC-LG (e).

4.4.5 Effect of pH, secondary minerals and colloids on REE distribution

The humidity cell leachates data were submitted to thermodynamical equilibrium calculations using the PHREEQC software using a database provided by the BRGM. The precipitation of secondary minerals and REE speciation calculations are discussed in the present section. The pH effect (pH between 2 and 11) on REE speciation is calculated using the mean water quality data from the FeC-HG humidity cell (richest lithology in REE); the results obtained are shown in Figure 4-9. The concentration of free REE^{3+} ion increase significantly at acidic pH values. The content of all REE^{3+} in the leachates is between 10^{-11} and 10^{-8} mg/l for pH values of 2.6-6.0. When pH increases from 6 to 10, the concentrations of REE^{3+} significantly decrease to

10^{-16} mg/l. This depletion on REE^{3+} concentration decreases can be explained by the REE precipitation as secondary minerals. The PHREEQC calculation suggests the precipitation of a variety of secondary oxy-hydroxides of Fe, Mn and Al (e.g. diaspore, gibbsite, greenalite, imogolite, bixbyite, ferrihydrite) as well as REE phosphates. This finding is coherent with the work of Sun et al., (2011), in which dissolved REE decreased from 520 to 0.875 µg/l, as the pH increased from acidic to neutral pH. Moreover, other authors demonstrated that REE and pH have a negative correlation (as pH increases a total dissolved REE decreases and vice versa) (Janssen and Verweij 2003; Leybourne et al., 2000; Sun et al., 2011; Verplanck et al., 2004). Therefore, in the range of pH values obtained in the humidity cell tests, Fe, Al, and Mn probably form secondary minerals and colloids, which may control the REE concentrations in the leachates (Figure 10). Other studies (Bau 1999; Prudêncio et al., 2015, 2017) showed that Fe and Mn secondary minerals mainly sequester LREE from the solution, while the Al oxyhydroxides mainly sorb HREE. On the other hand, REE fractionation may also be controlled by weathering reactions, surface adsorption, and solution chemistry (Yusoff et al., 2013; Stille et al., 2006).

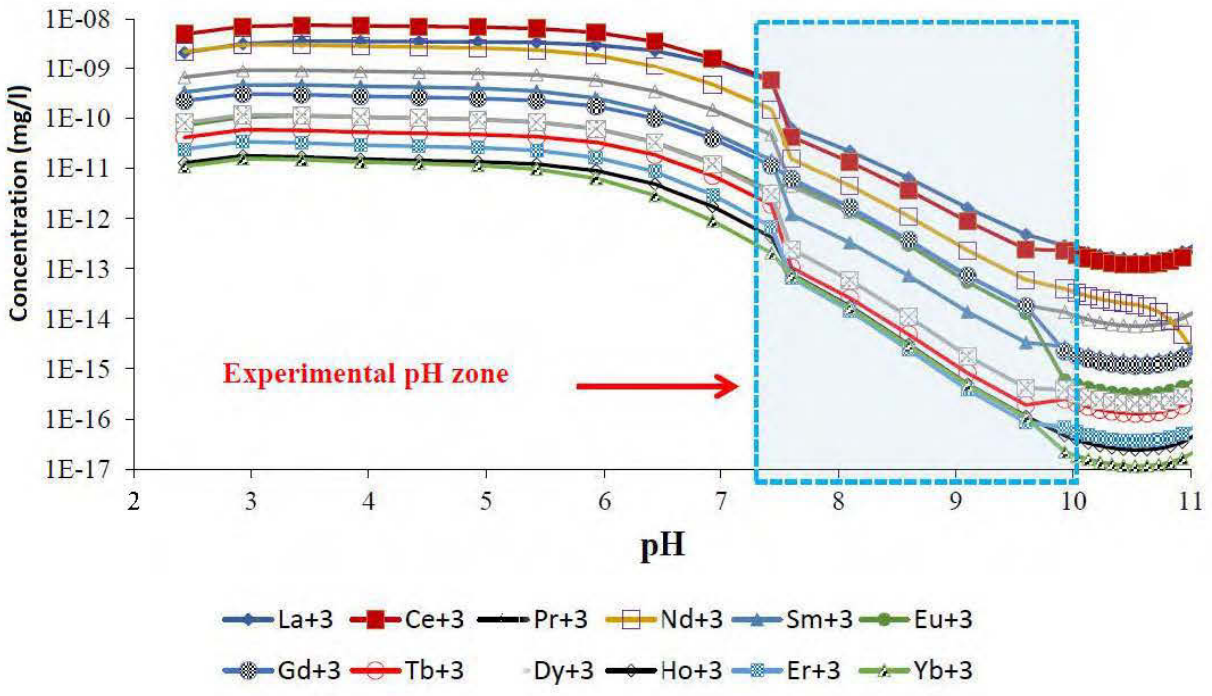

Figure 4-9 : Effect of pH on REE concentration.

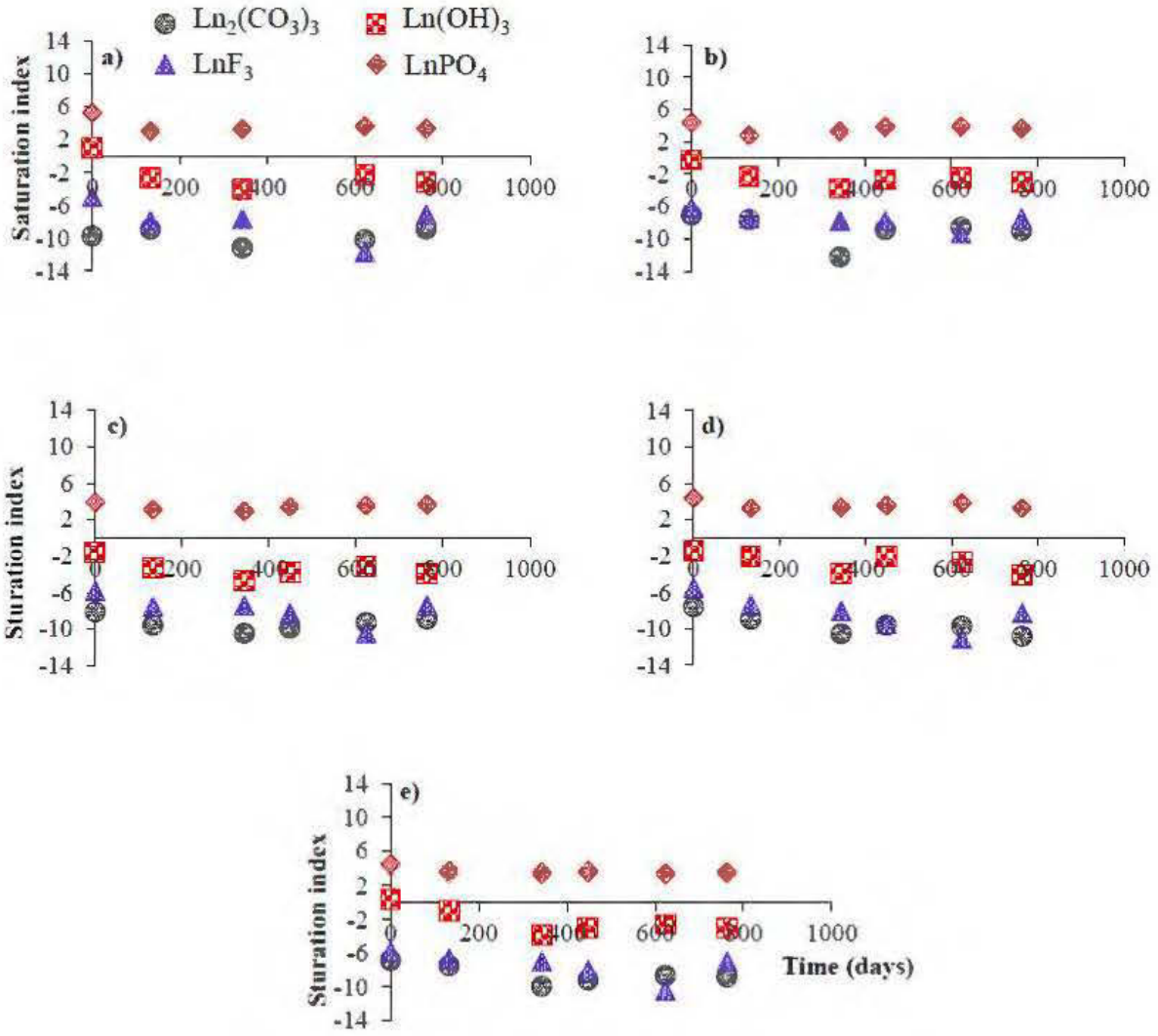

Figure 4-10 : Saluration indices of lanthanides (Ln) phosphates, fluorides, carbonates, and hydroxides on REE fractionation; a) Brec, b) CaC, c) FeC-HG, d) FeC-LG, and e) SiC-LG.

4.4.6 REE speciation in the leachates

The REE speciation could influence the mobility of REE, which, in some cases, could explain their distribution patterns in the leachates. REE are mainly associated with carbonates ligands in neutral or alkaline waters, and the greater stability of HREE-CO_3^{2-} complexes hinders the adsorptive removal of the HREE in comparison with the LREE (Gimeno et al., 2000). Because of the abundance of carbonates anions in the Montviel humidity cell leachates, sulfate and fluoride will not be the main ligands that may form aqueous complexes with the REE ($REEF_3$ and $REESO_4$ were always undersaturated as suggested by PHREEQC). The phosphorous concentrations (0.0045 to 0.056 mg/l) are low relative to sulfate (0.4 to 43 mg/l), and fluoride (0.01 to 3.18 mg/l). Despite lower phosphorus levels, they may exert a significant influence on

REE fractionation between aqueous and solid phases (Figure 4-11). Moreover, the speciation calculations show that the HREE carbonate and hydroxides complexes ($Ln(CO_3)^{2-}$, $(LnCO_3)^{+}$, $Ln(OH)^{2+}$) were more abundant (76 %) than those of LREE (47 %). Sulfate, phosphate, carbonates, and fluoride complexes $Ln(SO_4)^{+}$, $(LnHPO_4^{+})$, $Ln(HCO_3)^{2+}$, and $(LnF_2)^{+}$, constitute less than 4 % of the REE-complexes. The $CePO_{4(aq)}$, $GdPO_{4(aq)}$, $YbPO_{4(aq)}$ proportions are 48 %, 58 %, and 73 %, respectively. With respect to the free ion metal, HREE3+ proportions (14%) are lower in comparison with $LREE^{3+}$ proportions (32 %). Furthermore, the REE selective precipitation may occur with a fixed phosphorus concentration and variable pH (Figure 4-11), which suggest that LREE phosphates precipitate at pH =3.6-4.8, while HREE phosphates precipitate at pH =4-6. In other works, fluoride is strongly associated with Al^{3+} in acid waters (Gimeno et al., 2000), and phosphate forms preferentially ion pairs with calcium and magnesium (Johannesson et al., 1996). As a result, it is clear that all these parameters (i.e. pH, complexation, adsorption, precipitation or co-precipitation) could cause the REE fractionation and therefore influence their mobility. The quantification of this mobility may give important ideas on the degree of REE fractionation in humidity cells. HREE(s)/LREE(s) and LREE(aq)/HREE(aq) using the cumulative/ normalized were compared and defined as mobility.

$$\text{Mobility} = ((\text{HREE(s)}/\text{LREE(s)})\ )/(\ (\text{HREE(aq)}/\text{LREE(aq)}))$$

with s: solid and aq: aqueous

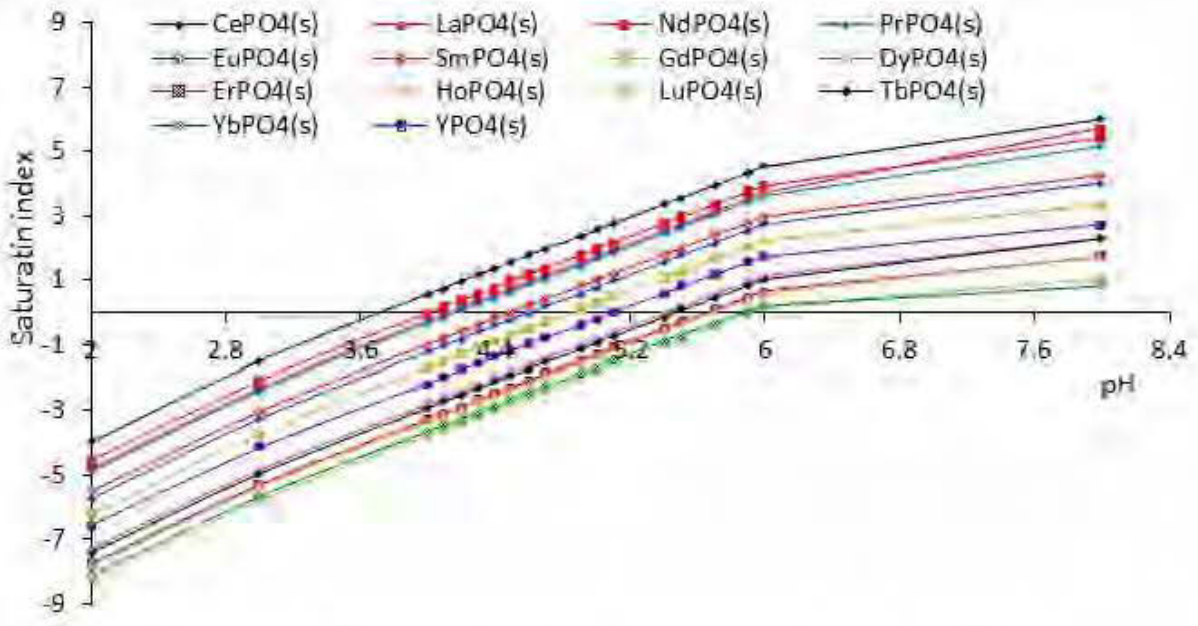

Figure 4-11 : Effect of pH on selective precipitation of REE phosphates.

When the mobility is equal to 1, The (HREE/LREE) ratios are equal in both solids and leachates. This suggest that there is no difference between LREE and HREE mobility. However, when mobility is lower than 1, the (HREE/LREE) ratio is higher in the leachates than in the solids. This also suggests that HREE are leached preferentially and/or that they are more mobile than LREE. Moreover, with the exception of SiC-LG, humidity cell results show that HREE mobility is higher compared to LREE (Table 4-4). This can be explained by: (i) LREE precipitation as suggested by PHREEQC, (ii) proprtion of $LREE^{3+}$ is higher compared to $HREE^{3+}$ (adsorption, precepitation and/or co precepitation are favorable), and (iii) high HREE complexation with carbonates and hydroxides accelerate their mobility. Morover, REE mobility may be influenced by several factors: (i) pH, (ii) ionic strength, (iii) presence or absence of organic matter, (iv) and temperature (Purdy 2014; Sapsford et al., 2012; Stille et al., 2006).

Tableau 4-4 : REE mobility in studied samples from Montviel waste rocks.

		Unit	Brec	CaC	FeC-LG	FeC-HG	SiC
Solid	$LREE_{(s)}$	mg/l	0.69	1.10	0.81	2.85	0.45
	$HREE_{(s)}$	mg/l	0.07	0.08	0.03	0.08	0.06
Leachate	$LREE_{(aq)}$	mg/l	0.14	0.09	0.07	0.15	0.12
	$HREE_{(aq)}$	mg/l	0.02	0.01	0.01	0.01	0.01
Mobility Parameters	HREE(s) / LREE(s)	-	0.10	0.07	0.04	0.03	0.12
	HREE(aq) / LREE(aq)	-	0.10	0.15	0.11	0.07	0.08
	Mobility	-	0.97	0.50	0.34	0.40	1.48

4.5 Conclusions

SEM-EDS results show that: (i) the REE are associated with carbonates; (ii) all analysed minerals contain mostly LREE (La, Ce, Pr, Nd, Sm, Eu and Gd); (iii) the sum of LREE in each analysed mineral varies between ~ 3 and 10 wt %; (iv) the HREE identified are Gd and Yb with less than 0.4 % in all REE-bearing minerals; (v) three groups of carbonate minerals were observed with variable concentrations of Ca, Na, and F; and (vi) the majority of REE-bearing minerals are contained in finer fraction (- 106 µm). Humidity cell results indicate that the leachability of REE from the studied samples is low in humidity cell conditions and HREE are leached preferentially and/or that they are more mobile than LREE.The pH, the precipitation of secondary minerals, and colloids of Fe, Al, Mn, and phosphorous could affect the fractionation of dissolved REE at different levels. The increase of pH produces a REE fractionation by precipitating them as insoluble salts (i.e. $REEPO_4$). The Mn and Fe in the solids have a negative

correlation with LREE (R^2 Mn 0.95, R^2 Fe 0.90), while it exhibits a positive correlation with Al (R^2 Al 0.98). This suggest that Fe and Mn oxides produce a LREE fractioation, while Al oxides increase REE mobility.

4.6 Acknowledgements

The authors thank the URSTM, staff for their support with laboratory work and NSERC/Geomega Resources for funding of this study.

References

Adam, K., Kourtis, A., Gazea, B., and Kontopoulos, A. (1997). Evaluation of static tests used to predict the potential for acid drainage generation at sulfide mine sites. Trans. Instn.Min.Metall. sect.A:min.industry. 106. January-April: A1-A8.

Bau, M., (1999). Scavenging of dissolved yttrium and rare earths by precipitating iron oxyhydroxide: experimental evidence for Ce oxidation, Y-Ho fractionation, and lanthanide tetrad effect. Geochimica et Cosmochimica Acta, 63(1): 67-77.

Benzaazoua, M., Bussiére, B., Dagenais, A. M., and Archambault, M. (2004). Kinetic tests comparison and interpretation for prediction of the Joutel tailings acid generation potential. Environmental Geology, 46(8), 1086-1101. doi:10.1007/s00254-004-1113-1.

Bussière, B. (2007). Colloquium 2004: Hydrogeotechnical properties of hard rock tailings from metal mines and emerging geoenvironmental disposal approaches. Canadian Geotechnical Journal, 44(9), 1019-1052. doi:10.1139/t07-040.

David, J., Dion, C., Goutier, J., Roy, P., Bandyayera, D., Legault, M., and Rhéaume, P. (2006). Datations U-Pb effectuées dans la Sous-province de l'Abitibi à la suite des travaux de 2004-2005. Ressources naturelles et Faune. RP 2006-04, Quebéc- Canada.

Desharnais, G., and Duplessis, C. (2011). Montviel core zone REE mineral resource estimate technical report, Quebec. Geomega Resources Inc. Member of SGS group (SGS SA).

Edahbi M., Plante B., Bouzahzah H., and Benzaazoua M. (2015). Mineralogical and geochemical study of rare earth elements from a carbonatite deposit. Proceedings of the 13th SGA biennial meeting, Nancy, France.

Gimeno Serrano MaJ., Auqué Sanz LF., and Nordstrom D.K. (2000). REE speciation in low-temperature acidic waters and the competitive effects of aluminum. Chemical Geology 165:167-180.

Gonzalez, V., Vignati, D. A. L., Leyval, C., and Giamberini, L. (2014). Environmental fate and ecotoxicity of lanthanides: Are they a uniform group beyond chemistry? Environment International, 71(0), 148-157.

Goutier, J. (2006). Géologie de la région du lac au Goéland (32F/15): Ressources naturelles et Faune, Québec.

Jaireth, S., Hoatson, D. M., and Miezitis, Y. (2014). Geological setting and resources of the major rare-earth-element deposits in Australia. Ore Geology Reviews, 62(0), 72-128.

Janssen, R. P. T., and Verweij, W. (2003). Geochemistry of some rare earth elements in groundwater, Vierlingsbeek, The Netherlands. Water Research, 37(6), 1320-1350.

Johannesson, K.H, Lyons, W.B, Yelken, M.A, Gaudette, H.E., Stetzenbach, K.J. (1996) Geochemistry of the rare-earth elements in hypersaline and dilute acidic natural terrestrial waters: complexation behavior and middle rare-earth element enrichments. Chem Geol 133(1-4):125–144.

Kato, Y., Fujinaga, K., Nakamura, K., Takaya, Y., Kitamura, K., Ohta, J., Iwamori, H. (2011). Deep-sea mud in the Pacific Ocean as a potential resource for rare-earth elements. Nature Geosci, 4(8), 535-539.

Kwitko-Ribeiro, R. (2012). New sample preparation developments to minimize mineral segregation in process mineralogy. Paper presented at the Proceedings of the 10th International Congress for Applied Mineralogy (ICAM).

Lawrence R., Wang Y. (1996). Determination of neutralization potential for acid rock drainage prediction. MEND project 1:38.

Leybourne, M. I., Goodfellow, W. D., Boyle, D. R., and Hall, G. M. (2000). Rapid development of negative Ce anomalies in surface waters and contrasting REE patterns in groundwaters associated with Zn–Pb massive sulphide deposits. Applied Geochemistry, 15(6), 695-723.

Lipin, B. R. (1989). Geochemistry and mineralogy of rare earth elements. Reviews in mineralogy, 21.

McLellan, B. C., Corder, G. D., Golev, A., and Ali, S. H. (2014). Sustainability of the Rare Earths Industry. Procedia Environmental Sciences, 20, 280-287.

Merkus, H. G. (2009). Particle size measurements: fundamentals, practice, quality (Vol. 17): Springer Science and Business Media.

Miekeley, N., Coutinho de Jesus, H., Porto da Silveira, C. L., Linsalata, P., and Morse, R. (1992). Rare-earth elements in groundwaters from the Osamu Utsumi mine and Morro do Ferro analogue study sites, Poços de Caldas, Brazil. Journal of Geochemical Exploration, 45(1), 365-387.

Nadeau, O., Stevenson, R., and Jébrak, M. (2016). Evolution of Montviel alkaline-carbonatite complex by coupled fractional crystallization, fluid mixing and metasomatism, part II: Trace element and Sm–Nd isotope geochemistry of metasomatic rocks: implications for REE-Nb mineralization. Ore Geology Reviews, 72, Part 1, 1163-1173.

Nadeau, O., Cayer, A., Pelletier, M., Stevenson, R., and Jébrak, M. (2015). The Paleoproterozoic Montviel carbonatite-hosted REE–Nb deposit, Abitibi, Canada: Geology, mineralogy, geochemistry and genesis. Ore Geology Reviews, 67, 314-335.

Nadeau, O., Cayer, A., Pelletier, M., Séguin, D., Stevenson, R., and Jébrak, M. (2014). Pétrométallogenèse du système alcalin carbonatitique (ETR-Nb) de Montviel, Abitibi. Conférences, séance 12.

Nadeau, O., Stevenson, R., and Jébrak, M. (2014). The Archean magmatic-hydrothermal system of Lac Shortt (Au-REE), Abitibi, Canada: Insights from carbonate fingerprinting. Chemical Geology, 387, 144-156.

Nordstrom, D.K. (2011). Hydrogeochemical processes governing the origin, transport and fate of major and trace elements from mine wastes and mineralized rock to surface waters. Applied Geochemistry 26, 1777-1791.

Parkhurst, D. L., and Appelo, C. (2013). Description of input and examples for PHREEQC version 3: a computer program for speciation, batch-reaction, one-dimensional transport, and inverse geochemical calculations (2328-7055).

Plante, B., Benzaazoua, M., and Bussière, B. (2010). Predicting Geochemical Behaviour of Waste Rock with Low Acid Generating Potential Using Laboratory Kinetic Tests. Mine Water and the Environment, 30(1), 2-21.

Plante, B., Bussière, B., and Benzaazoua, M. (2012). Static tests response on 5 Canadian hard rock mine tailings with low net acid-generating potentials. Journal of Geochemical Exploration, 114, 57-69. doi:10.1016/j.gexplo.2011.12.003.

Price, WA. (2009). Prediction manual for drainage chemistry from sulphidic geologic materials. MEND report 1:579.

Prinčič, T., Štukovnik, P., Pejovnik, S., De Schutter, G., and Bokan Bosiljkov, V. (2013). Observations on dedolomitization of carbonate concrete aggregates, implications for ACR and expansion. Cement and Concrete Research, 54, 151-160.

Prudêncio MI., Valente T., Marques R., Braga MAS., Pamplona J. (2017). Rare Earth Elements, Iron and Manganese in Ochre-precipitates and Wetland Soils of a Passive Treatment System for Acid Mine Drainage. Procedia Earth and Planetary Science 17:932-935.

Prudêncio, MI., Valente, T., Marques, R., Braga, MAS., Pamplona J. (2015). Geochemistry of rare earth elements in a passive treatment system built for acid mine drainage remediation. Chemosphere 138:691-700 .

Purdy, C. (2014). The Geochemical and Mineralogical Controls on the Environmental Mobility of Rare Earth Elements from Tailings, Nechalacho Deposit, Northwest Territories. Msc thesis, Queen's University.

Sapsford DJ., Bowell RJ., Geroni JN., Penman KM., Dey M. (2012). Factors influencing the release rate of uranium, thorium, yttrium and rare earth elements from a low grade ore. Minerals Engineering 39:165-172.

Sneller, F. E. C., Kalf, F. D., Weltje, L., and Wezel, A. P. V. (2000). Maximum Permissible Concentrations and Negligible Concentrations for Rare Earth Elements (REEs). Research for man and environnement

Sobek, A. (1978). Field and laboratory methods applicable to overburdens and minesoils: Industrial Environmental Research Laboratory, Office of Research and Development, US Environmental Protection Agency.

Steinmann, M., and Stille, P. (2008). Controls on transport and fractionation of the rare earth elements in stream water of a mixed basaltic–granitic catchment basin (Massif Central, France). Chemical Geology, 254(1-2), 1-18.

Stille P., Steinmann M., Pierret MC. (2006). The impact of vegetation on fractionation of rare earth elements (REE) during water–rock interaction. Journal of Geochemical Exploration 88:341-344.

Sun, H., Zhao, F., Zhang, M., and Li, J. (2011). Behavior of rare earth elements in acid coal mine drainage in Shanxi Province, China. Environmental Earth Sciences, 67(1), 205-213. doi:10.1007/s12665-011-1497-7.

Valente, T.M., Antunes, M., Braga, AS., Prudêncio, M., Marques, R., Pamplona, J. (2012). Mineralogical attenuation for metallic remediation in a passive system for mine water treatment. Environmental Earth Sciences 66:39-54.

Verplanck, P. L., Nordstrom, D. K., Taylor, H. E., and Kimball, B. A. (2004). Rare earth element partitioning between hydrous ferric oxides and acid mine water during iron oxidation. Applied Geochemistry, 19(8), 1339-1354.

Villeneuve, M., Bussière, B., Benzaazoua, M., and Aubertin, M. (2009). Assessment of interpretation methods for kinetic tests performed on tailings having a low acid generating potential. Proceedings, Securing the Future and 8th ICARD, Skelleftea, Sweden.

Villeneuve, M., Bussière, B., Benzaazoua, M., Aubertin, M., and Monroy, M. (2003). The influence of kinetic test type on the geochemical response of low acid generating potential tailings. Paper presented at the Proc, Tailings and Mine Waste.

Wang, L., and Liang, T. (2014). Effects of exogenous rare earth elements on phosphorus adsorption and desorption in different types of soils. Chemosphere, 103, 148-155.

Yang, X. J., Lin, A., Li, X.-L., Wu, Y., Zhou, W., and Chen, Z. (2013). China's ion-adsorption rare earth resources, mining consequences and preservation. Environmental Development, 8, 131-136.

Yusoff, ZM., Ngwenya, BT., Parsons, I. (2013). Mobility and fractionation of REEs during deep weathering of geochemically contrasting granites in a tropical setting, Malaysia. Chemical Geology 349–350:71-86.

CHAPITRE 5 ARTICLE 4 : RARE EARTH ELEMENTS (La, Ce, Pr, Nd, Sm) FROM A CARBONATITE DEPOSIT: MINERALOGICAL CHARACTERIZATION AND GEOCHEMICAL BEHAVIOR

Cet article est accepté dans la revue Minerals, 2018

Edahbi, M.[a]; Plante, B.[a]; Benzaazoua, M.[a]; Kormos, L.[b]; Pelletier, M.[C]

[a] Université du Québec en Abitibi-Témiscamingue (UQAT), 445 boul de l'Université, Rouyn-Noranda J9X 5E4, QC, Canada.

[b]XPS Consulting &Testwork Services, 6 Edison Road, Falconbridge, ON, P0M1S0, Canada

[C]Ressources Géoméga, St-Lambert, Canada

5.1 Abstract

Geochemical characterization including mineralogical measurements and kinetic testing was completed on samples from the Montviel carbonatite deposit, located in Quebec (Canada). Three main lithological units representing both waste and ore grades were sampled from drill core. A rare earth elements (REE) concentrate was produced through a combination of gravity and magnetic separation. All samples were characterized using several mineralogical techniques (i.e., quantitative evaluation of minerals by scanning electron microscopy or QEMSCAN, X-ray diffraction (XRD), and scanning electron microscopy with X-ray microanalysis or SEM-EDS) in order to quantify modal mineralogy, liberation, REE deportment and composition of REE-bearing phases. The REE concentrate was then submitted for kinetic testing (weathering cell) in order to investigate the REE leaching potential. The mineralogical results indicate that: (i) the main REE-bearing minerals in all samples are burbankite, kukharenkoite-Ce, monazite, and apatite; (ii) the samples are dominated by REE-free carbonates (i.e. calcite, ankerite, and siderite), and (iii) LREE is more abundant than HREE. Grades of REE minerals, sulfides and oxides are richer in the concentrate than in the host lithologies. The geochemical test results show that low concentrations of light REE are leached under kinetic testing conditions (8.8-139.6 µg/l total light REE). These results are explained by a low reactivity of the REE-bearing carbonates in the kinetic testing conditions, low amounts of REE in solids, and by precipitation of secondary REE minerals.

Keywords: Carbonatite; rare earth elements; Gravity Concentration; QEMSCAN® mineralogy; geochemical behavior; kinetic tests

5.2 Introduction

5.2.1 REE background

In recent decades, rare earth elements (REE), also called lanthanides (La to Lu, Sc, and Y), have been considered strategic metals, as they are a key component in the manufacturing of modern technologies. Their economic importance has grown as a result of their use in a wide range of industries including the manufacturing of products aimed at environmental conservation and sustainability. Applications include use in hybrid vehicles, radar systems, rechargeable batteries, mobile phones, flat screen display panels, compact fluorescent light bulbs, electronic products, etc.

These elements are often classified into two main categories: light (LREE, La to Gd) and heavy (HREE, Tb to Lu) rare earth elements. Currently, China produces 99 % of HREE and 87 % of LREE (Catinat, 2010) and has a significant influence on REE prices. The global demand for REE was expected to reach 160 000 tons in 2016 with the annual demand in China predicted to rise from 70 000 tons to 105,000 tons between 2011 and 2016 (Humphries, 2013). Because of their dominance in both production and research and development, China is well positioned in the industry compared to other countries. However, the global demand combined with REE importance to clean technology development has led countries, including USA, Japan, and the European Union to voice concerns regarding supply chain risk. As a result, more REE exploration projects are being funded around the world, particularly in the Americas (e.g., Canada, Brazil, USA) (Mariano and Mariano, 2012). Unfortunately, investment into REE exploration is still underfunded due to risks associated with relative scarcity and complexity of the deposits. Additional risk comes from price fluctuations created by changes in exports coming out of China. For example, in 2011 China reduced their REE exports which resulted in a significant increase of REE prices (Cox and Kynicky, 2017; Massari and Ruberti, 2013; Schlinkert and Boogaart, 2015). The REE industry (the exploration companies and the companies that have operations in production) is present worldwide through close to 30 companies (Cox and Kynicky, 2017), several of which are in serious financial difficulty (Chakhmouradian et al., 2015).

REE extraction from ores is challenging because of its complex mineralogy and complicated and costly processing. REE-bearing minerals have structural and chemical properties that do not facilitate their separation from gangue minerals (e.g., carbonates, phosphates, silicates, etc.). Each

mineralogical suite requires a unique processing flowsheet thus a successful process for one deposit may not work for a different deposit. REE are typically processed using flotation, magnetic and electrostatic separation, gravity upgrading (Mozley Table, Falcon and Knelson concentrators, etc.) as well as hydrometallurgical treatment, followed by acid or alkaline leaching.(Dehaine et al., 2015; Filippov et al., 2016; Jordens et al., 2016) Most operations have complex flowsheets using combinations of the above techniques.

REE ores are often contaminated with actinides such as thorium, niobium and uranium, and other contaminants (e.g., Ba, Sr, Mn, Ta) (Chakhmouradian et al., 2017; Nadeau et al., 2015). Social responsibility of REE producers is an important issue for investors. Several publications found in the literature have reported significant environmental issues caused by REE mining and refining(Hurst, 2010; Weber and Reisman, 2012). In China, the use of acids to recover REE leads to the deterioration in water quality in the surrounding environment. In Malaysia, radioactive wastes were stored in ambient surface conditions and consequently generated deleterious impacts on the environment (Pecht et al., 2011).

The distribution and concentrations of REE vary depending on the geological context (e.g., alkaline and hyperalkaline igneous rocks, carbonatites, cationic clays, sedimentary rocks) (Chakhmouradian and Zaitsev, 2012; Kynicky et al., 2012). Within magmatic deposits, REE are mainly concentrated by fractional crystallization (Chakhmouradian et al., 2017; Chakhmouradian and Wall, 2012; Orris and Grauch, 2002; Williams-Jones et al., 2012).The main REE-bearing phases are silicates, carbonates, fluocarbonates, oxides, phosphates, and sulfates (Chakhmouradian and Zaitsev, 2012; Edahbi et al., 2017; Kanazawa and Kamitani, 2006; Verplanck and Gosen, 2011; Zaitsev et al., 1998). Because REE deposits are characteristically large-tonnage, low-grade operations, recycling of many electronic products could be presented an alternative REE source (e.g., phosphor lamps, batteries, permanent magnets) (Binnemans et al., 2013). Worries over supply disruptions have fueled exploration for REE deposits in other parts of the world such as Australia (e.g., Mount Weld), USA (e.g., Mountain Pass), and Canada (e.g., Montviel, Kipawa). REE deposits can be found in different geological settings, especially associated with magmatism(Chakhmouradian and Wall, 2012; Schmid, 1981). Carbonatites are known for their LREE potential due to the favorable geological context for LREE-bearing minerals crystallization and formation (Andrade et al., 1999; Nadeau et al., 2015; Zaitsev et al., 2014b).

Carbonatites are igneous rocks containing more than 50 % primary carbonates and classified according to their content of CaO, MgO, ($FeO + Fe_2O_3 + MnO$), and SiO_2. The most common types of carbonatites are: calciocarbonatite, magnesiocarbonatites, ferrocarbonatite, and silico-carbonatites(Schmid, 1981). Carbonatites are characterized by: (i) abundant carbonates minerals (i.e. calcite, ankerite, dolomite, and siderite), (ii) various accessory minerals as phosphates, fluocarbonates, iron oxides, and REE-bearing minerals (e.g., burbankite, xenotime, bastnasite, carbocernaite, kukharenkoite, monazite etc.) (Chakhmouradian et al., 2017). Carbonatite deposits are known to be associated with alkaline intrusions. They are more enriched in LREE compared to HREE. One way this enrichment can be explained is by fractional crystallization (Nadeau et al., 2016) and chemical substitution between REE and other cations of carbonate minerals. During magma cooling, the LREE elements remain in the liquid phase while higher temperature minerals crystallize. REE crystallization with carbonate minerals occurs at the end of the fractionation process (Chakhmouradian and Wall, 2012).

Several carbonatite deposits in Canada have emerged as a possible resource for REE, such as the Montviel deposit (Lebel-sur-Quévillon, Québec, Canada). The REE-bearing minerals within the Montviel deposit are contained mainly in ferrocarbonatites, breccia, and calcio/silico-carbonatites.

5.2.2 Geochemical behavior of REE

REE can be found in three forms: (i) associated with suspended particles, (ii) associated with colloidal microparticles, and (iii) free and/or dissolved ions. With the exception of Ce (IV) and Eu (II), REE are in trivalent state (Ln^{3+}) (Bau, 1999; Censi et al., 2014). They tend to be fractionated by the other metallic elements M^{3+}. They can also be complexed with inorganic and/or organic ligands such as carbonates, halides, sulfates, phosphates, and organic matter.

REE mining operations, as in any mining operation, generate a lot of solid and liquid waste (i.e. waste rocks, tailings, and mining effluents). In addition, due to low-grades, only near surface, high-tonnage REE deposits can be economically exploited, usually by open-pit mining. These wastes, with no commercial value, are often stored on surface. This disposal of REE mine wastes represent serious environmental concern (Hurst, 2010). Indeed, several examples of environmental damage caused by REE extraction were reported in the literature such as in Malaysia, USA, and China (Weber and Reisman, 2012). REE mine wastes contain various contaminants such as metals, REE, and radioactive elements (e.g., thorium and niobium) (Edahbi et al., 2017; Massari and Ruberti,

2013). For example, the Mountain Pass mine produced approximately 3000 l/min of wastewater containing thorium and uranium.

There are significant knowledge gaps about REE-bearing mine wastes, particularly in terms of their reactivity, speciation, mobility, and toxicity (Sapsford et al., 2012). Partial or total dissolution of the REE-bearing minerals may release REE into surface and underground aquifers (Zhu et al., 2016). Water-rock interactions with mine waste influences the water quality associated with mine drainage. The release of REE and other associated elements is controlled by the mineralogical composition of the rocks and by pH, temperature, degree of saturation, secondary precipitation, and the presence of impurities within the reactive minerals.

In order to anticipate potential environmental impacts of REE mining, the prediction of REE leaching from mine wastes is required, even if these elements occur at low grades. Investigation of the geochemical behavior of REE mine waste requires extensive mineralogical characterization and kinetic testing on different lithologies of a given deposit. In order to better characterize REE-bearing minerals and to enhance the geochemical responses, a REE concentrate sample was prepared using gravity and magnetic separation (Dehaine et al., 2015; Jordens et al., 2014). The basic premise is that the weathering pattern observed for the concentrate is an amplified version of the original waste's behavior. This work aims to understand the geochemical behavior of the Montviel (carbonatite orebody) mine wastes including waste rocks and REE concentrate in order to predict the quality of the drainage water.

5.3 Materials and methods

The first part of this section presents a summary description of the Montviel mine site and the different procedures used to prepare and characterize the studied materials. The second part describes the main physical, chemical and mineralogical characteristics of samples (waste rocks and concentrate). Finally, the main geochemical results obtained from kinetic testing on the concentrate are presented.

5.3.1 Location and geological setting of Montviel deposit

The Montviel site is a future open-pit mine of rare earth elements. The Montviel deposit is located in the heart of the Canadian Shield, approximately 97 km north of Lebel-sur-Quévillon, Quebec, Canada. The REE mineralization within the deposit is hosted mainly in carbonatites, within the

Montviel alkaline proterozoic intrusion. The mining company GéoMéga Resources estimates the indicated resources to be approximately 183.9 Mt at 1.45 % total rare earth oxides (TREO) and an additional 66.7 Mt at 1.46 % TREO in the inferred resources category. The mineralized zone is mainly composed of five lithologies: silicocarbonatites, calciocarbonatites, magnesiocarbonatites, ferrocarbonatites and polygenic breccia. The mineralogical composition of these lithologies is mainly represented by carbonates (i.e. calcite, ankerite, siderite, barytocalcite, and strontianite), REE carbonates and REE-Ba-Sr mixtures(Goutier, 2006; Nadeau et al., 2015).

5.3.2 Sampling and preparation

The materials used in this work were supplied by Geomega Resources Inc. Approximately 5 kg of each lithology were sampled from exploration drill core: low-grade and high-grade ferrocarbonatites (FeC-LG and FeC-HG, respectively), and calciocarbonatite (CaC). Cores were crushed, then pulverized to mimic particle size distribution typical to the one targeted by ore processing.

In order to satisfy the characterization requirements (i.e. detection limit) and to more easily investigate the REE mineralogy and geochemical behavior during kinetic tests, REE were concentrated to increase the geochemical responses (Figure 5-1).

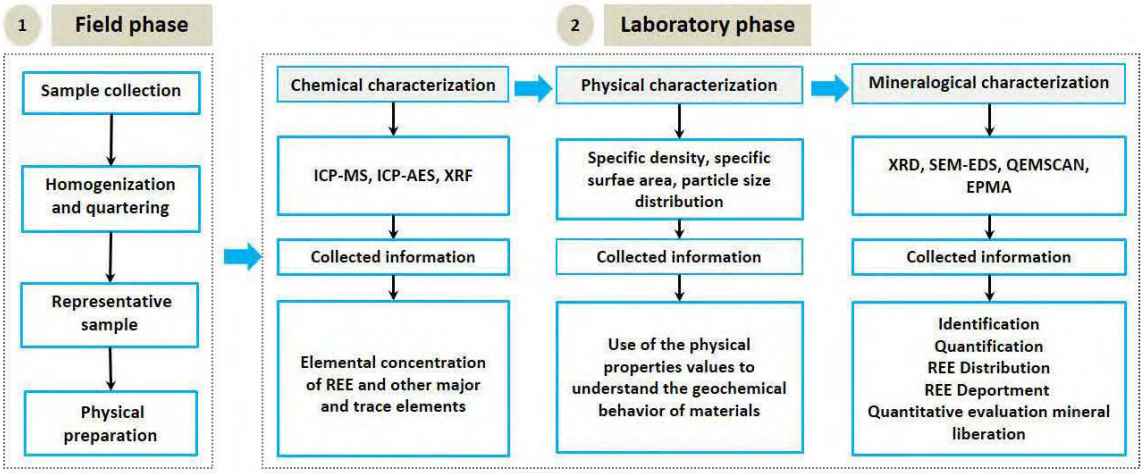

Figure 5-1 : REE-bearing minerals characterization methodology.

Due to their high density and magnetic properties, REE-bearing minerals were enriched using gravity and magnetic separation. Ferrocarbonatite high grade (FeC-HG) was used as feed for the enrichment process. The material was dried and sieved into four different fractions (-106 µm, -

315/+106 µm, -630/+315 µm, and -2 mm/+630 µm) to determine the REE distribution. The fractions were selected on the basis of the grain size distribution curve of the whole material to provide equivalent weight fractions. The heavier minerals appeared to be concentrated within the finest fraction, i.e. below 106 µm with 46275 ppm LREE (La, 16767 ppm; Ce, 27504 ppm; Pr, 2009 ppm). Slurry composed of water and solids (around 40 % solids) corresponding to each size fraction was prepared in the mixing tank before feeding the concentration process steps. Several stages of concentration using a Knelson concentrator and Mozley table were necessary to improve the grade of the concentrate (Figure 2). The final concentrate was created by mixing concentrates with the same initial proportions (raw sample FeC-HG). The separation efficiency was first verified through binocular loupe and then submitted to physical, chemical, and mineralogical characterization.

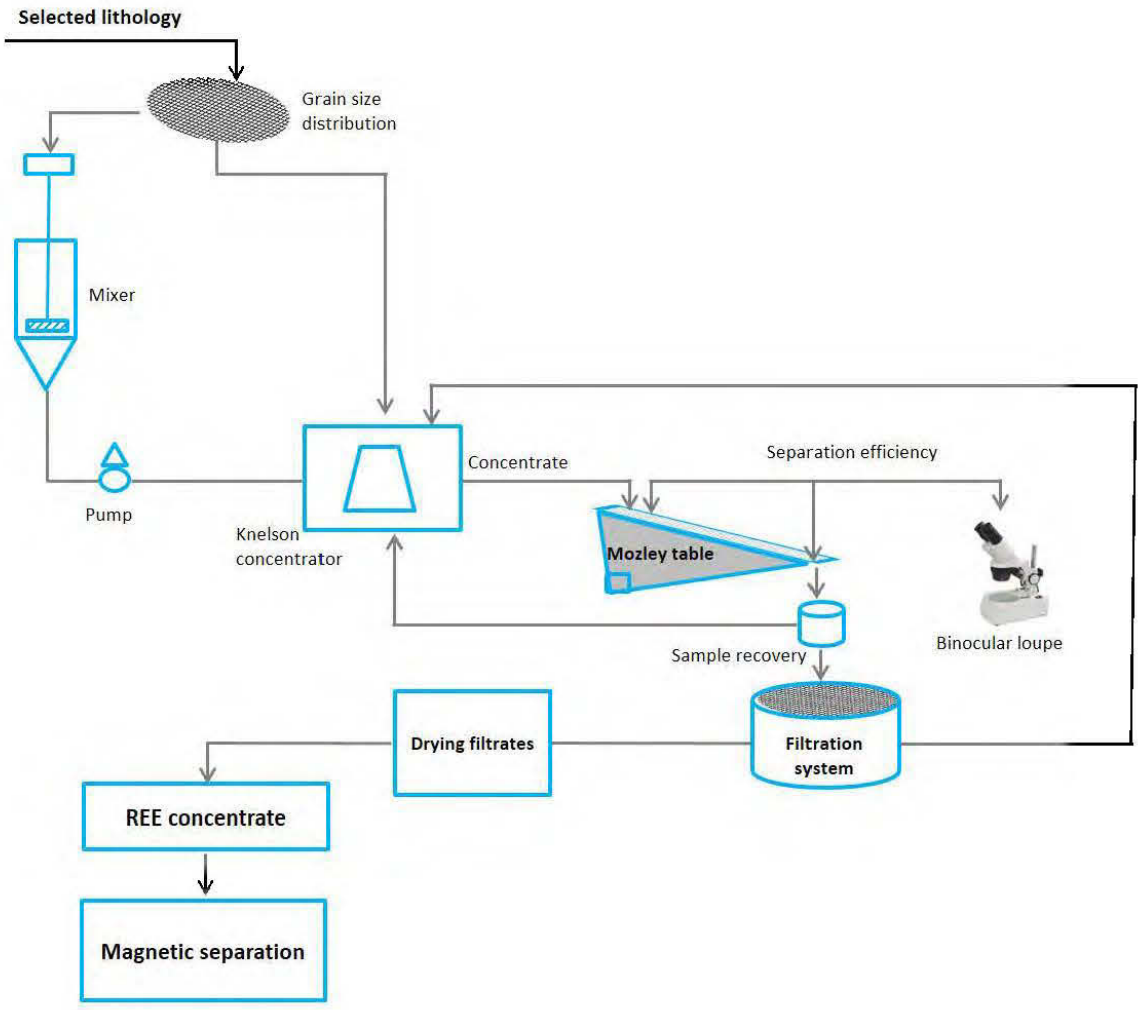

Figure 5-2 : Experimental set-up for the Mozley table and Knelson concentrator tests.

5.3.3 Physical and chemical analysis

The specific gravity (SG) was determined with a Micromeritics Helium Pycnometer. The particle size distributions were analyzed using a laser analyzer (Malvern Mastersizer S). The specific surface area (S.S.A.) was determined by using a Micromeritics Surface Area Analyser using the B.E.T. method(Brunauer et al., 1938).

The whole-rock analyses were performed using an X-ray Fluorescence (Bruker, Tiger Model), analyzer on a powdered aliquot of each sample to determine the major and minor elements. Chemical analyses were carried out by Inductively Coupled Plasma (ICP-AES/MS, Perkin Elmer Optima 3100-RL). Over 20 elements, to a 0.001 wt. % precision were analyzed after a multi-acid digestion (HCl, HNO3, and HF) Total sulfur and carbon grades were measured using an induction furnace analyzer (ELTRA CS-2000) with the detection limits are 0.05 % of carbon and 0.009 % of sulfur, respectively

The physicochemical parameters of the weathering cell leachates (pH, conductivity, Eh) were determined using a pH/Eh/electrical conductivity meter. The ICP-MS was used to analyze the REE concentrations in the weathering cell leachates, while the other elements were measured using the ICP-AES on an acidified (2 % HNO_3) and filtered (<0.45 μm) aliquot. The acid-base accounting (AP: acid-generating potential; NP: neutralization potential; NNP=NP-AP: net neutralization potential) was determined using the percentage of sulfur (AP=31.25 x % S) and carbon (NP=83.3 x % C).

5.3.4 Mineralogical characterization

The mineralogical composition was identified by X-ray diffraction (XRD; Brucker D8 Advance, with a detection limit and precision of approximately 1 to 5 %, operating with a copper cathode, Kα radiation) using the DIFFRACT.EVA program, and quantified with rietveld refinement using the Bruker's TOPAS 4.2 software (Young, 1993). In order to reconcile the final mineralogical results, chemical and mineralogical results are collected, compared, and adjusted to determine the percentages of mineral phases present within samples.

Mineralogical investigation and local X-Ray microanalysis were completed on a Hitachi S-3500N scanning electron microscope (SEM), equipped with an Energy-Dispersive X-ray Spectroscopy (EDS) probe (Oxford Instruments, Abingdon, Oxfordshire 20 mm^2 X-Max Silicon Drift Detector

(SDD). All analyses where carried out using an accelerating voltage of 20 kV, current of150 µA, pressure in the chamber fixed at 25 Pa and a working distance of 15 mm. The polished section observations were determined using backscattered electrons imaging mode (BSE). Electron probe microanalysis (EPMA), which has lower detection limits than the EDS-SEM system, were also used to analyze the trace metal composition of certain accessory minerals known for their affinity to REE, such as apatite. Electron microprobe mineralogical analyses (Cameca SX 100) were performed using an accelerating voltage of 20 kV and a beam current of 20 nA.

In order to further understand the effect of mineralogy, mineral size distributions, and effect of liberation on the geochemical behavior of REE-bearing minerals, a QEMSCAN (Quantitative Evaluation of Materials by Scanning Electron Microscopy) analysis was performed (Edahbi et al., 2017a; Smythe et al., 2013). QEMSCAN is an automated system that produces particle maps (color coded by mineral) through the collection of rapidly acquired X-Rays. The distribution and corresponding data files quantify the modal mineralogy, texture (mineral association), grain size, elemental deportment and liberation of samples analyzed. The polished sections were analyzed by PMA (particle mineralogy analysis) and TMS (trace mineral search) modes. Measurement resolution was set to 0.8 µm or 1 µm to capture the fine particle sizes (Jordens et al., 2016; Smythe et al., 2013). The mineralogical observations were performed on polished sections prepared carefully to avoid density segregation and ensure a homogenous dispersion of particles. The mineralogical observations were mainly focused on REE carbonates.

5.3.5 Weathering cells

A weathering cell test was used to evaluate the geochemistry of the REE concentrate following the procedures of Bouzahzah (Bouzahzah et al., 2015). The weathering cells consist of bi-weekly flushes by 50ml of deionized water on a sample weighing 67 g. The sample (particle size distribution <400 µm) is left to dry under ambient air between flushes. The bi-weekly (Mondays and Thursdays) leachates are combined and analyzed for their pH, Eh, electrical conductivity, and dissolved constituents. A more detailed description of the weathering cells is found in Plante (2010) and Villeneuve et al. (2003).

5.4 Results

5.4.1 Physical and chemical characteristics of the three Montviel lithologies and the REE concentrate

The physical and chemical properties of the samples studied are summarized in Table 5-1. The SG of the samples ranges from 3 to 3.60. The SG of the REE concentrate (3.60) is greater than that of all the lithological units (3.00-3.36) due to the increased content of sulfide and REE-bearing minerals. Fine grinding of the FeC-HG was required to ensure a high recovery of REE-bearing minerals to the REE concentrate.

The D_{50} and D_{90} values (the particle size passing 50 and 90 % on the cumulative grain size distribution curve, respectively) also highlight the particle size differences between the waste rocks samples and REE concentrate sample. The D_{50} and D_{90} values of the REE concentrate are significantly lower (124-209 µm) than for the waste rock samples (D_{50}: 2075-2775 µm and D_{90}: 5000-5500 µm).

The chemical characteristics results show that the REE concentrate sample contains higher concentrations of REE, Fe, Ca, Mg, Mn, Zn, Na, K, Ba, and Pb compared to the other samples. Indeed, the highest sum of LREE is recorded in the REE concentrate (36226 mg/l), while the lowest sum is found in the BreC (LG) (4400 mg/l). The samples are rich in LREE compared to HREE. Lanthanum (La), cerium (Ce), and neodymium (Nd) are the most abundant elements in all samples, with a maximum content in the REE concentrate and a minimum content in the breccia sample.

The acid-base accounting results show that the AP values are all lower ($4.1<AP<86.5$ kg $CaCO_3$/t) than the NP values ($44<NP<602$ kg $CaCO_3$/t), leading to NNP values undoubtedly within the non-acid generating zone (>20 kg $CaCO_3$/t).

Tableau 5-1 : Chemical and ABA characterization of the samples studied (elements in mg/l; AP, NP and NNP in kg $CaCO_3$/t).

Parameter	REE-ConC	CaC	FeC-LG	FeC-HG
Physical properties				
D_{50}	124	2075	2775	2250
D_{90}	209	5000	5500	5200
Specific gravity	3.60	3.10	3.36	3.30
Chemical composition				
Fe	155,700	12,000	20,000	16,000
Ca	70,130	19,000	11,000	9200

Mg	26,990	2300	4200	3300
Mn	11,570	1300	2100	1700
Zn	1186	62	81	29
Na	11,900	450	120	900
K	3240	910	750	960
Ba	35,000	1800	1400	1900
Pb	6363	12	8	8
Rare earth elements				
La	10,881	2500	2100	8900
Ce	19,302	5400	4200	14,000
Pr	1414	680	450	1400
Nd	4629	2200	1300	4100
Sm	420	330	150	390
Eu	80	77	31	78
Gd	156	270	99	290
Tb	0.9	20	6.2	15
Dy	28	74	16	31
Ho	2.9	11	2.0	3.3
Er	6.4	18	3.7	5.5
Tm	0.3	1.5	0.39	0.49
Yb	2.7	6.9	2.3	2.9
Lu	0.3	0.75	0.29	0.35
ΣLREE	36,226	10,780	8050	28,400
ΣHREE	698	800	298	804
Carbon	6.98	9.31	9.77	8.73
Sulfur	2.77	0.41	0.22	0.84
AP	86.5	7.8	4.1	20.3
NP	581.3	602	542	493
NNP	494.9	594.2	537.9	472.7

The relationship between LREE, Ba, and Sr shows a strong correlation with LREE ($R^2 > 0.90$), LREE vs Ba ($R^2 = 0.99$) and LREE vs Sr ($R^2 = 0.98$) (Figure 5-3). This is confirmed by the experimental constant relative proportions of (Ce/Nd) = 2.5, (Ce/Pr) = 12.75, and (Ce/La) = 1.6 in all samples. These relationships between LREE, Sr, and Ba, verified for all samples, suggest that these elements are associated in the same mineral phases. These geochemical anomalies are confirmed in the QEMSCAN analyses section.

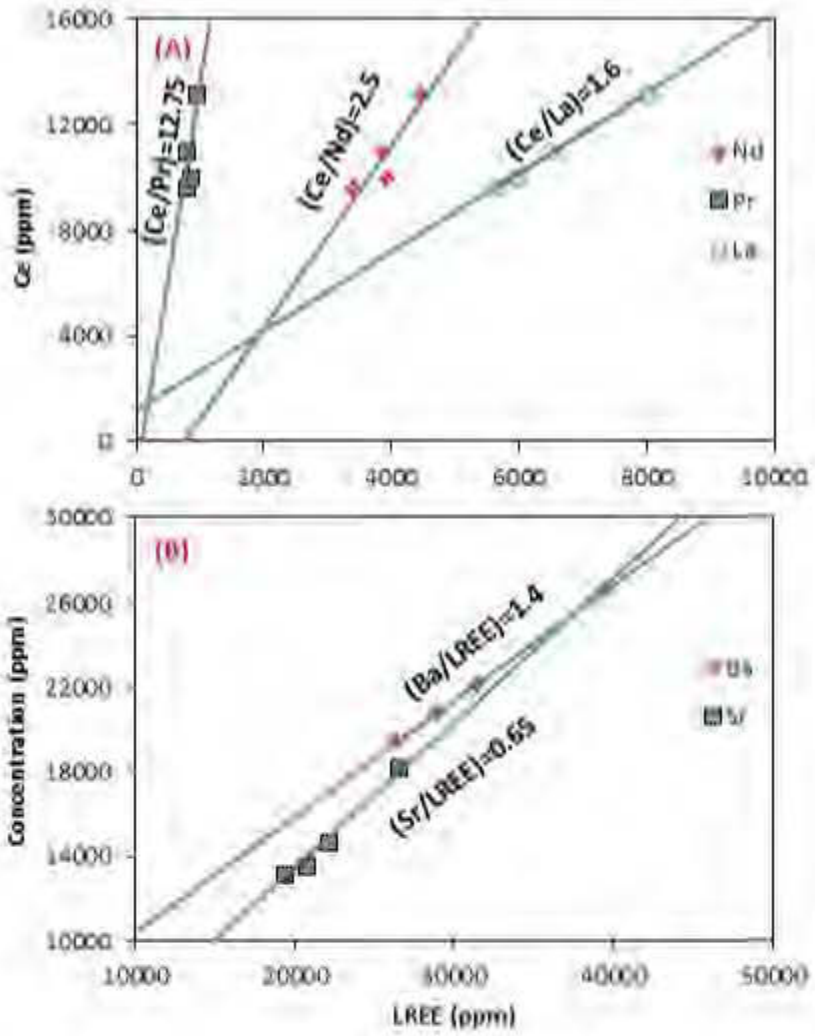

Figure 5-3 : Correlation between LREE (Ce vs La, R^2 =0.99; Ce vs Nd, R^2 =0.93; Ce vs Pr, R^2 =0.91), LREE vs Ba (R^2 =0.99) and LREE vs Sr (R^2 = 0.98).

5.4.2 Mineralogical characterization

The mineralogy of REE concentrate, determined by XRD analysis, is dominated by carbonates (i.e. ankerite, 34-43 wt. %, siderite, 12-16 wt. %, calcite, 8-11 wt. %), bassanite (3-5 wt. %), ilmenite (1 wt. %), biotite (7-16 wt. %), sulfides, and hematite (0-10 wt %). Two types of REE-bearing minerals are detected: burbankite, kukharenkoite, synchysite (carbonates) and monazite as main phosphate. However, the concentration of the possible Nb/Th-bearing minerals is too low to be detected by XRD. The mineralogical composition of the REE concentrate is shown in Table 5-2.

Tableau 5-2 : XRD mineralogical composition of REE concentrates.

Mineral	Chemical formula	Phase (wt. %)
Ankerite	$Ca(Fe,Mg,Mn)(CO_3)_2$	34.47
Siderite	$FeCO_3$	16
Monazite	$(La,Ce,Nd)PO_4$	3.4
Biotite	$K(Fe, Mg)_3(AlSi_3)O_{10}(F,OH)_2$	6.65
Burbankite	$(Na,Ca)_3(Sr,Ba,Ce)_3(CO_3)_5$	1.3
Strontianite	$SrCO_3$	0.23
Kukharenkoite	$Ba_2Ce(CO_3)_3F$	1.56
Calcite	$CaCO_3$	11.44
Pyrrhotite	$Fe_{(1-x)}S$	3.21
Pyrite	FeS_2	2.1
Quartz	SiO_2	3.25
Synchysite-Ce	$CaCe(CO_3)_2F$	0.26
Ilmenite	$FeTiO_3$	5.23
Bassanite	$2CaSO_4 \cdot (H_2O)$	9.62
Hematite	Fe_2O_3	1.12

These XRD results are confirmed by the other mineralogical techniques. SEM-EDS and QEMSCAN investigation show that: (i) REE are partially or totally liberated as free particles (kukharenkoite, burbankite, qaqarssukite, monazite) and/or associated with pyrochlore, baytocalcite, apatite, and Mg-Fe carbonates (Figure 5-4); (ii) all analyzed REE-bearing minerals contain LREE (La, Ce, Pr, Nd, Sm); (iii) two groups of REE-bearing minerals (carbonates and phosphates) were detected with variable REE grades, and (iv) pyrite and pyrrhotite were the most abundant sulfide minerals identified in the sample.

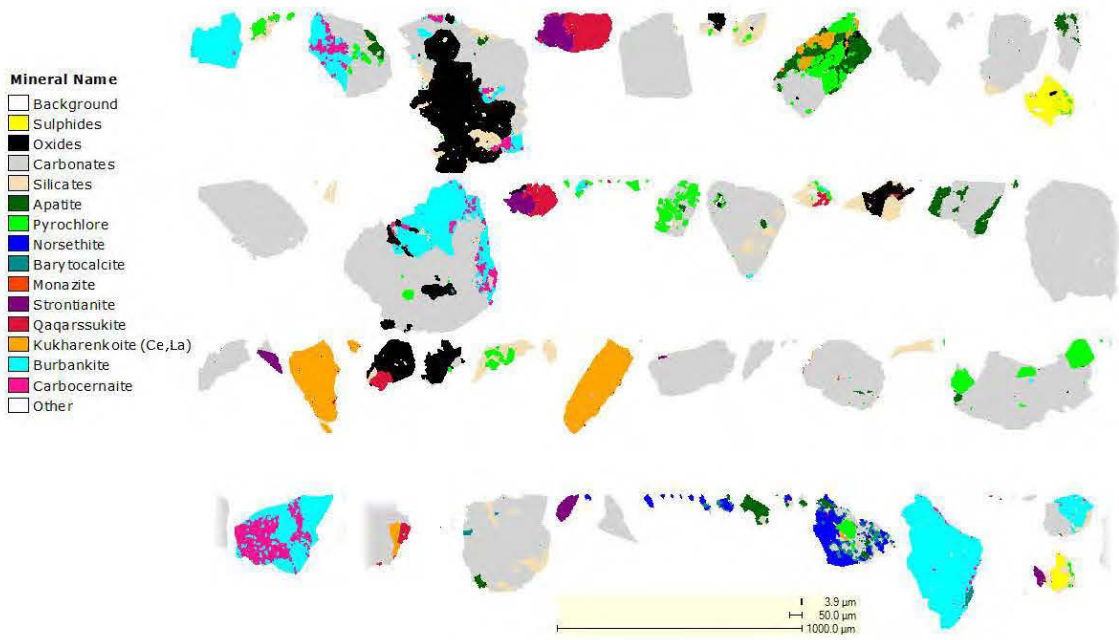

Figure 5-4 : QEMSCAN schematics of mineralogical associations in the REE concentrate.

In order to better investigate the REE mineralogy, all samples were submitted to mineralogical assessment using QEMSCAN. The main objective of the QEMSCAN work was to define the modal abundances, grain size, REE deportments and mineral liberation. The results of modal mineralogy show that REE minerals include: kukharenkoite $Ba_2(La,Ce)(CO_3)_3F$, burbankite $(Na,Ca)_3(Sr,Ba,Ce)_3(CO_3)_4$, ancylite $Sr(La,Ce)(CO_3)_2(OH)x(H_2O)$, carbocernaite $(Ca,Na)(Sr,Ce,Ba)(CO_3)_2$, qaqarssukite $Ba(Ce,REE)(CO_3)_2F$, and apatite $Ca_5(PO_4)_3F$ (Figure 5-5). The QEMSCAN mineralogical data shows that carbonernaite, ancylite, barytocalcite, and apatite minerals were undetectable by XRD.

Gangue minerals are dominated by carbonates that include calcite (most common in CAC), as well as ankerite, siderite, Mn siderite, and a Ca Mg Fe carbonates. Composites with higher levels of Fe have more ankerite, siderite, Ca Mg Fe carbonate compared to CAC. Silicates are dominated by biotite, chlorite with trace levels of amphiboles, pyroxene, feldspar, quartz, titanite and zircon. The QEMSCAN findings show that sulfides (mainly pyrite) and Fe-oxides are more abundant in the REE concentrate in comparison with the studied lithologies (Figure 5-5).

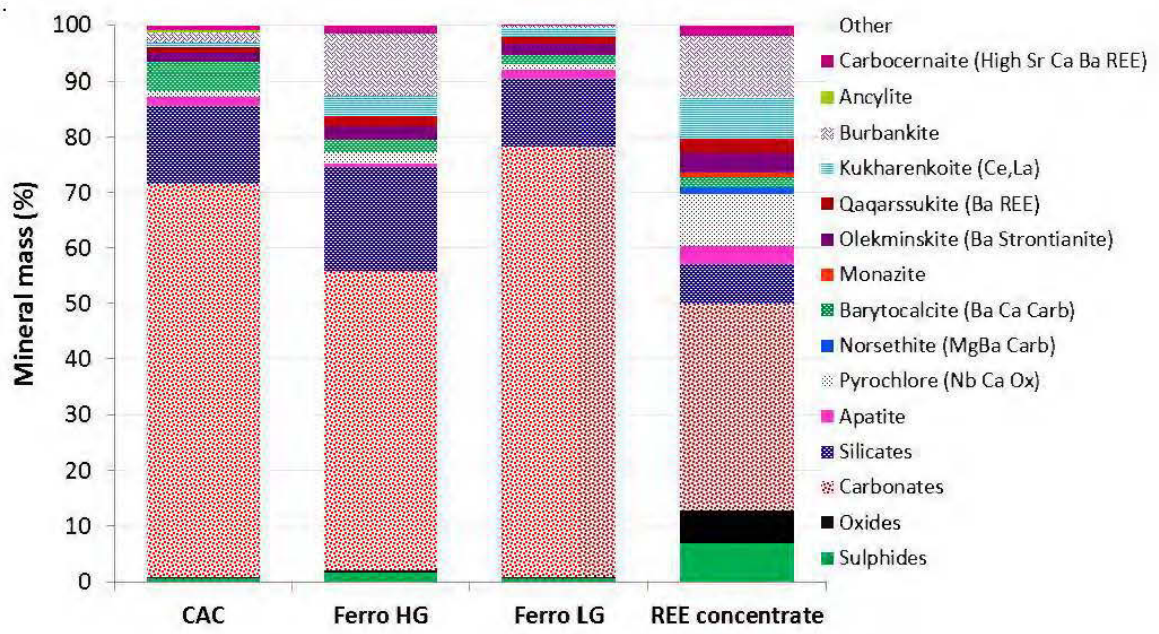

Figure 5-5 : QEMSCAN assessment of Montviel lithologies and REE concentrate.

The difference between XRD and QEMSCAN analyses is perhaps due to two reasons: (i) XRD is a semi-quantative method that has a detection limit in the 1-5 % range, and/or (ii) a representativeness problem of the tested sample. Given the sample preparation procedure, the latter is unlikely.

The QEMSCAN results shown in Figure 5-6 demonstrate that the concentration process successfully increased the grades of all REE-bearing phases, and decreased those of the non REE-bearing gangue minerals (carbonates and silicates). The degree of liberation of REE-bearing minerals is very important because it allows evaluation of mineral absolute reactivity. Liberation (based on area %) data is shown for combined REE minerals. At least, 50 % of the REE-bearing minerals are liberated (more than 15 % as free particles) within the samples, while the remaining particles are either included or locked within gangue minerals (e.g. silicates and carbonates) (Figure 5-6).

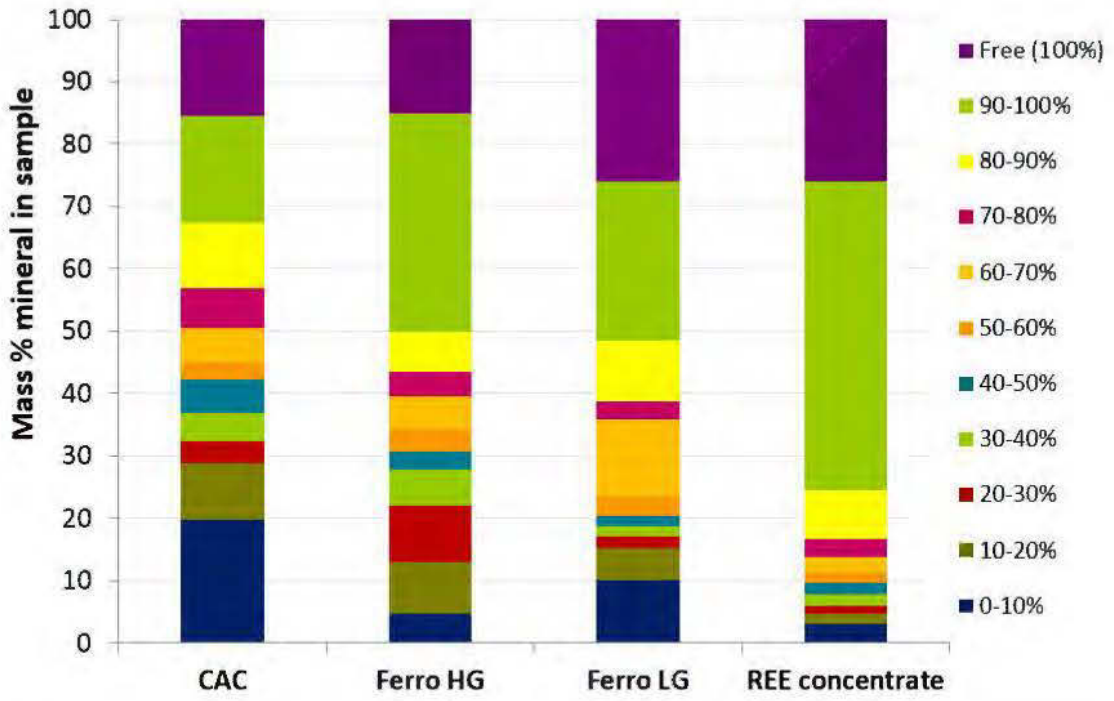

Figure 5-6 : The degree of liberation of REE-bearing minerals in Montviel lithologies and REE concentrate.

REE deportments for Ce, La, Nd, Pr and Sm have been calculated using the EPMA and QEMSCAN data. It is important to note that no deportment data is available for the REE that were not included in the EPMA analysis. Ce, La, Nd, Pr and Sm deportments are summarized in Figure 5-7. Ancylite, burbankite, carbonernaite, kukharenkoite, qaqarssnkite, monazite, strontianite and apatite mainly contain Ce and Nd, whereas Sm and La deport maiuly to monazite, ancylite, burbankite, carbonernaite, kukharenkoite, qaqarssnkite. The gangue minerals are maiuly represented by carbonates and silicates.

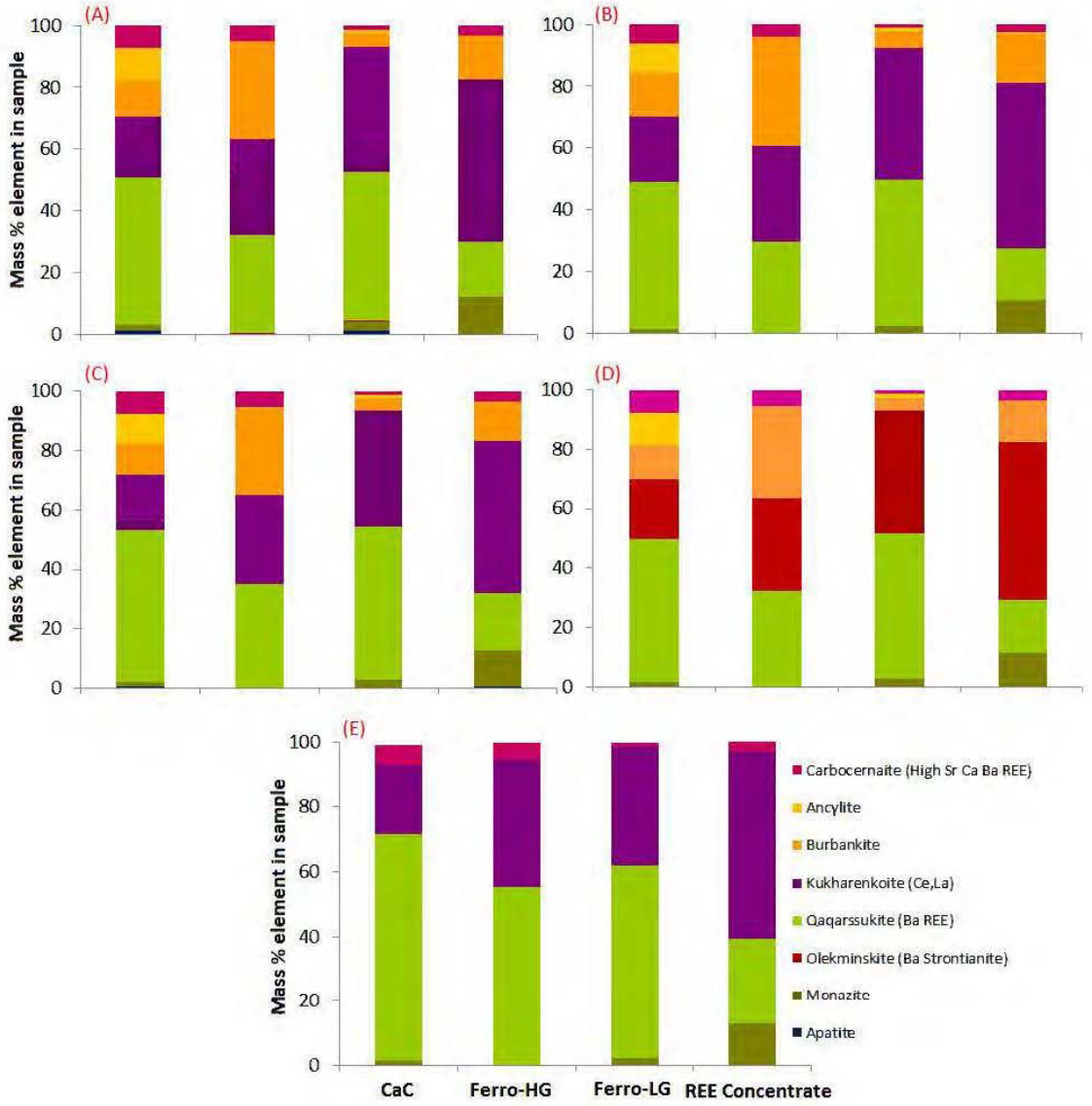

Figure 5-7 : Ce(a), La (b), Pr(c), Nd (d), and Sm (d) deportment in REE-bearing minerals.

As shown in Table 5-2, carbonate minerals are the most abundant mineral group in the REE concentrate. As a result, the materials were proven as being non-acid generating based on quantitative evaluation of mineralogy using QEMSCAN results and the calculation of degree of liberation.

5.4.3 Geochemical behavior

The weathering cell test results are shown in Figure 5-8 and 5-9. The pH of all the cell leachates remains alkaline (7.27-8.95) during the test. The electric conductivities of the leachates stabilize

rapidly between 117 and 169 µS/cm. The redox potential (Eh) varied from 228 to 553 mV. The alkalinity values stabilize between 37 and 110 mg $CaCO_3$/l, while the acidity is always below 5 mg$CaCO_3$/l. All these parameters stabilize after the approximately the first 60 days. The leaching concentrations of Th, Nb, Ni, Pb and Cu are not presented due to their low concentrations in the leachates from the REE concentrate. It is worth mentioning that these elemental concentrations were below the values fixed by Directive 019 (provincial legislations in Quebec). Leachate Ca concentrations vary between 0.003 and 20.6 mg/l after approximately 287 days. The Ba concentrations increase from the beginning of the test until approximately 231 days, after which they decrease until the end of the test and remain below the analytical detection limit (0.001 mg/l). The Sr (1.71-8.24 mg/l) and Mn (0.009–0.076 mg/l) concentrations generated from the concentrate sample show similar trends. The REE concentrate cell also generates detectable Mg and Si concentrations in the leachates (Mg: 0.05–3.4 mg/l and Na: 0.004–19.1 mg/l). The As, Cd, Bi, Co, Cr, Fe, Th, Ti and Zn values are typically under their respective detection limits and are therefore not shown.

The evolution of the elemental concentration of S (presumably as sulfate) Ca, Na, Ba, Mg, Fe, Sr, and REE suggests the dissolution of carbonates is a result of water-rock interaction and/or acid generated by sulfide oxidation. The LREE concentrations are higher in the leachates from the REE concentrate (1-133 µg/l) compared to those of HREE (0.03-61 µg/l). These results are consistent with those found by Edahbi et al. (2017) on the Kipawa alkaline intrusion REE deposit. In this geological context the leached REE is below 15 µg/l (Edahbi et al., 2017). Moreover, Purdy (2014) demonstrated that the REE concentrations in the leachate using shake flask tests on REE tailings of the Nechalacho Deposit, Northwest Territories, vary between 1 and 12 µg/l, with a maximum concentration in the tests using distilled deionized water and the minimum concentration in the tests using pilot plant water. The authors also demonstrated that more than 90 % of the leached REE were presented in the colloidal phase(Purdy, 2014). In addition, other authors showed that REE fractionation is promoted by an increase in pH (Edahbi et al., 2017; Janssen and Verweij, 2003; Leybourne et al., 2000). Edahbi et al. (2017) showed, using thermodynamic equilibrium calculations on the humidity cell leachate data, that REE concentrations decreased significantly (from 10^{-8} to 10^{-16} mg/l) when pH values increase from 2.6 to 10 (Edahbi et al., 2017)

The HREE (1387 mg/l) are in lower concentrations in the solid samples relative to the LREE (51220 mg/l). However, the ratio of LREE to HREE (2.5) leached during the weathering cell tests

are lower than their corresponding relative ratio in the solids (37). This suggests that the LREE have a lower mobility than HREE. This could be explained by the fact that the LREE have larger ionic radii than the HREE, which favors their precipitation as secondary minerals in weathering cell conditions.

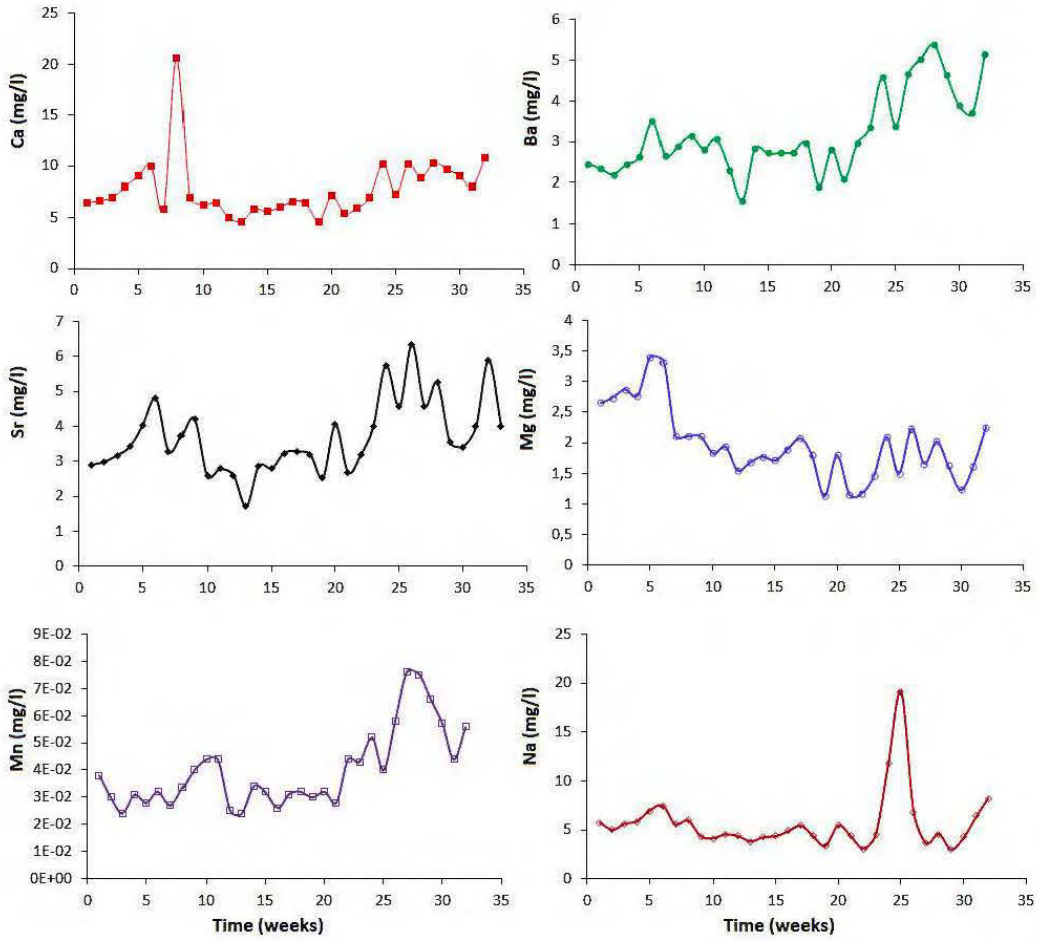

Figure 5-8 : Evolution of Ca, Ba, Sr, Mg, Mn and Na concentrations from weathering cell test.

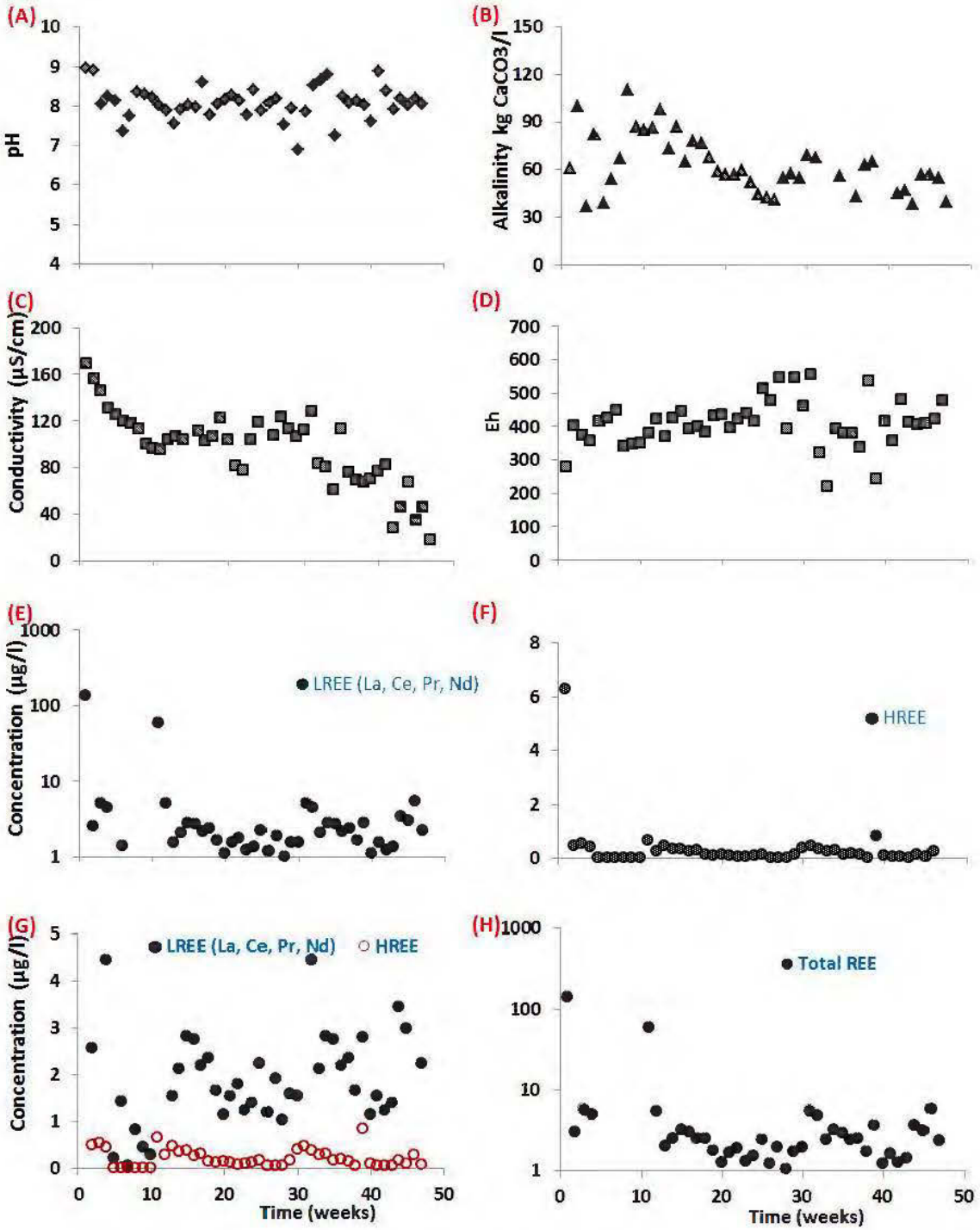

Figure 5-9 : Weathering cell results corresponding to REE concentrate.

5.5 Discussion

The mineralogy of REE and the geochemical behavior of the REE-bearing phases within the Montviel carbonatites were evaluated using QEMSCAN analyses and kinetic tests (weathering cells), and observations are discussed below.

5.5.1 Separation efficiency and environmental challenges

The chemical composition of the concentrate analyzed by XRF are shown in Table 5-3. In general, LREE concentrations increase with decreasing particle size. Sulfide minerals and iron oxides are also concentrated in the finest size fraction of the concentrate sample. The Nb, and Th display a similar trend (Figure 5-10). The majority of these elements are present in the -106 µm fraction (41 % of LREE, 36 % of Nb, and 19 % of Th). The concentration of LREE in the finer fractions is explained by preferential grinding of REE-bearing minerals compared to the gangue minerals (i.e. silicates, iron oxides, etc.).

Tableau 5-3 : Chemical analyses of the REE concentrate from the ten tests of gravity concentration; 2σ is the error of the XRF analyses.

	LREE		**Ba**		**Sr**	
	(ppm)	2σ	(ppm)	2σ	(ppm)	2σ
-106 µm	26612	1030	39487	732	18158	267
106-315 µm	22091	873	31438	542	14606	200
315-630 µm	19411	782	26239	441	13140	173
630 µm-2 mm	20748	845	28999	506	13474	184

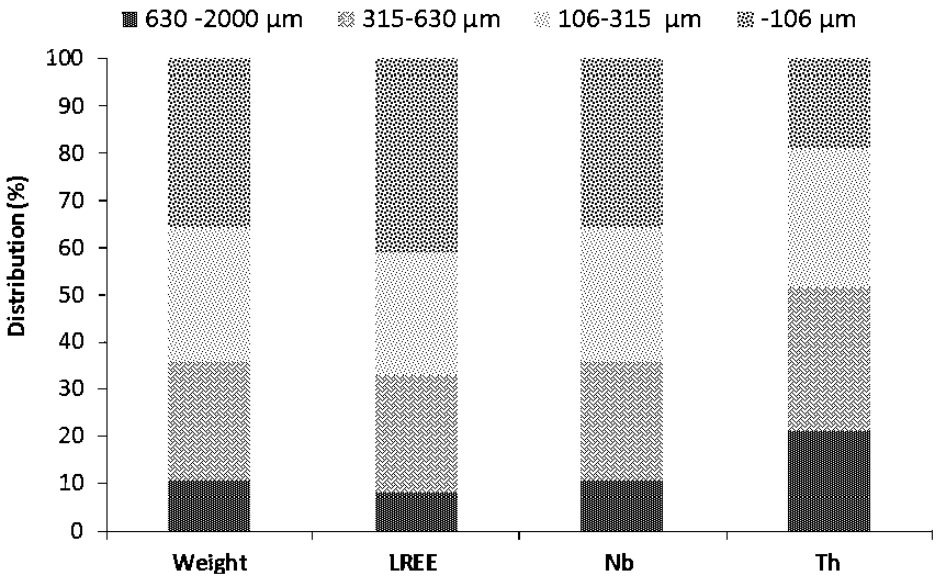

Figure 5-10 : LREE enrichment as a function of the particle size.

In the light of these findings, the finer fraction will be the most problematic fraction and will potentially require a focused strategy to mitigate the risk. Fine particles are the most reactive to water-rock interactions due to its higher specific surface area and degree of liberation. Therefore, they may release metals, REE, and other contaminants in the drainage waters, which might exceed regulatory limits. As a circumvention strategy, and in the context of sound REE production, this fraction could be separated by a screening operation and reprocessed with the ore (Figure 5-12). The least problematic coarse fraction could be sent to waste rock piles with suitable and specific environmental management and waste disposal strategies.

REE ores are often contaminated with actinides such as thorium, niobium and uranium, and other contaminants (e.g., Ba, Sr, Mn, Ta) (Chakhmouradian et al., 2017; Nadeau et al., 2015). Social responsibility of REE producers is an important issue for REE investors. Several publications found in the literature have reported significant environmental issues caused by REE mining and refining (Hurst, 2010; Weber and Reisman, 2012). In China, the use of acids to recover REE leads to the deterioration of the water quality in the surrounding environment. In Malaysia, radioactive wastes were stored in ambient surface conditions and consequently generated deleterious impacts on the environment(Pecht et al., 2011). REE ores are generally the deposits characterized by large-tonnage, low-grade operations which could generate significant quantities of liquid and solid wastes (e.g., waste rocks, tailings, and effluents). For example, the production of one tonne of REE

could be generated approximately 2000 tonnes of tailings (Hurst, 2010). In the case of Montviel project (Lebel-sur-Quévillon, Canada) 250 million tonnes (Mt) of REE-Nb carbonatites with a REE content estimated at 1.47 % of rare earth oxides (REO) could be extracted. The costs of processing, tailings, and environment of one metric tonne of is estimated to Canadian dollar 74.60 (Belzile Solutions Inc., 2015). In order to implement an integrated management strategy for the REE waste rocks, the base of the waste rocks pile should be compacted and tilted to promote lateral water flow, and it should be composed of materials from the least problematic lithology. The liquid effluents, collected around the pile, should be passed through a limestone drain for passive treatment.

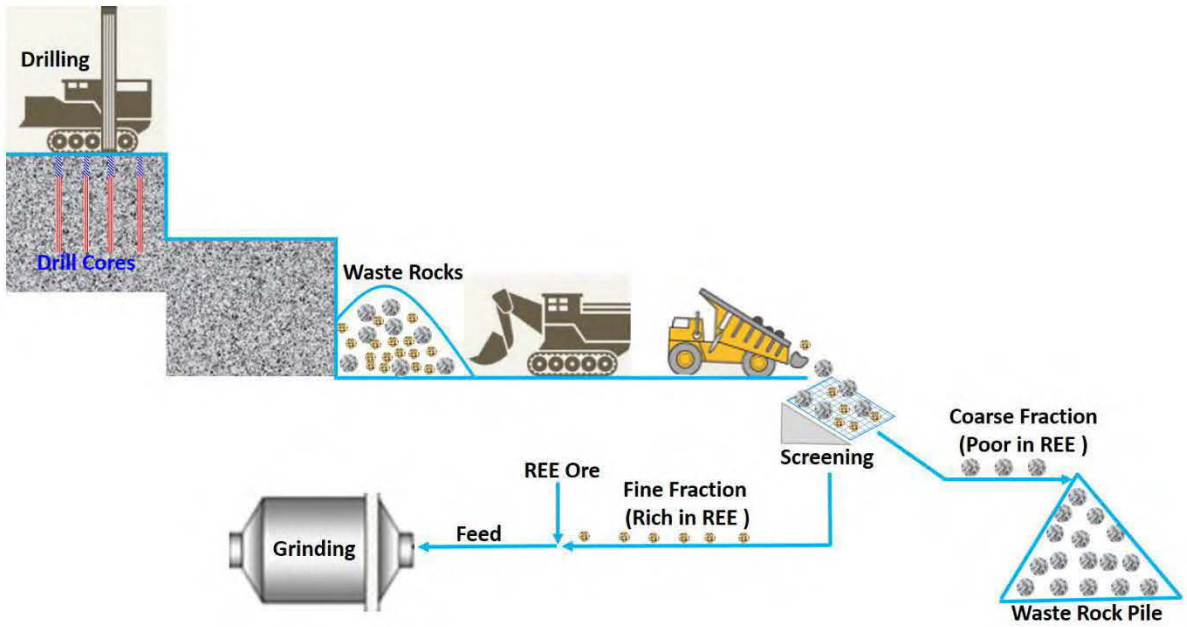

Figure 5-11 : Example of integrated management of REE mine wastes.

5.5.2 Geochemical behavior of REE

The weathering of the different lithologies within the Montviel deposit was studied in a previous study (Edahbi et al., 2017b), where it was demonstrated that the REE-bearing carbonates from the Montviel deposit generates various elements (e.g., Ba, Sr, F, Th, and REE) in mine drainage waters. It is known that the carbonates dissolution is incomplete in near neutral conditions (Chou et al., 1989; Morse and Arvidson, 2002; Morse et al., 2007), and that the carbonate dissolution rates are lowest in alkaline and neutral conditions and increase in acid conditions (Benzaazoua et al., 2004;

Sherlock et al., 1995). The presence of impurities within REE-bearing minerals weaken their crystal lattice and consequently increase their dissolution rate. In the case of the Montviel materials, REE-carbonates and non REE-carbonates neutralize the acidity produced by the sulfide oxidation or carried within acid rain, releasing REE and other associated elements in the leachates. However, it was demonstrated that the REE concentrations (and other associated elements) in the Montviel leachates are controlled by secondary precipitation and sorption phenomena. The behavior of the concentrate sample studied here is similar to that of the REE-bearing lithologies, although the residual REE concentrations in the leachates are higher (136 µg/l in the concentrate leachates compared to the lithologies, 9 µg/l). The use of a concentrate to mimic the behavior of REE in waste material is done in order to amplify the geochemical responses that could be obtained from mine wastes, and make measurement and interpretation more robust. This methodology was successfully applied in another context (Plante et al., 2011). Consequently, the interpretation of the weathering cell data will not be pushed further; the interested readers are invited to consult Edahbi et al. (2018).

5.5.3 Implications to the prediction of the geochemical behavior and water quality of REE mine wastes

Predicting the geochemical behavior of REE-bearing mine wastes and, ultimately, the mine drainage quality of those wastes, is not significantly different than for other metals. However, prediction of contaminated neutral drainage issued from REE mine wastes is particularly challenging because of the low reactivity and complex compositions of REE-bearing minerals. Therefore, in order to better understand the geochemical behavior of REE waste rocks and tailings and predict the quality of the drainage waters, the use of detailed chemical/mineralogical characterizations such as QEMSCAN, MLA, SEM and EPMA are valuable. Figure 5-13 illustrates a mine water quality prediction strategy that could be applied to REE-bearing mine wastes. The purpose of this approach is to meet the following challenges (Figure 5-13): (i) identify and quantify the different REE-bearing minerals (and associated potential contaminants) on representative samples of the different lithologies, (ii) evaluate the reactivity of the REE-bearing lithologies, (iii) propose an integrated management approach of the future REE- bearing waste rocks. In such an approach, representative samples of the different lithologies are submitted to percolation and leaching tests along with physical, chemical and mineralogical testing. The combination of these

results helps to identify risks associated with weathering of mine waste and to move towards prediction of mine water quality.

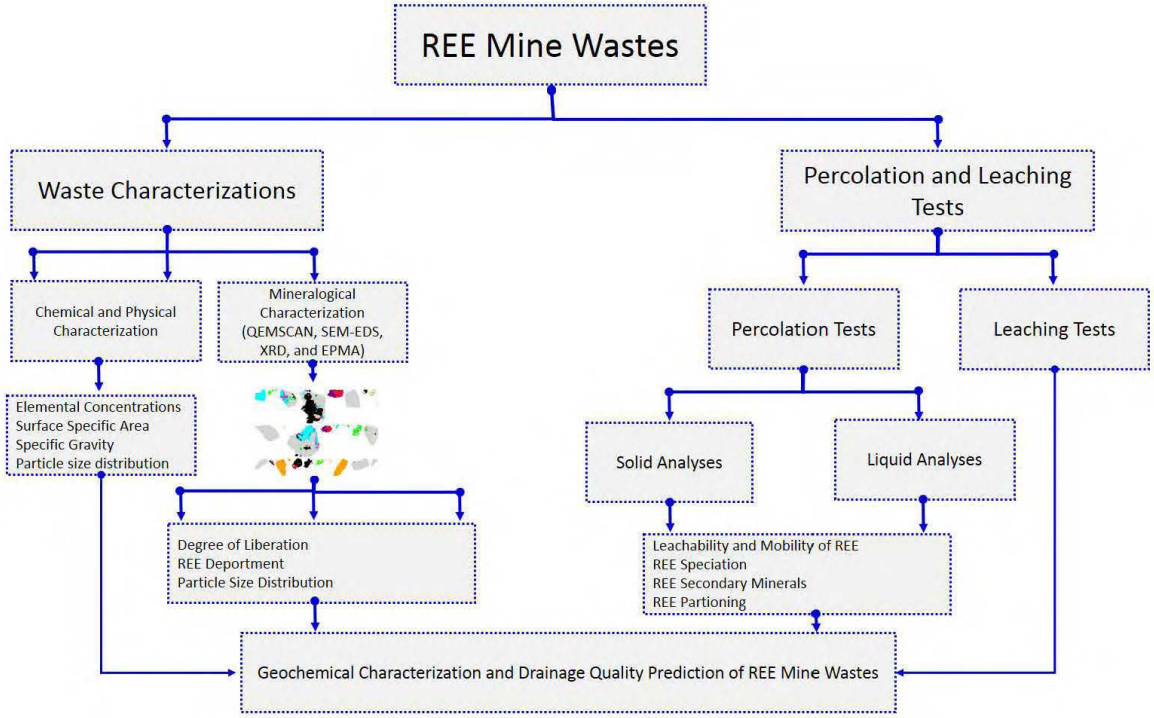

Figure 5-12 : Approach to predict geochemical behavior of REE mine wastes.

5.6 Conclusion

The main objectives of this study were: (1) to characterize REE-bearing minerals and to improve the counting statistics, analytical precision, and the geochemical interpretations using a REE concentrate sample prepared by gravity and magnetic processes, and (2) to evaluate the geochemical behavior of the REE-bearing materials using kinetic tests. Three lithological units chosen from exploration dill core to represent the heterogeneity of the GéoMéga waste rocks and a REE concentrate were tested. The lithologies were chosen to represent typical residue of REE mining and refining.

The main mineralogical conclusions drawn from this study indicate that: the main REE-bearing minerals in Montviel deposit are ancylite, burbankite, carbonernaite, kukharenkoite, qaqarssukite, monazite, strontianite and apatite. In addition, several accessory minerals contain REE, such as apatite and pyrochlore. At least 50 % of the REE-bearing minerals are liberated within the samples, while the remaining portion is either included or locked in gangue minerals (i.e. silicates and carbonates).

Geochemical results from both kinetic tests show a stable pH around 8 and alkalinity values between 37 and 110 mg$CaCO_3$/l. The main geochemical results from the kinetic tests are: (i) REE are good geochemical tracers of carbonate dissolution, and (ii) the leachability of REE from the studied carbonatite deposit is low and controlled by sorption processes in weathering cell conditions.

5.7 Acknowledgements

The authors thank the URSTM, staff for their support with laboratory work and NSERC/Geomega Resources for funding of this study. They also thank gratefully Agnico-Eagle mines and particularly Raphaël Mermillod-Blondin for technical support.

REFERENCES

Andrade, F.R.D., Möller, P., Lüders, V., Dulski, P. and Gilg, H.A., (1999). Hydrothermal rare earth elements mineralization in the Barra do Itapirapuã carbonatite, southern Brazil: behaviour of selected trace elements and stable isotopes (C, O). Chemical Geology, 155(1–2): 91-113.

Bau, M., (1999). Scavenging of dissolved yttrium and rare earths by precipitating iron oxyhydroxide: experimental evidence for Ce oxidation, Y-Ho fractionation, and lanthanide tetrad effect. Geochimica et Cosmochimica Acta, 63(1): 67-77.

Belzile Solutions Inc., (2015). NI 43-101 Technical Report Montviel Rare Earth Project Québec, Canada (accessed on March 16th, 2017).

Benzaazoua, M., Bussiére, B., Dagenais, A.M. and Archambault, M., (2004). Kinetic tests comparison and interpretation for prediction of the Joutel tailings acid generation potential. Environmental Geology, 46(8): 1086-1101.

Binnemans, K. et al., (2013). Recycling of rare earths: a critical review. Journal of Cleaner Production, 51: 1-22.

Bouzahzah, H., Benzaazoua, M., Plante, B. and Bussiere, B., (2015). A quantitative approach for the estimation of the "fizz rating" parameter in the acid-base accounting tests: A new adaptations of the Sobek test. Journal of Geochemical Exploration, 153: 53-65.

Brunauer, S., Emmett, P.H. and Teller, E., (1938). Adsorption of gases in multimolecular layers. Journal of the American chemical society, 60(2): 309-319.

Catinat, M., 2010. Critical Raw Materials for the EU—Report of the Ad-Hoc Working Group on Defining Critical Raw Materials. EC, Brussels, Belgium.

Censi, P., Saiano, F., Pisciotta, A. and Tuzzolino, N., (2014). Geochemical behaviour of rare earths in Vitis vinifera grafted onto different rootstocks and growing on several soils. Science of The Total Environment, 473–474: 597-608.

Chakhmouradian, A.R. et al., (2017). Apatite in carbonatitic rocks: Compositional variation, zoning, element partitioning and petrogenetic significance. Lithos, 274-275: 188-213.

Chakhmouradian, A.R., Smith, M.P. and Kynicky, J., (2015). From "strategic" tungsten to "green" neodymium: A century of critical metals at a glance. Ore Geology Reviews, 64, 455-458.

Chakhmouradian, A.R. and Wall, F., (2012). Rare Earth Elements: Minerals, Mines, Magnets (and More). Elements, 8(5): 333-340.

Chakhmouradian, A.R. and Zaitsev, A.N., (2012). Rare Earth Mineralization in Igneous Rocks: Sources and Processes. Elements, 8(5): 347-353.

Chou, L., Garrels, R.M. and Wollast, R., (1989). Comparative study of the kinetics and mechanisms of dissolution of carbonate minerals. Chemical Geology, 78(3-4): 269-282.

Cox, C. and Kynicky, J., (2017). The rapid evolution of speculative investment in the REE market before, during, and after the rare earth crisis of 2010–2012. The Extractive Industries and Society.

Dehaine, Q. and Filippov, L.O., (2015). Rare earth (La, Ce, Nd) and rare metals (Sn, Nb, W) as by-product of kaolin production, Cornwall: Part1: Selection and characterisation of the valuable stream. Minerals Engineering, 76: 141-153.

Edahbi, M., Benzaazoua, M., Plante, B., Doire, S. and Kormos, L., (2017). Mineralogical characterization using QEMSCAN® and leaching potential study of REE within silicate ores: A case study of the Matamec project, Québec, Canada. Journal of Geochemical Exploration, 185, 64-73.

Edahbi, M., B. Plante, M. Benzaazoua, and M. Pelletier. 2018. Geochemistry of rare earth elements within waste rocks from the Montviel carbonatite deposit, Québec, Canada. Environmental Science and Pollution Research DOI: 10.1007/s11356-018-1309-7.

Filippov, L.O., Dehaine, Q. and Filippova, I.V., (2016). Rare earths (La, Ce, Nd) and rare metals (Sn, Nb, W) as by-products of kaolin production – Part 3: Processing of fines using gravity and flotation. Minerals Engineering, 95: 96-106.

Goutier, J., (2006). Géologie de la région du lac au Goéland (32F/15). Ressources naturelles et Faune, Québec: Ville de Québec, QC, Canada.

Humphries, M., (2013). Rare Earth Elements: The Global Supply Chain. Congressional Research Service, 7-5700 (http://www.fas. org/sgp/crs/natsec/R41347.pdf) (accessed on August 16th, 2017).

Hurst, C., (2010). China's rare earth elements industry: What can the west learn?, Institute for the Analysis of Global Security Washington DC.

Janssen, R.P.T. and Verweij, W., (2003). Geochemistry of some rare earth elements in groundwater, Vierlingsbeek, The Netherlands. Water Research, 37(6): 1320-1350.

Jordens, A., Marion, C., Grammatikopoulos, T. and Waters, K.E., (2016). Understanding the effect of mineralogy on muscovite flotation using QEMSCAN. International Journal of Mineral Processing, 155: 6-12.

Jordens, A., Sheridan, R.S., Rowson, N.A. and Waters, K.E., (2014). Processing a rare earth mineral deposit using gravity and magnetic separation. Minerals Engineering, 62(0): 9-18.

Kanazawa, Y. and Kamitani, M., (2006). Rare earth minerals and resources in the world. Journal of Alloys and Compounds, 408–412(0): 1339-1343.

Kynicky, J., Smith, M.P. and Xu, C., (2012). Diversity of rare earth deposits: the key example of China. Elements, 8(5): 361-367.

Lawrence, R. and Wang, Y., (1996). Determination of neutralization potential for acid rock drainage prediction. MEND project, 1(3): 38.

Leal Filho, W., (2016). Chapter 17 - An Analysis of the Environmental Impacts of the Exploitation of Rare Earth Metals, Rare Earths Industry. Elsevier, Boston, pp. 269-277.

Leybourne, M.I., Goodfellow, W.D., Boyle, D.R. and Hall, G.M., (2000). Rapid development of negative Ce anomalies in surface waters and contrasting REE patterns in groundwaters associated with Zn–Pb massive sulphide deposits. Applied Geochemistry, 15(6): 695-723.

Mariano, A.N. and Mariano, A., (2012). Rare Earth Mining and Exploration in North America. Elements, 8(5): 369-376.

Massari, S. and Ruberti, M., (2013). Rare earth elements as critical raw materials: Focus on international markets and future strategies. Resources Policy, 38(1): 36-43.

Morse, J.W. and Arvidson, R.S., (2002). The dissolution kinetics of major sedimentary carbonate minerals. Earth-Science Reviews, 58(1): 51-84.

Morse, J.W., Arvidson, R.S. and Lüttge, A., (2007). Calcium carbonate formation and dissolution. Chemical reviews, 107(2): 342-381.

Nadeau, O., Cayer, A., Pelletier, M., Stevenson, R. and Jébrak, M., (2015). The Paleoproterozoic Montviel carbonatite-hosted REE–Nb deposit, Abitibi, Canada: Geology, mineralogy, geochemistry and genesis. Ore Geology Reviews, 67: 314-335.

Nadeau, O., Stevenson, R. and Jébrak, M., (2016). Evolution of Montviel alkaline-carbonatite complex by coupled fractional crystallization, fluid mixing and metasomatism — Part II: Trace element and Sm–Nd isotope geochemistry of metasomatic rocks: implications for REE-Nb mineralization. Ore Geology Reviews, 72, Part 1: 1163-1173.

Orris, G.J. and Grauch, R.I., (2002). Rare Earth Element Mine,Deposits, and Occurences. USGC (Science for a changing world): Reston, VA, USA.

Pecht, M. et al., (2011). Rare Earth Material: Insights and Concerns. CALCE EPSC Press, University of Maryland, College Park, MD.

Plante, B., Benzaazoua, M. and Bussière, B., (2011). Predicting geochemical behaviour of waste rock with low acid generating potential using laboratory kinetic tests. Mine Water and the Environment, 30(1): 2-21.

Purdy, C., (2014). The Geochemical and Mineralogical Controls on the Environmental Mobility of Rare Earth Elements from Tailings, Nechalacho Deposit, Northwest Territories. Master's thesis, Queen's University, Kingston, ON, Canada.

Sapsford, D.J., Bowell, R.J., Geroni, J.N., Penman, K.M. and Dey, M., (2012). Factors influencing the release rate of uranium, thorium, yttrium and rare earth elements from a low grade ore. Minerals Engineering, 39(0): 165-172.

Schlinkert, D. and van den Boogaart, K.G., (2015). The development of the market for rare earth elements: Insights from economic theory. Resources Policy, 46, Part 2: 272-280.

Schmid, R., (1981). Descriptive nomenclature and classification of pyroclastic deposits and fragments: Recommendations of the IUGS Subcommission on the Systematics of Igneous Rocks. Geology, 9(1): 41-43.

Schüler, D., Buchert, M., Liu, R., Dittrich, S. and Merz, C., (2011). Study on rare earths and their recycling. Öko-Institut eV Darmstadt.

Sherlock, E., Lawrence, R. and Poulin, R., (1995). On the neutralization of acid rock drainage by carbonate and silicate minerals. Environmental Geology, 25(1): 43-54.

Smythe, D.M., Lombard, A. and Coetzee, L.L., (2013). Rare Earth Element deportment studies utilising QEMSCAN technology. Minerals Engineering, 52: 52-61.

Verplanck, P.L. and Gosen, B.S.V., (2011). Carbonatite and alkaline intrusion-related rare earth element deposits-a deposit model; USGS: : Reston, VA, USA.

Weber, R.J. and Reisman, D.J., (2012). Rare earth elements: A review of production, processing, recycling, and associated environmental issues; US EPA Region: Washington, DC, USA.

Williams-Jones, A.E., Migdisov, A.A. and Samson, I.M., (2012). Hydrothermal mobilisation of the rare earth elements a Tale of "Ceria" and "Yttria". Elements, 8, 355-360.

Young, R.A., (1993). The rietveld method, 5. International union of crystallography, 5, 252–254.

Zaitsev, A.N.; Terry Williams, C.; Jeffries, T.E.; Strekopytov, S.; Moutte, J.; Ivashchenkova, O.V.; Spratt, J.; Petrov, S.V.; Wall, F.; Seltmann, R.; et al. (2014). Rare earth elements in phoscorites and carbonatites of the Devonian Kola Alkaline Province, Russia: Examples from Kovdor, Khibina, Vuoriyarvi and Turiy Mys complexes. Ore Geol. Rev. 2014, 61, 204–225.

Zaitsev, A.N., Wall, F. and Bas, M.J.L., (1998) . REE-Sr-Ba minerals from the Khibina carbonatites, Kola Peninsula, Russia: their mineralogy, paragenesis and evolution. Mineralogical Magazine, 62, 225-250.

Zhu, Z., Liu, C.-Q., Wang, Z.-L., Liu, X. and Li, J., (2016). Rare earth elements concentrations and speciation in rainwater from Guiyang, an acid rain impacted zone of Southwest China. Chemical Geology, 442: 23-34.

CHAPITRE 6 ARTICLE 5 : MINERALOGICAL CHARACTERIZATION USING QEMSCAN® AND LEACHING POTENTIAL STUDY OF REE WITHIN SILICATE ORES: A CASE STUDY OF THE MATAMEC PROJECT, QUÉBEC, CANADA

Cet article est accepté dans la revue Journal of Geochemical Exploration, 2017

Edahbi, M.[a]; Plante, B.[a]; Benzaazoua, M.[a]; Kormos, L.[c]; Doire, S.[d]

[a] Université du Québec en Abitibi-Témiscamingue (UQAT), 445 boul de l'Université, Rouyn-Noranda J9X 5E4, QC, Canada.

[c]XPS Consulting and Testwork Services, 6 Edison Road, Falconbridge, ON, P0M1S0, Canada

[d]Matamec Explorations Inc, Canada

6.1 Abstract

The mineralogy and leachability of the rare earth elements (REE) from the Kipawa deposit, a Heavy REE (HREE) mine project of Matamec Resources (Quebec, Canada), was investigated in order to predict their geochemical behavior and to evaluate the factors controlling the REE mobility in ambient conditions. All deposit lithologies defined, including ore and waste rocks, were sampled, characterized using a mineralogical multi-technique approach (automated SEM-EDS, EPMA-WDS, XRD), and then submitted to kinetic testing using weathering cells to investigate REE release potential. The mineralogical characterization shows that REE-bearing minerals are mainly represented by mosandrite, fluorbritholite, apatite, monazite and Zr silicates (i.e., aqualite, reidite). Mineralogical analysis indicates that REE particles are at least 70 % liberated and the remaining portion (around 30 %) is locked within gangue minerals, containing 100 % REE by area. The remaining fraction is either partially or totally locked in gangue minerals (i.e. carbonates, amphibole/pyroxene, and micas). The degree of liberation of these minerals is directly linked to their weathering. All kinetic test leachates showed a neutral to alkaline pH (7.0 to 9.5) and alkalinity values between 10 and 173mg$CaCO_3$/l. REE release from the materials are all below 15 µg/l. Thermodynamic equilibrium calculations using VMinteQ shows the possibility of secondary mineral precipitation (i.e. iron oxide and clays), which could be sorbed and/or co-precipitated the leached REE.

Keywords: Rare earth elements, mineralogy, QEMSCAN®, WDS, geochemical behavior, weathering cells, modelling.

6.2 Introduction

The rare earths industry is important to the world's economy. For example, the North American REE industry directly contributes to the economy with $795 million in shipments, employing nearly 1,050 workers with a payroll of $116 million (Rare Earth technology Alliance, 2014). Rare earth elements are used in hybrid vehicles, rechargeable batteries, clean energy (renewable energy), mobile (cell) phones, flat screen display panels, compact fluorescent light bulbs, laptop computers, disk drives, catalytic converters, etc. (Humphries, 2003). Currently, China fills 94 % of the global REE market (Chen, 2011; Hong, 2006; Lema et al., 2016). However, the supply is seen as a risk due to uncertainty related to political polices within China. The exploitation of REE deposits in Canada will reduce this dependence on the Chinese REE industry, and mitigate the risk associated with supply disruptions. (Biennemas et al., 2013; Edahbi et al., 2015).

The group of rare earth elements (REE), called also lanthanides, is composed of seventeen chemical elements (fifteen lanthanides, La to Lu, as well as Y and Sc). These REE are found in various geological settings such as igneous, sedimentary and metamorphic environments, and are associated with several mineral phases such as apatite (Calas, 2012). The lanthanides exhibit similar chemical and physical properties and differ only in the number of electrons in the 4f shell (Lipin and Mckay., 1989). In addition, the difference in the size of REE ions increases their cationic exchange with other elements in different minerals (i.e. calcite and apatite) (Jia 1991; Lipin and Mckay, 1989).

In Canada, the legislation forces mining companies to manage their waste products in order to minimize environmental impacts, the mining industry is properly regulated, except for REE mines. But nevertheless, the mine waste rocks and tailings are generally stored at the surface and exposed to ambient conditions. The reaction between water, oxygen, and some reactive minerals such as sulfides (i.e. pyrite, pyrrhotite, chalcopyrite, sphalerite, etc.) can generate contaminated mine drainage. Like any kind of mine, REE mining and refining are known to generate certain amounts of liquid and solid residue, but there is no evidence of their negative effects on the environment (Cheng et al., 2013). However, REE deposits are known to be associated to several radioactive elements such as thorium (Th), niobium (Nb), and uranium (U) (Dai et al., 2013; Hao et al., 2015).

The release of REE and associated elements should be tested in order to define appropriate management scenarios and thus avoid possible adverse environmental effects.

In the framework of sustainable development, social acceptability, and environmental regulations, it is now necessary to integrate environmental studies as early as possible in the design and development of mining projects. Unfortunately, knowledge on REE release from mine wastes is very limited, despite existence of several REE mine projects around the world which are currently at the feasibility stage. A lack of knowledge related to mobility and toxicity of REE has led to either an absence or insufficient international environmental mining regulations.

The purpose of this paper is to: (i) study the mineralogy of REE Kipawa deposit, (ii) evaluate the distribution of REE within the ore and waste rock lithologies, and (iii) evaluate the leaching potential of REE-bearing minerals from the Kipawa deposit (Canada). This knowledge will enable the mining company to understand the geochemical behavior of REE during rock-water interactions, which could be helpful to predict the water quality of the future REE mine wastes and contribute to minimizing their potential environmental impacts.

6.3 Materials and methods

Mineralogical techniques, namely automated mineralogy (QEMSCAN®), X-ray diffraction (XRD), scanning electron microscopy (SEM-EDS), and electron micro-probe (EPMA), as well as weathering cell tests were used to characterize and study the REE leaching potential of six lithologies from the Kipawa deposit (five waste rock lithologies and an ore concentrate sample). The following describes the case study, sampling and methodology used in this work (Figure 6-1).

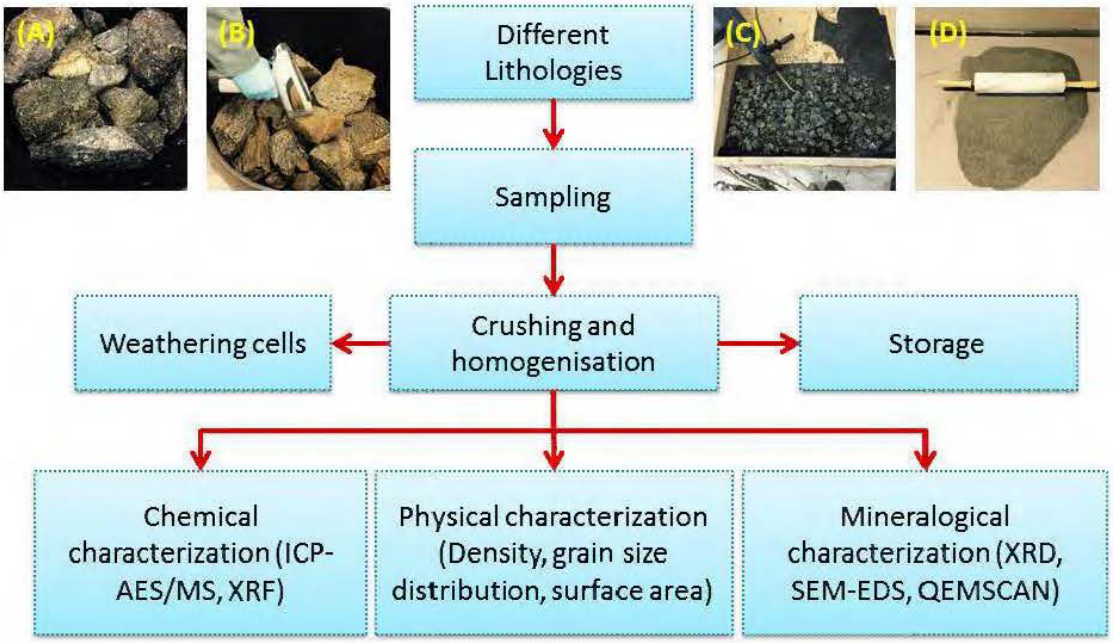

Figure 6-1 : Methodology used for preparing samples.

6.3.1 Location and geological setting of Kipawa deposit

The Kipawa REE Project is located approximately 50km east of the town of Témiscamingue, Quebec province, Canada. The Kipawa deposit contains both light (LREE) and heavy (HREE) rare earth elements but is especially enriched with HREE. The Kipawa HREE mineralisation is contained within syenite lithologies associated to the Kipawa alkaline complex. Matamec Explorations Inc., majority owner of the property, estimates the indicated resources to be approximately 10.2Mt at 0.44 % total rare earth oxides (TREO) with an additional inferred resource of 9.6Mt at 0.38 % TREO. (Roche et al., 2012). The HREE mineralization is also associated with yttrium (Y) and zirconium (Zr). REE-Y-Zr elements in Kipawa orebody are associated with silicate minerals within the Kipawa deposit: mainly eudialyte (a sodic silicate), yttro-titanite/mosandrite (titanite silicate), and britholite (calcic silicophosphate) (Roche et al., 2012).

6.3.2 Sampling and preparation

Approximately 10 kg of five waste rock lithologies, described as syenite waste (SW), calcite-poor waste (WCCP), calcite-rich waste (WCCR), peralkaline gneiss (PG), and monzonitic basement gneiss (MBG), were sampled from exploration drill cores, while a magnetic concentrate (MC) was provided by Matamec Explorations Inc.. The MC sample, prepared by Matamec Explorations Inc.

using magnetic separation on the ore, was used in order to increase the geochemical response of the materials during weathering cells. The samples were selected with great care in order to ensure good representivity of the waste rocks. They were crushed to <¼ inch, pulverized to <300 µm, homogenized separately, and submitted to chemical and physical characterizations (Figure 6-1). For the mineralogical investigations, all samples were crushed to <850 µm, homogenized, and then fixed in polished sections.

6.3.3 Weathering cell tests

Weathering cell tests are used to predict the geochemical behavior of mine wastes under leaching conditions. A Buchner-type funnel containing 67 g of samples arranged uniformly on a filter paper was used, and then the sample was subjected to bi-weekly 50 ml leaching cycles for a duration of 19 weeks (Benzaazoua et al., 2004). The leachates were analyzed for pH, conductivity, redox potential, and elemental concentrations (e.g., LREE, or La to Gd, and HREE, or Tb to Lu as well as Y)).

6.3.4 Physical, chemical, and mineralogical characterizations

The grain size distribution was measured using a laser analyzer (Malvern Mastersizer). The specific gravity (SG) was analyzed with a helium gas pycnometer (Micromeritics Accupyc 1330). The specific surface area was determined by helium adsorption using a BET interpretation (Brunauer et al. 1938).

The major and trace elements of the solid materials were determined both by XRF and Inductively Coupled Plasma (ICP-AES/MS) analysis after a multi-acid digestion (HCl, HNO_3, Br_2, and HF). The sulfide sulfur in the solids was determined by subtraction of the sulfate sulfur (determined by a 40 % HCl extraction; method adapted from Sobek et al., 1978) from the total sulfur (ICP-AES analysis). The S and C content were determined using an ELTRA CS-2000 induction furnace.

The REE in the leachates were analyzed with ICP-MS, while ICP- AES was used to analyze other elements such as S, Ca, Mg, Mn, Fe, Sr, F, P, K , Zn, Pb, Si, and Na. The leachates were filtered (0.45 µm) and acidified (2 % HNO_3) for ICP analyses. Pore water, pH, Eh, and electrical conductivity measurements were determined immediately with a pH/mV meter and an electrical conductivity meter (EC meter).

The mineralogy of all samples (waste rocks and magnetic concentrate) were determined by the X-ray diffraction (Bruker AXS Advance D8), using a copper cathode (K_α radiation). The DiffracPlus EVA software was used to identify the detected minerals and the TOPAS software was used to quantify their abundance using Rietveld refinement (Raudsepp and Pani, 2003; Ruffell and Wiltshire, 2004).

A scanning electron microscope (SEM) Hitachi S-3500N, equipped with a microanalysis system (energy dispersive spectroscopy, or EDS) was used in order to confirm the presence of the phases detected by XRD, to analyze the elemental composition of the REE-bearing minerals present in samples, and to detect minerals in concentrations lower than the XRD detection limit. All analyses where carried out using an accelerating voltage of 20 kV, current of 150 μA, low pressure in the chamber fixed at 25 Pa and working distance approximately 15 mm. The analyses were performed on polished sections of the six samples, prepared using a method allowing to avoid density segregation and enhance particle dispersion (Bouzahzah et al., 2015).

The QEMSCAN® (quantitative evaluation of minerals by scanning electron microscopy) automated mineralogical analysis tool enables quantitative chemical analysis of materials and generation of high-resolution mineral maps and images. Measurement resolution was set to 0.8 μm or 1 μm to capture the fine particle sizes. It was used to evaluate the distribution, modal abundances, and deportment of REE in all samples. Each sample was measured using PMA (particle mineral analysis) and TMS (trace mineral search). Electron microprobe mineralogical analyses (Cameca SX 100) using an accelerating voltage of 20 kV and beam current of 20 nA, were also performed on selected minerals in order to define REE contents of minerals with more accuracy (low detection limits (0.14-0.35 %)). The deportment data is calculated based on the mass of a mineral in the sample and the amount of the element in the composition of that mineral (from mineral composition data produced by EPMA). Note that only the elements quantified by EPMA are included in the deportment calculations. This mineralogical information with assay reconciliation is linked to the material's reactivities and is therefore crucial to understand the geochemical behavior of the REE-bearing minerals (Peelman et al., 2016).

6.4 Results and discussion

6.4.1 Sample physical and chemical characteristics

The particle size distribution has a great importance in the interpretation of kinetic test results (Erguler et al., 2015), since fine particles are more reactive than coarse particles. The particle size distributions of the materials are shown in Table 6-1. The lithologies were prepared in order to show a particle size distribution similar to that of the magnetic concentrate (MC); the D_{50} values vary between 18 and 30 µm (Table 6-1) for all samples.

The other physical properties are summarized in Table 6-1. The specific gravity was similar in all samples (2.8-3.16 $g.cm^{-3}$). The specific surface area of MC (5.17 $m^2.g^{-1}$) was higher than for the waste rocks (1.75-3.14 $m^2.g^{-1}$).

The chemical compositions of the samples are shown in Table 6-1. The whole-rock analyses of the waste rocks samples (WS, WCCP) and the ore (MC) show similar concentrations of SiO_2 (52–54 %), Al_2O_3 (6–7 %), Fe_2O_3 (8–9 %), Na_2O (4–6 wt.%), and K_2O (1.78–3 %), and higher variation in MgO (6–14 %) and CaO (6.64–11.99 %) (Table 6-1).

The whole-rock analyses of the PG and MBG samples show similar concentrations of SiO_2 (60–70 %), Al_2O_3 (11–13 %), Fe_2O_3 (6–9 %), and Na_2O (4.65–7.8 %) (Table 6-1). In comparison with these samples, WCCR has a higher concentration of CaO (29.5 %) and a lower concentration of SiO_2 (19.02 %). The WCCR material is the only one with significant carbonate content; therefore, it shows the highest carbon concentration (6.36 %) in comparison to the other samples (less than 0.14 %). The sulfur content is less than 0.07 % in all samples. The chemical composition of all samples is highlighted in Table 6-1.

The results in Table 6-1 show that all samples are richer in LREE (412-6117 mg/l) than in HREE (103.2-5547.46 mg/l). The concentrate MC has the highest concentration of LREE, while the MBG contains the lowest concentration. Yttrium is the most abundant element in all samples, with a maximum in the MC (11 712 mg/l) and a minimum in the MBG sample (524 mg/l).

Tableau 6-1 : Physical and chemical compositions of WS, WCCP, WCCR, MC, PG and MBG samples.

	Unit	WS	WCCP	WCCR	MC	PG	MBG
Physical properties							
Specific gravity	$g.cm^{-3}$	3.01	3.12	2.96	3.16	2.91	2.8
Specific surface area	$m^2.g^{-1}$	2.28	2.25	3.14	5.17	2.49	1.75
D_{90}	µm	110	115	60	60	110	60
D_{80}	µm	70	80	50	50	70	42
D_{50}	µm	25	30	20	20	25	18
Chemical composition							
C total	%	0.07	0.06	6.36	0.14	0.06	0.03
S total	%	0.02	0.02	0.02	0.04	0.07	0.01
SiO_2	%	55.98	52.92	19.02	54.3	60.42	70.18
Al_2O_3	%	6.89	5.93	0.66	7.06	13.76	11.18
Fe_2O_3	%	6.29	4.26	0.5	7.95	8.99	6.09
MgO	%	10.5	14.2	24.78	6.88	0.84	0.15
CaO	%	6.64	11.19	29.5	9.38	2.31	0.61
Na_2O	%	6.1	4.43	0.18	6.19	7.85	4.64
K_2O	%	2.99	1.78	0.36	2.15	3.05	5.03
TiO_2	%	0.33	0.26	0.02	0.84	0.96	0.39
P_2O_5	%	0.21	0.42	0.01	0.45	0.28	0.05
MnO	%	0.31	0.27	0.03	0.51	0.19	0.13
Cr_2O_3	%	0.04	0.04	0.05	0.08	0.04	0.1
V_2O_5	%	< 0.01	< 0.01	< 0.01	0.01	< 0.01	< 0.01
LOI	%	0.92	0.94	23.28	1.39	0.52	0.19
Rare earth elements							
Sc	mg/l	37.25	21.64	1.09	37.91	9.09	2.65
Y	mg/l	450.35	413.99	218.17	4497.99	409.94	83.06
La	mg/l	201.39	166.24	116.5	1208.74	146.17	103.76
Ce	mg/l	393.09	360.13	188.15	2687.22	300.66	190.72
Pr	mg/l	44.07	42.6	18.66	320.19	36.53	21.82
Nd	mg/l	163.5	163.96	64.62	1287.3	144.84	80.03
Sm	mg/l	31.2	33.81	12.06	297.47	29.95	12.34
Eu	mg/l	3.73	4.08	1.42	37.51	3.83	0.98
Gd	mg/l	27.83	29.27	10.51	278.41	27.75	8.35
Tb	mg/l	5.14	5.18	1.88	51.56	5.01	1.13
Dy	mg/l	35.01	36.2	13.21	368.84	35.94	6.7
Ho	mg/l	7.81	7.79	2.95	78.03	7.6	1.28

Er	mg/l	29.27	28.87	10.62	267.38	25.87	4.06
Tm	mg/l	4.91	4.93	1.52	38.73	3.63	0.65
Yb	mg/l	43.09	43.97	10.3	254.93	24.34	6.32

6.4.2 Mineralogical characterization

The mineralogical composition of the materials determined by XRD is summarized in Figure 6-2. All samples that were studied, except WCCR, are generally composed of same mineralogical phases but with different proportions: quartz (SiO_2), biotite ($K(Mg,Fe)_3(AlSi_3O_{10}(OH,F)_2$), diopside ($CaMgSi_2O_6$), aegirine-augite ($(Ca,Na)(Mg,Fe_2)(Si_2O_6)$), actinolite ($Ca_2(Mg,Fe)_5Si_8O_{22}(OH)_2$), calcite ($CaCO_3$), and microcline ($KAlSi_3O_8$). Other accessory minerals identified include zircon ($ZrSiO_4$), magnesio/ferri-katophorite $Na_2Ca(Fe,Mg)_4Fe(Si_7Al)O_{22}(OH)_2$, dolomite $CaMg(CO_3)_2$, and titanite ($CaTiSiO_5$). Calcite represents more than 70 % of the WCCCR sample and the remaining phases are mainly silicates minerals (i.e., biotite, diopside, quartz, aegirine/augite, and albite).

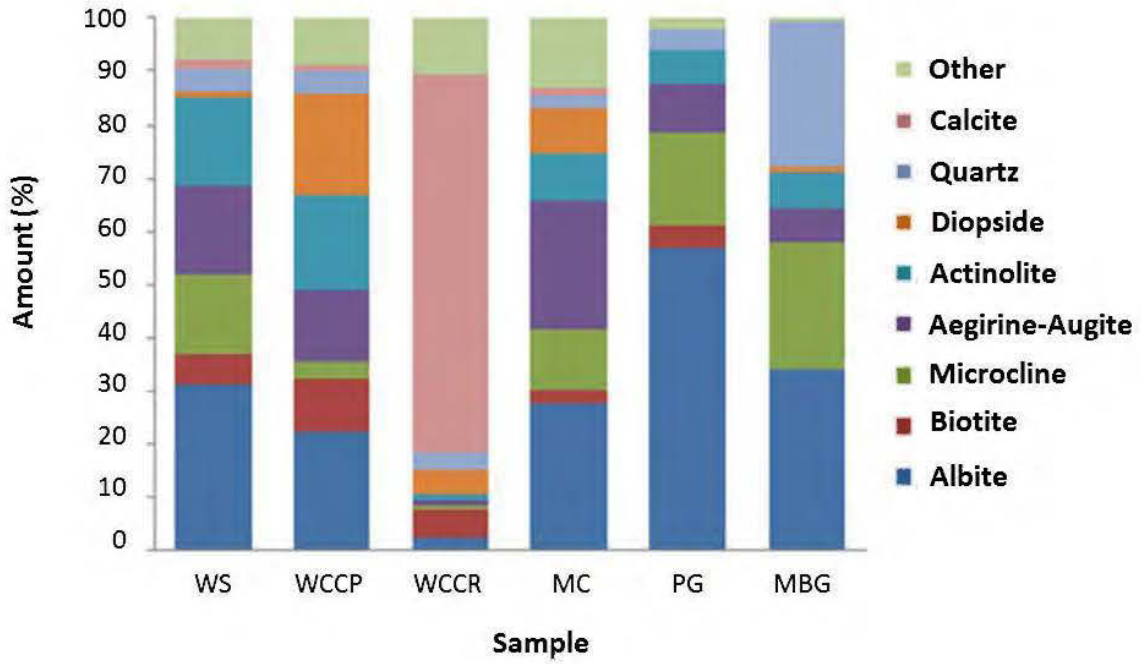

Figure 6-2 : Quantification of crystalline phase minerals in WS, WCCP, WCCR, MC, PG and MBG samples.

SEM-EDS investigation shows that: (i) the REE are liberated and/or associated with magnesiokatophorite/katophorite, apatite, zircon, albite (the partially liberated phases are called

middiling category; Figure 6-3); (ii) all analysed minerals contain mostly LREE (La, Ce, Pr, Nd, Sm, and Y); (iii) three groups of silicate minerals were detected with variable concentrations of Y. Sulfide particles (pyrite, pyrrhotite, galena, and sphalerite) were also identified in all samples.

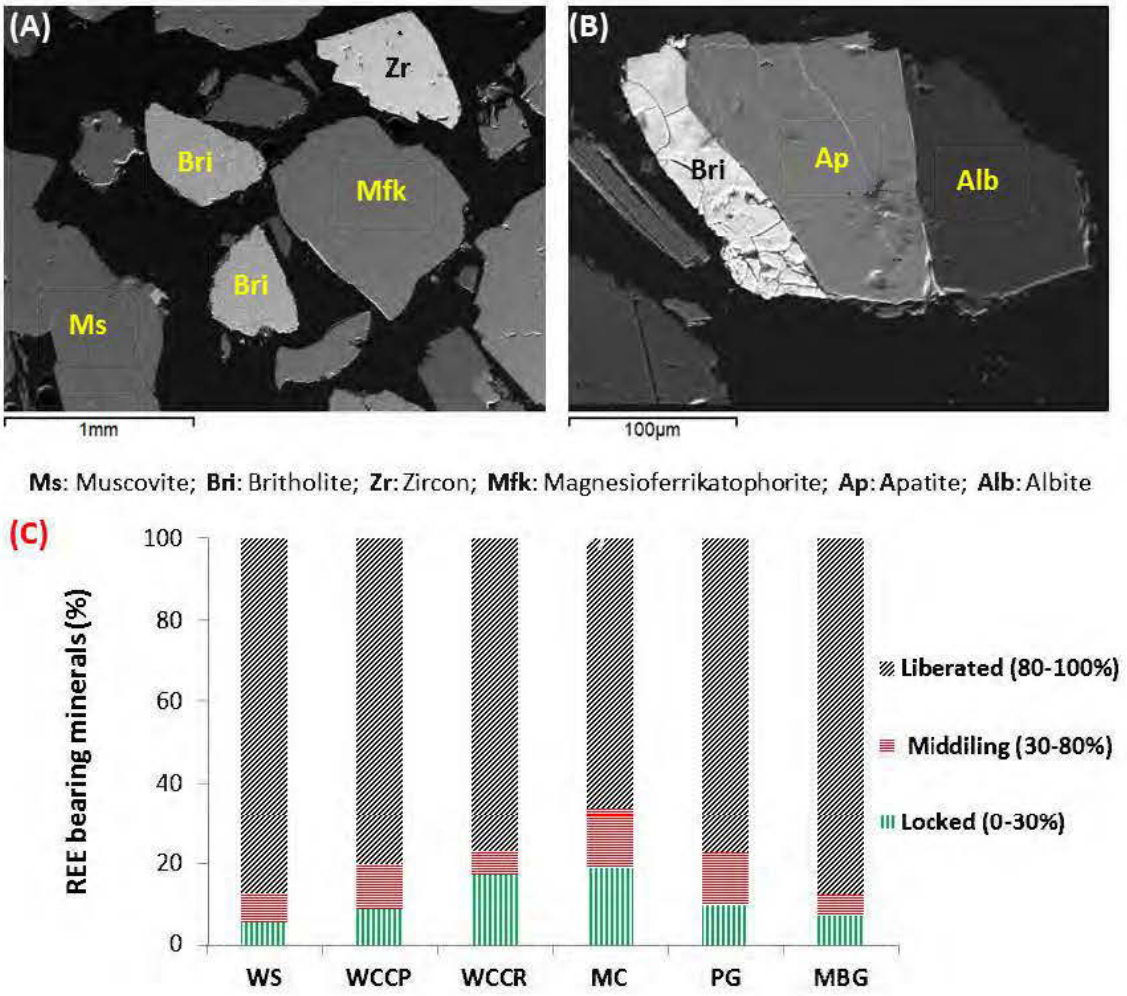

Figure 6-3 : Scanning Electron Microscope (SEM) electron micrograph showing gangue minerals, REE-bearing minerals (A), and their mineralogical associations (B) and liberation of the REE-bearing minerals (C).

The mineralogical modal composition of the studied samples obtained using QEMSCAN® is shown in Figure 6-4. The definition of each mineral category is summarized in Table 6-2. The results show that all samples are dominated by feldspar, amphibole, and biotite. However, MC is dominated by two other phases, namely calcite and chondrodite (Na-Mg Silicate). The XRD results are consistent with those of the quantitative mineralogy obtained by QEMSCAN® analyses.

Sulphides minerals occur at trace levels mainly as pyrite (FeS_2), sphalerite (ZnS), galena (PbS), pyrrhotite ($Fe_{(1-X)}S$), and chalcopyrite ($CuFeS_2$). The gangue minerals of the studied samples are maiuly composed of iron oxides, carbonates (ankerite, dolomite, and calcite), plagioclase (albite), barite, quartz, and micas (biotite). The REE minerals are mosandrite $(Na(Na,Ca)_2(Ca,Ce,Y)_4(Ti,Nb,Zr)(Si_2O_7)_2(O,F)_2F_3)$, monazite $(La,Ce,Nd,Sm)PO_4)$, fluorbritholite $(Ca,Ce,La,Na)_5(SiO_4,PO_4)_3(OH,F)$, apatite $(Ca_5(PO_4)_3F)$, aqualite $((H_3O)_8(Na,K,Sr)_5Ca_6Zr_3Si_{26}O_{66}(OH)_9Cl)$, and thorosteepstrupine, whereas the Zr silicates include reidite ($ZrSiO_4$) and catapleiite ($(Na,Ca)_2ZrSi_3O_9•2(H_2O)$) (Table 6-2).

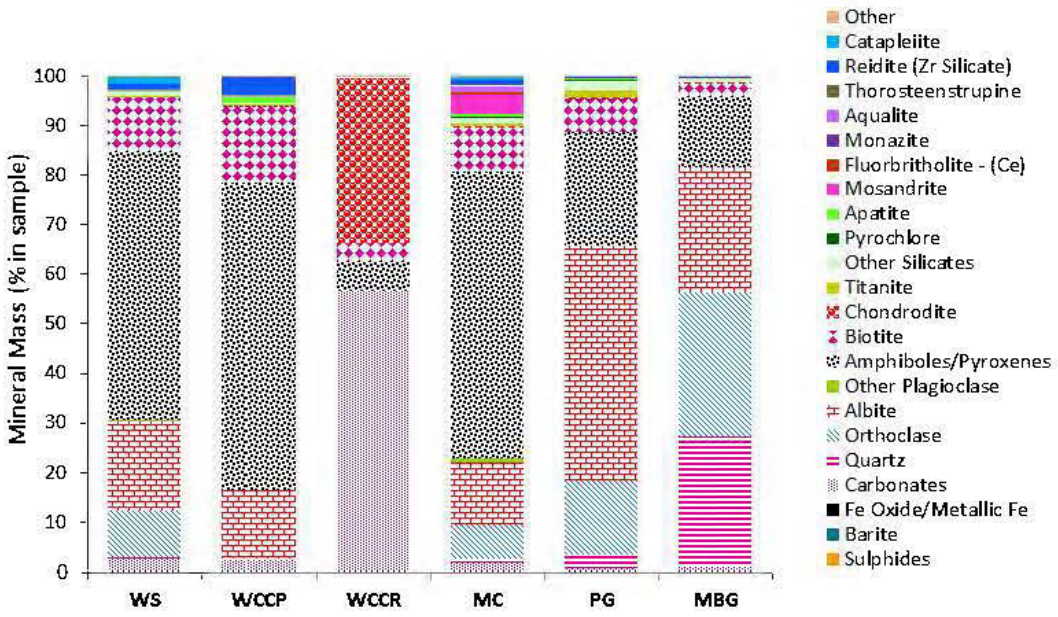

Figure 6-4 : Mineralogical characterization of REE-bearing minerals using QEMSCAN®.

Tableau 6-2 : Description of mineral category obtained by QEMSCAN®.

Mineral category	Grouping Includes
Sulphides	Chalcopyrite, Sphalerite, Galena, Pyrite, Pyrrhotite
Barite	Barite
Fe Oxide/Metallic Fe	Magnetite/Hematite, Fe Metal Shards
Carbonates	Calcite, Siderite, Ca Mg Fe Carbonate
Quartz	Quartz
Orthoclase	Orthoclase
Ankerite/Dolomite	Ankerite, Dolomite
Albite	Albite, Albite Boundaries with Other Silicates

Other Plagioclase	Plagioclase An20-80
Orthoclase	Orthoclase
Amphiboles	Actinolite/Tremolite, Aegirine, Arfveedsonite
Biotite	Biotite, Biotite Boundaries with Silicates
Chondrodite	Chondrodite, Boundaries with Silicates
Titanite	Titanite
Other Silicates	Chlorite, Muscovite, Epidote, Catapleiite
Pyrochlore	Pyrochlore
Apatite	Apatite, Apatite Boundaries
Mosandrite	Mosandrite
Fluorobritholite - Ce	Fluorbritholite - Ce, Fluorbritholite - Ce Boundaries
Monazite	Titanite
Aqualite	Pyroxenes, Amphiboles, Epidote, Zircon
Thorosteepstrupine	Titanite
Reidite	Zr Silicate, Zircon

An example of typical association of REE-bearing minerals with silicate minerals is provided in Figure 6-5 (a, b, d, e, f, and g). The QEMSCAN® mineralogical investigation provide with the main following observations: (i) the REE are associated or included with amphibole/pyroxenes, Zr silicates (i.e. aqualite), and pyrochlore. In addition, monazite often occurs as inclusions within fluorbritholite-Ce (Figure 6-5c).

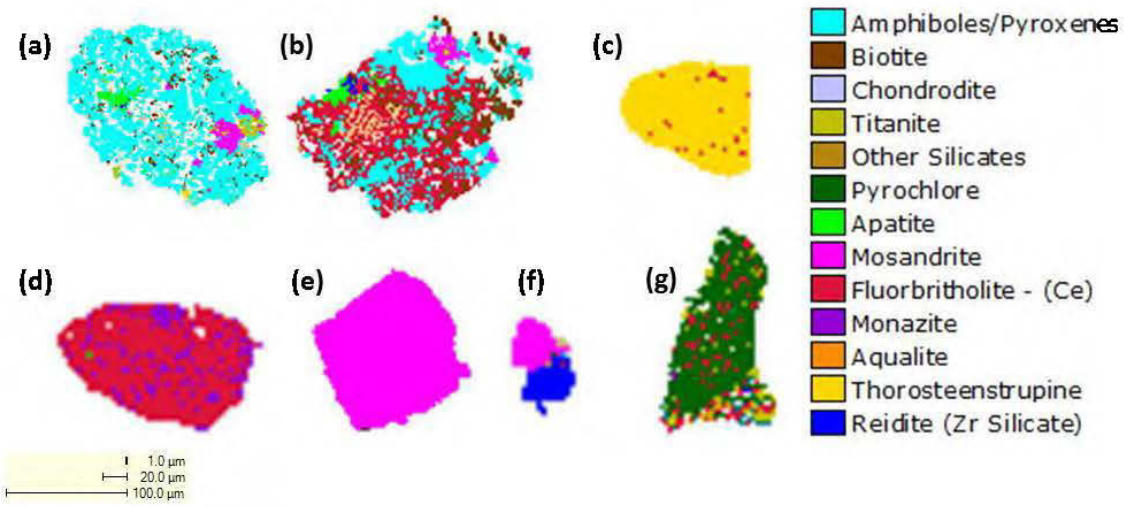

Figure 6-5 : REE typical associations in Kipawa lithologies by QEMSCAN® analysis: (a and b) REE inclusion in amphibole/pyroxenes, (c) REE inclusions in aqualite, (d) Monazite inclusions

in fluorbritholite, (e) liberated REE particle, (f) REE associated with Zr silicates and (g) REE inclusions within pyrochlore.

Figure 6-6 illustrates the degree of liberation of REE-bearing minerals and Zr silicates found in the samples once finely ground (extreme reactivity condition mimicking REE ore processing): particles are free, well-liberated (more than 70 %), associated with other minerals (i.e. silicate minerals, mainly amphibole/pyroxene), and included within other gangue minerals (Table 6-2). Therefore, the absolute reactivity of the majority of REE-bearing minerals is expected to be significant due to their high degree of liberation of the materials once milled. The Zr-bearing silicates show similar liberation as the REE-bearing minerals. The QEMSCAN® results also show that the REE distribution is more concentrated in the finer fractions (Figure 6-7).

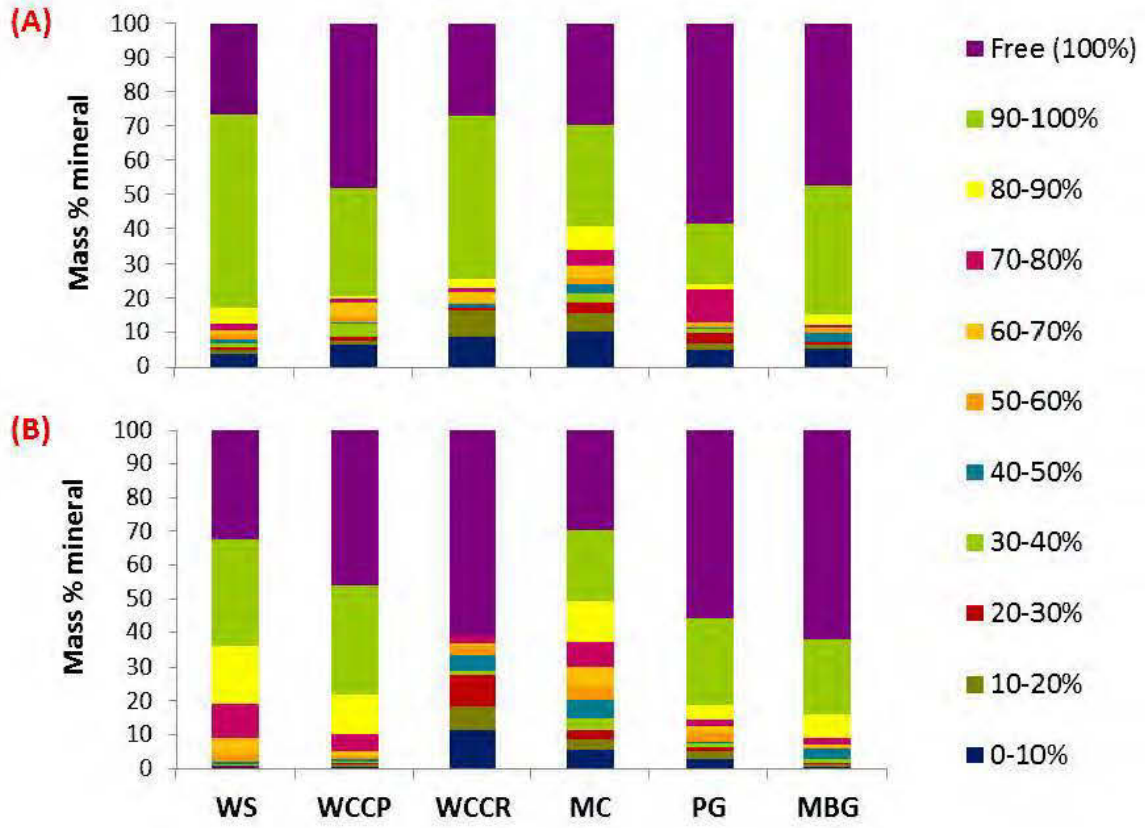

Figure 6-6 : The degree of liberation of REE-bearing minerals and Zr silicates within Kipawa lithologies.

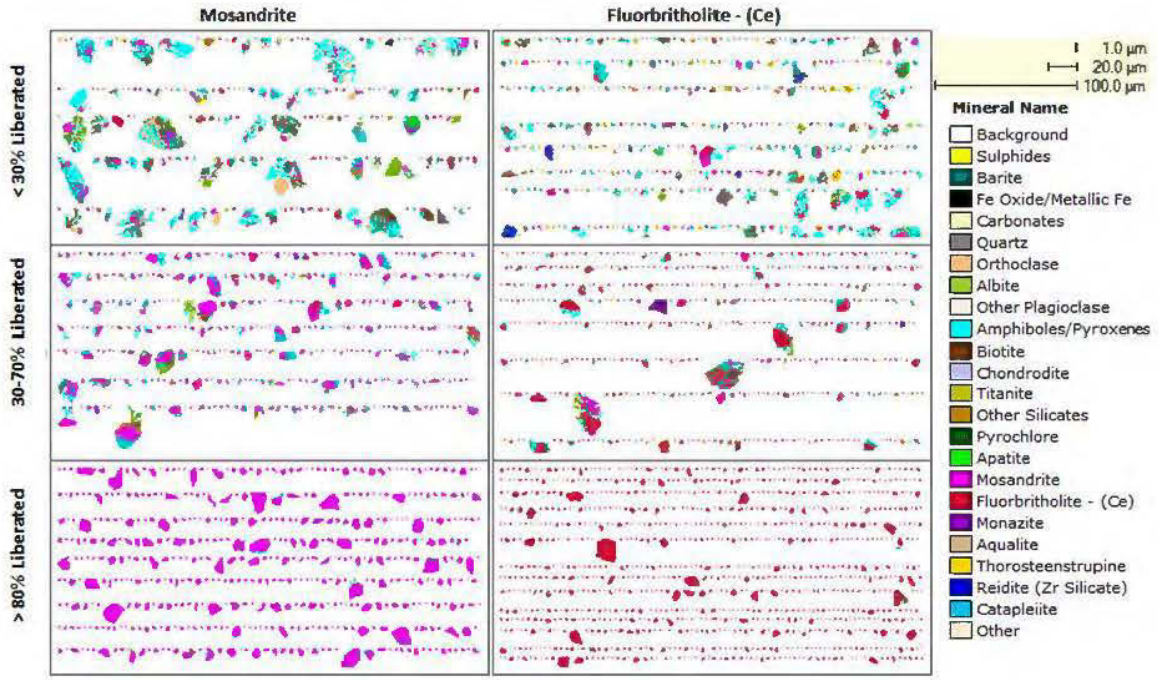

Figure 6-7 : The degree of liberation of mosandrite and fluobritholite within Kipawa lithologies.

QA/QC protocols for QEMSCAN measurements include comparison of chemical assays to assays calculated from the mineralogical measurements. The objective of the reconciliation is to ensure that the sample measurements are representative. The difference between elemental assays provided by QEMSCAN® and those obtained by chemical analyses using ICP is shown in Table 6-3. The assays obtained by both methods are generally of the same order. The discrepancies observed are acceptable and might be potentially due to: (i) the dissemination of the REE mineralization at fine sizes (<1 µm) in the gangue minerals, which is challenging to quantify by QEMSCAN®, (ii) the Kipawa mineralogy is complex. Each mineral phase which was grouped into mineral "bins" to create a simplified QEMSCAN® list, has a range of compositions. Average chemistry was applied to each bin for processing and reporting. (iii) the difficulties to dissolve some refractory minerals such Zr silicates for the chemical analyses, which leads to an underestimation of the associated elements, (vi) the effect of particle size, since the particles used in polished sections are coarser compared to those used for chemical analyses (Andersen et al., 2009; Goodall et al., 2005; Rollinson et al., 2011; Mackay et al., 2016). These cause homogenization problems and, consequently, the discrepancies between two techniques

Tableau 6-3 : Comparison of La, Ce, Nd, Pr, and Y determined by QEMSCAN® and chemical assays (ICP-MS) within Kipawa lithologies; QA and CA values in mg/l.

	Ce			La			Nd			Pr			Y		
	QA[a]	CA[b]	diff[c]	QA[a]	CA[b]	diff[c]	QA[a]	CA[b]	diff[c]	QA[a]	CA[b]	diff[c]	QA[a]	CA[b]	diff[c]
WS	373	390	-4.55	178	200	-11	112	160	-30	37	44	-15.90	163	450	-63.77
WCCP	608	360	40.78	309	166	86.14	205	160	28.12	63	43	46.51	84	400	-79
WCCR	145	188	-29.65	81	120	-32.5	30	18	66.66	13	19	-31.57	14	200	-93
MC	2851	2680	5.99	1186	1210	-1.98	1019	1280	-20.39	310	300	3.33	2272	4500	-49.51
PG	296	300	-1.35	119	150	-20.66	77	100	-23	25	30	-16.66	93	410	-77.31
MBG	217	190	12.44	110	104	5.76	72	80	-10	21	22	-4.54	6	83	-92.77

[a]: ∑(Ce, La, Nd, Pr, Sm, and Y) from quantitative values of minerals detected by QEMSCAN analyses.

[b]: Element value from chemical analyses.

[c]: Difference between QA and CA, in %.

6.4.3 REE deportment

Figure 6-8 shows the distribution of Nd, Pr, Ce, and La between the minerals identified in the samples. The results are shown as % wt. of the element in the sample. Nd, Pr, Ce, and La deportments indicate that the majority of REE are locked within mosandrite, fluorbritholite, apatite, monazite, aqualite, titanite, and thorosteestrupine. Figure 6-8 shows that Ce and La deport in similar contents within fluobritholite, apatite, and mosandrite. However, Nd deports at greater levels into apatite and mosandrite compared to La and Ce. However, all HREE but Y (0.22-4.81 %) are under the EPMA detection limit. The Y is mainly associated with mosandrite, monazite, fluoroapatite, fluobritholite, aqualite, thorosteenstrupine, and titanite, with the highest contents in mosandrite (4.81 %) and the lowest in titanite (0.22 %).

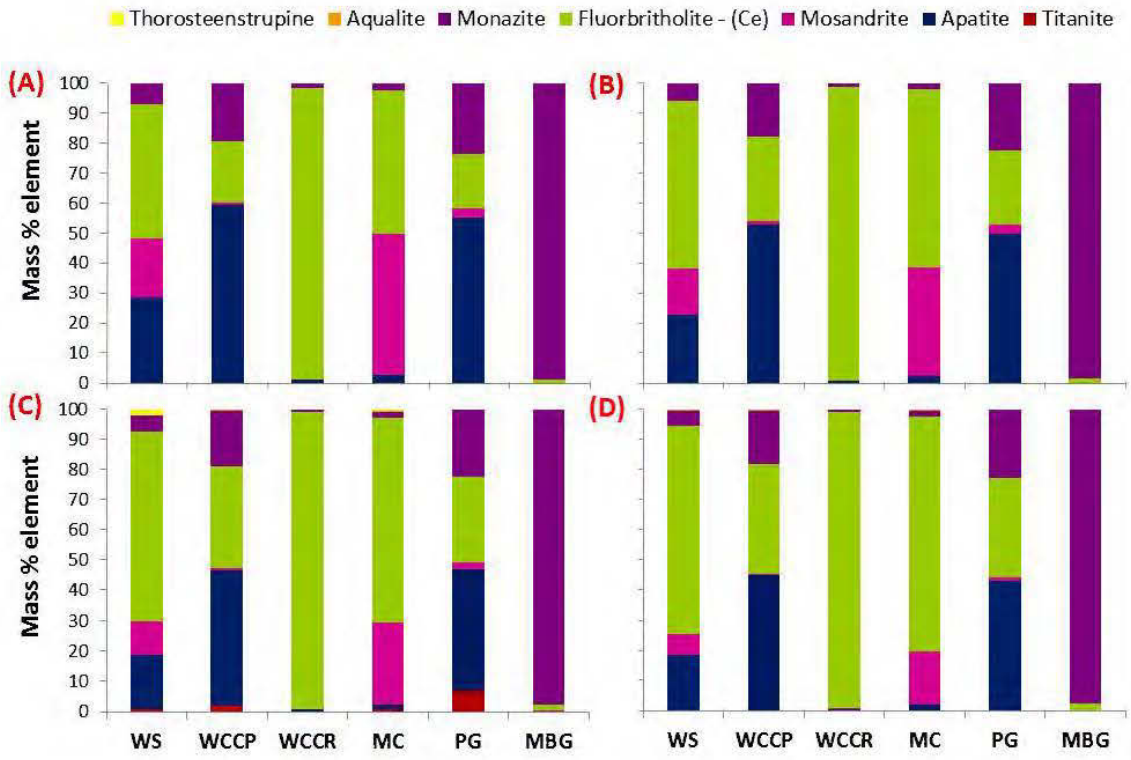

Figure 6-8 : Nd (A), Pr (B), Ce (C) and La (D) deportment in REE-bearing minerals.

6.4.4 Geochemical behavior

The geochemical behavior of the materials was evaluated using weathering cells during 40 cycles (20 weeks). The pH, electrical conductivity, Eh, and alkalinity values of the weathering cell

leachates are shown in Figures 6-9a, 6-9b, 6-9c and 6-9d, respectively. The leachates of all samples had a relatively stable pH, varying between 7.0 and 9.8. The leachates of the WCCR and WCCP showed a higher pH, varying between 8.5 and 9.78 while the MC, PG, and MBG samples showed a pH varying between 7.0 and 9.5. The electrical conductivity of the samples varied between 30 and 168 µS/cm. The redox potential varied from 428 to 816 mV, while the alkalinity values stabilized below 100 mg/l. These results confirmed the weak reactivity of silicates in weathering cell conditions.

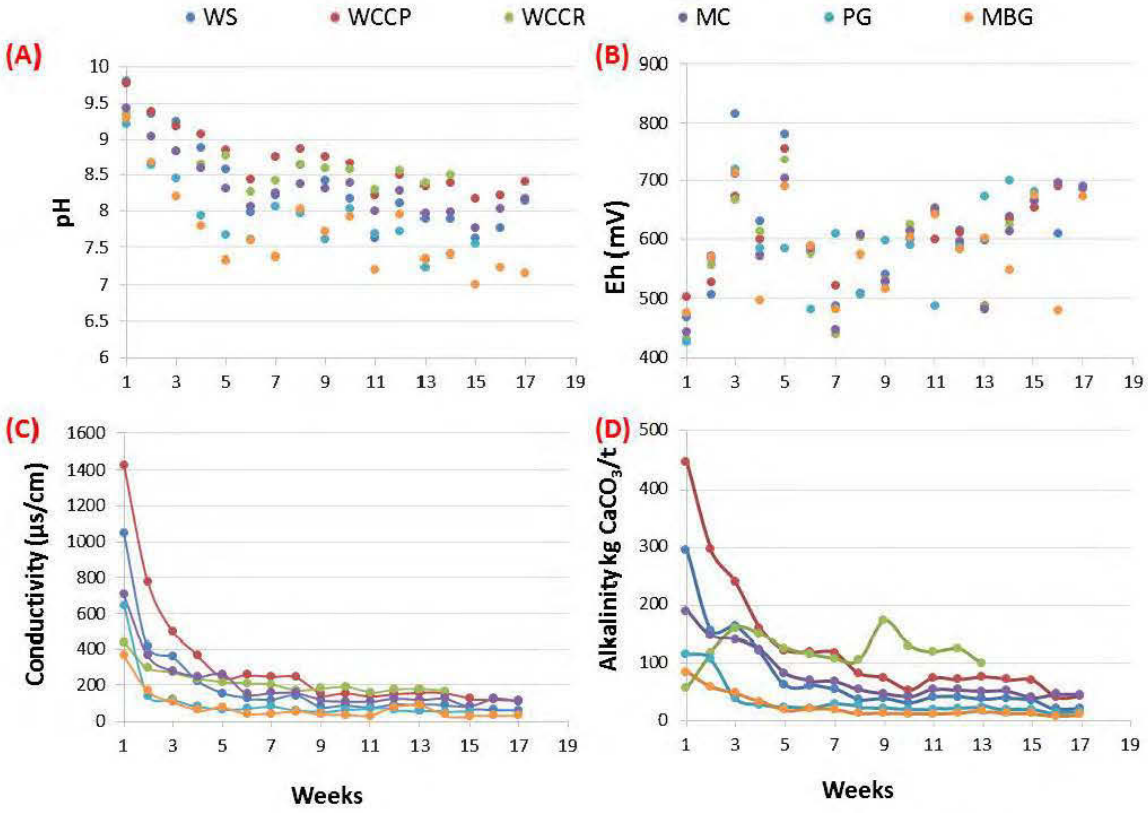

Figure 6-9 : pH (a), electrical conductivity (µS/cm) (b), Eh (mV) (c), and alkalinity values (d) of the weathering cell leachates.

The concentrations of dissolved elements (sulfates, metals, and REE) are displayed in Figures 6-10a to 6-10f. The concentrations of S, most probably occurs as sulfates (47.7 mg/l), Ca (22.5 mg/l), Zn (0.084 mg/l), and Mn (0.31 mg/l), in the MC were higher than in other samples (SW, WCCP, WCCR, PG, and MBG). The concentration of Th was analyzed in all leachates and was under the detection limit (0.1 ppb) of the ICP-MS method used. The elements Nb and U were less abundant than Th and were not analyzed in the leachates. The concentrations were often higher in the first

flushes due to a combination of the leaching of already oxidized products formed prior to the kinetic test, the rapid reaction of the finer particles and their depletion, and the surface passivation of the minerals (Benzaazoua et al., 2004). The highest sum of released LREE (Figure 6-10f) was recorded in concentrate sample MC (31 µg/l), while the lowest sum was found in the WCCR (4 µg/l). The leached concentrations of HREE are between 3.5 and 70 µg/l, with the maximum observed for MC and the minimum for WCCR. The low leaching of REE is mainly due to: (i) the low reactivity of REE silicates under these leaching conditions, (ii) the sorption phenomena of the leached REE on secondary minerals surfaces within weathering cells (i.e., iron oxyhydroxides), and (iii) the precipitation of secondary REE-bearing minerals. Indeed, the REE-bearing minerals leach low concentrations of REE, that get to be sorbed or precipitated as secondary minerals, which explains the low REE concentrations measured in the leachates. Despite the abundance of LREE compared to HREE in all solid samples, the HREE concentrations in the leachates are higher compared to the LREE. In fact, the LREE/HREE ratio is lower in the leachates than in the solids. This also suggests that HREE are leached preferentially and/or that they are more mobile than LREE.

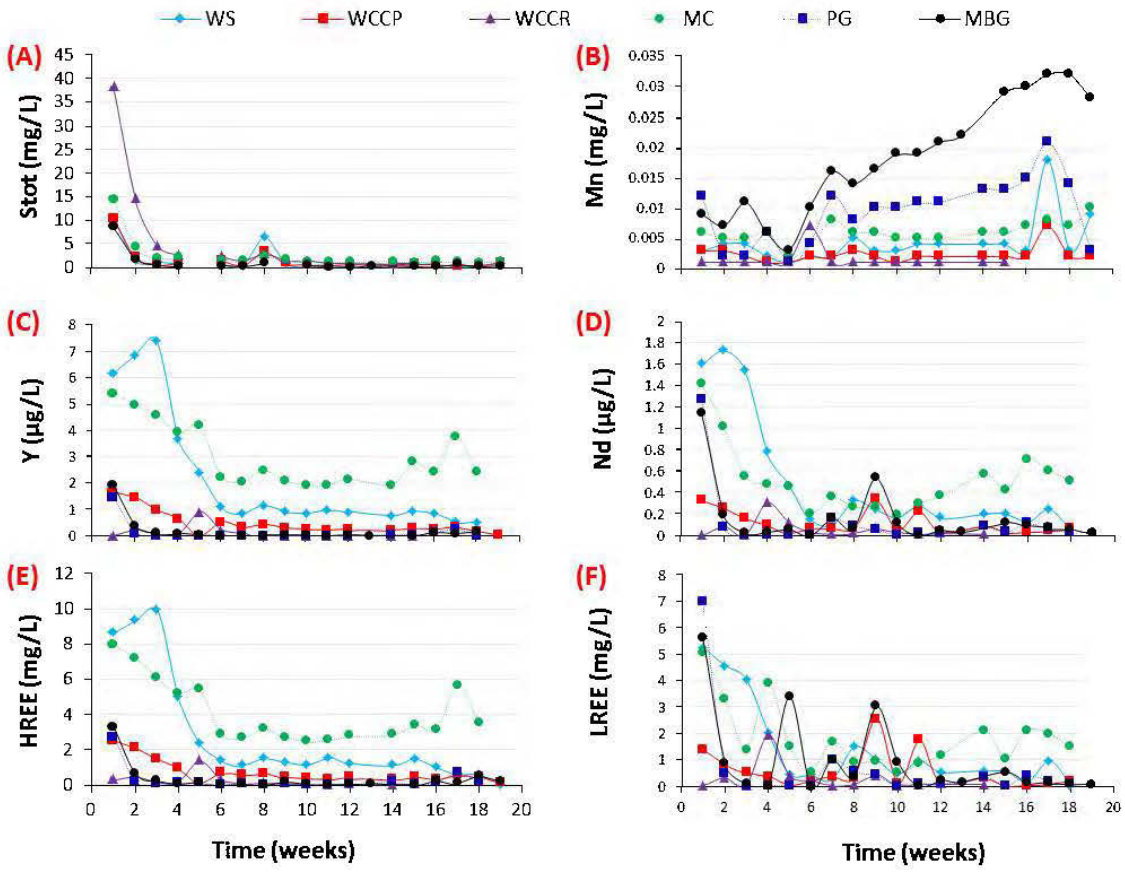

Figure 6-10 : Leachates punctual concentrations of studied samples: total sulfur (A), Mn (B), Y (C), Nd (D), HREE (E) and LREE (F).

The weathering cells leachates of the magnetic concentrate MC (where concentrations are significantly higher) were submitted to thermodynamical equilibrium calculations using the VMinteq code (Jon Petter Gustafsson, 2000). In the weathering cell conditions of the present study (neutral to alkaline conditions), REE, Fe, Al, Mg, and Mn are, according to the modelling, predicted to precipitate as various secondary minerals such as $REE(OH)_3$, hematite Fe_2O_3, goethite $FeO(OH)$, kaolinite $Al_2Si_2O_5(OH)_4$, magnesioferrite $Mg(Fe^{3+})_2O_4$, lepidocrocite $Fe^{3+}O(OH)$, and Ferrihydrite $(Fe^{3+})_2O_3 \times 0.5H_2O$ (Figure 6-11). In the case of all the other samples, the modelling showed similar results. These secondary minerals could precipitate, co-precipitate, and/or adsorb REE, which could explain the low REE concentrations in the leachates. This geochemical behavior could be explained through the following assumptions: (i) ionic radius; LREE have a higher ionic radius relative to HREE, which makes them less stable in the crystal matrix, and (ii) geochemical affinity (sorption) of the LREE to carbonates, iron/manganese oxyhydroxides, clays, and phosphates.

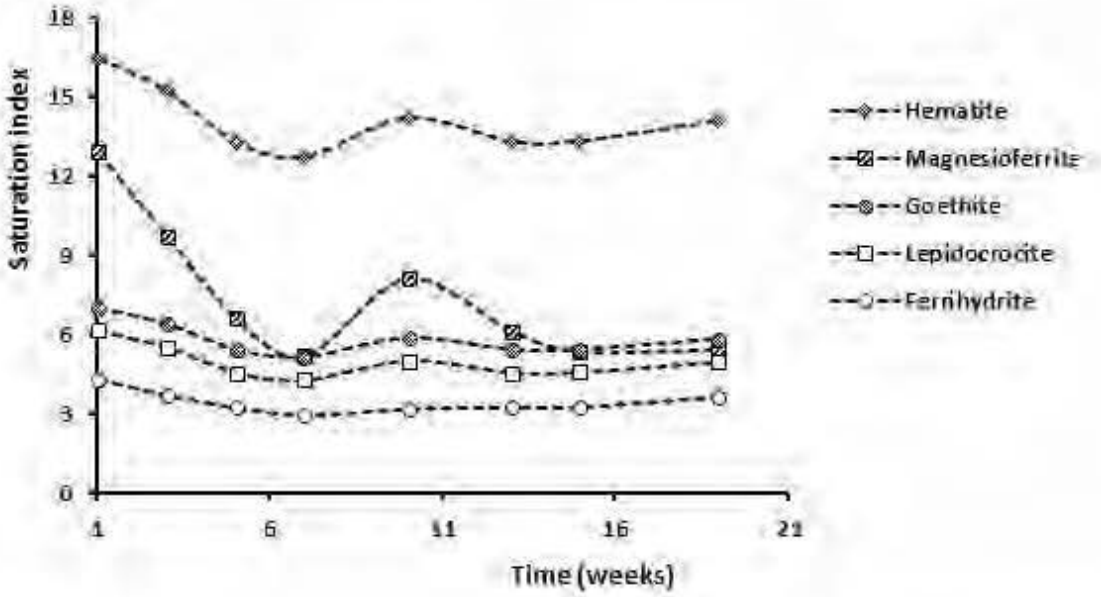

Figure 6-11 : Saturation indexes of secondary minerals throughout MC weathering cell flushes.

6.5 Conclusion

The mineralogical characterization and the geochemical behavior of REE-bearing minerals from different lithologies and a REE concentrate were investigated in this study. A detailed characterization of these samples showed that the majority of REE-bearing minerals are liberated when finely ground, and the remaining fraction (less than 30 %) is associated or locked within gangue minerals (amphibole/pyroxene, feldspar and micas). The main REE-bearing minerals are fluobritholite, mosandrite, apatite, and Zr-bearing silicates. The QEMSCAN® analyses coupled with EPMA and chemical assays confirm that REE are more concentrated in the finer fractions with a high degree of liberation (>70 %) which favours their dissolution in contact with water and oxygen during kinetic tests.

Geochemical results from kinetic tests show that:

- The leachability of REE from the studied silicates deposit is low in weathering cell conditions.
- The LREE/HREE ratio is lower in the leachates than in the solids. This also suggests that HREE are leached preferentially and/or that they are more mobile than LREE.
- Degree of liberation of minerals linked to reactivity.

- Several secondary minerals could contribute to control the solubility of REE upon their leaching, such as iron, manganese hydro/oxides.

In order to better understand the geochemical behavior of REE, further research is required: (i) advanced chemical and physical characterizations using EXAFS and XPS techniques, (ii) comparison of field tests results with those of laboratory tests, and (iii) determination and testing the various REE-bearing secondary minerals that can form during kinetic tests in order to deduce the factors affecting the REE leach rates.

6.6 Acknowledgements

The authors thank the URSTM, staff for their support with laboratory work and NSERC for funding of this study. The authors thank gratefully the mining company Matamec Explorations for the great help, especially in the sampling steps.

REFERENCES

Andersen, J C., Rollinson, G.K., Snook, B., Herrington, R., and Fairhurst, R.J. (2009). Use of QEMSCAN® for the characterization of Ni-rich and Ni-poor goethite in laterite ores. Minerals Engineering, vol. 22, no 13, p. 1119-1129.

Benzaazoua, M., Bussière, B., Dagenais, A.M., and Archambault, M. (2004). Kinetic tests comparison and interpretation for prediction of the Joutel tailings acid generation potential. Environmental Geology 46, 1086-1101.

Biennemas, K., Jones, P.T., Blanpain, B., Gerven, T.V., Yang, Y., Walton, A., and Buchert, M. (2013). Recycling of rare earth earths: a critical review. Journal of cleaner production 51, 1-22.

Bouzahzah H., Benzaazoua M., and Bussière B. (2014). Prediction of Acid Mine Drainage: Importance of Mineralogy and the Test Protocols for Static and Kinetic Tests Mine Water and the Environment. Mine Water and the Environment", Mine Water and the Environment, 33:54–65.

Bouzahzah H., Benzaazoua M., Mermillod-Blondin, R., and Pirard, E. (2015). A novel procedure for polished section preparation for automated mineralogy avoiding internal particle settlement. 12th International Congress for Applied Mineralogy (ICAM). Istanbul (Turkey), 10-12 August 2015.

Brunauer, S., Emmett, P.H., and Teller, E. (1938). Adsorption of gases in multimolecular loyers. Journal of the American Chemical Society, 60: 309-319.

Calas, G. (2012). Elements. International Magazine of Mineralogy, Geochemistry, and Petrology, vol. 8, no ISSN: 1811-5209.

Chakhmouradian, A. R., and Wall, F. (2012). Rare Earth Elements: Minerals, Mines, Magnets (and More). Elements, vol. 8, no 5, p. 3.

Cheng. Z. (2011). Global rare earth resources and scenarios of future rare earth industry. Journal of Rare Earths, vol. 29, no 1, p. 1-6.

Cheng, Z., Jingkun, J., Oscar, F., Shuxiao, W., and Jiming, H. (2013). Characteristics and health impacts of particulate matter pollution in China (2001–2011). Atmospheric Environment, vol. 65, no 0, p. 186-194.

Dai, S., Panpan, X., Shaohui, J., Colin, W., James, C., Xiaoyun, Y., David, F. (2017). Enrichment of U-Re-V-Cr-Se and rare earth elements in the Late Permian coals of the Moxinpo Coalfield, Chongqing, China: Genetic implications from geochemical and mineralogical data. Ore Geology Reviews, vol. 80, p. 1-17.

Edahbi, M., Plante, B., Bouzahzah, H., Benzaazoua, M., and Plettier.M. (2015). Mineralogical and geochemical study of rare earth elements from a carbonatite deposit. Proceedings of the 13th SGA biennial meeting, Nancy, France, 24-27 août 2015.

Elzinga, E. J., Reeder, R. J. S., Withers, H., Peale, R. E., Mason, R. A., Beck K. M., and Hess, W. P. (2002). EXAFS study of rare-earth element coordination in calcite. Geochimica et Cosmochimica Acta, vol. 66, no 16, p. 2875-2885.

Erguler, Z., and Güzide, K. (2015). The effect of particle size on acid mine drainage generation: Kinetic column tests. Minerals Engineering, vol. 76, p. 154-167.

Goodall, R., Peter, J., and Alan, R. (2005). The use of QEMSCAN® and diagnostic leaching in the characterisation of visible gold in complex ores. Minerals Engineering, vol. 18, no 8, p. 877-886.

Hao, Z., Yonghua, L., Hairong, L., Binggan, W., Xiaoyong, L., Tao, L., and Jiangping, Y. (2015). Levels of rare earth elements, heavy metals and uranium in a population living in Baiyun Obo, Inner Mongolia, China: A pilot study. Chemosphere, vol. 128, p. 161-170.

Hong, F. (2006). Rare Earth: Production, Trade and Demand. Journal of Iron and Steel Research, International, vol. 13, p. 33-38.

Humphries, M. (2013). Rare Earth Elements: The Global Supply Chain. Congressional Research Service, 7-5700 (http://www.fas. org/sgp/crs/natsec/R41347.pdf).

Jia, Y. Q. (1991). Crystal radii and effective ionic radii of the rare earth ions. Journal of Solid State Chemistry, vol. 95, no 1, p. 184-187.

Lema. I.B., and Leal Filho,W. (2016). Rare earth industry, Technological, Economic, and environnemental Implications.

Lipin, B.R, and Mackay, G.A. (1989). Geochemistry and mineralogy of rare earth elements. Mineralogical society of America, volume 21.

Mackay, D. A. R., G. J. Simandl, W., Redfearn, M., and Gravel, J. (2016). Indicator mineral-based exploration for carbonatites and related specialty metal deposits — A QEMSCAN®®

orientation survey, British Columbia, Canada. Journal of Geochemical Exploration, vol. 165, p. 159-173.

Peelman, S., Zhi, H. I., Sun, Ji, J., Yongxiang, Y. (2016). Leaching of Rare Earth Elements: Review of Past and Present Technologies A2 - Lima, Ismar Borges De. In Rare Earths Industry, Walter Leal Filho, chapter 21, p 319-334. Boston: Elsevier.

Plante, B., Bussière, B., Benzaazoua, M. (2014). Lab to field scale effects on contaminated neutral drainage prediction from the Tio mine waste rocks. Journal of Geochemical Exploration 137, 37-47.

Plante, B., M. Benzaazoua, and B. Bussière. (2010b). Kinetic Testing and Sorption Studies by Modified Weathering Cells to Characterize the Potential to Generate Contaminated Neutral Drainage. Mine Water and the Environment 30 (1) (December 19): 22–37.

Roche in collaboration with SGS, Golder and Genivar. (2012). Feasibility study for Kipawa project, Temescamingue Area, Québec, Canada. http://www.matamec.com/vns-site/uploads/ documents/ matamecfs 2013sedar.pdf (accessed on August 15th, 2017).

Rare Earth Technology Alliance (RETA). (2014). The Economic Benefits of the North American Rare Earths Industry.

Raudsepp M., and Pani A. (2003). Application of Rietveld analysis to environmental mineralogy. In environmental Aspects of MINE WASTES, Chapter 8. Editors J.L. Jambor, D.W. Blowes and A.I.M.Ritchie. Short Course Serie, Vol.31, 165-180.

Rollinson, K., Jens, C., Andersen, Ross, J., Maria, B. and Rob, F. (2011). Characterisation of non-sulphide zinc deposits using QEMSCAN®®. Minerals Engineering, vol. 24, no 8, p. 778-787.

Ruffell A., and Wiltshire P.(2004). Conjunctive use of quantitative and qualitative X-ray diffraction analysis of soils and rocks for forensic analysis. Forensic science international, 145, 13-23.

Sapsford, D. J., Bowell, R. J., Geroni, J. N., Penman, K. M., and Dey, M. (2012). Factors influencing the release rate of uranium, thorium, yttrium and rare earth elements from a low grade ore. Minerals Engineering, vol. 39, p. 165-172.

Sobek, A., Schuller, W., Freeman, J., and Smith, R. (1978). Field and laboratory methods applicable to overburdens and minerals. U.S. Environmental Protection Agency, EPA-600/2–78–054 (PB-280–495).

CHAPITRE 7 DISCUSSION

Les caractérisations minéralogiques, chimiques, physiques et les résultats des évaluations environnementales traités dans les Chapitres 3, 4, 5 et 6 ont permis de bien comprendre à la fois la minéralogie et le degré de libération des minéraux porteurs de REE, ainsi que les différents processus réactionnels impliqués dans le comportement géochimique des roches stériles et des minerais de REE des deux sites d'étude Montviel et Kipawa. Des échantillons représentatifs de roches stériles et de minerai de Montviel ont été soumis à des cellules humides tandis que ceux de Kipawa ont été soumis à des mini-cellules d'altération. Malgré l'agressivité de ces deux tests par rapport aux conditions de terrain, l'objectif était de comprendre et d'évaluer le comportement géochimique de divers matériaux porteurs de terres rares et en particulier la mobilité de ces dernières afin d'anticiper et de prédire leur relargage dans les eaux de drainage minier durant les interactions eau-roche. Plus spécifiquement, il a été démontré aux Chapitre 3, 4, 5 et 6 que la lixiviation des terres rares est faible dans les conditions de laboratoire, même si les minéraux de terres rares dans les carbonatites de Montviel ou dans les silicates de Kipawa sont sous forme de particules libres à plus 70 % (au moins 70 % de surface est disponible à la réaction). Cet aspect, qui est expliqué dans les Chapitres 4, 5 et 6, serait dû essentiellement aux processus géochimiques suivants : (i) les REE sont lixiviées dans un premier temps et elles précipitent ensuite sous forme des minéraux secondaires de terres rares, et/ou (ii) les REE sont retenus dans la gangue des matériaux des essais cinétiques via des mécanismes de sorption (Chapitre 3). En outre, les stériles de Montviel possèdent une importante capacité de sorption vis à vis des terres rares ainsi que d'autres métaux (Chapitre 3).

Bien que les travaux nous aient permis de mieux comprendre leur comportement environnemental, une discussion de certains aspects qui ne sont pas discutés dans les chapitres précedents sont utiles à la prise des décisions au sujet de l'évaluation environnementale des minerais à REE. Ainsi, dans cette discussion, les points suivants seront abordés : (i) la comparaison des résultats géochimiques des essais cinétiques (les cellules humides et les mini-cellules d'altération) avec les essais de lixiviation TCLP, SPLP et CTEU-9, renforcée par une analyse des données en composante principale (ACP); (ii) l'effet d'échelle entre les résultats d'essais cinétiques obtenus au laboratoire et sur le terrain, et (iii) une proposition d'une approche d'entreposage des rejets miniers porteurs des REE basée sur leur comportement géochimique. Enfin, une approche d'évaluation

environnementale, qui découle essentiellement des résultats de cette thèse, sera proposée dans le but de mieux prédire le comportement géochimique des matériaux géologiques porteurs de REE.

Tableau 7-1 : Méthodologies suivies pour la réalisation des essais de lixiviation.

Essai	Agent lixiviant	Paramètres de l'essai
TCLP (U.S. EPA Method 1311)	Solution d'acide acétique (pH 4,93)	Granulométrie: 9,5 mm Ratio liquide/solide: 20 Durée de l'essai: 18 heures
SPLP (U.S. EPA Method 1312)	Mélange d'acide nitrique et d'acide sulfurique (pH 4,2)	Granulométrie: 9,5 mm Ratio liquide/solide: 20 Durée de l'essai: 18 heures
CTEU-9 (Stegemann and Cote1991)	Eau déionisée (pH 7)	Granulométrie: 150 µm Ratio liquide/solide: 4 Durée de l'essai: 7 jours

7.1 Comparaison des résultats géochimiques des essais cinétiques et les essais de lixiviation TCLP, SPLP et CTEU-9

L'interprétation des résultats des cellules humides réalisées sur les stériles des carbonatites de Montviel ayant été présentés dans le Chapitre 4, une comparaison entre les résultats des cellules humides et des essais de lixiviation tels que TCLP (Toxicity Charaterisitic Leachning Procedure), SPLP (Synthetic Precipitation Leaching Procedure) et CTEU-9 (Centre technologique des eaux usées – méthode 9) sera présentée ici. Ces derniers font partie des essais en batch qui sont largement utilisés au Québec pour prédire le comportement environnemental des différents matériaux (Benzaazoua et al., 2006; CEAEQ 2012; Lim et al., 2009). Les conditions opératoires pour la conception et la réalisation de ces essais, ainsi que les différents points à prendre en considération au moment de la comparaison, sont résumées dans le Tableau 7-1. Il faut noter que la comparaison est parfois ardue en raison des différences notables en termes de conditions de réalisation de ces essais (Al-Abed et al., 2006; Bassolé, 2016).

7.1.1 Cellules humides

Les lixiviats des cellules humides sont récupérés après quelques heures de contact des eaux de rinçage et les rejets. La durée des essais réalisés est de plus de 800 jours. Les paramètres physico-chimiques et géochimiques des lixiviats sont mesurés immédiatement après leur récupération. Les valeurs de pH sont basiques pour tous les échantillons et dépassent la valeur supérieure de la Directive 019 (pH 9.5) durant les sept premiers rinçages, après quoi ils montrent une tendance à la baisse au fil du le temps. La baisse du pH peut être attribuable à l'épuisement de la fraction fine et/ou à l'oxydation acidogène des sulfures. Les détails des paramètres physico-chimiques sont discutés dans le Chapitre 3. Les métaux et les métalloïdes analysés dans les lixiviats sont comparés aux normes de la Directive 019 sur les effluents miniers du Québec, le règlement sur les effluents des mines de métaux du Canada (REMM) et les critères de la politique de protection des sols et de réhabilitation des terrains contaminés au Québec. Les concentrations mesurées en termes d'As, Cu, Fe, Ni, Pb et Zn sont en dessous des limites exigées par la Directive 019 et les critères du REMM du Canada (Figures 7-1). Pour ce qui est des critères applicables en cas de contamination des eaux souterraines (critère aux fins de consommation), tous les paramètres sont respectés à l'exception du fluorure (concentration > 1,5 mg/l limite exigée pour les eaux souterraines destinées aux fins de consommation). Le barium respecte les règles mais sa concentration tend à augmenter au fil du temps, ce qui peut engendrer un drainage neutre contaminé en Ba quelques années suite à l'entreposage des stériles en surface, s'il n'y a pas d'atténuation naturelle.

Figure 7-1 : Grille d'évaluation environnementale pour les carbonatites de Montviel.

Les REE sont faiblement lixiviées (entre 0.15 et 9 µg/l; concentrations REE totales issues des cellules humides) en conditions de laboratoire. La teneur de LREE étant plus élevée dans les différentes lithologies et par conséquent leurs concentrations dans les lixiviats sont plus élevées par rapport aux HREE (Figure 7-2). Par ailleurs, dans le cas du concentré de terres rares, le rapport LREE / HREE étant faible dans les lixiviats (rapport 2.5) par rapport aux échantillons solides (rapport 37), cela suggère que les HREE seraient libérées préférentiellement et / ou plus seraient mobiles comparativement aux LREE.

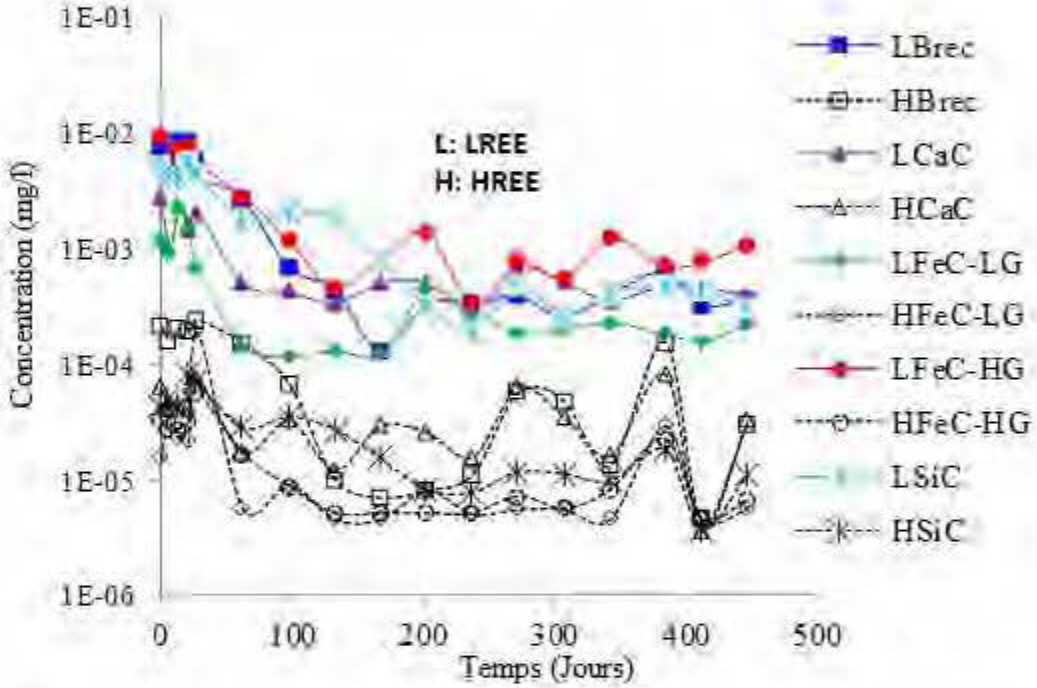

Figure 7-2 : Mobilité des LREE vs HREE issus des cellules humides pour les carbonatites de Montviel.

Tel que démontré dans les Chapitres 4, 5 et 6, les REE sont associés aux éléments radioactifs comme Th, Ra, Nb et U. (Hierro et al., 2012). Dans le cas des carbonatites de Montviel, les isotopes radioactifs détectés dans les lixiviats des cellules humides sont le radium (Ra-226, et Ra-228) et l'uranium (U-234, U-235, et U-238) (Figure 7-3). Les résultats montrent que toutes les concentrations en ces éléments radioactifs sont sous la limite prescrite par la Directive 019 et en respect avec les lignes directrices canadiennes pour la gestion des matières radioactives naturelles

(MRN) : la limite de rejet dérivée pour la famille uranium U238 (et tous ses descendants) qui est 1 Bq/l et la limite pratique dérivée pour le radium qui est 5 Bq/l.

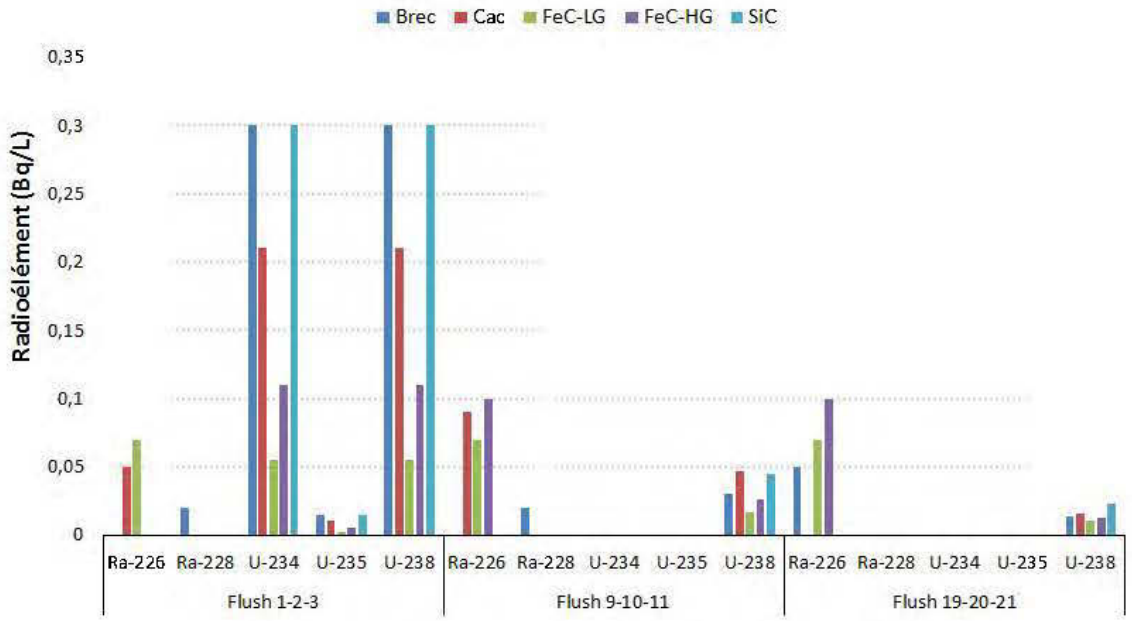

Figure 7-3 : La radioactivité des éléments radioactifs détectés dans les lixiviats des cellules humides des carbonatites de Montviel.

7.1.2 Comparaison des résultats issus des essais TCLP, SPLP et CTEU-9

Au Québec, les essais de lixiviation en batch sont utilisés pour les évalnations environnementales des rejets miniers (roches stériles et résidus). Cependant, leurs conditions opératoires sont différentes en termes de pH de l'agent lixiviant, de la durée de l'expérience, de la granulométrie, entre autres. L'essai TCLP est conçu pour simuler le scénario de lixiviation des métaux et des métalloïdes dans des conditions acides, alors que les tests SPLP et CTEU-9 sont conçus pour simuler l'effet de la 10 mg/l et l'effet des eaux naturelles sur la dissolution des matériaux organiques et inorganiques (CEAEQ 2012; US EPA, 1995).

La comparaison entre les essais TCLP et SPLP (Figure 7-4A) montre que les éléments Zn, Ba, Mn, Fe, Pb et les REE sont plus lixiviés par les essais TCLP que par les SPLP, qui extraient plus de Cu, B, As, F, Th et U. Ces résultats sont en accord avec les résultats trouvés par d'autres chercheurs (Lackovic et al., 1997; Lewis et Hugo, 2000; Özverdi and Erdem 2010; Shieh, 2001). De plus, les travaux de Bassolé (2016) ont démontré qu'il n'y a pas une différence significative entre les

quantités d'arsenic extraites par les deux tests. Les différences entre les tests TCLP et SPLP sont dues essentiellement au type de solution d'extraction utilisée : plus la solution est acide, plus la dissolution est importante (Al-Abed et al., 2008, Hooper, 1998).

La comparaison du test TCLP au test CTEU-9 (Figure 7-4B) montre que le test TCLP est plus agressif par rapport à l'essai CTEU-9. Ce dernier extrait plus de SO4, de F, d'As, d'U et de Th, tandis que l'essai TCLP extrait plus des autres métaux et métalloïdes. Cette différence est expliquée par les conditions différentes de réalisation : le test TCLP est réalisé dans des conditions acides comparativement au test CTEU-9 qui est effectué dans des conditions neutres (Tableau 7-1).

7.1.3 Comparaison des résultats des cellules humides avec les résultats des essais TCLP, SPLP et CTEU-9

Les résultats géochimiques issus des essais de lixiviation en batch (TCLP, SPLP et CTEU-9) comparés avec ceux issus des cellules humides sont présentés dans le but de montrer les différences en termes de concentrations des contaminants dans les lixiviats. Les concentrations des cellules humides utilisées dans cette comparaison sont les concentrations moyennes de la portion stabilisée allant de 63 à 819 jours.

7.1.3.1 TCLP vs cellules humides

Pour TCLP, le Fe, le Ba et le Pb sont libérés dans les lixiviats tandis que dans les essais en cellules humide, le Fe est sous la limite recommandée par la Directive 019 (3 mg/l; Figure 7-4D). Les concentrations de Ba, de Pb et de Zn avec l'essai TCLP dépassent les critères applicables en cas de contamination des eaux souterraines seulement dans les breccias, ferrocarbonatites LG et HGet silicocarbonatites. Dans les calciocarbonatites, le Zn est le seul élément qui est libéré en raison de sa mobilité dans les conditions neutres et alcalines. Les concentrations de REE varient entre 6, et 28 mg/l, tandis que celles des éléments U et Th sont inférieures à 0.02 mg/l et 0.0004 mg/l respectivement.

7.1.3.2 SPLP vs cellules humides

Pour la comparaison des essais SPLP et des cellules humides, les concentrations des métaux analysés sont inférieures aux critères de la Directive 019. Dans les essais SPLP, seul le pH qui dépasse la limite supérieure recommandée par la Directive 019 (pH 9,5; Figure 7-4E). Les

concentrations des métaux issus des essais SPLP sont supérieures à celles des cellules humides (Figure 7-4E). Ceci pourrait être attribuable au pH des solutions utilisées dans les deux tests. Les essais SPLP utilisent des acides, ce qui conduit à une exagération de la dissolution des métaux comparativement aux cellules humides qui utilisent de l'eau déionisée.

7.1.3.3 CTEU-9 vs cellules humides

Pour les extractions CTEU-9, les essais sont réalisés à l'eau déminéralisée avec un ajustement du pH à 7 pendant 7 jours d'agitation. Après 7 jours, le pH se situe entre 8 et 9 et le F dépasse les critères applicables en cas de contamination des eaux souterraines (4 mg/l) dans tous les échantillons (Figure 7-4F). Le Ba (> 5,3 mg/l), le Mo (1.13 mg/l) et le F (30 mg/l) dépassent les limites recommandées par les critères relatifs à l'eau potable et à la politique de protection des sols et de réhabilitation des terrains contaminés (Ba : 1 mg/l; Mo : 0,07 mg/l; F : 1,5 mg/l) et les critères applicables en cas de contamination des eaux souterraines (critères aux fins de consommation; (Ba : 5,3 mg/l; Mo : 2 mg/l; F : 4 mg/l) pour les ferrocarbonatites LG et HG, les breccia et les calciocarbonatites.

En conclusion, on peut dire que les essais de lixiviation en batch, en particulier les essais TCLP et SPLP, conduisent à la dissolution des éléments en plus grande concentration par rapport aux essais en cellules humides. Ceci est attribuable à : (i) l'énergie de l'agitation par culbutage, (ii) le milieu fermé, (iii) la durée d'extractions (18 heures) et (iv) aux acides utilisés pour l'extraction dans les essais de TCLP et SPLP contrairement aux essais en cellules humides. De tous les éléments lessivés, le F est le seul élément à être libéré dans les deux types d'essais au-delà de la limite permise par les critères applicables en cas de contamination des eaux souterraines (critères aux fins de consommation).

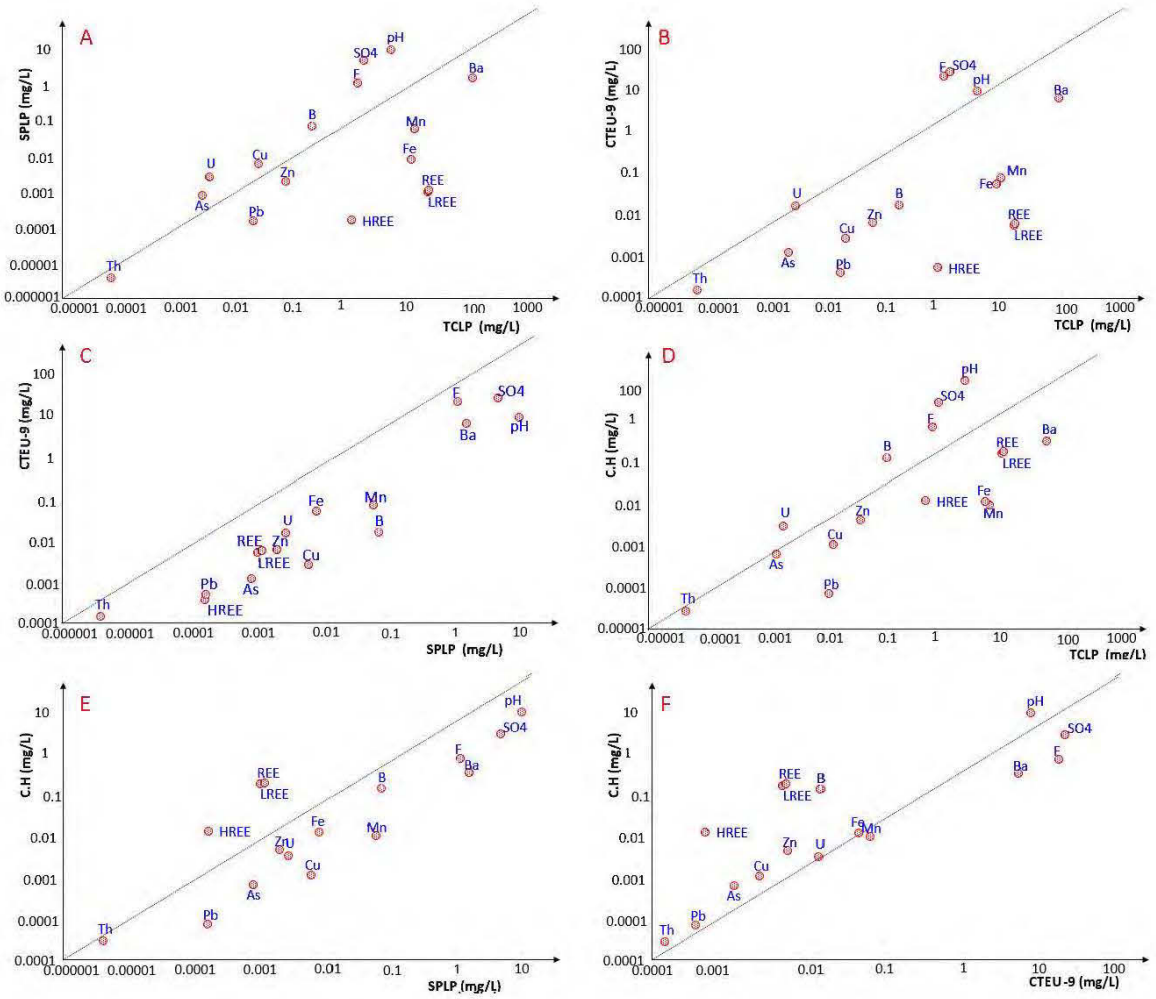

Figure 7-4 : Comparaison des résultats des essais de lixiviation (TCLP, SPLP et CTEU-9) et les cellules humides.

Les essais TCLP et SPLP lixivient plus de REE que les essais CTEU-9 et en cellules humides. Les essais CTEU-9 et SPLP sont les essais les plus semblables aux cellules humides (Figure 7-5), ce qui peut être attribuable aux pH plus similaires (Tableau 7-1). Dans l'avenir et pour des évaluations environnementales des roches stériles et de minerai de REE, on recommande beaucoup plus les essais de CTEU-9 qui possèdent des conditions très similaires à celles qu'on trouve dans le terrain surtout en terme de pH, bien que le système d'extraction des essais CTEU-9 soit fermé.

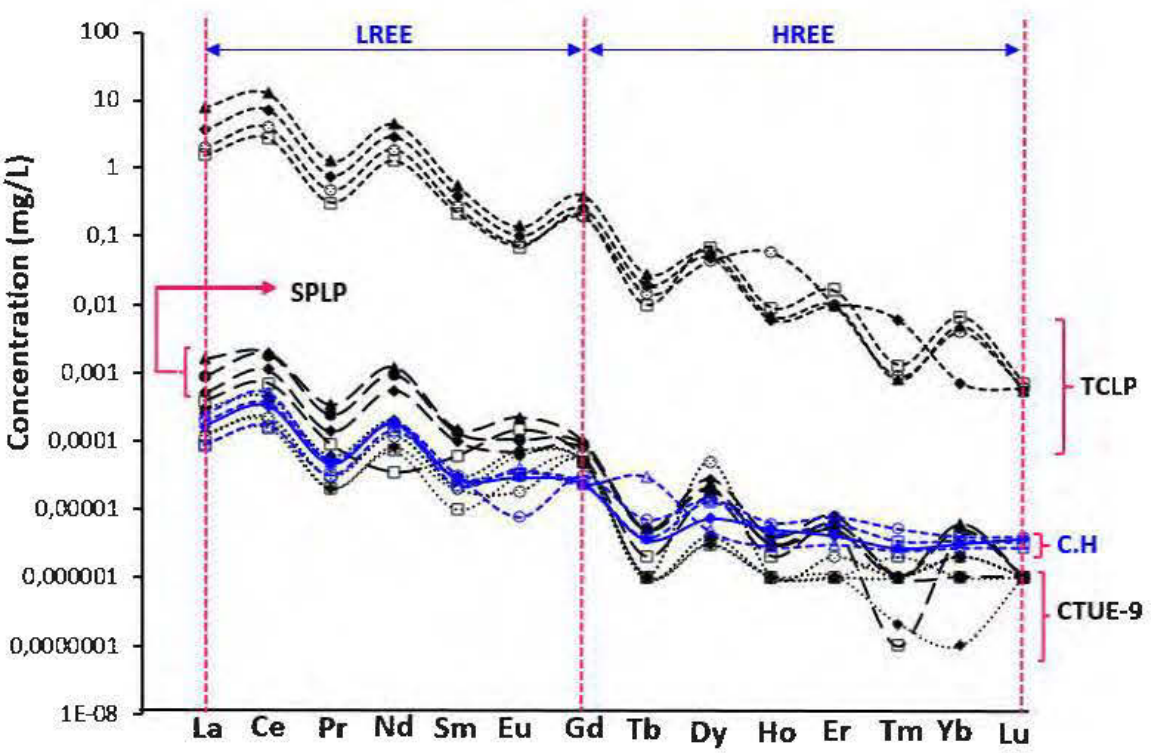

Figure 7-5 : Comparaison des résultats d'essais de lixiviation des REE par les essais de lixiviation (TCLP, SPLP, et CTEU-9) et les cellules humides.

L'analyse des données des résultats issus des essais cinétiques en cellules humides (CH) et des essais TCLP, SPLP et CTEU-9 au moyen de l'analyse par composante principale (ACP) permet de montrer les relations entre les éléments majeurs et en traces. Seuls les résultats de l'ACP des calciocarbonatites seront présentés car toutes les autres lithologies montrent des comparaisons similaires. Les deux premières composantes (PC1 et PC2) représentent plus de 98 % de la variabilité cumulée des données (Figure 7-6A). La représentation des éléments dans le plan déterminé par PC1- PC2 montre cinq groupes distincts (Figure 7-6B).

La projection des échantillons (TCLP, SPLP, CTEU-9 et CH) sur le plan factoriel PC1-PC2 (Figure 7-6C) indique que PC1 et PC2 sont liées aux types des essais (essais de lixiviation ou cinétiques). Les groupes 1 et 4 sont fortement corrélés avec CTEU-9, tandis que les groupes 2 et 3 sont positivement corrélés avec les essais TCLP, et négativement avec les essais SPLP et CH. Ceci suggère que les REE (LREE et HREE) et les autres métaux sont trop lixiviés par l'essai TCLP caractérisé par un pH acide contrairement aux essais SPLP, CTEU-9 et en CH. Cependant, les éléments des gronpes 1 et 4 ont tendance à se lixivier préférentiellement par le CTEU-9. Les

groupes 2 et 3 sont négativement corrélés avec le pH, ce qui indique que la mise en solution des REE et d'autres éléments métalliques se fait principalement dans les conditions acides.

La Figure 7-6D (cercle de corrélation) montre les résultats géochimiques des cellules humides forment quatre cinq groupes : groupe 1, composé de SO_4, Th, As et F; groupe 2, contenant B; groupe 3, composé de REE, LREE, HREE, Cu, Zn, Pb, Fe, Ba et Mn; groupe 4, constitué de U; et groupe 5, représenté par pH. Le groupe 3 peut se diviser en deux sous-groupes caractérisés par des fortes corrélations : (i) REE, LREE, HREE, et (ii) Cu, Zn, Pb, Fe, Ba et Mn (Figure 7-6B). Noter que le REE représente le total des éléments des terres rares.

D'un point de vue géochimique, la relation suggérée par ACP, en particulier entre les REE et SO_4, signifie que l'oxydation des sulfures (présence des SO_4) peut augmenter la lixiviation des REE en réponse à l'acidité générée. Cependant, d'un point de vue minéralogique, la forte corrélation entre les REE et le Ba indique que ces derniers sont portés par les mêmes phases minérales (i.e. mélange REE-Ba tel que démontré par les analyses minéralogiques; Chapitres 2 et 3). De même, le regroupement de Th et F suggéré par ACP peut être attribué à une association minéralogique portant les deux éléments (i.e. fluoroapatite).

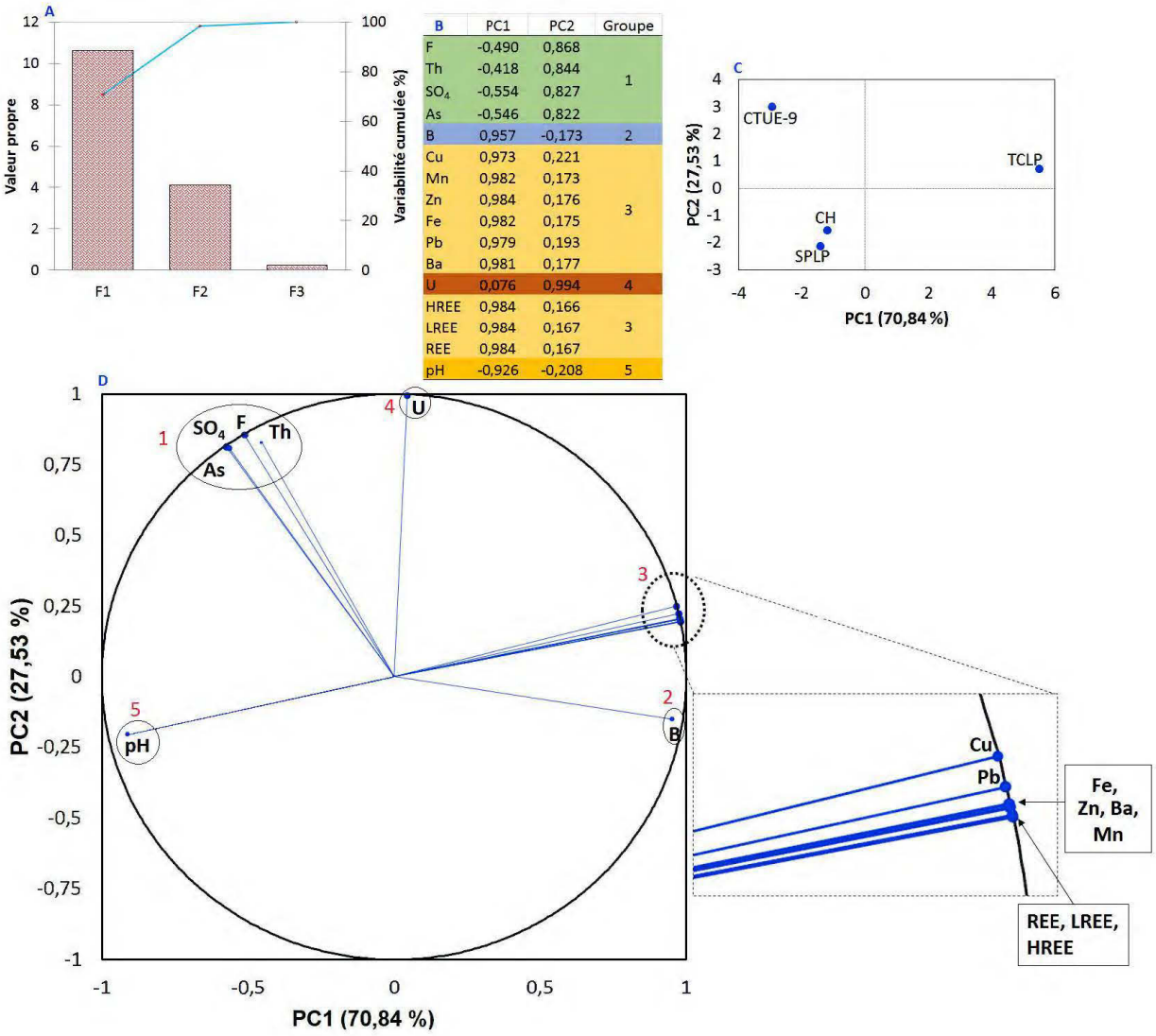

Figure 7-6 : Analyse par composante principale (ACP) des données géochimiques des calciocarbonatites (concentrations moyennes des celules humides sur 819 jours) de Montviel issues des essais de lixiviation et des cellules humides.

7.2 Comparaisons des comportements géochimiques à différentes échelles

Cette section a pour objectif de comparer les résultats géochimiques des matériaux de Montviel entre les essais du laboratoire et les barils du terrain. Aucune étude n'est trouvée dans la littérature qui étudie l'effet d'échelle sur la lixiviation des REE. Dans cette section, les principaux résultats

géochimiques issus des barils de terrain ainsi que les principales différences observées entre les essais *in situ* et au laboratoire sont présentées.

La prédiction du comportement environnemental des rejets miniers (roches stériles et résidus) dans la plupart des cas se fait par des essais statiques et/ou cinétiques de laboratoire. Cependant, des différences significatives sont observés entre les conditions de laboratoire et du terrain (pH, granulométrie, consommation d'oxygène, ratio solide/liquide, température, processus géochimiques de surface comme la sorption, etc.). En conséquence, les résultats des essais de laboratoire ne reflètent pas nécessairement les résultats des essais de terrain en termes de concentrations des polluants (métaux et metalloïdes). Pour l'instant, les géochimistes démontrent qu'il est très difficile de simuler les résultats de terrain à partir des essais de laboratoire (Kandji et al., 2016; Levesque et al., 2016; Plante et al., 2010a et b). La prise de décision sur le comportement environnemental des rejets miniers nécessite la compréhension de l'effet d'échelle sur les facteurs influençant les mécanismes de dissolution de ces rejets (Lin et al., 1981; Lapakko, 1994; Bennet et al., 2000; Malmström et al., 2000; Hellmann et al., 2002; Miller et al., 2003; Frostad et al., 2005; Gu et Evans, 2007; Ganor et al., 2007; Pepin, 2009; Sapsford et al., 2009).

L'interprétation des résultats cinétiques de laboratoire doit se faire en tenant compte des effets d'échelle pour rendre la prédiction environnementale des rejets miniers plus réaliste. La réactivité des minéraux porteurs de contaminants (i.e., métaux et REE) dépend des paramètres hydrogéologiques, géochimiques et minéralogiques (Guy et al., 1999; Zendah et al., 2013). La mobilité des contaminants sur le terrain, entre autres les REE, peut être réduite par rapport aux essais de laboratoire via plusieurs processus géochimiques comme la précipitation des minéraux secondaires résultant des équilibres thermodynamiques et géochimiques des solutions (Fernández-Caliani et al., 2009; Gschneidner et al., 2006; Yusoff et al., 2013). En outre, les mécanismes de dissolution sont contrôlés essentiellement par la réactivité des minéraux (carbonates ou silicates), les pourcentages des fractions fines, et les surfaces spécifiques élevées (Erguler et al., 2015). Ces conditions ne sont pas trouvées dans les matériaux de carbonatites de Montviel qui sont caractérisés comme des matériaux faiblement réactifs (Edahbi et al., 2015; Chapitres 4 et 5). La qualité des eaux de drainage minier de Montviel dépend principalement de la concentration des REE et contaminants associés résultants de la dissolution des carbonates (porteurs ou non de REE) et de l'oxydation des sulfures, en particulier la pyrrhotite contenant Ni et Co en impuretés. Les carbonatites de Montviel sont composés à plus de 60 % de carbonates, incluant les carbonates

porteurs de terres rares. Cette réactivité peut être influencée par la température et l'acidité de la solution de lixiviation (Alkattan et al., 1998; Coto et al., 2012). Les températures moyennes sur le site varient entre -18 °C en janvier et 17°C en juillet. Ce type de climat peut diminuer la réactivité des sulfures, et favorise la solubilité du dioxyde de carbone (CO_2), qui peut diminuer le pH des eaux de drainage.

7.2.1 Matériaux et méthodes

Seuls les matériaux et les essais en barils seront décrits dans cette partie. Les détails des essais cinétiques et les matériaux utilisés au laboratoire sont trouvés aux Chapitres 3, 4 et 5 de cette thèse.

7.2.1.1 Matériaux utilisés en essais de terrain

Les matériaux choisis pour ce test ont été sélectionnés pour représenter les différentes lithologies et le minerai des carbonatites de Montviel (calciocarbonatites, breccia, ferrocarbonatites, et silicocarbonatites). La masse nécessaire pour la réalisation des essais en barils (environ 200-240 kg) est issue de plusieurs carottes de forage pour chaque échantillon. Après la sélection des carottes de la cartothèque, les échantillons ont subi un concassage pour réduire leur dimension et assurer une homogénéisation avant de les mettre en barils. Au total, sept barils sont montés *in situ* pour évaluer l'effet d'échelle sur le comportement géochimique des roches stériles et de minerais porteurs de REE des carbonatites de Montviel (Figure 7-7). Ces essais ont été mis en place et suivis par le personnel de la compagnie Géoméga. Les barils utilisés sont en plastique avec une capacité d'environ 180 litres. À la base de chaque baril, une sortie est percée avec un embout en géotextile pour collecter les lixiviats. Les particules fines sont maintenues à l'intérieur des barils par une petite couche de sable à la base des barils, qui permet également de filtrer les lixiviats et éviter le bouchage de la sortie. Le sommet des barils demeure toujours ouvert pour permettre l'entrée des eaux de pluie. Les lixiviats sont collectés dans des contenants en plastique munis d'un couvercle pour éviter la contamination et/ou la dilution des lixiviats par la pluie.

Figure 7-7 : Essais en barils des matériaux des carbonatites de Montviel.

La comparaison des essais de laboratoire et les essais en barils *in situ* nécessite le rappel de certains paramètres de chaque type d'essais qui sont indispensables à la compréhension de l'effet d'échelle sur le comportement géochimique des REE. Ces derniers sont résumés dans le Tableau 7-2.

Tableau 7-2 : Paramètres des essais cinétiques utilisés pour comparer l'effet d'échelle.

Essai	Masse (kg)	Distribution granulométrique	Ratio liquide/solide (l/kg/semaine)	Rinçage
Cellules humides	1	< 6,3 mm	1	Une fois par semaines
Essais en barils	200-240	< 120 mm	(0.023)	75,7 mm/mois

Les compositions chimiques des eaux de lixiviats ont été déterminées pour les comparer aux critères de la Directive 019. Seuls les paramètres supérieurs à la limite de détection et qui ont un intérêt pour la compréhension de l'effet d'échelle seront présentés, tels que le pH, la conductivité électrique, quelques métaux (Pb, Zn, Ba, Ca, Cd, etc.), les REE et un métalloïde (As). Tous les

paramètres mesurés dans les lixiviats *in situ* respectent les limites de la Directive 019 sans exception (Figure 7-8, 7-10 et 7-11).

Le Tableau 7-2 compare les résultats géochimiques des lithologies pour quelques éléments d'intérêt issus des essais terrain (barils) et de laboratoire (cellules humides). La libération des éléments géochimiques dans les lixiviats est contrôlée par plusieurs facteurs, dont le rapport liquide/solide. Le rapport liquide/solide sur le terrain est estimé à 0.023 l/kg/semaine et à 1 l/kg/semaine en cellules humides (Tableau 7-2). Ce rapport au laboratoire est environ 44 fois supérieur à celui du terrain.

Le pH demeure toujours entre 8 et 8,5 grâce à l'abondance des minéraux neutralisants, en particulier les carbonates. Les valeurs de pH *in situ* (8,13-8,64) sont légèrement supérieures à celles mesurés au laboratoire (7,08-9,96). Ceci peut être expliqué par l'augmentation de la dissolution des neutralisants causée par les températures plus faibles et l'effet des pluies acides *in situ*.

Les mesures de la conductivité électrique traduisent la quantité des anions et cations en solution. Les conductivités électriques mesurées *in situ* sont plus élevées que celles mesurées au laboratoire. Cette différence peut être attribuable à l'eau de pluie acide et à l'effet de la température, qui augmente d'une façon significative la dissolution des carbonates sur le terrain.

Les valeurs d'alcalinité des lixiviats *in situ* oscillent entre 54 et 260 mg CaCO3/l, plus élevées que celles mesurées au laboratoire (variant entre 10 et 30 mg CaCO3/l). Cette différence entre le terrain et le laboratoire est un autre indice qui suggère la plus grande dissolution des carbonates sur le terrain comparativement au laboratoire. Les alcalinités sont plus élevées dans les lixiviats des silicocarbonatites *in situ* et au laboratoire.

Le calcium est un des éléments les plus abondants dans les matériaux de Montviel, leur teneur en oxyde CaO dans les tous échantillons varie de 15,7 au 30,2 % (Tableau 3-1). Les minéraux porteurs de Ca sont essentiellement les carbonates (calcite, ankérite) tel que démontré par les analyses minéralogiques par DRX, et QEMSCAN; les détails se trouvent dans les Chapitres 3 et 4. Les concentrations dans les lixiviats *in situ* (2.19-35 mg/l) sont un ordre de grandeur supérieur aux essais de laboratoire (0.53-10.1 mg/l). Cette différence peut être due à la différence entre le laboratoire et le terrain en termes de température et le ratio solide/liquide.

Les sulfates dans lixiviats *in situ* et au laboratoire est un produit de l'oxydation des sulfures présents dans les échantillons solides, en particulier la pyrite, la galène, pyrrhotite et/ou de la dissolution

des sulfates comme la célestine ($SrSO_4$) (Tableau 3-3). De plus, les eaux de pluie contiennent une certaine concentration de sulfate. Les ions H3O+ sont un autre produit de l'oxydation des sulfures qui consomment l'alcalinité de la solution et contribuent à la diminution du pH des lixiviats. Le suivi de l'évolution de ces deux éléments lors des essais cinétiques est un paramètre-clé pour l'interprétation des résultats géochimiques. Les mesures des concentrations des sulfates sont environ deux ordres de grandeur supérieures pour les essais *in situ*. Pour les essais de laboratoire, les valeurs sont stabilisées autour de 1,6 mg/l, tandis que celles mesurées *in situ* se stabilisent autour de 143 mg/l.

Le barium est porté principalement par la barytocalcite, et un mélange de REE-Ba-Sr. Les données ponctuelles mesurées *in situ* sont d'un ordre de grandeur inférieures à celles du laboratoire (0,05-0.86 mg/l). Les conditions de terrain en termes de température, la dissolution de CO_2, et l'effet des pluies acides (présence de sulfates dans la pluie) favorisent la dissolution des minéraux porteurs du barium, mais les concentrations élevées de SO_4 *in situ* par rapport au laboratoire permettent probablement de contrôler les concentrations de Ba en solution en le précipitant sous forme de barite ($BaSO_4$) : indice de saturation de la barite terrain : 0.35-8.2 (sursaturation); labo < 0 (sous saturation).

Les terres rares proviennent essentiellement des carbonates de REE (i.e. burbankite, kukhrenkoite, bastnaésite, etc.) tel que démontré dans les Chapitres 3 et 4 (cellules humides; 0,15-9 µg/l). Les valeurs mesurées sur les lixiviats *in situ* varient entre 0.0006 et 0.039 mg/l avec un maximum dans les silicocarbonatites et un minimum dans les ferrocarbonatites. Les concentrations au laboratoire sont inférieures aux essais *in situ* par plusieurs ordres de grandeurs. Cet écart entre les essais *in situ* et au laboratoire peut être expliqué par : (i) l'effet de la température (la température plus faible *in situ* augmente la dissolution des carbonates), (ii) la surface spécifique (plus élevée au laboratoire par rapport au terrain) et la précipitation des REE sous forme des minéraux secondaires ou leur sorption sur les surfaces des minéraux primaires à l'intérieur des essais du laboratoire par les mécanismes de sorption, tel que démontré dans le Chapitre 3.

Tableau 7-3 : Comparaison de quelques résultats géochimiques issus des différentes échelles.

		Essais terrain				Cellules humides			
	Unité	BreC	CaC	FeC	SiC	BreC	CaC	FeC	SiC
pH		8,15-8,64	8,13-8,45	8,28-8,44	8,24-8,64	7,47-9,94	7,41-9,56	7,44-9,31	7,08-9,69
Conductivité	uS/cm	246-736	150-972	377-1010	852-1140	45,4-334	36-96,2	38,9-126,5	51-207
OH	mg/l CaCO3	2	2	2	2	1	1	1	1-5
CO_3^{2-}	mg/l CaCO3	3,5-21,5	2-7	2-6	2	1-27	1-1,42	1-4	1-16
HCO_3^-	mg/l CaCO3	74,5-173,5	54-183	135-186	143-260	16-66	16-62	16-35	16-63
F	mg/l	0,73-2,14	0,37-2,26	2,07-3,05	0,67-1,24	0,01-1,95	0,01-0,64	0,01-0,31	0,01-1,89
SO_4	mg/l	38-165	15-230	27-130	85-330	0,8-10	0,5-2,1	0,5-1,43	0,04-4,4
Al	mg/l	0,074-0,29	0,046-0,39	0,024-0,273	0,069-2,11	0,1-0,74	0,004-0,13	0,07-0,28	0,04-0,29
As	mg/l	0,004-0,006	0,0016-0,006	0,002-0,005	0,04-0,06	0,0001-0,0031	0-0,0006	0-0,0004	0-0,0007
Ba	mg/l	0,07-0,22	0,03-0,07	0,09-0,207	0,05-0,2	0,051-0,52	0,12-0,6	0,14-0,86	0,05-0,846
Ca	mg/l	9,24-29,9	2,19-35	5,77-21,5	2,56-21,1	0,53-10,1	0,56-5,24	0,65-4,88	0,53-8,59
P	mg/l	0,03-0,05	0,03-0,06	0,03	0,03-0,11	0,0045-0,552	0-0,025	0-0,022	0-0,026
Zn	mg/l	0,002-0,078	0,002-0,079	0,003-0,061	0,006-0,1	0,001-0,074	0-0,014	0-0,011	0-0,018
REE	mg/l	0,0008-0,008	0,0008-0,011	0,0006-0,004	0,0006-0,039	$0,0002\text{-}0,00891 \times 10^{-03}$	$0,0003\text{-}0,0033 \times 10^{-03}$	$0\text{-}0,009 \times 10^{-03}$	$0,0003\text{-}0,0057 \times 10^{-03}$

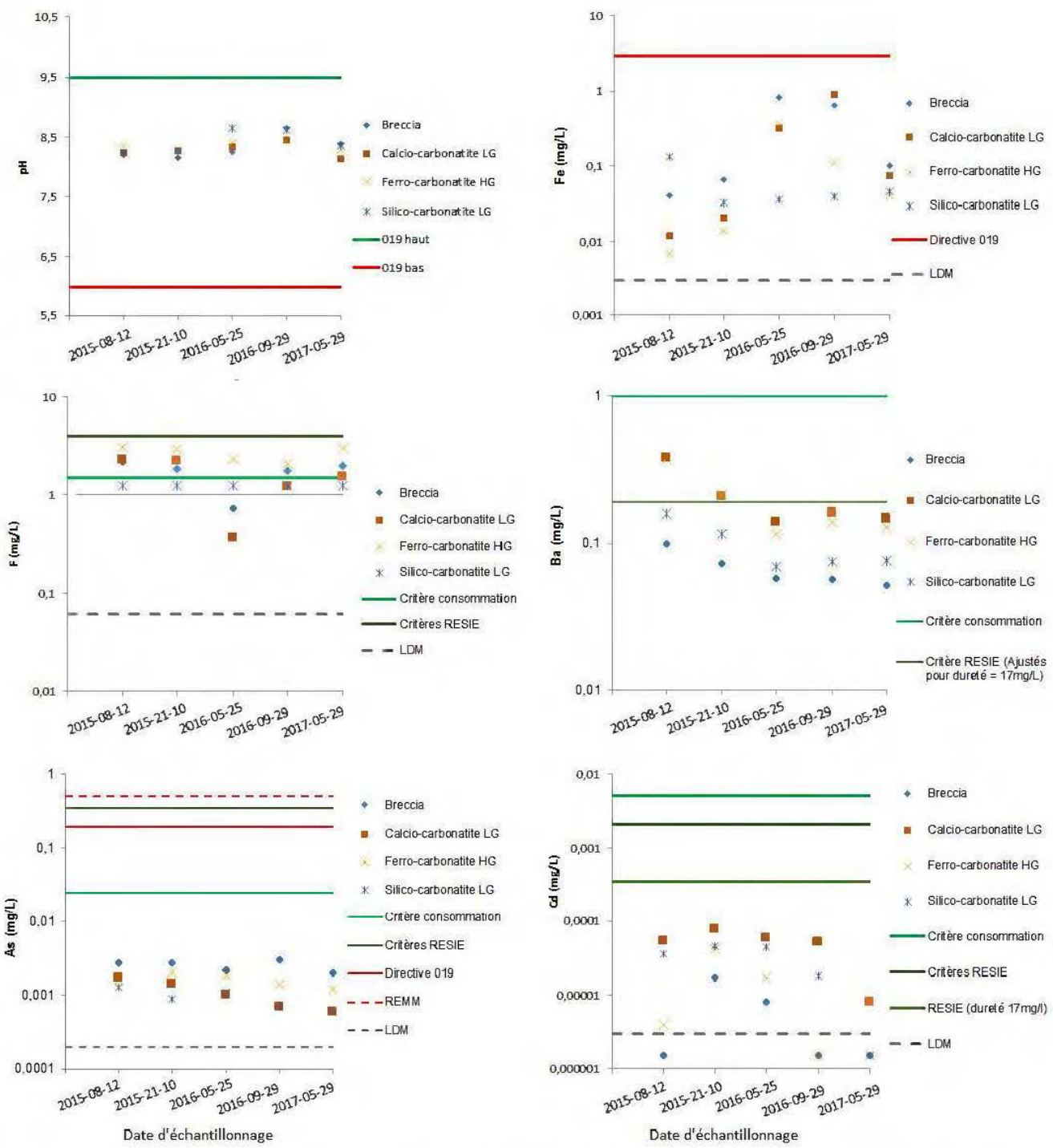

Figure 7-8 : Comparaison des paramètres (pH, Fe, F, Ba, As et Cd) mesurés dans les lixiviats *in situ* avec les critères de réglementation tels que Directive 019, RESIE, critères de consommation, et limite de détection.

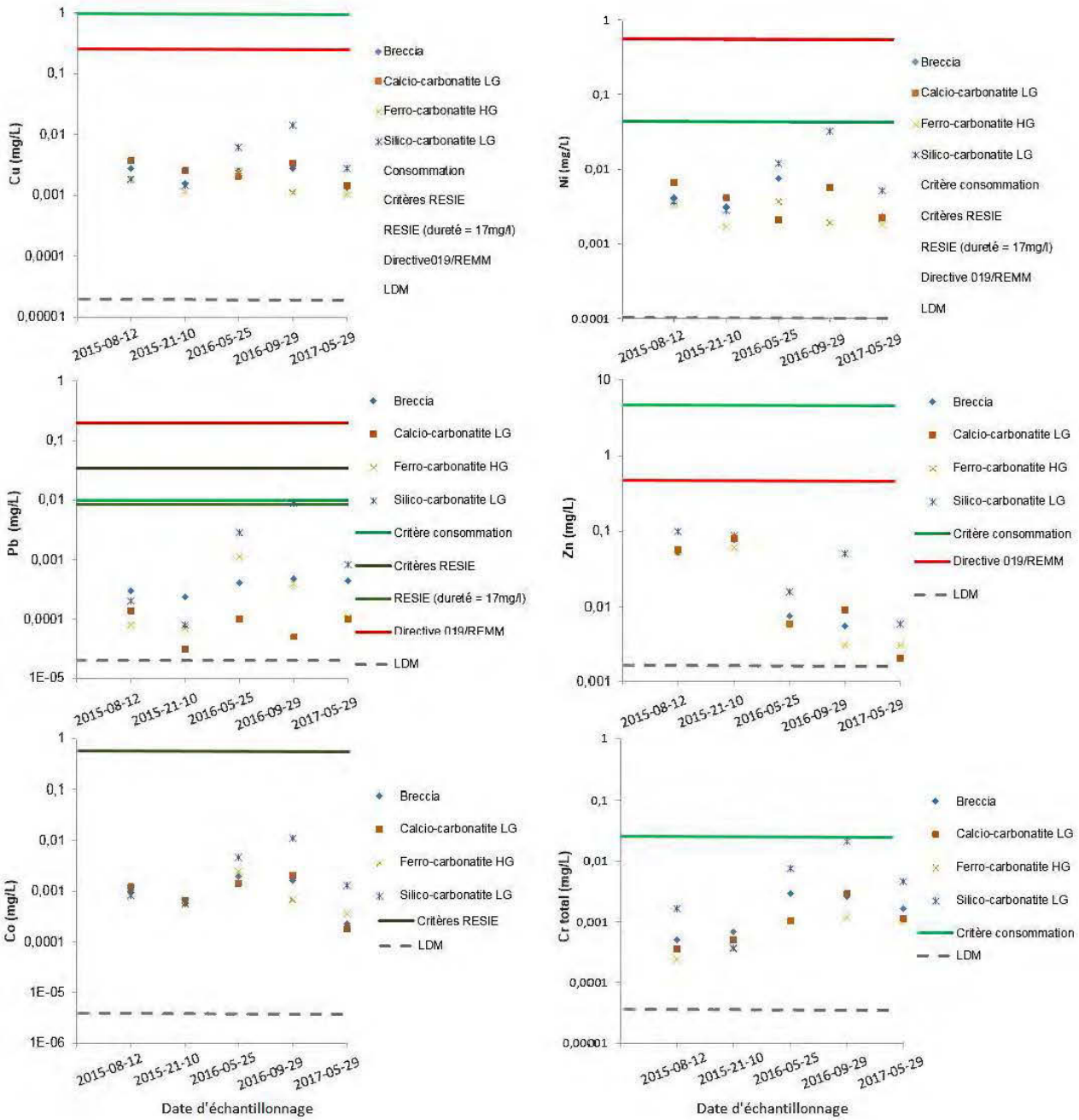

Figure 7-9 : Comparaison des paramètres (Cu, Ni, Pb, Zn, Co et Cr) mesurés dans les lixiviats *in situ* avec les critères de réglementation tels que Directive 019, RESIE, critères de consommation, et limite de détection.

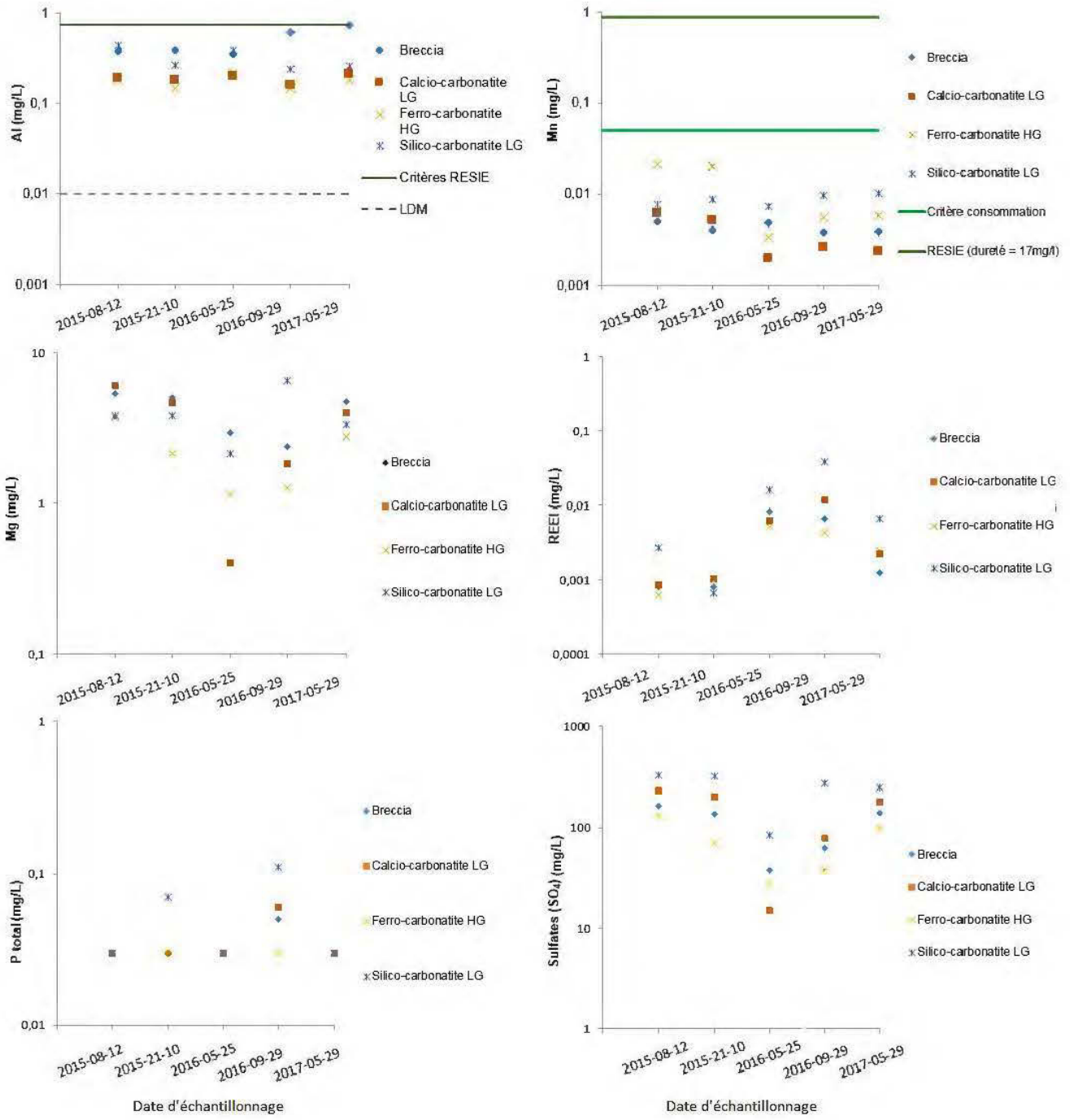

Figure 7-10 : Comparaison des paramètres (Al, Mn, Mg, REE, P et SO4) mesurés dans les lixiviats *in situ* avec les critères de réglementation tels que Directive 019, RESIE, critères de consommation, et limite de détection.

Les taux de relargages instantanés des éléments (mg/l/jour) sont calculés en divisant les charges cumulées normalisées, extraites des cellules humides, par rapport au temps (mg/l/jour). Les

résultats obtenus montrent que toutes les lithologies de Montviel ont des tendances similaires en termes des taux de relargage instantanés. En effet, seules les données issues de ferrocarbonatites sont présentées pour quelques éléments d'intérêt qui sont importants pour la compréhension de l'effet d'échelle entre les essais terrain et du laboratoire (Figure 7-11; les taux de relargages instantanés des éléments sont calculés à partir des concentrations moyennes). Les taux instantanés de quelques éléments issus des essais du laboratoire et terrain en fonction du temps sont présentés à la Figure 7-12. D'importantes différences dans les taux de relargages instantanés sont observées pour la plupart des éléments: Ca terrain : $3{,}13 \times 10^{-4}$ mg/l/jour – labo : 0,41 mg/l/jour; Ba terrain : $4{,}56 \times 10^{-6}$ mg/l/jour – labo : 0,71 mg/l/jour; Mg terrain : $5{,}22 \times 10^{-5}$ mg/l/jour – labo : 0,70 mg/l/jour; S terrain : $0{,}47 \times 10^{-4}$ mg/l/jour – labo : 0,10 mg/l/jour; P terrain : $9{,}21 \times 10^{-8}$ mg/l/jour – labo : 0,0012 mg/l/jour; REE terrain : $8{,}11 \times 10^{-8}$ mg/l/jour – labo : $1{,}5 \times 10^{-4}$ mg/l/jour. Pour le soufre, les taux de relargage instantanés ne correspondent pas aux taux d'oxydation des minéraux sulfureux, en particulier la pyrite (sulfure majoritaire), car les sulfates pourraient précipiter sous forme des minéraux secondaires tel que suggéré par les calculs thermodynamiques (Figure 7-13).

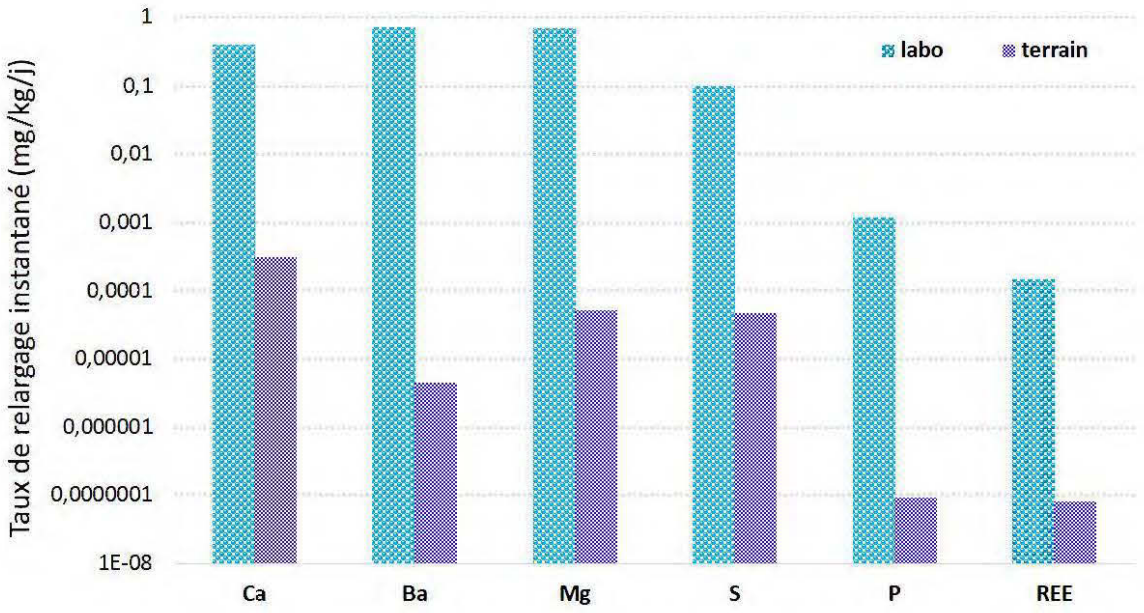

Figure 7-11 : Comparaison des taux de relargage instantanés obtenus en cellule humide et en baril de terrain (terrain) pour les ferrocarbonatites de Montviel.

Les taux de relargages instantanés issus des cellules humides sont supérieurs à ceux issus des essais terrain pour toutes les lithologies. Ces différences entre les différentes échelles pourraient être dues à la précipitation de minéraux secondaires et/ou aux phénomènes de sorption, aux granulométries

différentes et au rapport solide/liquide (voir Chapitres 3, 4, 5 et 6). De plus, les conditions hydrogéologiques du terrain (teneurs en éléments dissous élevées, temps de contact élevé, rapport solide/liquide faible) sont favorables à la précipitation des REE (i.e. $REEPO_4$), du Ba (i.e. barite), du Fe (i.e. goethite, hématite) et du P (i.e. hydroxyapatite) que dans les conditions d'essais de laboratoire (Figure 7-13). Certains de ces minéraux secondaires précipités (particulièrement goethite et hématite) pourraient également réduire la mobilité des REE via des phénomènes de sorption.

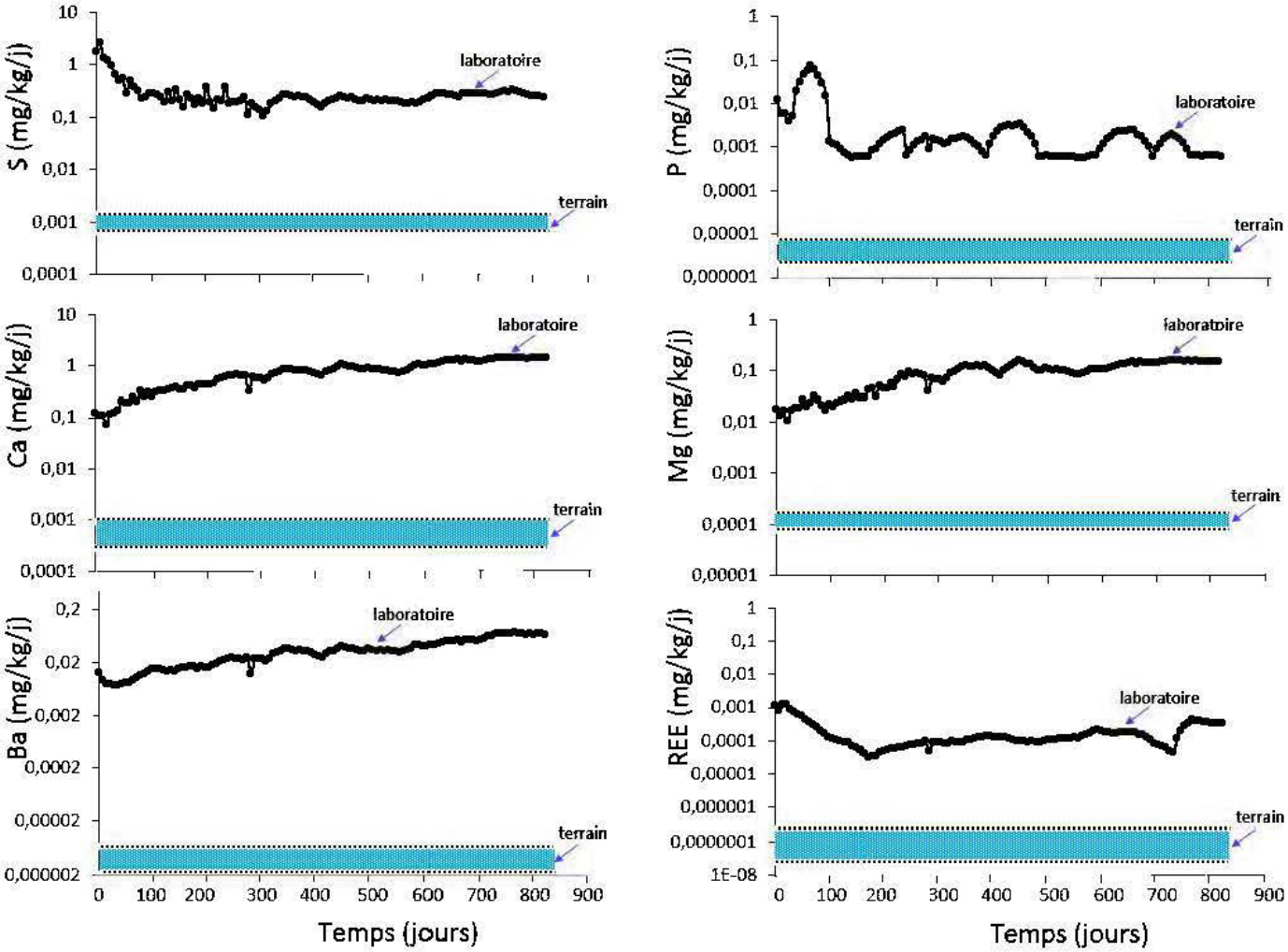

Figure 7-12 : Taux de relargages instantanés des éléments associés aux ferrocarbonatites entre les essais terrain et du laboratoire.

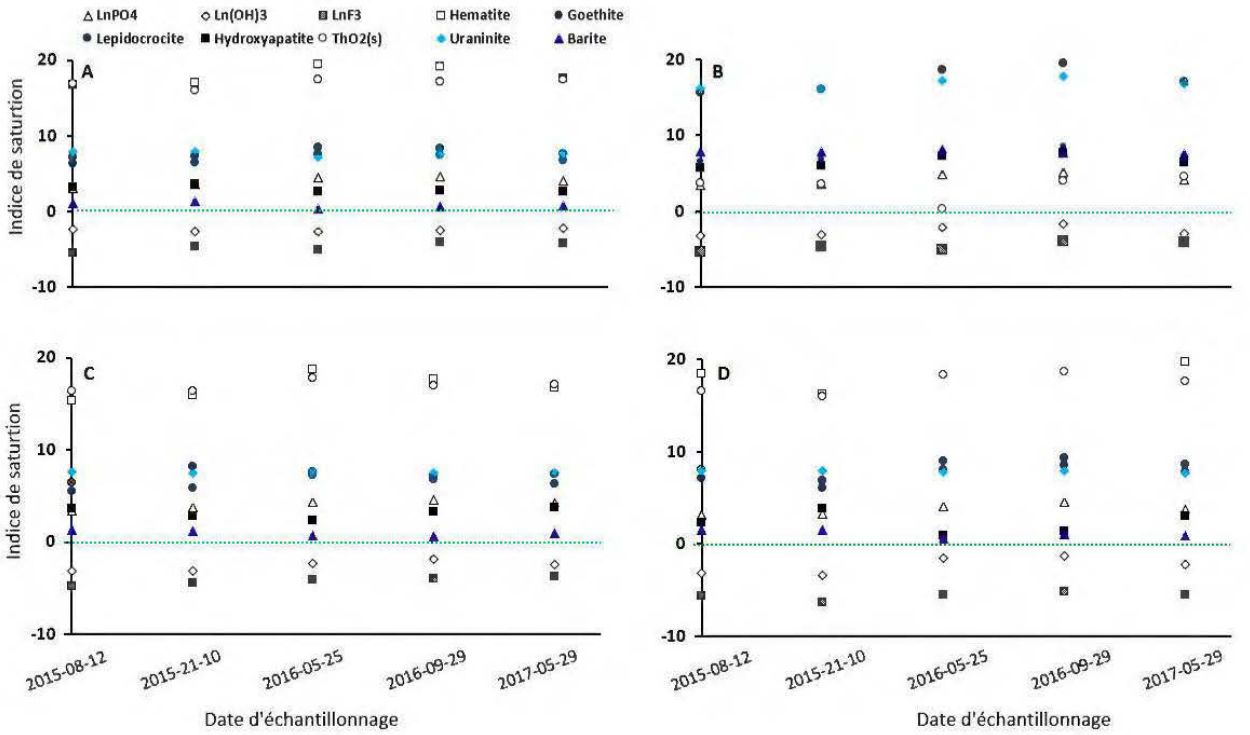

Figure 7-13 : Indices de saturation des minéraux secondaires dans les des essais terrain.

Enfin, les taux de relargages des éléments sont contrôlés par des facteurs d'ordres physiques, hydrogéologiques et minéralogiques. La différence de granulométrie entre les carbonates (porteurs ou non des REE) présents aux différentes échelles est significative. Les minéraux soumis aux cellules humides sont plus fins par rapport à ceux présents dans les essais terrain (Tableau 7-2). Comme la fraction fine est plus réactive que la fraction grossière, les cellules humides présentent des taux de relargages instantanés plus élevés par rapport aux essais terrain. De plus, la différence entre les essais de laboratoire et du terrain en terme du rapport liquide/solide, allant de 0,023 à 1 l/kg/semaine, pourrait aussi avoir un impact significatif sur la lixiviation des éléments. Les conditions hydrologiques du terrain (le temps de rétention hydraulique, perméabilité et diffusion de l'eau et des gaz, etc.) pourraient aussi avoir un impact sur le relargage des éléments dans les essais de terrain.

7.2.2 Effet de la température sur le taux de relargage instantané des éléments

La loi d'Arrhenius (équation 7.1) permet de mettre en évidence l'effet de la température sur la variation de la vitesse d'une réaction chimique (i.e. taux d'oxydation des sulfures). L'équation générale qui décrit la loi d'Arrhenius est la suivante :

$$K = Ae^{-\frac{Ea}{RT}} \quad (7.1)$$

k : taux d'oxydation (mg/s)

A : constante appelé aussi facteur de fréquence (même unité que k)

E_a : énergie d'activation (J/mol)

R : constante universelle des gaz parfaits (8,314472 $kJ.mol^{-1}. K^{-1}$)

T : température (Kelvin, K)

Pour deux températures (T_1 et T_2) avec T2 > T1, avec T_1 et T_2 représentant respectivement la température du terrain et du laboratoire, l'équation de la loi d'Arrhenius devient :

$$\ln\frac{k2}{k1} = \frac{Ea}{R}\left(\frac{1}{T1} - \frac{1}{T2}\right) \quad (7.2)$$

La pyrite est le minéral sulfureux le plus abondant dans les matériaux de Montviel. L'énergie d'activation (E_a) de ce minéral varie en fonction du pH. Par exemple, les valeurs de E_a sont comprises entre 4 et 94 kJ/mol pour des pH entre 6 et 8 (Nicholson et al., 1988, 1994; Blowes et al., 2003). Pour avoir une idée de l'effet de la température sur les taux de réaction de la pyrite dans les matériaux de Montviel, différents scénarios sont simulés. Les scénarios pour des températures variant entre 1 et 24°C et pour des énergies d'activation de 5, 10, 20, 40, 80 et 94 kJ/mol sont présentés à la Figure 7-14. Le paramètre k(24)/k(T) représente le rapport des taux d'oxydation entre la température du terrain k(T) et la température du laboratoire k(24). Ces scénarios montrent d'importantes différences entre les essais terrain et de laboratoire en termes du taux d'oxydation de la pyrite, allant jusqu'à un ordre de grandeur supérieur pour les essais de laboratoire. D'autres chercheurs ont remarqué la même observation pour différents matériaux (Day et al., 2005; Plante et al., 2010).

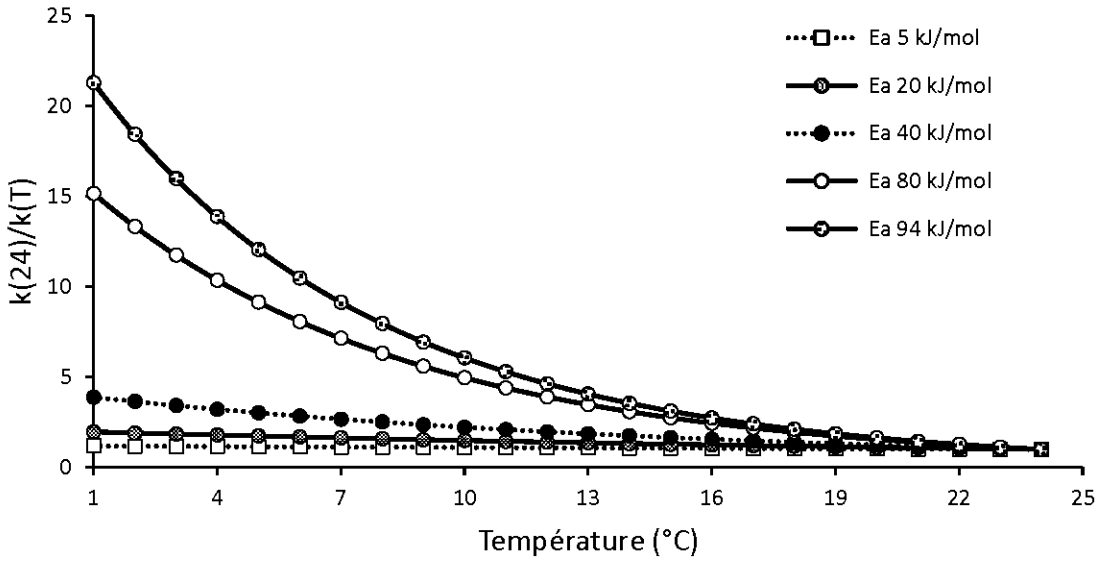

Figure 7-14 : Taux d'oxydation de la pyrite en fonction de la température pour différentes énergies d'activation.

La Figure 7-14 montre que les différences de températures moyennes entre le laboratoire et le terrain peuvent avoir un effet significatif sur les taux d'oxydation de la pyrite. À des températures auxquelles se sont déroulées les essais (22°C en laboratoire et 1°C *in situ*), les taux d'oxydation sont 21 fois plus rapide en laboratoire pour l'énergie d'acivation (E_a) égale à 90 kJ/mol. Durant l'oxydation-neutralisation, on suppose que les taux de génération des autres éléments pourraient être influencés par un facteur similaire à celui de l'oxydation de la pyrite vue que les neutralisants se dissolvent en réponse à l'oxydation des sulfures. Par conséquent, les taux de génération des principaux métaux générés ont été corrigés pour l'effet de la température par un facteur de 21 (division par 21 des taux en laboratoire) (Figure 15). Plante et al., 2014 et d'autres chercheurs ont appliqué des corrections similaires pour visualiser les différences géochimiques inter-échelles (e.g. Bennett et al., 2000; Frostad et al., 2005; Plante et al., 2014).

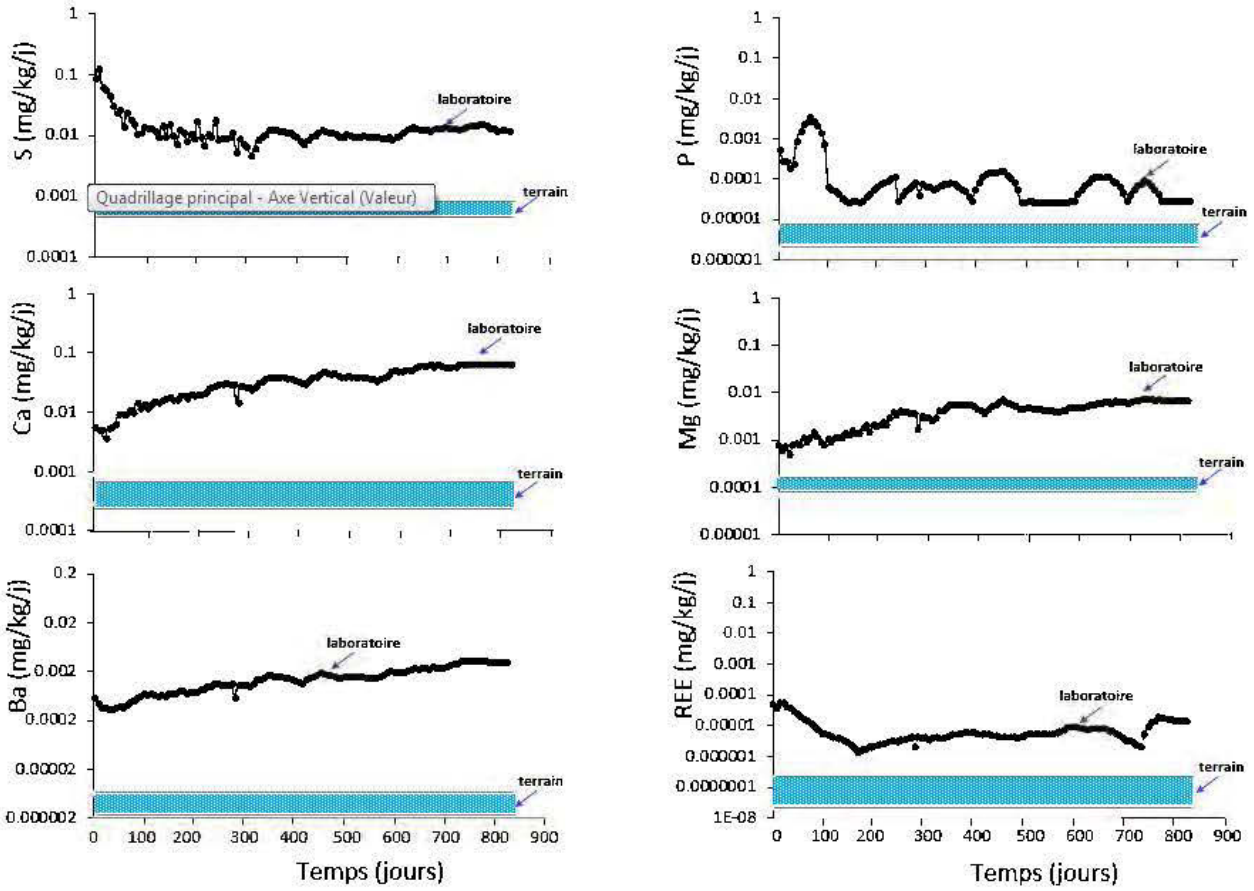

Figure 7-15 : Comparaison des taux de génération des métaux à différentes échelles, corrigés pour la température.

7.3 Comparaison du comportement géochimique des REE dans les carbonatites et les silicates

Pour mieux comprendre les différences et les similarités entre le comportement géochimique des REE issus des carbonatites de Montviel et les silicates de Kipawa, les résultats de deux types d'essais, cellules humides pour les carbonatites et mini-cellules d'altération pour les silicates, ainsi que ceux de deux concentrés de minéraux porteurs de REE représentant le minerai des deux sites, sont comparés. Les concentrés sont soumis aux mini-cellules d'altérations de laboratoire pour une durée de 140 jours.

Pour comparer les résultats géochimiques, il est pertinent de rappeler les différences minéralogiques entre les dépôts de carbonatites et de silicates étudiés dans cette thèse. Ces différences sont résumées dans le Tableau 7-4.

Tableau 7-4 : Les principales phases porteuses des REE dans les carbonatites de Montviel et les silicates de Kipawa.

	Minéraux des terres rares	$LREE_2O_3$ (%)	$HREE_2O_3$ (%)	Élément de terres rares
Carbonatites de Montviel	Monazite $(REE)PO_4$	50,87	-	Ce, La, Sm
	Synchysite $CaREE(CO_3)_2F$	51,41	-	Ce, La
	Burbankite $(Na,Ca)_3(Sr,Ba,REE)_3(CO_3)_5$	6,97	-	Ce, La
	Kukhareukoite $Ba_2REE(CO_3)_3F$	18,36	-	Ce, La, Pr, Nd
	Apatite $(Ca, REE)_5(PO_4)_3F$	1-3	-	Ce, La, Nd
Silicates de Kipawa	Mosandrite $Na(Na,Ca)_2(Ca,Ce,Y)_4(Ti,Nb,Zr)(Si_2O_7)_2(O,F)_2F_3$	26,95	6,18	Ce, Y
	Britholite $(Ce,Ca,Th,La,Nd)_5(SiO_4,PO_4)_3(OH,F)$	32,32	-	Ce, La, Nd, Y
	Eudialyte $Na_4(Ca,Ce)_2(Fe,Mn,Y)ZrSi_8O_{22}(OH,Cl)_2$	8,27	1,14	Ce, Y

Les minéraux de gangue du gisement Montviel sont composés de plus de 60 % de carbonates (i.e., calcite, ankérite, sidérite, etc.), tandis que ceux de Kipawa sont principalement composés d'aluminosilicates. Le détail de ces caractérisations minéralogiques des deux dépôts se trouvent dans les Chapitres 4, 5 et 6.

La comparaison des résultats géochimiques issus des cellules humides des carbonatites et des mini-cellules d'altération des silicates montre des concentrations plusieurs ordres de grandeur supérieures pour les essais des silicates en mini-cellules d'altération. Cet écart est associé essentiellement à la différence entre les conditions de réalisation des deux essais (i.e,. la granulométrie, ratio solide/liquide, etc.) ainsi qu'au degré de libération des minéraux porteurs de REE. La distribution granulochimique et granulominéralogique montrent que la fraction fine (<106 µm) pour les deux matériaux (silicates et carbonatites) est plus riche en REE par rapport aux fractions grossières (voir Chapitres 4 et 5). L'étude par XANES (Chapitre 3) montre que toutes les terres rares dans les solides se trouvent sous forme REE^{3+}. Après leur libération dans les lixiviats,

il est supposé qu'elles demeurent sous forme de cations trivalents dans les lixiviats vu les conditions environnementales en termes de pH-Eh et leurs concentrations (Figure 7-16). La projection de Ce et Eu issus des cellules humides de Montviel et les mini-cellules d'altération de Kipawa dans le diagramme pH-Eh (Figure 7-16) montre que ces éléments sont sous frome d'ions trivalens libres (Ce^{3+} et Eu^{3+}). Ces éléments pourraient se fractionner sous forme de minéraux secondaires et/ou en présence des matériaux possédant des capacités d'adsorption importantes tels que les carbonates, les oxyhydroxydes de fer et les argiles. Ils peuvent aussi se complexer avec des ligands inorganiques (carbonates, les sulfates, les phosphates, etc.) pour former des complexes stables (voir Chapitre 3). Cependant, les charges cumulées normalisées des REE dans les lixiviats sont relativement faibles pour toutes les lithologies des carbonatites (0,001-0,05 mg/l) de Montviel et pour celles de Kipawa (0,5-50 mg/l). Cette faible lixiviation des REE est due à la précipitation des REE sous forme des minéraux secondaires, à leur coprécipitation par les oxyhydroxides de fer, et/ou à leur sorption sur les surfaces des matériaux après leur lixiviation. Ces aspects ont été vérifiées par une étude de sorption des REE sur les matériaux de Montviel et par les calculs d'équilibres thermodynamiques. En effet, les REE se complexent avec PO_4^{3-} pour former des sels stables de REE (Chapitres 4 et 5).

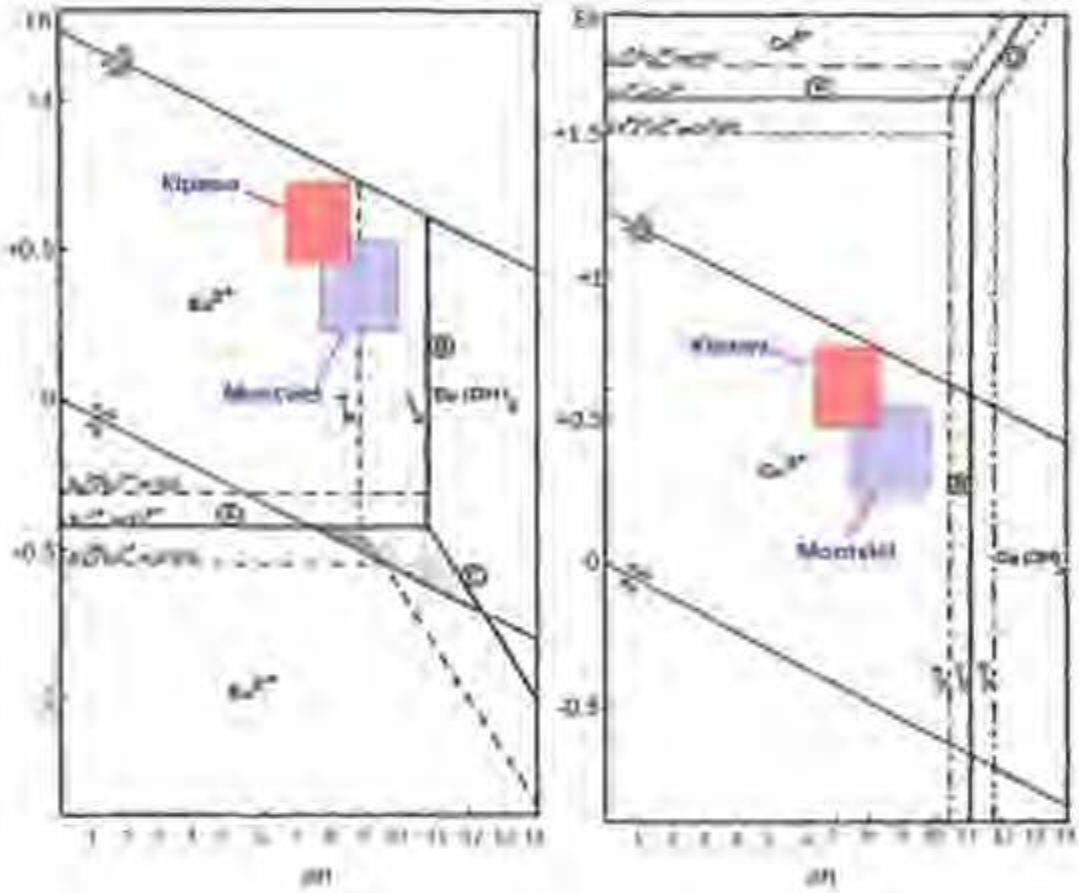

Figure 7-16 : Diagramme Eh-pH du cérium et de l'europium dans les lixiviats de Montviel et de Matamec (Bonnot-Courtois, 1981).

Pour comparer la réactivité des carbonates et celle des silicates des terres rares, un concentré de carbonates de REE et un concentré de silicates de REE sont soumis à des essais en mini-cellules d'altération. Les différences de charges cumulées normalisées issues des mini-cellules d'altération de concentré de carbonates de REE (valeurs) et celui de silicates de REE (valeurs) varient d'un à 2 ordres de grandeur (Figure 7-17). Comme les deux concentrés ont les mêmes caractéristiques (i.e. la granulométrie, le rapport liquide/solide, le degré de libération, etc.), les différences en termes de charges cumulées normalisées pourraient être dûes principalement à la différence de réactivité entre les deux concentrés. Le concentré de carbonates de REE semble plus réactif que le concentré de silicates de REE.

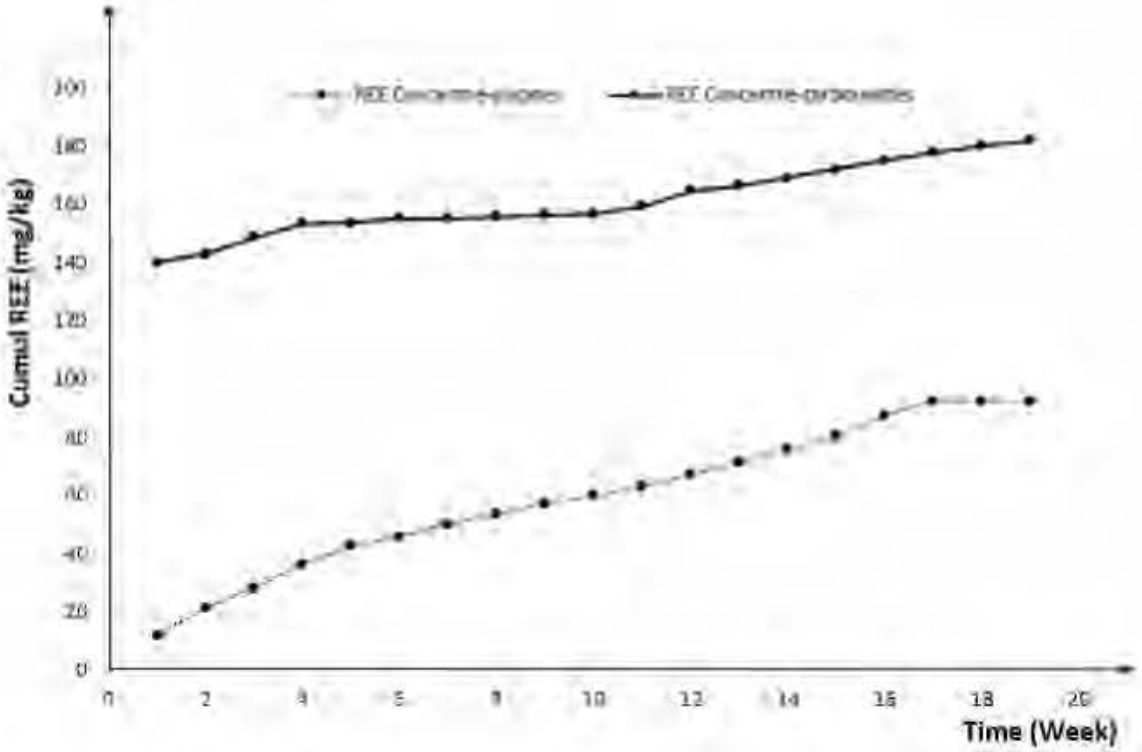

Figure 7-17 : Comparaison de la lixiviation des REE issus des mini-cellules d'altération entre un concentré des REE des silicates et celui des carbonatites.

7.4 Approche d'entreposage des matériaux de Montviel et de Kipawa pour assurer une gestion intégrée

Les rejets miniers sont stockés en surface dans des haldes à stériles et dans des parcs à résidus. En cas d'absence des minéraux neutralisants, l'oxydation des minéraux sulfureux (i.e. pyrite, pyrrhotite, etc.) présents dans ces résidus miniers pourrait générer du drainage minier acide (DMA). Les lixiviats de DMA sont caractérisés par un pH acide, ainsi que par des concentrations élevées en sulfates et en métaux lourds. Dans le cas de présence des minéraux neutralisants en quantité suffisante, le pH des lixiviats pourrait être compris entre 6,5 et 9,5 (cas des matériaux de Montviel et Matamec); on parle d'un drainage neutre contaminé (DNC). Dans ces conditions, certains métaux caractérisés par une mobilité importante comme le zinc, le nickel, le plomb et l'arsenic pourraient atteindre, dans les eaux de drainage, des concentrations supérieures aux normes en vigueur. Dans les minerais de REE, les matériaux géologiques (carbonatites et silicates) sont faiblement réactifs et les REE sont souvent associés avec des contaminants (par exemple, Ba, F,

Sr, Nb, U et Th). Les minéraux porteurs de REE peuvent se présenter sous forme de minéraux purs ou être présents en inclusion dans les autres minéraux de gangue. En cas d'absence d'atténuation naturelle, leur dissolution pourrait engendrer des conditions du DNC.

Pour faire face à ce problème de drainage minier contaminé, les méthodes de restauration visent à limiter l'accès de l'eau ou de l'oxygène aux résidus réactifs, dépendamment du type du climat. En climat sec, on peut limiter le mouvement de l'eau vers les résidus en utilisant la méthode stockage et relargage (store and release). Cependant, en climat humide, on préfère limiter le mouvement de l'oxygène en utilisant, par exemple, des couvertures à effets de barrière capillaire (CEBC) ou la méthode de la monocouche avec nappe surélevée. Comme les résidus de mines de REE ne génèrent pas de DMA, le recours à d'autres techniques de restauration moins coûteuses et plus appropriées aux problématiques de DNC pourrait être envisagé.

Dans la littérature actuelle sur la restauration des rejets miniers de terres rares, aucune étude n'a été trouvée sur la façon de restaurer les haldes à stériles ou les aires d'accumulation de résidus de mines de terres rares. Les réflexions présentées dans ce qui suit sont basées sur les résultats de cette thèse afin de suggérer des voies permettant de restaurer des aires d'accumulation de rejets des terres rares. Parmi les suggestions proposées pour restaurer les aires d'accumulation de rejets de mines de terres rares, on cite :

- ✓ Techniques d'imperméabilisation, en particulier l'utilisation des argiles ou de la gangue issue des futures exploitations pour assurer une déviation des écoulements d'eau (favoriser les écoulements horizontaux). Ces techniques pourraient réduire à un certain niveau la percolation des eaux de pluie au sein des rejets. Par conséquent, les volumes d'eau contaminées à gérer seront plus faibles. Dans les climats arides, cette technique peut être très prometteuse pour contraindre la percolation des eaux, vue les faibles précipitations annuelles (Knidiri, 2015). Cependant, en climat humide, la limitation de la percolation de l'eau est un défi. La limitation de la percolationpourrait être prometteuse pour restaurer les sites des résidus de mines de terres rares, en permettant de réduire le débit à traiter mais avec des risques de concentrations plus élevées (moins de dilution). L'atténuation naturelle pourrait être significative vue la présence des quantités importantes des carbonates et/ou de silicates de calcium et de magnésium, qui ont des capacités de rétention importantes des métaux et des REE en solution. Un traitement passif pour enlever les métaux résiduels à la

sortie des haldes pourrait être nécessaire avant que les effluents rejoignent le milieu naturel (Figure 7-18).

- ✓ Techniques d'effet de barrière capillaire avec une déviation des eaux de surface suivant une pente pour assurer un bon drainage des eaux. Les résidus miniers peuvent servir aussi comme matériaux de la couche de rétention d'eau tel que discuté précédemment.
- ✓ Mettre les matériaux des lithologies à forte capacité de sorption en alternance avec les autres matériaux à faible capacité de sorption au fur et à mesure de la construction des aires d'accumulation des rejets.
- ✓ Mettre les matériaux de grande capacité de sorption à la base des aires d'accumulation qui vont servir comme un filtre pour les effluents percolant à travers les rejets (Figure 7-18).

7.4.1 Restauration et conception de la halde à stérile de Montviel

Dans le cas de Montviel, l'accès au minerai de REE se fait à travers la lithologie des silicocarbonatites. Les résultats de caractérisation minéralogique, des essais cinétiques de laboratoire et des essais de sorption montrent que cette dernière contient très peu de sulfures et de minéraux de REE, qu'elle libère moins de REE et d'autres métaux, et qu'elle possède une grande capacité de sorption des métaux par rapport aux autres lithologies. La prise en considération de tous ces paramètres, et la morphologie du gisement, permet de concevoir la future halde à stérile issue de l'exploitation du gisement Montviel (Figure 7-18). Afin de traiter toute contamination résiduelle à la sortie de la halde à stérile et la disponibilité des carbonates *in situ*, un traitement passif par drains calcaires pourrait être utilisé avant que les effluents ne rejoignent le milieu naturel (Figure 7-18).

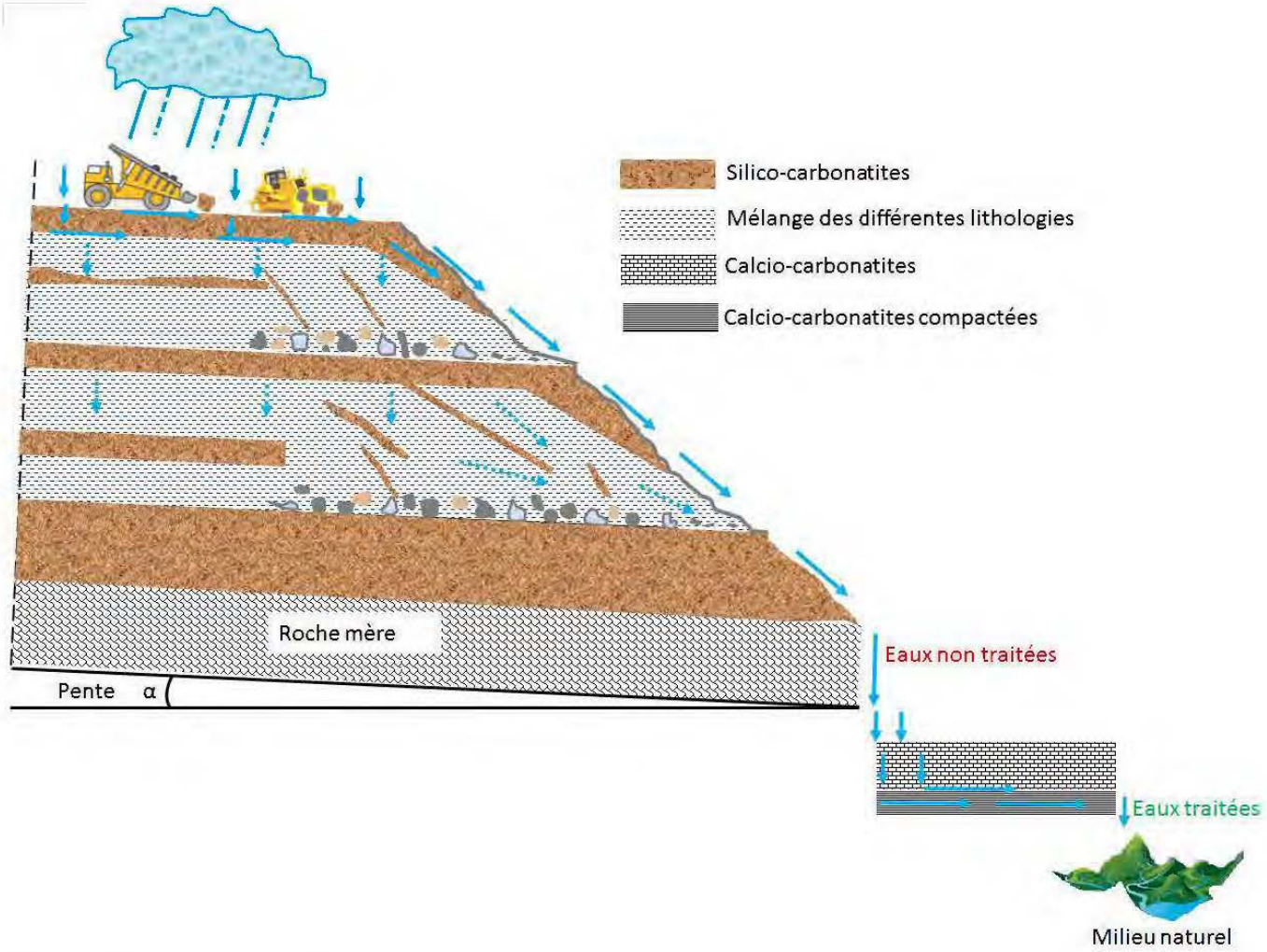

Figure 7-18 : Approche d'entreposage proposée pour les rejets miniers porteurs de terres rares de Montviel (inspirée de Aubertin et al., 2002).

La présente étude a mis en évidence le rôle de la minéralogie et la géochimie des stériles et des minerais dans la prédiction du comportement enviromemental des différents matériaux géologiques porteurs de REE (silicates et carbonatites). L'étude de deux types de gisements à différentes échelles (laboratoire et terrain) pourrait apporter une contribution importante dans la compréhension des phénomènes (sorption, dissolution, précipitation de minéraux et oxydation des sulfures) à considérer durant la phase de la prédiction du comportement enviromemental des rejets miniers porteurs des terres rares potentiellement générateurs de DNC. La prise en considération de ces phénomènes dès les phases de faisabilité et/ou préfaisabilité des projets miniers de terres rares permet de proposer une gestion appropriée de ces rejets durant et après l'exploitation.

Les résultats présentés tout long de cette thèse sont obtenus par l'adaptation d'une approche en plusieurs phases cohérente avec le guide proposé par IRME-UQAT pour la caractérisation des résidus miniers et du minerai (Plante et al., 2015). L'approche adaptée a pour objectif de soulever les défis suivants (Figure 7-19) : (i) identifier et quantifier les différents minéraux porteurs des REE associés à différents gisements de REE, (ii) déterminer à l'avance le potentiel polluant de certaines espèces qui pourraient être libérées pendant le stockage des rejets miniers en surface, et (iii) proposer une approche de gestion intégrée et des voies de valorisations des rejets miniers porteurs de terres rares. L'approche utilisée est constituée de trois piliers fondamentaux : (i) échantillonnage exhaustif sur le terrain, (ii) caractérisation détaillée (minéralogique, chimique, et physique), et (iii) prédiction du comportement environnemental des REE via l'utilisation des essais cinétiques (cellules humides, mini-cellules d'altération et barils de terrain).

La pertinence des résultats de caractérisations minéralogique, chimique, physique, et géochimiques issus des différents essais de prédiction dépend de la représentativité des échantillons. Avant de commencer l'étape d'échantillonnage, il est pertinent de consulter les cartes géologiques et les forages effectués en exploration. La consultation de ces cartes permettra de savoir le nombre de lithologies, la profondeur du forage, la distribution des carottes, le pendage des carottes, et la composition minéralogique. Ces informations aident à la réalisation d'un plan d'échantillonnage : maille d'échantillonnage, choix et le repérage des carottes, estimation de la quantité à échantillonner en lien avec les besoins expérimentaux, etc. Il est recommandé d'échantillonner séparément les lithologies et faire par la suite un échantillon composite pour l'étudier. Ceci permet de mieux cerner une lithologie problématique d'un point de vue environnemental pour la gérer séparément (mise en place d'une approche d'entreposage des rejets miniers).

Comme c'est parfois difficile d'identifier à l'œil nu la composition minéralogique des carottes, il est conseillé d'être outillé d'un XRF portatif qui aidera à améliorer la représentativité des échantillons en se basant sur la composition chimique des éléments majeurs. Une fois repérées les sections de carottes à échantillonner, on propose de les diviser, d'en concasser un aliquot et de les homogénéiser, selon la quantité nécessaire pour répondre aux besoins expérimentaux. Pour la caractérisation chimique et minéralogique des minéraux porteurs de REE, il est important de prendre en considération la distribution granulochimique des REE et leur densité au moment de préparation des sections polies. Quant aux analyses chimiques suite à une digestion acide, il est nécessaire d'avoir recours à des méthodes évitant l'acide sulfurique et l'acide fluoridrique, qui

pourraient précipiter les REE et, par conséquent, sous-estimer les résultats. Pour la préparation des sections polies, il faut s'assurer de l'annulation de l'effet de la densité des minéraux des REEE par l'ajout de carbone graphitique qui va assurer une distribution homogène des grains. Sur le plan environnemental, la détermination de la composition chimique et minéralogique des échantillons en question permettra d'identifier et quantifier les minéraux acidogènes, neutralisants, et porteurs de contaminants potentiels afin de mieux statuer sur le potentiel de génération d'acidité et de drainage neutre contaminés des matériaux étudiés.

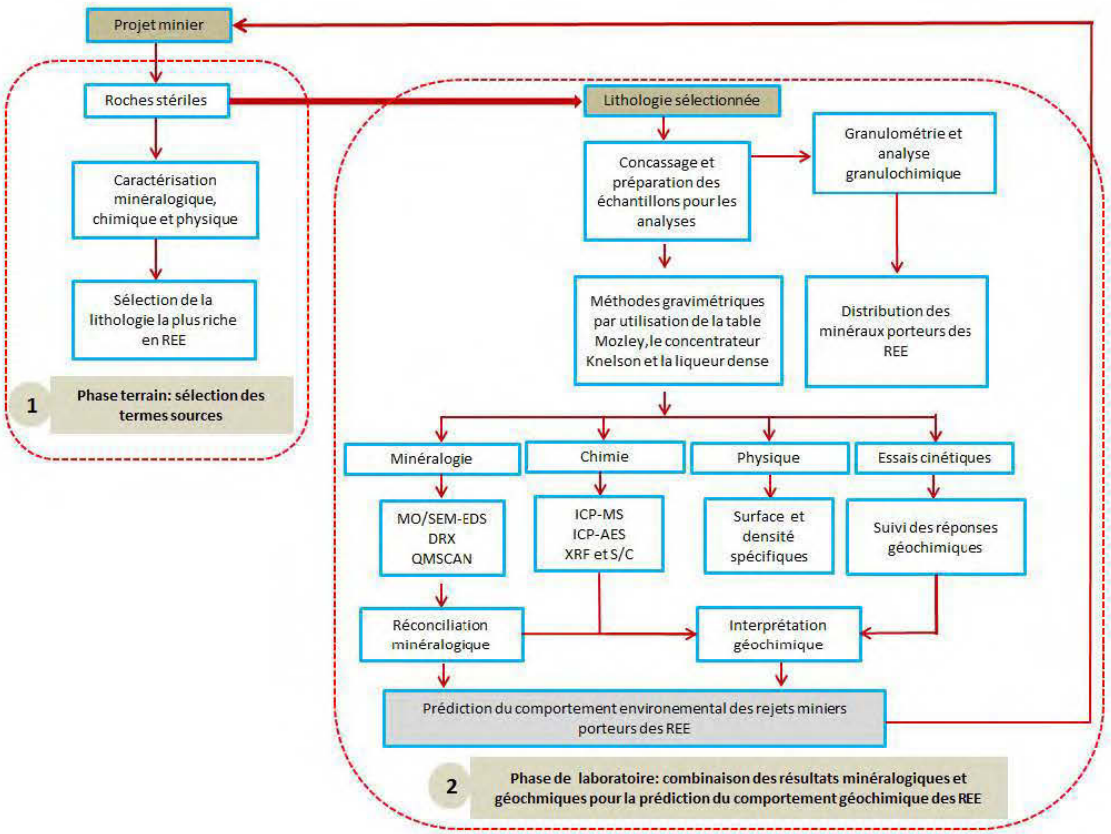

Figure 7-19 : approche adaptée pour l'évaluation environnemental des roches stériles porteurs des REE.

L'intégration des différentes phases de cette approche dès l'étape d'exploration permettrait de faciliter la prise de décisions associée à l'approche d'entreposage durant l'exploitation et, par conséquent, les techniques de restauration. Sur le plan pratique, cette approche pourrait être un bon intermédiaire entre le législateur et la compagnie minière. Du côté du législateur, elle permet d'avoir des éléments de réponse pour statuer sur l'acceptabilité du projet. Du côté de la compagnie

minière, ces étapes contribueraient à répondre aux exigences du législateur sur les impacts environnementaux.

Références

Al-Abed, S. R., Jegadeesan, G., Purandare, J., and Allen, D. (2008). Leaching behavior of mineral processing waste: comparison of batch and column investigations. Journal of hazardous materials, 153(3), 1088-1092.

Al-Abed, S. R., Hageman, P. L., Jegadeesan, G., Madhavan, N., and Allen, D. (2006). Comparative evaluation of short-term leach tests for heavy metal release from mineral processing waste. The Science of the total environment, 364(1-3), 14-23.

Alkattan, M., Eric, H., Oelkers, J., and Schott, J. (1998). An experimental study of calcite and limestone dissolution rates as a function of pH from −1 to 3 and temperature from 25 to 80°C. Chemical Geology, vol. 151, no 1–4, p. 199-214.

Anawar, H. (2015). Sustainable rehabilitation of mining waste and acid mine drainage using geochemistry, mine type, mineralogy, texture, ore extraction and climate knowledge. Journal of Environmental Management, vol. 158, p. 111-121.

Appelo, C.A.J., and Postma, D. (2005). Geochemistry, groundwater and pollution, Editor: A.A. Balkeman Publishers, 2nd edition.

Arvidson, S., Inci Evren, E., James, E., and Andreas, L. (2003). Variation in calcite dissolution rates: A fundamental problem. Geochimica et Cosmochimica Acta, vol. 67, no 9, p. 1623-1634.

Aubertin, M., and Bussiere, B. (2002). Environnement Minier Et Gestion Des Rejets Miniers. Presses Polytechnique Montreal.

Bassolé, M. (2016). Pertinence des essais de lixiviation en batch dans la prédiction du comportement hydrogéochimique des rejets miniers. Mémoire. Rouyn-Noranda, Université du Québec en Abitibi-Témiscamingue, Science appliquées, 238 p.

Bennett, J. W., Comarmond, M. J., and Jeffrey, J. (2000). Comparison of sulfidic oxidation rates measured in the laboratory and the field. Proceedings from the jh JCARD, Denver, 1, pp.171-180.

Bennett, P. C., Melcer, M. E., Siegel, D. I., and Hassett, J. P. (1988). The dissolution of quartz in dilute aqueous solutions of organic acids at 25°C. Geochimica et Cosmochimica Acta, vol. 52, no 6, p. 1521-1530.

Benzaazoua, M., Fiset, J. F., Bussière, B., Villeneuve, M., and Plante, B. (2006). Sludge recycling within cemented paste backfill: Study of the mechanical and leachability properties. Minerals Engineering, 19(5), 420-432.

Benzaazoua, M., Bussière, B., Dagenais, A.M., and Archambault, M. (2004). Kinetic tests comparison and interpretation for prediction of the Joutel tailings acid generation potential. Environmental Geology 46, 1086-1101.

Bian, X., Shao-hua, Y., Yao, L., and Wen-yuan, W. (2011). Leaching kinetics of bastnaesite concentrate in HCl solution. Transactions of Nonferrous Metals Society of China, vol. 21, no 10, p. 2306-2310.

Bouzahzah, H., Benzaazoua, M., and Bussière, B. (2014). Prediction of Acid Mine Drainage: Importance of Mineralogy and the Test Protocols for Static and Kinetic Tests Mine Water and the Environment. Mine Water and the Environment", Mine Water and the Environment, 33:54–65.

Bussière B., and Aubertin M. (1999). Clean tailings as cover material for preventing acid mine drainage: an *in situ* experiment. Conférence présentée au Sudbury '99 Mining and the Environment II, Sudbury, Ontario, 13–17 September 1999. Edited by N.B.D. Goldstack, P. Yearwood, and G. Hall. Vol. 1.pp: 19–28.

CEAEQ. (2012). Protocole de lixiviation pour les espèces inorganiques, MA. 100 – Lix.com.1.1, Rév. 1. Ministère du Développement durable, de l'Environnement, de la Faune et des Parcs du Québec, 07(1), 1-17.

Chang, Hongtao, Mei Li, Zhaogang Liu, Yanhong Hu and Fushun. Z. (2010). Study on separation of rare earth elements in complex system. Journal of Rare Earths, vol. 28, Supplement 1, no 0, p. 116-119.

Coto, B., C. Martos, J. L. Peña, R. Rodríguez, and Pastor. G. (2012). Effects in the solubility of CaCO3: Experimental study and model description. Fluid Phase Equilibria, vol. 324, no 0, p. 1-7.

Day, S., Sexsmith, K., MacGregor, D., Mehling, P., Shaw, S., and Kestler, U. (2005). Cold temperature effects on geochemical weathering. Proceedings from the 1 jh an nuai British

Columbia-MEND MLIARD workshop, Challenges in the prediction of drainage chemistry. Vancouver, British Columbia, Canada.

Demers I., Bussière B., Aachib M.., and Aubertin M. (2011). Repeatability evaluation of instrumented column tests in cover efficiency evaluation for the prevention of acid mine drainage. Water, Air, and Soil Pollution 219, pp : 113-128.

Duzgoren-Aydin, N. S., and Aydin. A. (2009). Distribution of rare earth elements and oxyhydroxide phases within a weathered felsic igneous profile in Hong Kong. Journal of Asian Earth Sciences, vol. 34, no 1, p. 1-9.

Edahbi, M., Plante, B., Bouzahzah, H., Benzaazoua, M., and Plettier, M. (2015). Mineralogical and geochemical study of rare earth elements from a carbonatite deposit. Proceedings of the 13th SGA biennial meeting, Nancy, France, 24-27 août 2015.

Elzinga, E. J., R. J. Reeder, S. H. Withers, R. E. Peale, R. A. Mason, K. M. Beck and Hess, W. P. (2002). EXAFS study of rare-earth element coordination in calcite. Geochimica et Cosmochimica Acta, vol. 66, no 16, p. 2875-2885.

Erguler, Z., and Güzide, K. (2015). The effect of particle size on acid mine drainage generation: Kinetic column tests. Minerals Engineering, vol. 76, p. 154-167.

Fernández-Caliani, J. C., Barba-Brioso, C., and De la Rosa. J. D. (2009). Mobility and speciation of rare earth elements in acid minesoils and geochemical implications for river waters in the southwestern Iberian margin». Geoderma, vol. 149, no 3–4, p. 393-401.

Frostad, S., Klein, B., and Lawrence, R. W. (2005). Determining the weathering characteristics of a waste dump with field tests. International Journal of Surface Mining, Reclamation and Environment 19, 132-143.

Ganor, J., Lu, P., Zheng, Z., and Zhu, C. (2007). Bridging the gap between laboratory measurements and field estimations of silicate weathering using simple calculations.Environmental Geology 53, 599-610.

González, V. (2015). "Lanthanide ecotoxicity: First attempt to measure environmental risk for aquatic organisms." Environmental Pollution 199(Supplement C): 139-147.

Gonzalez, V. (2014). Environmental fate and ecotoxicity of lanthanides: Are they a uniform group beyond chemistry?. Environment International 71(Supplement C): 148-157.

Gschneidner, A., Jean-Claude, and Vitalij. G. (2006). Handbook on the Physics and Chemistry of Rare Earths. vol. 36, p. 521.

Gu ,X, and Evans, L. (2007) Modelling the adsorption of Cd(II), Cu(II), Ni(II), Pb(II), and Zn(II) onto Fithian illite. J Coll Interf Sei 307: 317-325.

Guy, C., Daux. V., and Schott. J. (1999). Behaviour of rare earth elements during seawater/basalt interactions in the Mururoa Massif. Chemical Geology, vol. 158, no 1–2, p. 21-35.

Hellmann. R., and Scott A. (2002). Water-Rock Interactions, Ore Deposits, and Environmental Geochemistry A Tribute to David A. Crerar. The geochemical society. Special publication N°.7.

Hierro, A., Bolivar, J.P., Vaca, F., and Borrego, J. (2012). Behavior of natural radionuclides in surficial sediments from an estuary impacted by acid mine discharge and industrial effluents in Southwest Spain. Journal of Environmental Radioactivity 110, 13-23.

Hooper, K. I. M. (1998). TCLP fails to extract oxoanion-forming elements that are extracted by municipal solid waste leachates.

Kandji, E. H. B. (2017). Kinetic testing to evaluate the mineral carbonation and metal leaching potential of ultramafic tailings: Case study of the Dumont Nickel Project, Amos, Québec. Applied Geochemistry 84(Supplement C): 262-276.

Knidiri, J. (2015). Évaluation de l'effet de la pente sur le comportement hydrogéologique d'un recouvrement alternatif de type stockage-relargage constitué de rejets calcaires phosphatés en climat aride (Doctoral dissertation, École Polytechnique de Montréal).

Lackovic, J. A., Nikolaidis, N. P., Chheda, P., Carley, R. J., and Patton, E. (1997). Evaluation of batch leaching procedures for estimating metal mobility in glaciated soils (pp. 231-240).

Lappako, K. A. (1994). Evaluation of neutralization potential determinations for metal mine waste and a proposed alternative. International Land Reclamation and Mine Drainage Conference and the Third International Conference on the Abatement of Acidic Drainage. Pittsburg, USA.

Lévesque Michaud, M. (2016). Développement d'une méthode de prédiction cinétique du drainage neutre contaminé avec agent complexant : application au projet minier blackrock. Mémoire

de maitrise. Rouyn-noranda, université du Québec en Abitibi-Témiscamingue, sciences appliquées, 238 p.

Lewis, A. E., and Hugo, A. (2000). Characterization and batch testing of a secondary lead slag. (October), 365-370.

Lin, F., and Charles, V. (1981). The dissolution kinetics of brucite, antigorite, talc, and phlogopite at room temperature and pressure. American Mineralogist, vol. 66, no 7-8, p. 801-806.

Malmström, M. E., Destouni, G., Banwart, S. A., and Stromberg, B. H. E. (2000). Resolving the scale-dependence of mineral weathering rates. Environmental Science and Technology 34, 1375-1378.

Mbonimpa M., Aubertin M., Aachib M., and Bussière B. (2003). Diffusion and consumption of oxygen in unsaturated cover materials. Canadian Geotechnical Journal 40(5), pp: 916-932.

Miller, S., Andrina, J., et Richards, D. (2003). Overburden Geochemistry and Acid Rock Drainage Scale-Up Investigations at the Grasberg Mine, Papua Province, Indonesia.Proceedings ofthe 6thiCARD. Cairns, North Queensland, Australia, pp. 1ll-121.

Nicholson, R. V. (1994). Iron-sulfide oxidation mechanisms: laboratory studies. Dans The Environmental Geochemistry of Sulfide Mine-wastes (eds. J. L. Jambor and D. W. Blowes). Mineralogical Association of Canada, Nepean, ON, vol.22, pp.l64-183.

Nicholson, R. V., Gillham, R. W., Cherry, J. A., and Reardon, E. J. (1988). Pyrite oxidation in carbonate-buffered solutions: 1. Experimental kinetics. Geochimica Cosmochimica Acta 52, 1077-1085.

Özverdİ, A., and Erdem, M. (2010). Environmental risk assessment and stabilization/solidification of zinc extraction residue: I. Environmental risk assessment. Hydrometallurgy, 100(3-4), 103-109.

Pepin, G. (2009). Évaluation du comportement géochimique de stériles potentiellement générateurs de drainage neutre contaminé à l'aide de cellules expérimentales *in situ*". Mémoire de maîtrise, Département des génies civil, géologique et des mines. École Polytechnique de Montréal, Montreal, Québec, Canada.

Plante, B., Bussiére, B., Bouzahzah, H., Benzaazoua, M., Demers, I., Kandji, B., and Cassista, M. A. (2015). Revue de littérature en vue de la mise à jour du guide de caractérisation des résidus miniers et du minerai.

Plante, B., Benzaazoua, M., and Bussière, B. (2010a). Predicting Geochemical Behaviour of Waste Rock with Low Acid Generating Potential Using Laboratory Kinetic Tests. Mine Water and the Environment, 30(1), 2-21.

Plante, B., Benzaazoua, M., Bussière, B., Biesinger, M. C., and Pratt, A. R. (2010b). Study of Ni sorption onto Tio mine waste rock surfaces. Applied Geochemistry, 25(12), 1830-1844.

Romero-Freire, A. (2018). Assessment of baseline ecotoxicity of sediments from a prospective mining area enriched in light rare earth elements. Science of The Total Environment 612(Supplement C): 831-839.

Sapsford, D. J., Bowell, R. J., Dey, M., and Williams, K. P. (2009). Humidity cell tests for the prediction of acid rock drainage. Minerais Engineering 22, 25-36.

Shieh, C. (2001). Criteria of selecting toxicity characteristics leaching procedure (TCLP) and synthetic precipitation leaching procedure (SPLP) tests to characterize special wastes. Florida Center for Solid and Hazardous Waste Management, University of Florida, Report, 01-2.

Stegemann, J., and Cote, P. (1991). Investigation of test methods for solidified waste evaluation. Appendix B: Test methods for solidified waste evaluation. Environment Canada Manuscript Series.

US EPA. (1995). Applicability of the toxicity characteristic leaching procedure to mineral processing wastes. Technical Background Document Supporting the Supplemental Proposed Rule Applying Phase IV Land Disposal Restrictions to Newly Identified Mineral Processing Wastes (December).

Yusoff, M., Bryne, T., and Parsons, I. (2013). Mobility and fractionation of REEs during deep weathering of geochemically contrasting granites in a tropical setting, Malaysia. Chemical Geology, vol. 349–350, no 0, p. 71-86.

Zendah, H., Khattech, I., and Jemal.M. (2013). Thermochemical and kinetic studies of the acid attack of "B" type carbonate fluorapatites at different temperatures (25–55)°C. Thermochimica Acta, vol. 565, no 0, p. 46-51.

Zhang, Y., and Xuelu, G. (2015). Rare earth elements in surface sediments of a marine coast under heavy anthropogenic influence: The Bohai Bay, China. Estuarine, Coastal and Shelf Science, vol. 164, p. 86-93.

CHAPITRE 8 CONCLUSIONS ET RECOMMANDATIONS

8.1 Sommaire des résultats obtenus

Plusieurs projets de mines de terres rares sont actuellement en développement au Canada (i.e, Montviel, Kipawa, Strange Lake). Or, les exploitations minières de terres rares sont connues pour générer des grandes quantités de rejets (rejets de concentrateur et roches stériles) qui sont entreposés en surface dans des parcs à rejets ou empilées dans les haldes à stériles (Hurst, 2010). Les eaux de pluie et de la fonte des neiges percolant par-dessus et au travers des rejets miniers porteurs des terres rares forment les eaux de drainage minier. Ces effluents pourraient être contaminés par plusieurs polluants provenant de la dissolution totale ou incongruente des phases minérales constituant les rejets miniers. La gestion et le traitement des effluents contaminés présente un défi majeur pour les compagnies minières, puisque les eaux rejetées dans l'environnement doivent absolument respecter les normes environnementales en vigueur avant de rejoindre le milieu naturel. Au Québec, les valeurs des paramètres physico-chimiques (i.e. pH), les concentrations en métaux (Ba, Sr, F, Cu, Zn, Pb, etc.) et métalloïdes (i.e. As), et la toxicité ne doivent pas dépasser les limites consignées dans la nouvelle Directive019. On peut distinguer différents types de drainage minier : acide (DMA), neutre contaminé (DNC) et alcalin (DA). Contrairement au DMA (pH acide, concentrations élevées en métaux), le DNC a un pH respectant les normes environnementales. Cependant, ce type de drainage peut contenir des métaux en concentrations qui peuvent dépasser les limites réglementaires; en particulier, les éléments chimiques les plus mobiles et les incompatibles tels que le zinc, le nickel etc. Les éléments des terres rares peuvent aussi être impliqués mais leur géochimie demeure mal connue et il n'existe pas de législation les concernant.

Ainsi, depuis plusieurs années, la recherche scientifique s'efforce pour comprendre la formation du drainage minier contaminé, les mécanismes géochimiques responsables de sa génération et les outils de prédiction de la qualité de l'eau. Cependant, les approches utilisées pour l'évaluation environnementale associée à l'exploitation des gisements polymétalliques (matériaux très réactifs) ne sont pas forcement applicable dans le cas de l'exploitation des gisements de terres rares (réputés comme des matériaux géologiques faiblement réactifs). Par conséquent, le comportement géochimique de rejets miniers porteurs des terres rares n'est pas maîtrisé et, de surcroît, n'a fait

l'objet que de très rares recherches jusqu'à maintenant. La revue de littérature indique ainsi une grande méconnaissance sur la géochimie des terres rares, la réactivité des minéraux porteurs des terres rares, et les processus géochimiques (sorption, précipitation et co-précipitation) qui contrôlent leur fractionnement et leur mobilité dans les conditions environnementales proches de la neutralité. Il est donc difficile de statuer sur la gestion des rejets miniers porteurs des terres rares. Les lithologies renfermant des terres rares ne sont en général pas riches en sulfures et donc à l'abris d'un potentiel de génération d'acidité.

Lors des cinq dernières années, plusieurs projets de mines de terres rares au Canada ont été considérés pour leur mise en valeur (Strange Lake, Montviel, Kipawa, etc.), ce qui nécessite la prédiction du comportement géochimique des rejets miniers de terres rares qui seront issus de ces futures exploitations. Le comportement géochimique des futurs rejets miniers porteurs de terres rares, la minéralogie des phases porteurs des terres rares, la géochimie des lixiviats et les processus géochimiques impliqués dans les conditions de DNC pour les roches stériles porteuses des terres rares ont été discutés tout le long de cette thèse de doctorat. Les résultats des travaux de laboratoire indiquent que : (i) les roches stériles et les minerais des deux gisements (Montviel et Matamec) ne sont pas générateurs d'acide, (ii) la lixiviation de terres rares est relativement faible dans les conditions contrôlées de laboratoire, (iii) les terres rares légères présentent une plus mobilité faible par rapport aux terres rares lourdes, et (iv) les phosphates, les carbonates et les oxyhydroxydes de fer sont les principales phases minérales qui contrôlent le fractionnement des terres rares en solution. De plus, les essais de terrain ont montré : (i) la présence d'un effet d'échelle significatif à comparer avec les essais de laboratoire et *in situ*, (ii) une augmentation de la dissolution des carbonates dans les conditions météorologiques du terrain, (iii) les eaux de drainage respectent les exigences environnementales de la Directive 019 en termes des métaux et les radionucléides. Les taux de relargage instantanés des terres rares aux échelles du terrain sont inférieurs d'environ 4 ordres de grandeur aux taux de relargage à l'échelle du laboratoire.

En parallèle, il a été démontré que l'atténuation naturelle par les phénomènes de sorption, de précipitation et de co-précipitation pourrait réduire significativement la mobilité des terres rares dans des conditions de lixiviation, tel que démontré aux Chapitres 3, 4, 5, et 6. Le potentiel d'atténuation serait contrôlé par plusieurs facteurs comme la température, la surface spécifique, la granulométrie, la saturation des solutions, etc. Ces facteurs expliquent en partie l'effet d'échelle relevé au niveau de la qualité des eaux entre les essais *in situ* et en laboratoire. Les roches stériles

des essais *in situ* génèrent davantage de terres rares dans les lixiviats que les essais en laboratoire via une dissolution plus importante des carbonates des terres rares sur le terrain.

Les lithologies des carbonatites de Montviel ont été soumises à des essais en cellules humides (Chapitre 4), tandis que celles de Kipawa ont été soumises à des essais en mini-cellules d'altération (Chapitre 6); les deux types de tests ont été démontrés équivalents lors d'études antérieures (Bassolé, 2016; Benzaazoua et al., 2004; Maest and Nordstrom, 2017; Plante et al., 2010). Les principaux résultats géochimiques fournis par ces deux types d'essais montrent que les matériaux de Kipawa relarguent plus de terres rares que ceux de Montviel. Ceci s'expliquerait par le fait que les mini-cellules sont plus agressives et, par conséquent, elles provoquent une dissolution exagérée des minéraux porteurs des terres rares. Cependant, la comparaison entre les résultats des mini-cellules d'altération de deux concentrés de terres rares (un de Montviel et l'autre de Kipawa) indique que les carbonates de terres rares sont plus réactifs que les silicates de terres rares (carbonates des REE relarguent 3 à 4 fois plus les terres rares que les silicates).

Des cellules de sorption en terres rares ont été utilisées pour évaluer le potentiel de sorption des lithologies de Montviel. Les résultats (Chapitre 3) montrent que les terres rares retenues peuvent être sous différentes formes sorbées, précipitées, et/ou co-précipitées à travers d'autres phases. Dans la partie discussion (Chapitre 7), d'autres aspects d' importance pour la compréhension du comportement géochimique des terres rares non discutés dans les chapitres précédents, comme la comparaison des résultats des essais de lixiviation TCLP, SPLP, et CTEU-9 et les essais cinétiques de laboratoire (cellules humides et mini-cellules d'altération), l'effet d'échelle entre les essais de laboratoire et du terrain réalisés sur les roches stériles porteuses des terres rares de Montviel, ainsi qu'une approche d'entreposage des rejets miniers porteurs des terres rares.

8.1.1 Chapitre 2

Ce chapitre portait principal sur une revue de littérature sur : (i) les différents types de gisements porteurs des terres rares, (ii) les caractéristiques de ces dernières, (iii) leurs applications, (iv) leur recyclage, (v) leur comportement géochimique en le milieu aqueux, (vi) la réactivité de leurs phases porteuses, et (vii) les impacts potentiels de leur relargage dans l'environnement. Ce chapitre a permis de mettre notamment l'emphase sur de nombreuses lacunes associés au cycle de vie des mines de terres rares (de l'exploration à la restauration). Il présente les différents aspects

environnementaux associés à une exploitation des gisements de terres rares, ainsi que les différents types de rejets associés à l'exploitation et à la valorisation des REE.

8.1.2 Chapitre 3

Dans ce chapitre, vu les nombreuses lacunes sur la géochimie des terres rares, une étude qui se veut fondamentale permettant de comprendre le comportement géochimique des terres rares a été réalisée. Des carbonates, des phosphates, et des oxy-hydroxydes de fer ont été synthétisés par voie chimiques et mélangés avec des carbonates commerciaux de synthèse avec du cérium (Ce) et du lanthane (La). Une concentration de 5 % de pyrite est ajoutée à chaque mélange pour stimuler les conditions similaires à celles trouvées dans les carbonatites de Montviel qui renferment un peu de sulfures. Chaque mélange mettait l'emphase sur l'effet de chaque phase minérale sur la mobilité Ce et du La. En total cinq mélanges ont été formulés et soumis à des essais en mini-cellules d'altération pendant vingt-quatre semaines afin de suivre les concentrations des terres rares dans les lixiviats. L'analyse des concentrations en terres rares et en métaux associés permet d'évaluer leurs taux élémentaires de lixiviation et d'estimer l'effet de chaque phase minérale sur le relargage des terres rares. Il a été aussi question de construire les courbes d'oxydation-neutralisation permettant de statuer sur la génération d'acidité à long terme des différents mélanges. L'interprétation des résultats géochimiques issus de ces essais a mis en évidence l'impact des carbonates, des phosphates et des oxy-hydroxydes de fer sur la mobilité des terres rares. Les carbonates, qui représentent les principales phases minérales dans les carbonatites de Montviel, et les phosphates souvent associés aux terres rares se dissolvent et lixivient du calcium en neutralisant l'acide généré par l'oxydation des sulfures. Par conséquent, le mélange des carbonates est non générateur de DMA alors que les mélanges de phosphates et d'oxy-hydroxydes de fer sont potentiellement générateurs de DMA. Les profils des concentrations des terres rares montrent que ce sont les carbonates qui sorbent le plus de terres rares, suivis des phosphates et des oxy-hydroxydes de fer. Ces résultats ont mis en évidence le fait que les lithologies de Montviel peuvent présenter un potentiel de rétention de terres rares par sorption, précipitation et co-précipitation qui pourraient être intéressant pour réduire la contamination des eaux de drainage.

La deuxième partie de ce chapitre consistait à évaluer les capacités de sorption des lithologies du dépôt Montviel. Les capacités de rétention ont été évaluées par des essais en cellules de sorption (mini-cellules d'altération modifiées) à partir des solutions synthétiques simulant celles issues des

cellules humides des différentes lithologies de Montviel. Les solutions de rinçages contenaient 1 mg/l de Ce avec un pH ajusté à 8 et une force ionique fixe (ajustée par du nitrate de sodium ($NaNO_3$) à 0.05 M). Les lithologies soumises aux essais de sorption à savoir les formation brêchiques, les calciocarbonatites, les ferrocarbonatites-LG, les ferrocarbonatites-HG et les silicocarbonatites. Cependant, les capacités maximales de sorption n'ont pas été atteintes, probablement à cause des faibles concentrations utilisées lors de ces essais. Par conséquent, la quantité de terres rares retenues est faible et il est difficile de statuer exactement sur les mécanisme géochimiques (sorption, précipitation et/ou co-précipitation) responsables de leur rétention, malgré l'utilisation des différents types de méthodes spectroscopiques (XPS et DRIFT) et cristallochimiques (XAFS) utilisées. Les extractions séquentielles montrent que la majorité des terres rares sorbées sont associées aux carbonates, un résultat cohérent avec les résultats minéralogiques par QEMSCAN.

8.1.3 Chapitres 4 et 5

Dans ces chapitres, les roches stériles et le minerai de Montviel ont été soumis à des essais en cellules humides, tandis qu'un concentré de terres rares du même minerai a été soumis à une mini-cellule d'altération. Le concentré de terres rares a été obtenu suite à une combinaison de plusieurs techniques gravimétriques (table à Mozley, concentrateur de Knelson, liqueur dense) et métallurgiques (flottation). Les concentrations obtenues dans les lixiviats issus de la mini-cellule d'altération sont supérieures à celles des cellules humides. Cela est dû principalement à une dissolution exagérée des phases porteuses de terres rares par la mini-cellules d'altération, et aux pourcentages des minéraux des terres rares dans le concentré, leur plus faible granulométrie et à leur plus grande teneur en sulfures. L'acidité générée par l'oxydation des sulfures provoque la dissolution des carbonates de terres rares. Dans les lithologies, les sulfures sont sous forme de traces (inférieurs à 1 %) tandis que les carbonates représentent plus que 60 % des échantillons. Par conséquent, le potentiel net de neutralisation est largement supérieur à 20 kg de mg $CaCO_3$/t. Ceci suggère que les lithologies ne sont pas potentiellement génératrices d'acide à long terme. Les résultats montrent que les carbonates de terres rares s'altèrent en contact avec les eaux de rinçages en lixiviant du Ca (2,87–5,75 mg/l), du Mg (0,38–0,83 mg/l), du Mn (0,008–0,02 mg/l), du Ba (0,25–0,49 mg/l), du F (0,22–0,33 mg/l), et des REE (0,0007–0,0014 mg/l), alors que les silicates s'altèrent plus lentement et constituent une source mineure de Si, de Al, de Ca, et de Fe dans les

lixiviats. Lors de ces essais, tous les éléments chimiques analysés ont respecté les exigences environnementales. Cependant, le barium a augmenté tout le long de la période des essais. Ceci suggère qu'en absence d'atténuation naturelle, il y a possibilité de formation d'un drainage neutre contaminé en Ba. Les faibles taux de lixiviation des terres rares peuvent être expliqués par leur rétention dans la phase solide une fois dissouts. En effet, les résultats de la modélisation géochimique montrent la possibilité de la précipitation de minéraux secondaires tels que les phosphates de terres rares et les oxy-hydroxydes de fer. En effet, les calculs d'équilibre thermodynamiques par PhreeqC montrent que la spéciation des terres rares est représentée essentiellement par les espèces suivantes : $REEF_3$, $REEPO_4$, $REEOH^{2+}$, $REE(OH)_3$, $REESO_4^+$, $REE_2(SO_4)_3$, $REE_2(CO_3)_3$ et $REECO_3^{2+}$. Ces essais cinétiques confirment que la mobilité des terres rares lourdes est plus importante que celle des terres légères et ce, en tenant compte de leurs teneurs dans les solides et leurs concentrations dans les lixiviats.

La combinaison des techniques de caractérisation suivi des essais cinétiques ont permis de mieux de comprendre le comportement géochimique des terres rares de Montviel. La dissolution des phases minérales lors de leur soumission aux essais cinétiques dépend de la réactivité, qui dépend à son tour du degré de libération des minéraux en question. Ce dernier a été mis en évidence via l'utilisation d'une étude minéralogique par QEMSCAN. Plus de 70 % des carbonates de terres rares sont libres et disponibles à la réaction lors des interactions. La proportion restante est associée avec des minéraux de gangue comme les silicates, les oxydes de fer et les sulfures. Les principaux minéraux porteurs des terres rares sont la carbocernaite, la burbankite, l'ancylite, l'apatite, la kukharenkoite, et la monazite, tandis que les minéraux de gangue sont principalement représentés par les silicates (quartz, albite, diopside, biotite, et chlorite), les carbonates (calcite, ankerite, sidérite, barytocalcite, et strontianite), les sulfates (célestine) et les sulfures en traces (pyrite, pyrrhotite, chalcopyrite, sphalérite et galène).

8.1.4 Chapitre 6

Le chapitre 6 présente le comportement géochimique des principales lithologies et du concentré du gisement de terres rares de Kipawa. Les échantillons ont fait l'objet d'une caractérisation minéralogique approfondie par QEMSCAN permettant de mieux comprendre les résultats géochimiques. L'analyse minéralogique montre que plus que 70 % des minéraux sont libres à la réaction. La fraction restante (30 %) est sous forme d'association ou d'inclusions avec les minéraux

de gangue (amphiboles et pyroxènes). Les observations QEMSCAN montrent aussi que les principaux minéraux porteurs de terres rares sont l'eudyalite, la mosandrite, la fluobritholite et l'apatite, etc.

Des échantillons composites représentant les différentes lithologies de Kipawa, ont été soumis à des essais en mini-cellules d'altération dans le but de mieux comprendre le comportement géochimique des roches stériles et d'un concentré de terres rares issu de minerai correspondant. La dissolution des minéraux de terres rares est responsable des concentrations en terres rares détectées dans les lixiviats (<15 µg/l, concentrations moyennes des mini-cellules). Par ailleurs, le concentré relargue comme attendu des concentrations plus importantes en terres rares par rapport aux lithologies. Ceci suggère que cette réponse géochimique élevée est conditionnée par la plus grande concentration des minéraux porteurs de terres rares et par la plus faible proportion des minéraux de gangue qui pourraient retenir les terres rares après leur lixiviation. Les sulfures, en particulier la pyrrhotite, se concentre avec les minéraux de terres rares lors de la séparation magnétique. Ceci pourrait aussi avoir un impact sur la signature géochimique en terres rares dans les lixiviats.

L'yttrium est l'élément le plus abondant dans les lixiviats issus des mini-cellules d'altération des matériaux du Kipawa. Le fer, le zinc, le plomb et le cuivre se présentent en très faibles concentrations dans les lixiviats. Le pH oscille autour de 7 et respecte les normes environnementales tout le long de la période des essais. Les concentrations en métaux et en terres rares diminuent au cours du temps pour se stabiliser après 4 à 5 semaines d'essais. Le pH proche de la neutralité favorise la précipitation de plusieurs minéraux secondaires comme les oxy-hydroxydes de fer, les phosphates et les argiles. Ceci réduit d'une façon significative la mobilité des terres rares une fois dissouts. Les lithologies présentent une composition minéralogique similaires à l'exception de la lithologie calcite riche qui est riche en calcite, pour laquelle le pH des lixiviats est alcalin (pH 8 - 9,5). Les lixiviats issus de la lithologie syénite (teneur la plus importante des REE dans les lithologies) engendrent les concentrations les plus élevées en terres rares par rapport aux autres lithologies.

8.1.5 Chapitre 7

Les travaux effectués dans les chapitres 3, 4, 5 et 6 ont permis de mieux comprendre le comportement géochimique des terres rares associées à deux types de gisements. L'objectif principal de ce chapitre est de mettre l'emphase sur les analyses des radionucléides, de comparer

les résultats des cellules humides en milieux percolés avec les essais de lixiviation batch en milieux fermés TCLP, SPLP et CTEU-9, d'évaluer l'effet d'échelle entre les essais de laboratoire et les essais du terrain dans le cas des matériaux de Montviel. Le chapitre 7 finit par proposer une approche d'entreposage innovante qui pourrait fournir les solutions nécessaires à une gestion durable des rejets miniers porteurs des terres rares. Les résultats montrent que les minéraux porteurs des terres rares sont associés aux éléments radioactifs Th, Ra, Nb, U. Pour Montviel, les isotopes radioactifs détectés dans les lixiviats issus des cellules humides sont le radium (Ra-226, et Ra-228) et l'uranium (U-234, U-235, et U-238), tandis que pour Kipawa, les isotopes radioactifs sont inférieurs à la limite de détection. Les résultats d'analyse indiquent des concentrations sous la limite recommandée par la Directive 019 et en respect avec les lignes directrices canadiennes pour la gestion des matières radioactives naturelles (MRN).

Les essais de lixiviation en batch, en particulier TCLP et SPLP, favorisent une dissolution exagérée des minéraux porteurs de terres rares et les éléments associés par rapport aux essais en cellules humides. Ceci peut être attribuable aux solutions d'extraction utilisées dans les essais de TCLP et SPLP (solutions acides) contrairement aux essais en cellules humides qui utilisent de l'eau déionisée. L'essai CTEU-9 est le seul essai de lixiviation qui présente des résultats similaires à ceux issus des cellules humides. Le F libéré par les essais de TCLP et SPLP est le seul élément qui dépasse la limite permise par les critères applicables en cas de contamination des eaux souterraines (critère aux fins de consommation).

L'analyse des données des résultats géochimiques issus des essais cinétiques (cellules humides) et des essais de lixiviation TCLP, SPLP, CTEU-9 par analyse en composante principale (ACP) permet de mettre en évidence les relations entre les différents paramètres géochimiques analysés. Les résultats de l'ACP montrent l'existence de cinq groupes distincts; groupe 1 composé de SO_4, Th, As, et F; groupe 2 contenant B; groupe 3 composé de REE, LREE, HREE, Cu, Zn, Pb, Fe, Ba, Mn; groupe 4 constitué de U, et groupe 5 représenté par pH. La corrélation négative avec le pH indique que la mise en solution des REE et d'autres éléments métalliques se fait principalement dans les conditions acides. La relation entre les terres rares et SO_4 signifie que l'oxydation des sulfures (SO_4 comme produit d'oxydation) pourrait être à l'origine de la lixiviation des REE.

La comparaison des taux de relargage des terres rares au laboratoire et sur le terrain confirme la présence d'un effet d'échelle. La lixiviation des terres rares est plusieurs ordres de grandeur

supérieure pour les essais *in situ*. Ceci peut être expliqué par l'augmentation de la dissolution des carbonates de REE causée par la température plus faible sur le terrain. Par conséquent, les taux d'oxydation des sulfures dans les barils de terrain vont être plus faibles et la dissolution des carbonates va être plus grande par rapport aux conditions de laboratoire. Le barium présente des concentrations d'un ordre de grandeur inférieures dans les lixiviats des essais *in situ* à cause de sa précipitation sous forme de barite causée par l'effet des pluies acides (teneur en sulfates inférieure à 10 mg/l dans l'eau de pluie) tel que suggéré par les calculs thermodynamiques.

La comparaison des résultats géochimiques (les concentrations moyennes) issus des cellules humides des carbonatites et des mini-cellules d'altération des silicates montre plusieurs ordres de grandeur supérieur pour les essais des silicates en mini-cellules d'altération. Cet écart est associé essentiellement à la différence entre les conditions de réalisation des deux essais (i.e. la granulométrie, ratio solide/liquide, la composition minéralogique) ainsi qu'au degré de libération des minéraux porteurs ou non REE. Cependant, la comparaison entre les résultats des deux concentrés (Montviel et Kipawa) issus des mini-cellules d'altération montrent que la réactivité des carbonates de terres rares est plus élevée que celle des silicates des terres rares.

Enfin, une approche d'entreposage des rejets du dépôt Montviel a été proposée afin d'assurer une gestion appropriée qui respecte l'environnement. La méthode suggérée préconise de mettre les matériaux de grande capacité de sorption et à faibles teneurs en contaminants à la base des aires d'accumulation qui vont servir comme filtre pour les effluents percolant à travers les rejets. Il est également proposé d'utiliser un traitement passif secour par des drains calcaires en utilisant les lithologies carbonatées avant que les effluents rejoignent le milieu naturel.

8.2 Recommandations

Des investigations supplémentaires seraient requises pour mieux comprendre certains aspects soulevés dans ce projet de doctorat. Des travaux supplémentaires de terrain (constructions de parcelles du terrain), de laboratoire (i.e. étude isotopique sur les essais en colonnes) et des simulations numériques par MIN3P, prenant compte les conditions hydrogéologiques de terrain, sont recommandés pour compléter l'évaluation du comportement environnemental des rejets miniers porteurs des REE. Voici quelques pistes permettant d'affiner la prédiction du comportement géochimique des rejets miniers porteurs des terres rares :

1) Les cellules expérimentales *in situ* sont recommandées pour valider les différents sénarios de restauration proposés durant cette thése et permettant d'assurer une gestion intégrée des rejets miniers porteurs des terres rares. Il sera également possible de mettre en évidence la pertinence de l'étude isotopique pour éclaircir les mécanismes géochimiques responsables de la rétention des terres rares dans les essais cinétiques de laboratoire et du terrain.
2) Pour les essais en colonnes, il pourrait aussi être avantageux de tester les différentes fractions granulométriques. Ceci permettrait de mieux statuer sur le comportement environnemental des roches stériles et des résidus de porteurs de REE.
3) Afin de mettre en évidence l'impact de la température et du ratio liquide/solide sur la dissolution des carbonates de REE, des essais en batch pourraient être intéressants à réaliser (les réactions de dissolution, les cinétiques des réactions et les concentrations des éléments). Les résultats de ces essais pourraient être utiles dans les simulations numériques par MIN3P pour prédire le comportement des rejets miniers de REE.
4) Pour évaluer les mécanismes géochimiques responsables du fractionnement des terres rares, il serait intéressant de réaliser des travaux des isotopes (Ce, La, Nd) sur les parcelles expérimentales du terrain.
5) Certains indicateurs de séquestration de carbone par les matériaux de Montviel ont été observés et méritent des investigations supplémentaires à l'image de ce qui a été fait sur les stériles de Royal Ni (Kandji, 2017; Pronost et al., 2011).
6) Pour valoriser tous les résultats de cratérisation chimique, physique, minéralogique, et les résultats géochimiques issus des différents essais statiques et cinétiques et les rendre à la disposition des décideurs, une application géoinformatique pourrait être prometteuse pour élaborer un modèle géo-environnemental englobant l'ensemble des résultats. Le modèle pourrait être flexible avec une interface interactive qui permettrait à l'utilisateur de choisir les paramètres (i.e. minéralogiques, géochimiques, physiques etc.) selon son choix afin de localiser les zones ayant des propriétés données. Les résultats du modèle pourraient fournir des réponses d'ordres minéralogiques et géochimiques nécessaires à une saine gestion des rejets miniers de carbonatites de Montviel. De plus, la visualisation en 3D des résultats pourrait aider à élaborer des pistes de solution afin de prévenir la génération d'un éventuel drainage contaminé et d'agir au bon moment, comme par exemple de séparer des lithologies ou de les entreposer selon une certaine disposition dans les haldes à stériles. Une version

préliminaire d'un tel modèle a été déjà réalisée dans le cadre de ce travail et sera améliorée avant de sa présentation officielle.

BIBLIOGRAPHIE

Adam, K., Kourtis, A., Gazea, B., and Kontopoulos, A. (1997). Evaluation of static tests used to predict the potential for acid drainage generation at sulfide mine sites. Trans. Instn.Min.Metall. sect.A:min.industry. 106. january-april: A1-A8.

Al-Abed, S. R., Jegadeesan, G., Purandare, J., and Allen, D. (2008). Leaching behavior of mineral processing waste: comparison of batch and column investigations. Journal of hazardous materials, 153(3), 1088-1092.

Al-Abed, S. R., Hageman, P. L., Jegadeesan, G., Madhavan, N., and Allen, D. (2006). Comparative evaluation of short-term leach tests for heavy metal release from mineral processing waste. The Science of the total environment, 364(1-3), 14-23.

Al-Harahsheh, M., and Kingman, S. (2004). Microwave-assisted leaching—a review. Hydrometallurgy, 73(3), 189-203.

Alex, P., Suri, A. K., and Gupta, C. K. (1998). Processing of xenotime concentrate. Hydrometallurgy, 50(3), 331-338.

Ali, S. H. (2014). Social and environmental impact of the rare earth industries. Resources, 3(1), 123-134.

Alkattan, M., Eric, H., Oelkers, J., and Schott, J. (1998). An experimental study of calcite and limestone dissolution rates as a function of pH from −1 to 3 and temperature from 25 to 80°C. Chemical Geology, vol. 151, no 1–4, p. 199-214.

Anawar, H. M. (2015). Sustainable rehabilitation of mining waste and acid mine drainage using geochemistry, mine type, mineralogy, texture, ore extraction and climate knowledge. Journal of Environmental Management, 158, 111-121.

Andersen, J C., Rollinson, G.K., Snook, B., Herrington, R., and Fairhurst, R.J. (2009). Use of QEMSCAN® for the characterization of Ni-rich and Ni-poor goethite in laterite ores. Minerals Engineering, vol. 22, no 13, p. 1119-1129.

Andrade, F.R.D., Möller, P., Lüders, V., Dulski, P. and Gilg, H.A., (1999). Hydrothermal rare earth elements mineralization in the Barra do Itapirapuã carbonatite, southern Brazil: behaviour of selected trace elements and stable isotopes (C, O). Chemical Geology, 155(1–2): 91-113.

Appelo, C.A.J., and Postma, D. (2005). Geochemistry, groundwater and pollution, Editor: A.A. Balkeman Publishers, 2nd edition.

Arvidson, S., Inci Evren, E., James, E., and Andreas, L. (2003). Variation in calcite dissolution rates: A fundamental problem. Geochimica et Cosmochimica Acta, vol. 67, no 9, p. 1623-1634.

Association minére du Canada (2015). Faits et chiffres de l'industrie miniére canadienne. http://mining.ca/sites/default/files/documents/Faits-et-chiffres-2015.pdf (accessed on October 14th, 2017).

Aubertin, M., and Bussiere, B. (2002). Environnement Minier Et Gestion Des Rejets Miniers. Presses Polytechnique Montreal.

Baral, S. S., Shekar, K. R., Sharma, M., and Rao, P. V. (2014). Optimization of leaching parameters for the extraction of rare earth metal using decision making method. Hydrometallurgy, 143, 60-67. doi:10.1016/j.hydromet.2014.01.006.

Barman, A. K., Varadachari, C., and Ghosh, K. (1992). Weathering of silicate minerals by organic acids. I. Nature of cation solubilisation. Geoderma, 53(1-2), 45-63.

Bassolé, M. (2016). Pertinence des essais de lixiviation en batch dans la prédiction du comportement hydrogéochimique des rejets miniers. Mémoire. Rouyn-Noranda, Université du Québec en Abitibi-Témiscamingue, Science appliquées, 238 p.

Bau, M., (1999). Scavenging of dissolved yttrium and rare earths by precipitating iron oxyhydroxide: experimental evidence for Ce oxidation, Y-Ho fractionation, and lanthanide tetrad effect. Geochimica et Cosmochimica Acta, 63(1): 67-77.

Belzile Solutions Inc., (2015). NI 43-101 Technical Report Montviel Rare Earth Project Québec, Canada (accessed on March 16th, 2017).

Bennett, J. W., Comarmond, M. J., and Jeffrey, J. (2000). Comparison of sulfidic oxidation rates measured in the laboratory and the field. Proceedings from the jh JCARD, Denver, 1, pp.171-180.

Bennett, P. C., Melcer, M. E., Siegel, D. I., and Hassett, J. P. (1988). The dissolution of quartz in dilute aqueous solutions of organic acids at 25°C. Geochimica et Cosmochimica Acta, vol. 52, no 6, p. 1521-1530.

Benzaazoua, M., Fiset, J. F., Bussière, B., Villeneuve, M., and Plante, B. (2006). Sludge recycling within cemented paste backfill: Study of the mechanical and leachability properties. Minerals Engineering, 19(5), 420-432.

Benzaazoua, M., Bussiére, B., Dagenais, A. M., and Archambault, M. (2004). Kinetic tests comparison and interpretation for prediction of the Joutel tailings acid generation potential. Environmental Geology, 46(8), 1086-1101. doi:10.1007/s00254-004-1113-1.

Bian, X., Yin, S.-h., Luo, Y., and Wu, W.Y. (2011). Leaching kinetics of bastnaesite concentrate in HCl solution. Transactions of Nonferrous Metals Society of China, 21(10), 2306-2310.

Bilal, E., Marciano, V., Marques, Correia Neves, J., Fuzikawa, K., Riffel, B. F., . . . Nasraoui, M. (1998). Altération hydrothermale des monazites-(Ce) des pegmatites du district de Santa Maria de Itabira (Minas Gerais, Brésil). Comptes Rendus de l'Académie des Sciences - Series IIA - Earth and Planetary Science, 326(10), 693-700.

Binnemans, K., Jones, P. T., Blanpain, B., Van Gerven, T., Yang, Y., Walton, A., and Buchert, M. (2013).. Recycling of rare earths: a critical review. Journal of Cleaner Production, 51: 1-22.

Blowes, D. W., Ptacek, C. J., Jambor, J. L., and Weisener, C. G. (2003). 9.05 - The Geochemistry of Acid Mine Drainage A2 - Turekian, Heinrich D. HollandKarl K Treatise on Geochemistry (pp. 149-204). Oxford: Pergamon.

Blowes, D.W., Ptacek, C.J., Jambor, J.L. and Weisener, C.G. (2003). Treatise on Geochemistry, pp. 149-204, Pergamon, Oxford.

Blowes, D., and Ptacek, C. (1994). Acid-neutralization mechanisms in inactive mine tailings. National Water Research Institute.

Bouzahzah, H., Benzaazoua, M., Plante, B., and Bussiere, B., (2015). A quantitative approach for the estimation of the “fizz rating” parameter in the acid-base accounting tests: A new adaptations of the Sobek test. Journal of Geochemical Exploration, 153: 53-65.

Bouzahzah, H., Benzaazoua, M., and Bussière, B. (2014). Prediction of Acid Mine Drainage: Importance of Mineralogy and the Test Protocols for Static and Kinetic Tests Mine Water and the Environment. Mine Water and the Environment", Mine Water and the Environment, 33:54–65.

Bouzahzah, H. (2013). Modification et amélioration des tests statiques et cinétiques pour une prédiction fiable du drainage minier acide (Doctoral dissertation, Université du Québec en Abitibi-Témiscamingue).

Brunauer, S., Emmett, P.H. and Teller, E. (1938). Adsorption of gases in multimolecular layers. Journal of the American chemical society, 60(2): 309-319.

Buckau, G., Artinger, R., Geyer, S., Wolf, M., Fritz, P., and Kim, J. I. (2000). Groundwater in-situ generation of aquatic humic and fulvic acids and the mineralization of sedimentary organic carbon. Applied Geochemistry, 15(6), 819-832.

Bussière, B. (2007). Colloquium 2004: Hydrogeotechnical properties of hard rock tailings from metal mines and emerging geoenvironmental disposal approaches. Canadian Geotechnical Journal, 44(9), 1019-1052. doi:10.1139/t07-040.

Bussière B., and Aubertin M. (1999). Clean tailings as cover material for preventing acid mine drainage: an *in situ* experiment. Conférence présentée au Sudbury '99 Mining and the Environment II, Sudbury, Ontario, 13–17 September 1999. Edited by N.B.D. Goldstack, P. Yearwood, and G. Hall. Vol. 1. pp: 19–28.

Calas, G. (2012). Elements. International Magazine of Mineralogy, Geochemistry, and Petrology, vol. 8, no ISSN: 1811-5209.

Catinat, M., (2010). Critical Raw Materials for the EU—Report of the Ad-Hoc Working Group on Defining Critical Raw Materials. EC, Brussels, Belgium.

CEAEQ. (2012). Protocole de lixiviation pour les espèces inorganiques, MA. 100 – Lix.com.1.1, Rév. 1. Ministère du Développement durable, de l'Environnement, de la Faune et des Parcs du Québec, 07(1), 1-17.

Censi, P., Saiano, F., Pisciotta, A. and Tuzzolino, N., (2014). Geochemical behaviour of rare earths in Vitis vinifera grafted onto different rootstocks and growing on several soils. Science of The Total Environment, 473–474: 597-608.

Chakhmouradian, A. R., Reguir, E. P., Zaitsev, A. N., Couëslan, C., Xu, C., Kynický, J., and Yang, P. (2017). Apatite in carbonatitic rocks: Compositional variation, zoning, element partitioning and petrogenetic significance. Lithos, 274-275: 188-213.

Chakhmouradian, A.R., Smith, M.P., and Kynicky, J., (2015). From "strategic" tungsten to "green" neodymium: A century of critical metals at a glance. Elsevier.

Chakhmouradian, A. R., and Wall, F. (2012). Rare Earth Elements: Minerals, Mines, Magnets (and More). Elements, 8(5), 333-340. doi:10.2113/gselements.8.5.333

Chakhmouradian, A. R., and Zaitsev, A. N. (2012). Rare Earth Mineralization in Igneous Rocks: Sources and Processes. Elements, 8(5), 347-353. doi:10.2113/gselements.8.5.347

Chen, L., Ma, T., Du, Y., and Xiao, C. (2017). Dissolved Rare Earth Elements of Different Waters in Qaidam Basin, Northwestern China. Procedia Earth and Planetary Science, 17, 61-64.

Chen, Y., Tian, Q., Chen, B., Shi, X., and Liao, T. (2011). Preparation of lithium carbonate from spodumene by a sodium carbonate autoclave process. Hydrometallurgy, 109(1–2), 43-46.

Chen, Z. (2011). Global rare earth resources and scenarios of future rare earth industry. Journal of Rare Earths, 29(1), 1-6.

Cheng, Z., Jiang, J., Fajardo, O., Wang, S., and Hao, J. (2013). Characteristics and health impacts of particulate matter pollution in China (2001–2011). Atmospheric Environment, 65(0), 186-194.

Cheng. Z. (2011). Global rare earth resources and scenarios of future rare earth industry. Journal of Rare Earths, vol. 29, no 1, p. 1-6.

Chang, Hongtao, Mei Li, Zhaogang Liu, Yanhong Hu et Fushun Zhang. (2010). Study on separation of rare earth elements in complex system. Journal of Rare Earths, vol. 28, Supplement 1, no 0, p. 116-119.

Cherifa, A. B., Rogez, J., Jemal, M., and CMathieu, J. (2000). Dissolution de l'hydroxyapatite et du phosphate tricalcique β dans les solutions d'acide nitrique. Journal of Thermal Analysis and Calorimetry, 63, 689–697.

Chou, L., Garrels, R.M., and Wollast, R., (1989). Comparative study of the kinetics and mechanisms of dissolution of carbonate minerals. Chemical Geology, 78(3-4): 269-282.

Coto, B., C. Martos, J. L. Peña, R. Rodríguez et G. Pastor. (2012). Effects in the solubility of CaCO3: Experimental study and model description. Fluid Phase Equilibria, vol. 324, no 0, p. 1-7.

County, S.B. (2004). Final Environmental Impact Report for Molycorp, Inc. Mountain Pass Mine 30-year Plan, ENSR International. Department, S.B.C.L.U.S., Molycorp, I., Development, S.B.C.E. and Group, P.S.

Cox, C. and Kynicky, J. (2017). The rapid evolution of speculative investment in the REE market before, during, and after the rare earth crisis of 2010–2012. The Extractive Industries and Society.

Dai, S., Panpan, X., Shaohui, J., Colin, W., James, C., Xiaoyun, Y., David, F. (2017). Enrichment of U-Re-V-Cr-Se and rare earth elements in the Late Permian coals of the Moxinpo Coalfield, Chongqing, China: Genetic implications from geochemical and mineralogical data. Ore Geology Reviews, vol. 80, p. 1-17.

Das, N., and Das, D. (2013). Recovery of rare earth metals through biosorption: An overview. Journal of Rare Earths, 31(10), 933-943.

David, J., Dion, C., Goutier, J., Roy, P., Bandyayera, D., Legault, M., and Rhéaume, P. (2006). Datations U-Pb effectuées dans la Sous-province de l'Abitibi à la suite des travaux de 2004-2005. Ressources naturelles et Faune. RP 2006-04, Quebéc- Canada.

David, R. (2000). LIDE (ed.),"CRC Handbook of Chemistry and Physics": CRC Press LLC, Inc. USA.

Davris, P., Stopic, S., Balomenos, E., Panias, D., Paspaliaris, I., and Friedrich, B. (2017). Leaching of rare earth elements from eudialyte concentrate by suppressing silica gel formation. Minerals Engineering, 108, 115-122.

Day, S., Sexsmith, K., MacGregor, D., Mehling, P., Shaw, S., and Kestler, U. (2005). Cold temperature effects on geochemical weathering. Proceedings from the 1 jh an nuai British Columbia-MEND MLIARD workshop, Challenges in the prediction of drainage chemistry. Vancouver, British Columbia, Canada.

Dehaine, Q. and Filippov, L.O. (2015). Rare earth (La, Ce, Nd) and rare metals (Sn, Nb, W) as by-product of kaolin production, Cornwall: Part1: Selection and characterisation of the valuable stream. Minerals Engineering, 76: 141-153.

Delgado, J., Pérez-López, R., Galván, L., Nieto, J. M., and Boski, T. (2012). Enrichment of rare earth elements as environmental tracers of contamination by acid mine drainage in salt marshes: A new perspective. Marine Pollution Bulletin, 64(9), 1799-1808.

Demers I., Bussière B., Aachib M. et Aubertin M. (2011). Repeatability evaluation of instrumented column tests in cover efficiency evaluation for the prevention of acid mine drainage. Water, Air, and Soil Pollution 219, pp : 113-128.

Demers, I., Bouda, M., Mbonimpa, M., Benzaazoua, M., Bois, D., and Gagnon, M. (2015). Valorization of acid mine drainage treatment sludge as remediation component to control acid generation from mine wastes, part 2: Field experimentation. Minerals Engineering, 76, 117-125.

Desharnais, G., and Duplessis, C. (2011). Montviel core zone REE mineral resource estimate technical report, Quebec. Geomega Resources Inc. Member of SGS group (SGS SA).

Dibbs, H. P. (1972). The determination of the zeta potential of minerals. Information Canada.

Ding, R., and WooD, S. A. (2002). The aqueous geochemistry of the rare earth elements and yttrium. Part X. Potentiometric determination of stability constants of acetate complexes of La^{3+}, Nd^{3+}, $Gd^{3+}$and Yb^{3+} at 25–70 C and 1 bar. Water-Rock Interactions, Ore Deposits, and Environmental Geochemistry: A Tribute to David A. Crerar, The Geochemical Society Special Publication No, 7.

Dorozhkin, S. V. (2002). A review on the dissolution models of calcium apatites. Progress in Crystal Growth and Characterization of Materials, 44(1), 45-61.

Duzgoren-Aydin, N. S., and Aydin, A. (2009). Distribution of rare earth elements and oxyhydroxide phases within a weathered felsic igneous profile in Hong Kong. Journal of Asian Earth Sciences, 34(1), 1-9.

Edahbi, M., Plante. B., Benzaazoua. M., and Pelletier. M. (2018). Geochemistry of rare earth elements within waste rocks from the Montviel carbonatite deposit, Québec, Canada. Environmental Science and Pollution Research DOI: 10.1007/s11356-018-1309-7.

Edahbi, M., Benzaazoua, M., Plante, B., Doire, S. and Kormos, L., (2017). Mineralogical characterization using QEMSCAN® and leaching potential study of REE within silicate ores: A case study of the Matamec project, Québec, Canada. Journal of Geochemical Exploration.

Edahbi, M., Plante, B., Bouzahzah, H., Benzaazoua, M., and Plettier.M. (2015). Mineralogical and geochemical study of rare earth elements from a carbonatite deposit. Proceedings of the 13th SGA biennial meeting, Nancy, France, 24-27 août 2015.

Einsele, G. (2013). Sedimentary basins: evolution, facies, and sediment budget: Springer Science and Business Media.

Elzinga, E. J., R. J. Reeder, S. H. Withers, R. E. Peale, R. A. Mason, K. M. Beck and Hess. W. P. (2002). EXAFS study of rare-earth element coordination in calcite. Geochimica et Cosmochimica Acta, vol. 66, no 16, p. 2875-2885.

Erguler, Z. A., and Erguler, G. (2015). The effect of particle size on acid mine drainage generation: Kinetic column tests. Minerals Engineering, 76, 154-167.

Feng, C., Bi, X., Liu, S., and Hu, R. (2014). Fluid inclusion, rare earth element geochemistry, and isotopic characteristics of the eastern ore zone of the Baiyangping polymetallic Ore district, northwestern Yunnan Province, China. Journal of Asian Earth Sciences, 85(0), 140-153.

Fernández-Caliani, J. C., Barba-Brioso, C., and De la Rosa, J. D. (2009). Mobility and speciation of rare earth elements in acid minesoils and geochemical implications for river waters in the southwestern Iberian margin. Geoderma, 149(3–4), 393-401.

Filippov, L.O., Dehaine, Q., and Filippova, I.V., (2016). Rare earths (La, Ce, Nd) and rare metals (Sn, Nb, W) as by-products of kaolin production – Part 3: Processing of fines using gravity and flotation. Minerals Engineering, 95: 96-106.

Firsching, F. H., and Kell, J. C. (1993). The solubility of the rare-earth-metal phosphates in sea water. Journal of Chemical and Engineering Data, 38(1), 132-133.

Firsching, F. H., and Mohammadzadei, J. (1986). Solubility products of the rare-earth carbonates. Journal of Chemical and Engineering Data, 31(1), 40-42.

Franchi, F., Hofmann, A., Cavalazzi, B., Wilson, A., and Barbieri, R. (2015). Differentiating marine vs hydrothermal processes in Devonian carbonatemounds using rare earth elements (Kess Kess mounds, Anti-Atlas, Morocco). Chemical Geology, 409, 69-86.

Free, M. L. (2014). Chapter 2.8 - Biohydrometallurgy A2 - Seetharaman, Seshadri Treatise on Process Metallurgy (pp. 983-993). Boston: Elsevier.

Frostad, S., Klein, B., and Lawrence, R. W. (2005). Determining the weathering characteristics of a waste dump with field tests. International Journal of Surface Mining, Reclamation and Environment 19, 132-143.

Ganor, J., Lu, P., Zheng, Z., and Zhu, C. (2007). Bridging the gap between laboratory measurements and field estimations of silicate weathering using simple calculations.Environmental Geology 53, 599-610.

Gence, N., and Ozbay, N. (2006). pH dependence of electrokinetic behavior of dolomite and magnesite in aqueous electrolyte solutions. Applied surface science, 252(23), 8057-8061.

Gibert, B. (2012). Ressources minérales et matériaux pour l'énergie. Laboratoire Géosciences Montpellier-Bât.22 - 2eme étage, France.

Gimeno Serrano MaJ., Auqué Sanz LF., and Nordstrom D.K. (2000). REE speciation in low-temperature acidic waters and the competitive effects of aluminum. Chemical Geology 165:167-180.

González, V. (2015). Lanthanide ecotoxicity: First attempt to measure environmental risk for aquatic organisms. Environmental Pollution 199(Supplement C): 139-147.

Gonzalez, V., Vignati, D. A. L., Leyval, C., and Giamberini, L. (2014). Environmental fate and ecotoxicity of lanthanides: Are they a uniform group beyond chemistry? Environment International, 71(0), 148-157.

Goodall, R., Peter, J., and Alan, R. (2005). The use of QEMSCAN® and diagnostic leaching in the characterisation of visible gold in complex ores. Minerals Engineering, vol. 18, no 8, p. 877-886.

Goutier, J. (2006). Géologie de la région du lac au Goéland (32F/15): Ressources naturelles et Faune, Québec.

Goyne, K. W., Brantley, S. L., and Chorover, J. (2010). Rare earth element release from phosphate minerals in the presence of organic acids. Chemical Geology, 278(1–2), 1-14.

Goutier, J., (2006). Géologie de la région du lac au Goéland (32F/15). Ressources naturelles et Faune, Québec: Ville de Québec, QC, Canada.

Gruber, C., Kutuzov, I., and Ganor, J. (2016). The combined effect of temperature and pH on albite dissolution rate under far-from-equilibrium conditions. Geochimica et Cosmochimica Acta, 186, 154-167.

Gschneidner, A., Jean-Claude, and Vitalij, G. (2006). Handbook on the Physics and Chemistry of Rare Earths. vol. 36, p. 521.

Gu ,X, and Evans, L. (2007) Modelling the adsorption of Cd(II), Cu(II), Ni(II), Pb(II), and Zn(II) onto Fithian illite. J Coll Interf Sei 307: 317-325.

Gupta, C. K., and Krishnamurthy, N. (1992). Extractive metallurgy of rare earths. International Materials Review, 37(5), 197–248.

Guy, C., Daux. V., and Schott. J. 1999. Behaviour of rare earth elements during seawater/basalt interactions in the Mururoa Massif. Chemical Geology, vol. 158, no 1–2, p. 21-35.

Hanson, S. L., Simmons, W. B., Webber, K. L., and Falster, A. U. (1992). Rare-earth-element mineralogy of granitic pegmatites in the Trout Creek Pass District, Chaffee County, Colorado. The Canadian Mineralogist, 30(3), 673-686.

Hao, Z., Yonghua, L., Hairong, L., Binggan, W., Xiaoyong, L., Tao, L., and Jiangping, Y. (2015). Levels of rare earth elements, heavy metals and uranium in a population living in Baiyun Obo, Inner Mongolia, China: A pilot study. Chemosphere, vol. 128, p. 161-170.

Hellmann. R., and Scott A. (2002). Water-Rock Interactions, Ore Deposits, and Environmental Geochemistry A Tribute to David A. Crerar. The geochemical society. Special publication N°.7.

Herrmann, H., Nolde, J., Berger, S., and Heise, S. (2016). Aquatic ecotoxicity of lanthanum – A review and an attempt to derive water and sediment quality criteria. Ecotoxicology and Environmental Safety, 124, 213-238.

Hierro, A., Bolivar, J.P., Vaca, F., and Borrego, J. (2012). Behavior of natural radionuclides in surficial sediments from an estuary impacted by acid mine discharge and industrial effluents in Southwest Spain. Journal of Environmental Radioactivity 110, 13-23.

Hong, F. (2006). Rare Earth: Production, Trade and Demand. Journal of Iron and Steel Research, International, vol. 13, p. 33-38.

Hooper, K. I. M. (1998). TCLP fails to extract oxoanion-forming elements that are extracted by municipal solid waste leachates.

Huang, X., Deng, H., Zheng, C., and Cao, G. (2016). Hydrogeochemical signatures and evolution of groundwater impacted by the Bayan Obo tailing pond in northwest China. Science of the total environment, 543, 357-372.

Humphries, M., (2013). Rare Earth Elements: The Global Supply Chain. Congressional Research Service, 7-5700 (http://www.fas. org/sgp/crs/natsec/R41347.pdf) (accessed on August 16th, 2017).

Hurst, C., (2010). China's rare earth elements industry: What can the west learn?, Institute for the Analysis of Global Security Washington DC.

Inguaggiato, C., Censi, P., Zuddas, P., Londoño, J. M., Chacón, Z., Alzate, D., . . . D'Alessandro, W. (2015). Geochemistry of REE, Zr and Hf in a wide range of pH and water composition: The Nevado del Ruiz volcano-hydrothermal system (Colombia). Chemical Geology, 417, 125-133.

Ippolito, N. M., Innocenzi, V., De Michelis, I., Medici, F., and Vegliò, F. (2017). Rare earth elements recovery from fluorescent lamps: A new thermal pretreatment to improve the efficiency of the hydrometallurgical process. Journal of Cleaner Production, 153, 287-298.

Jaireth, S., Hoatson, D. M., and Miezitis, Y. (2014). Geological setting and resources of the major rare-earth-element deposits in Australia. Ore Geology Reviews, 62(0), 72-128.

Janssen, R. P. T., and Verweij, W. (2003). Geochemistry of some rare earth elements in groundwater, Vierlingsbeek, The Netherlands. Water Research, 37(6), 1320-1350.

Jia, Y. Q. (1991). Crystal radii and effective ionic radii of the rare earth ions. Journal of Solid State Chemistry, vol. 95, no 1, p. 184-187.

Jiang, S.-Y., Yu, J.-M., and Lu, J.-J. (2004). Trace and rare-earth element geochemistry in tourmaline and cassiterite from the Yunlong tin deposit, Yunnan, China: implication for migmatitic–hydrothermal fluid evolution and ore genesis. Chemical Geology, 209(3–4), 193-213.

Johannesson, K.H, Lyons, W.B, Yelken, M.A, Gaudette, H.E., Stetzenbach, K.J. (1996) Geochemistry of the rare-earth elements in hypersaline and dilute acidic natural terrestrial waters: complexation behavior and middle rare-earth element enrichments. Chem Geol 133(1-4):125–144.

Jordens, A., Marion, C., Grammatikopoulos, T. and Waters, K.E., (2016). Understanding the effect of mineralogy on muscovite flotation using QEMSCAN. International Journal of Mineral Processing, 155: 6-12.

Jordens, A., Sheridan, R.S., Rowson, N.A. and Waters, K.E., (2014). Processing a rare earth mineral deposit using gravity and magnetic separation. Minerals Engineering, 62(0): 9-18.

Jorjani, E., Bagherieh, A. H., Mesroghli, S., and Chelgani, S. C. (2008). Prediction of yttrium, lanthanum, cerium, and neodymium leaching recovery from apatite concentrate using artificial neural networks. Journal of University of Science and Technology Beijing, Mineral, Metallurgy, Material, 15(4), 367-374.

Kanazawa, Y., and Kamitani, M. (2006). Rare earth minerals and resources in the world. Journal of Alloys and Compounds, 408–412(0), 1339-1343.

Kandji, E. H. B. (2017). Kinetic testing to evaluate the mineral carbonation and metal leaching potential of ultramafic tailings: Case study of the Dumont Nickel Project, Amos, Québec. Applied Geochemistry 84(Supplement C): 262-276.

Kato, Y., Fujinaga, K., Nakamura, K., Takaya, Y., Kitamura, K., Ohta, J., Iwamori, H. (2011). Deep-sea mud in the Pacific Ocean as a potential resource for rare-earth elements. Nature Geoscience, 4(8), 535-539. doi:10.1038/ngeo1185

Knidiri, J. (2015). Évaluation de l'effet de la pente sur le comportement hydrogéologique d'un recouvrement alternatif de type stockage-relargage constitué de rejets calcaires phosphatés en climat aride (Doctoral dissertation, École Polytechnique de Montréal).

Knutson, H.-K., Max-Hansen, M., Jönsson, C., Borg, N., and Nilsson, B. (2014). Experimental productivity rate optimization of rare earth element separation through preparative solid phase extraction chromatography. Journal of Chromatography A, 1348(0), 47-51.

Kodama, H., and Schnitzer, M. (1973). Dissolution of chlorite minerals by fulvic acid. Canadian Journal of Soil Science, 53(2), 240-243.

Koriko, M., Tchangbedji, G., Baba, G., Kili, A. K., and Gnandi, K. (2007). Effets de l'acidité et de la nature de l'acide sur la dissolution du phosphate naturel de Hahotoé-Kpogamé (Togo) par quelques acides conventionnels. Comptes Rendus Chimie, 10(6), 529-534.

Kwitko-Ribeiro, R. (2012). New sample preparation developments to minimize mineral segregation in process mineralogy. Paper presented at the Proceedings of the 10th International Congress for Applied Mineralogy (ICAM).

Kynicky, J., Smith, M.P. and Xu, C., (2012). Diversity of rare earth deposits: the key example of China. Elements, 8(5): 361-367.

Lackovic, J. A., Nikolaidis, N. P., Chheda, P., Carley, R. J., and Patton, E. (1997). Evaluation of batch leaching procedures for estimating metal mobility in glaciated soils (pp. 231-240).

Lappako, K. A. (1994). Evaluation of neutralization potential determinations for metal mine waste and a proposed alternative. International Land Reclamation and Mine Drainage Conference and the Third International Conference on the Abatement of Acidic Drainage. Pittsburg, USA.

Lawrence, R. and Wang, Y., (1996). Determination of neutralization potential for acid rock drainage prediction. MEND project, 1(3): 38.

Leal Filho, W., (2016). An Analysis of the Environmental Impacts of the Exploitation of Rare Earth Metals, Rare Earths Industry-Chapter 17, Elsevier, Boston, pp. 269-277.

Le Bouffant, L., Daniel, H., Martin, J. C., and BruyÈRe, S. (1982). Effect of impurities and associated minerals on quartz toxicity. The Annals of Occupational Hygiene, 26(5), 625-634.

Lee, J., Kim, D., Lee, S., and Kim, H. (2012). Effect of rare-earth elements on the plasma etching behavior of the RE–Si–Al–O glasses. Journal of Non-Crystalline Solids, 358(5), 898-902.

Lema. I.B., and Leal Filho,W. (2016). Rare earth industry, Technological, Economic, and environnemental Implications.

Lammers, K., Smith, M. M., and Carroll, S. A. (2017). Muscovite dissolution kinetics as a function of pH at elevated temperature. Chemical Geology.

Lévesque Michaud, M. (2016). Développement d'une méthode de prédiction cinétique du drainage neutre contaminé avec agent complexant : application au projet minier blackrock. Mémoire de maitrise. rouyn-noranda, université du Québec en Abitibi-Témiscamingue, science appliquées, 238 p.

Lewis, A. E., Hugo, A. (2000). Characterization and batch testing of a secondary lead slag. (October), 365-370.

Leybourne, M. I., Goodfellow, W. D., Boyle, D. R., and Hall, G. M. (2000). Rapid development of negative Ce anomalies in surface waters and contrasting REE patterns in groundwaters associated with Zn–Pb massive sulphide deposits. Applied Geochemistry, 15(6), 695-723.

Li, D. (2017). A review on yttrium solvent extraction chemistry and separation process. Journal of Rare Earths, 35(2), 107-119.

Li, J., and Duan, Z. (2011). A thermodynamic model for the prediction of phase equilibria and speciation in the H2O–CO2–NaCl–CaCO3–CaSO4 system from 0 to 250°C, 1 to 1000 bar with NaCl concentrations up to halite saturation. Geochimica et Cosmochimica Acta, 75(15), 4351-4376.

Li, L., Li, H., Wang, D., and Zhang, C. (2009). Trace Elements and Rare Earth Elements Geochemistry and Its Metallogenic Significance for Cu-Zn Ore Deposits in Tongbai Area, Henan Province, China. Earth Science Frontiers, 16(6), 325-336.

Li, X., Chen, Z., Chen, Z., and Zhang, Y. (2013). A human health risk assessment of rare earth elements in soil and vegetables from a mining area in Fujian Province, Southeast China. Chemosphere, 93(6), 1240-1246.

Lin, F., and Charles, V. (1981). The dissolution kinetics of brucite, antigorite, talc, and phlogopite at room temperature and pressure. American Mineralogist, vol. 66, no 7-8, p. 801-806.

Lingawi, H., Barbour, M., Lynch, R., and Anderson, P. (2011). Effect of Zinc Ions (zn2+) on Hydroxyapatite Dissolution Kinetics Studied Using Scanning Microradiography. Caries Research, 45(2), 195.

Linnen, R. L., Samson, I. M., Williams-Jones, A. E., and Chakhmouradian, A. R. (2014). 13.21 - Geochemistry of the Rare-Earth Element, Nb, Ta, Hf, and Zr Deposits. In H. D. Holland and K. K. Turekian (Eds.), Treatise on Geochemistry (Second Edition) (pp. 543-568). Oxford: Elsevier.

Lim, H., Ibana, D., and Eksteen, J. (2016). Leaching of rare earths from fine-grained zirconosilicate ore. Journal of Rare Earths, 34(9), 908-916.

Lipin, B.R, and Mackay, G.A. (1989). Geochemistry and mineralogy of rare earth elements. Mineralogical society of America, volume 21.

Lisboa, J. V., de Oliveira, D. P. S., Rocha, F., Oliveira, A., and Carvalho, J. (2015). Patterns of rare earth and other trace elements in Paleogene and Miocene clayey sediments from the Mondego platform (Central Portugal). Chemie der Erde - Geochemistry, 75(3), 389-401.

Liu, H., Guo, H., Xing, L., Zhan, Y., Li, F., Shao, J., and Li, C. (2016). Geochemical behaviors of rare earth elements in groundwater along a flow path in the North China Plain. Journal of Asian Earth Sciences, 117, 33-51.

Liu, H., Zhang, S., Pan, D., Tian, J., Yang, M., Wu, M., and Volinsky, A. A. (2014). Rare earth elements recycling from waste phosphor by dual hydrochloric acid dissolution. Journal of Hazardous Materials, 272, 96-101.

Mackay, D. A. R., Simandl, G. J., Ma, W., Redfearn, M., and Gravel, J. (2016). Indicator mineral-based exploration for carbonatites and related specialty metal deposits — A QEMSCAN® orientation survey, British Columbia, Canada. Journal of Geochemical Exploration, 165, 159-173.

McLellan, B. C., Corder, G. D., Golev, A., and Ali, S. H. (2014). Sustainability of the Rare Earths Industry. Procedia Environmental Sciences, 20, 280-287.

Malmström, M. E., Destouni, G., Banwart, S. A., et Strömberg, B. H. E. (2000). Resolving the scale-dependence of mineral weathering rates. Environmental Science and Technology 34, 1375-1378.

Manuela Vinha G. Silva, M., M.S. Cabral Pinto, M., and Carvalho, P. C. S. (2016). Major, trace and REE geochemistry of recent sediments from lower Catumbela River (Angola). Journal of African Earth Sciences, 115, 203-217.

Mariano, A.N. and Mariano, A., (2012). Rare Earth Mining and Exploration in North America. Elements, 8(5): 369-376.

Massari, S. and Ruberti, M., (2013). Rare earth elements as critical raw materials: Focus on international markets and future strategies. Resources Policy, 38(1): 36-43.

Mayfield, D. B., and Fairbrother, A. (2014). Examination of rare earth element concentration patterns in freshwater fish tissues. Chemosphere, 120(0), 68-74.

Mbonimpa M., Aubertin M., Aachib M., and Bussière B. (2003). Diffusion and consumption of oxygen in unsaturated cover materials. Canadian Geotechnical Journal 40(5), pp: 916-932.

McLellan, B. C., Corder, G. D., Golev, A., and Ali, S. H. (2014). Sustainability of the Rare Earths Industry. Procedia Environmental Sciences, 20(0), 280-287.

Medas, D., Cidu, R., De Giudici, G., and Podda, F. (2013). Geochemistry of rare earth elements in water and solid materials at abandoned mines in SW Sardinia (Italy). Journal of Geochemical Exploration, 133, 149-159.

Merkus, H. G. (2009). Particle size measurements: fundamentals, practice, quality (Vol. 17): Springer Science and Business Media.

Miekeley, N., Coutinho de Jesus, H., Porto da Silveira, C. L., Linsalata, P., and Morse, R. (1992). Rare-earth elements in groundwaters from the Osamu Utsumi mine and Morro do Ferro analogue study sites, Poços de Caldas, Brazil. Journal of Geochemical Exploration, 45(1), 365-387.

Mihajlovic, Stärk, J., H.-J., and Rinklebe. J. (2017). Rare earth elements and their release dynamics under pre-definite redox conditions in a floodplain soil. Chemosphere 181:313-319.

Miller, R. R., Heaman, L. M., and Birkett, T. C. (1997). U□Pb zircon age of the Strange Lake peralkaline complex: implications for Mesoproterozoic peralkaline magmatism in north-central Labrador. Precambrian Research, 81(1–2), 67-82.

Miretzky, P., and Fernandez-Cirelli, A. (2008). Phosphates for Pb immobilization in soils: a review. Environmental Chemistry Letters, 6(3), 121-133.

Moldoveanu, G. A., and Papangelakis, V. G. (2013). Recovery of rare earth elements adsorbed on clay minerals: II. Leaching with ammonium sulfate. Hydrometallurgy, 131–132(0), 158-166.

Moncur, M. C., Ptacek, C. J., Blowes, D. W., and Jambor, J. L. (2005). Release, transport and attenuation of metals from an old tailings impoundment. Applied Geochemistry, 20(3), 639-659.

Morse, J.W. and Arvidson, R.S., (2002). The dissolution kinetics of major sedimentary carbonate minerals. Earth-Science Reviews, 58(1): 51-84.

Morse, J.W., Arvidson, R.S. and Lüttge, A., (2007). Calcium carbonate formation and dissolution. Chemical reviews, 107(2): 342-381.

Nadeau, O., Stevenson, R. and Jébrak, M., (2016). Evolution of Montviel alkaline-carbonatite complex by coupled fractional crystallization, fluid mixing and metasomatism — Part II: Trace element and Sm–Nd isotope geochemistry of metasomatic rocks: implications for REE-Nb mineralization. Ore Geology Reviews, 72, Part 1: 1163-1173.

Nadeau, O., Cayer, A., Pelletier, M., Stevenson, R. and Jébrak, M., (2015). The Paleoproterozoic Montviel carbonatite-hosted REE–Nb deposit, Abitibi, Canada: Geology, mineralogy, geochemistry and genesis. Ore Geology Reviews, 67: 314-335.

Nadeau, O., Cayer, A., Pelletier, M., Séguin, D., Stevenson, R., and Jébrak, M. (2014). Pétrométallogenèse du système alcalin carbonatitique (ETR-Nb) de Montviel, Abitibi. Conférences, séance 12.

Nadeau, O., Stevenson, R., and Jébrak, M. (2014). The Archean magmatic-hydrothermal system of Lac Shortt (Au-REE), Abitibi, Canada: Insights from carbonate fingerprinting. Chemical Geology, 387, 144-156.

Nicolas-Alonso, L. F., and Gomez-Gil, J. (2012). Brain computer interfaces, a review. Sensors, 12(2), 1211-1279.

Nicholson, R. V. (1994). Iron-sulfide oxidation mechanisms: laboratory studies. Dans The Environmental Geochemistry of Sulfide Mine-wastes (eds. J. L. Jambor and D. W. Blowes). Mineralogical Association of Canada, Nepean, ON, vol.22, pp.l64-183.

Nicholson, R. V., Gillham, R. W., Cherry, J. A., and Reardon, E. J. (1988). Pyrite oxidation in carbonate-buffered solutions: 1. Experimental kinetics. Geochimica Cosmochimica Acta 52, 1077-1085 Nieto, A., Guelly, K., and Kleit, A. (2013). Addressing criticality for rare earth elements in petroleum refining: The key supply factors approach. Resources Policy, 38(4), 496-503.

Nordstrom, K. D. (2012). Models, validation, and applied geochemistry: Issues in science, communication, and philosophy. Applied Geochemistry, 27(10), 1899-1919.

Oelkers, E. H., and Poitrasson, F. (2002). An experimental study of the dissolution stoichiometry and rates of a natural monazite as a function of temperature from 50 to 230 °C and pH from 1.5 to 10. Chemical Geology, 191, 73 – 87.

Oral, R., Pagano, G., Siciliano, A., Gravina, M., Palumbo, A., Castellano, I., Trifuoggi, M. (2017). Heavy rare earth elements affect early life stages in Paracentrotus lividus and Arbacia lixula sea urchins. Environmental Research, 154, 240-246.

Orris, G. J., and Grauch, R. I. (2002). Rare Earth Element Mine,Deposits, and Occurences. USGC (Science for a changing world).

Özverd. İ, A., and Erdem, M. (2010). Environmental risk assessment and stabilization /solidification of zinc extraction residue: I. Environmental risk assessment. Hydrometallurgy, 100(3-4), 103-109.

Panda, R., Kumari, A., Jha, M. K., Hait, J., Kumar, V., Rajesh Kumar, J., and Lee, J. Y. (2014). Leaching of rare earth metals (REMs) from Korean monazite concentrate. Journal of Industrial and Engineering Chemistry, 20(4), 2035-2042.

Parkhurst, D. L., and Appelo, C. (2013). Description of input and examples for PHREEQC version 3: a computer program for speciation, batch-reaction, one-dimensional transport, and inverse geochemical calculations (2328-7055).

Peelman, S., Zhi, H. I., Sun, Ji, J., Yongxiang, Y. (2016). Leaching of Rare Earth Elements: Review of Past and Present Technologies A2 - Lima, Ismar Borges De. In Rare Earths Industry, Walter Leal Filho, chapter 21 -, p. 319-334. Boston: Elsevier.

Pecht, M., Kaczmarek, R., Song, X., Hazelwood, D., Kavetsky, R., and Anand, D. (2011). Rare Earth Material: Insights and Concerns. CALCE EPSC Press, University of Maryland, College Park, MD.

Peng, C., Crawshaw, J. P., Maitland, G. C., & Trusler, J. M. (2015). Kinetics of calcite dissolution in CO2-saturated water at temperatures between (323 and 373) K and pressures up to 13.8 MPa. Chemical Geology, 403, 74-85.

Pepin, G. (2009). Évaluation du comportement géochimique de stériles potentiellement générateurs de drainage neutre contaminé à l'aide de cellules expérimentales *in situ*". Mémoire de maîtrise, Département des génies civil, géologique et des mines. École Polytechnique de Montréal, Montreal, Québec, Canada.

Pingitore, N., Clague, J., and Gorski, D. (2014). Round Top Mountain rhyolite (Texas, USA), a massive, unique Y-bearing-fluorite-hosted heavy rare earth element (HREE) deposit. Journal of Rare Earths, 32(1), 90-96.

Plante, B., Bussière, B., and Benzaazoua, M. (2014). Lab to field scale effects on contaminated neutral drainage prediction from the Tio mine waste rocks. Journal of Geochemical Exploration, 137, 37--47. http://doi.org/10.1016/j.gexplo.2013.11.004.

Plante, B., Benzaazoua, M. and Bussière, B. (2011). Predicting geochemical behaviour of waste rock with low acid generating potential using laboratory kinetic tests. Mine Water and the Environment, 30(1): 2-21.

Plante, B., Bussiére, B., Bouzahzah, H., Benzaazoua, M., Demers, I., Kandji, B., and Cassista, M. A. (2015). Revue de littérature en vue de la mise à jour du guide de caractérisation des résidus miniers et du minerai.

Plante, B., Benzaazoua, M., and Bussière, B. (2010a). Predicting Geochemical Behaviour of Waste Rock with Low Acid Generating Potential Using Laboratory Kinetic Tests. Mine Water and the Environment, 30(1), 2-21. doi:10.1007/s10230-010-0127-z

Plante, B., Benzaazoua, M., Bussière, B., Biesinger, M. C., and Pratt, A. R. (2010b). Study of Ni sorption onto Tio mine waste rock surfaces. Applied Geochemistry, 25(12), 1830-1844.

Price, WA. (2009). Prediction manual for drainage chemistry from sulphidic geologic materials. MEND report 1:579.

Prigiobbe, V., and Mazzotti, M. (2013). Precipitation of Mg-carbonates at elevated temperature and partial pressure of CO2. Chemical Engineering Journal, 223, 755-763.

Prinčič, T., Štukovnik, P., Pejovnik, S., De Schutter, G., and Bokan Bosiljkov, V. (2013). Observations on dedolomitization of carbonate concrete aggregates, implications for ACR and expansion. Cement and Concrete Research, 54, 151-160.

Pronost, J., Beaudoin, G., Tremblay, J., Larachi, F., Duchesne, J., Hébert, R., and Constantin, M. (2011). Carbon sequestration kinetic and storage capacity of ultramafic mining waste. Environmental science & technology, 45(21), 9413-9420.

Prudêncio MI., Valente T., Marques R., Braga MAS., Pamplona J. (2017). Rare Earth Elements, Iron and Manganese in Ochre-precipitates and Wetland Soils of a Passive Treatment System for Acid Mine Drainage. Procedia Earth and Planetary Science 17:932-935.

Prudêncio, MI., Valente, T., Marques, R., Braga, MAS., Pamplona J. (2015). Geochemistry of rare earth elements in a passive treatment system built for acid mine drainage remediation. Chemosphere 138:691-700 .

Ptáček, P., Bartoníčková, E., Švec, J., Opravil, T., Šoukal, F., Wasserbauer, J., and Másilko, J. (2015). Preparation, kinetics of sinter-crystallization and properties of hexagonal strontium-yttrate-silicate apatite phase: SrY4[SiO4]3O. Ceramics International, 41(1, Part B), 1779-1795.

Purdy, C. (2014). The Geochemical and Mineralogical Controls on the Environmental Mobility of Rare Earth Elements from Tailings, Nechalacho Deposit, Northwest Territories.

QUÉBEC, Vérificateur Général. (2012). Rapport du Vérificateur général du Québec à l'Assemblée nationale pour l'année 2012-2013: Suivi d'une vérification de l'optimisation des ressources, chapitre 7: Interventions gouvernementales dans le secteur minier.

Quinn, J. E., Soldenhoff, K. H., and Stevens, G. W. (2017). Solvent extraction of rare earth elements using a bifunctional ionic liquid. Part 2: Separation of rare earth elements. Hydrometallurgy, 169, 621-628.

Rare Earth Technology Alliance (RETA). (2014). The Economic Benefits of the North American Rare Earths Industry.

Raudsepp M., and Pani A. (2003). Application of Rietveld analysis to environmental mineralogy. In environmental Aspects of MINE WASTES, Chapter 8. Editors J.L. Jambor, D.W. Blowes and A.I.M.Ritchie. Short Course Serie, Vol.31, 165-180.

Robertson, J. A., and Gould, K. L. (1983). Uranium and thorium deposits of northern Ontario (No. 25). Ontario Ministry of Natural Resources Rocha, E., Nasraoui, M., Soubiès, F., Bilal, E., and de Parseval, P. (2001). Évolution géochimique du pyrochlore au cours de l'altération météorique du gisement de Catalão II (Goiás, Brésil). Comptes Rendus de l'Académie des Sciences - Series IIA - Earth and Planetary Science, 332(2), 91-98.

Roche in collaboration with SGS, Golder and Genivar. (2012). Feasibility study for Kipawa project, Temescamingue Area, Québec, Canada. http://www.matamec.com/vns-site/uploads/ documents/ matamecfs 2013sedar.pdf (accessed on August 15th, 2017).

Rollinson, K., Jens, C., Andersen, Ross, J., Maria, B. and Rob, F. (2011). Characterisation of non-sulphide zinc deposits using QEMSCAN®®. Minerals Engineering, vol. 24, no 8, p. 778-787.

Ruffell A., and Wiltshire P.(2004). Conjunctive use of quantitative and qualitative X-ray diffraction analysis of soils and rocks for forensic analysis. Forensic science international, 145, 13-23.

Saldi, G. D., Daval, D., Morvan, G., and Knauss, K. G. (2013). The role of Fe and redox conditions in olivine carbonation rates: an experimental study of the rate limiting reactions at 90 and 150 C in open and closed systems. Geochimica et Cosmochimica Acta, 118, 157-183.

Sapsford, D. J., Bowell, R. J., Geroni, J. N., Penman, K. M., and Dey, M. (2012). Factors influencing the release rate of uranium, thorium, yttrium and rare earth elements from a low grade ore. Minerals Engineering, 39(0), 165-172.

Sapsford, D. J., Bowell, R. J., Dey, M., et Williams, K. P. (2009). Humidity cell tests for the prediction of acid rock drainage. Minerais Engineering 22, 25-36.

Romero-Freire, A. (2018). Assessment of baseline ecotoxicity of sediments from a prospective mining area enriched in light rare earth elements. Science of The Total Environment 612(Supplement C): 831-839.

Schlinkert, D., and Boogaart, K. G. (2015). The development of the market for rare earth elements: Insights from economic theory. Resources Policy, 46, Part 2, 272-280.

Schmid, R. (1981). Descriptive nomenclature and classification of pyroclastic deposits and fragments: Recommendations of the IUGS Subcommission on the Systematics of Igneous Rocks. Geology, 9(1): 41-43.

Schüler, D., Buchert, M., Liu, R., Dittrich, S. and Merz, C. (2011). Study on rare earths and their recycling. Öko-Institut eV Darmstadt.

Schreiber, A., Marx, J., Zapp, P., Hake, J.-F., Voßenkaul, D., and Friedrich, B. (2016). Environmental impacts of rare earth mining and separation based on eudialyte: A new European way. Resources, 5(4), 32.

Sherlock, E., Lawrence, R. and Poulin, R. (1995). On the neutralization of acid rock drainage by carbonate and silicate minerals. Environmental Geology, 25(1): 43-54.

Shieh, C. (2001). Criteria of selecting toxicity characteristics leaching procedure (TCLP) and synthetic precipitation leaching procedure (SPLP) tests to characterize special wastes. Florida Center for Solid and Hazardous Waste Management, University of Florida, Report, 01-2.

Sholkovitz, E. R. (1995). The aquatic chemistry of rare earth elements in rivers and estuaries. Aquatic Geochemistry, 1(1), 1-34.

Smith, M. M., and Carroll, S. A. (2016). Chlorite dissolution kinetics at pH3–10 and temperature to 275°C. Chemical Geology, 421, 55-64.

Smythe, D.M., Lombard, A. and Coetzee, L.L. (2013). Rare Earth Element deportment studies utilising QEMSCAN technology. Minerals Engineering, 52: 52-61.

Sneller, F. E. C., Kalf, F. D., Weltje, L., and Wezel, A. P. V. (2000). Maximum Permissible Concentrations and Negligible Concentrations for Rare Earth Elements (REEs). Research for man and environnement RIVM report 601501011.

Sobek, A., Schuller, W., Freeman, J., and Smith, R. (1978). Field and laboratory methods applicable to overburdens and minerals. U.S. Environmental Protection Agency, EPA-600/2–78–054 (PB-280–495).

Stegemann, J., and Cote, P. (1991). Investigation of test methods for solidified waste evaluation. Appendix B: Test methods for solidified waste evaluation. Environment Canada Manuscript Series.

Steinmann, M., and Stille, P. (2008). Controls on transport and fractionation of the rare earth elements in stream water of a mixed basaltic–granitic catchment basin (Massif Central, France). Chemical Geology, 254(1-2), 1-18.

Stille P., Steinmann M., Pierret MC. (2006). The impact of vegetation on fractionation of rare earth elements (REE) during water–rock interaction. Journal of Geochemical Exploration 88:341-344.

Sun, H., Zhao, F., Zhang, M., and Li, J. (2011). Behavior of rare earth elements in acid coal mine drainage in Shanxi Province, China. Environmental Earth Sciences, 67(1), 205-213. doi:10.1007/s12665-011-1497-7

Tang, H., Wang, X., Shuai, W., and Liu, Y. (2016). Immobilization of Rare Earth Elements of the Mine Tailings Using Phosphates and Lime. Procedia Environmental Sciences, 31, 255-263.

Tamir, G., Shenker, M., Heller, H., Bloom, P. R., Fine, P., and Bar-Tal, A. (2013). Organic N mineralization and transformations in soils treated with animal waste in relation to carbonate dissolution and precipitation. Geoderma, 209–210(0), 50-56.

Tatarko, P., and Kašiarová, M. (2015). 2 - Silicon nitride based ceramic composites toughened by rare-earth oxide additives A2 - Qin, Qinghua. In J. Ye (Ed.), Toughening Mechanisms in Composite Materials (pp. 35-71): Woodhead Publishing.

Tavares, L. M., Costa, E. M. d., Andrade, J. J. d. O., Hubler, R., and Huet, B. Effect of calcium carbonate on low carbon steel corrosion behavior in Saline co2 high pressure environmentals. Applied Surface Science.

Thomas, P. J., Carpenter, D., Boutin, C., and Allison, J. E. (2014). Rare earth elements (REEs): Effects on germination and growth of selected crop and native plant species. Chemosphere, 96(0), 57-66.

Tsamis, A., and Coyne, M. (2015). Recovery of rare earths from electronic wastes: An opportunity for High-Tech SMEs. Directorate general for internal policies policy department a: economic and scientific policy.

Tunsu, C., Ekberg, C., and Retegan, T. (2014). Characterization and leaching of real fluorescent lamp waste for the recovery of rare earth metals and mercury. Hydrometallurgy, 144, 91-98.

Turetta, C., Barbaro, E., Capodaglio, G., and Barbante, C. (2017). Dissolved rare earth elements in the central-western sector of the Ross Sea, Southern Ocean: Geochemical tracing of seawater masses. Chemosphere, 183, 444-453.

Tyler, G., and Olsson, T. (2001). Plant uptake of major and minor mineral elements as influenced by soil acidity and liming. Plant and Soil, 230(2), 307-321.

US EPA. (1995). Applicability of the toxicity characteristic leaching procedure to mineral processing wastes. Technical Background Document Supporting the Supplemental Proposed Rule Applying Phase IV Land Disposal Restrictions to Newly Identified Mineral Processing Wastes (December).

Valente, T.M., Antunes, M., Braga, AS., Prudêncio, M., Marques, R., Pamplona, J. (2012). Mineralogical attenuation for metallic remediation in a passive system for mine water treatment. Environmental Earth Sciences 66:39-54.

Verplanck, P. L., and Gosen, B. S. V. (2011). Carbonatite and alkaline intrusion-related rare earth element deposits-a deposit model USGS.

Verplanck, P. L., Nordstrom, D. K., Taylor, H. E., and Kimball, B. A. (2004). Rare earth element partitioning between hydrous ferric oxides and acid mine water during iron oxidation. Applied Geochemistry, 19(8), 1339-1354.

Vijayalakshmi, R., Mishra, S. L., Singh, H., and Gupta, C. K. (2001). Processing of xenotime concentrate by sulphuric acid digestion and selective thorium precipitation for separation of rare earths. Hydrometallurgy, 61(2), 75-80.

Villeneuve, M., Bussière, B., Benzaazoua, M., and Aubertin, M. (2009). Assessment of interpretation methods for kinetic tests performed on tailings having a low acid generating potential. Proceedings, Securing the Future and 8th ICARD, Skelleftea, Sweden.

Villeneuve, M. (2004). Évaluation du comportement géochimique à long terme de rejets miniers à faib le potentiel de génération d 'acide à l'aide d'essais cinétiques. Maîtrise, Université de Montréal - Ecole Polytechnique Montréal.

Villeneuve, M., Bussière, B., Benzaazoua, M., Aubertin, M., and Monroy, M. (2003). The influence of kinetic test type on the geochemical response of low acid generating potential tailings. Paper presented at the Proc, Tailings and Mine Waste.

Walker, S. (2010). Breaking the rare-earth monopoly. Engineering and Mining Journal, 211(10), 46.

Wang, C., Liang, Y., and Xu, W. (2015). On the significance of temperatures derived from major element and REE based two-pyroxene thermometers for mantle xenoliths from the North China Craton. Lithos, 224–225, 101-113.

Wang, L., and Liang, T. (2014a). Accumulation and fractionation of rare earth elements in atmospheric particulates around a mine tailing in Baotou, China. Atmospheric Environment, 88(0), 23-29.

Wang, L., and Liang, T. (2014b). Effects of exogenous rare earth elements on phosphorus adsorption and desorption in different types of soils. Chemosphere, 103(0), 148-155.

Wang, L., Liang, T., Zhang, Q., and Li, K. (2014). Rare earth element components in atmospheric particulates in the Bayan Obo mine region. Environmental Research, 131(0), 64-70.

Weber, R.J. and Reisman, D.J. (2012). Rare earth elements: A review of production, processing, recycling, and associated environmental issues. US EPA Region.

Weltje, L., Verhoof, L. R., Verweij, W., and Hamers, T. (2004). Lutetium speciation and toxicity in a microbial bioassay: testing the free-ion model for lanthanides. Environ Sci Technol, 38(24), 6597-6604.

White, A. F., and Brantley, S. L. (2003). The effect of time on the weathering of silicate minerals: why do weathering rates differ in the laboratory and field? Chemical Geology, 202(3–4), 479-506.

Williams-Jones, A.E., Migdisov, A.A. and Samson, I.M. (2012). Hydrothermal mobilisation of the rare earth elements a Tale of "Ceria" and "Yttria". Elements, 8.

Wübbeke, J. (2013). Rare earth elements in China: Policies and narratives of reinventing an industry. Resources Policy, 38(3), 384-394.

Xie, F., Zhang, T. A., Dreisinger, D., and Doyle, F. (2014). A critical review on solvent extraction of rare earths from aqueous solutions. Minerals Engineering, 56, 10-28.

Yang, X. J., Lin, A., Li, X.-L., Wu, Y., Zhou, W., and Chen, Z. (2013). China's ion-adsorption rare earth resources, mining consequences and preservation. Environmental Development, 8, 131-136.

Yang, K.-F., Fan, H.-R., Santosh, M., Hu, F.-F., and Wang, K.-Y. (2011). Mesoproterozoic carbonatitic magmatism in the Bayan Obo deposit, Inner Mongolia, North China: Constraints for the mechanism of super accumulation of rare earth elements. Ore Geology Reviews, 40(1), 122-131.

Yong, R., and Zheng, L. (1993). Adsorption and desorption of rare earth elements on soils and synthetic oxides. Acta Scientiae Circumstantiae, 13, 288.

Yörükoğlu, A., Obut, A., and Girgin, İ. (2003). Effect of thiourea on sulphuric acid leaching of bastnaesite. Hydrometallurgy, 68(1–3), 195-202.

Yoshida, S., Muramatsu, Y., Tagami, K., and Uchida, S. (1998). Concentrations of lanthanide elements, Th, and U in 77 Japanese surface soils. Environment International, 24(3), 275-286.

Young, R.A., (1993). The rietveld method, 5. International union of crystallography.

Yusoff, M., Bryne, T., and Parsons, I. (2013). Mobility and fractionation of REEs during deep weathering of geochemically contrasting granites in a tropical setting, Malaysia. Chemical Geology, vol. 349–350, no 0, p. 71-86.

Zaitsev, A.N.; Terry Williams, C.; Jeffries, T.E.; Strekopytov, S.; Moutte, J.; Ivashchenkova, O.V.; Spratt, J.; Petrov, S.V.; Wall, F.; Seltmann, R., and Borozdin, A.P. (2014). Rare earth elements in phoscorites and carbonatites of the Devonian Kola Alkaline Province, Russia: Examples from Kovdor, Khibina, Vuoriyarvi and Turiy Mys complexes. Ore Geol. Rev. 2014, 61, 204–225.

Zaitsev, A.N., Wall, F. and Bas, M.J.L. (1998) . REE-Sr-Ba minerals from the Khibina carbonatites, Kola Peninsula, Russia: their mineralogy, paragenesis and evolution. Mineralogical Magazine, 62, 225-250.

Zendah, H., Khattech, I., and Jemal.M. (2013). Thermochemical and kinetic studies of the acid attack of "B" type carbonate fluorapatites at different temperatures (25–55)°C. Thermochimica Acta, vol. 565, no 0, p. 46-51.

Zhang, S., Ding, Y., Liu, B., and Chang, C. C. (2017). Supply and demand of some critical metals and present status of their recycling in WEEE. Waste Management, 65, 113-127.

Zhang, Y., and Gao, X. (2015). Rare earth elements in surface sediments of a marine coast under heavy anthropogenic influence: The Bohai Bay, China. Estuarine, Coastal and Shelf Science, vol. 164, p. 86-93

Zhao, Y., Yu, R., Hu, G., Lin, X., and Liu, X. (2017). Characteristics and environmental significance of rare earth elements in PM2.5 of Nanchang, China. Journal of Rare Earths, 35(1), 98-106.

Zheng, Q., Wu, W., and Bian, X. (2017). Investigations on mineralogical characteristics of rare earth minerals in Bayan Obo tailings during the roasting process. Journal of Rare Earths, 35(3), 300-308.

Zhu, Z., Liu, C.-Q., Wang, Z.-L., Liu, X., and Li, J. (2016). Rare earth elements concentrations and speciation in rainwater from Guiyang, an acid rain impacted zone of Southwest China. Chemical Geology, 442: 23-34.

ANNEXES

ANNEXE A - ARTICLE 6 - MINERALOGICAL AND GEOCHEMICAL STUDY OF RARE EARTH ELEMENTS FROM A CARBONATITE DEPOSIT

Cet article est présenté à la conférence 13th SGA Biennial meeting at Nancy, France en 2015

Edahbi. M[a]; Plante. B[a]; Bouzahzah. H[a]; Benzaazoua. M[a]

[a] Université du Québec en Abitibi-Témiscamingue (UQAT), 445 boul de l'Université, Rouyn-Noranda J9X 5E4, QC, Canada.

Abstract

Five samples coming from a carbonatite deposit were characterized and rare earth element (REE) grades were measured. Mineralogical examination by SEM-EDS shows the following observations: (i) The rare earths are associated with carbonates, (ii) all analysed minerals contain preferably light REE (La, Ce, Pr, Nd, Sm and Eu), (iii) the sum of LREE in each analysed mineral varies between ~ 3 and 10 wt. %, (iv) the only heavy REE identified are Gd and Yb with a content lower than 0.4 wt. %, and (v) three groups of carbonate minerals were observed containing variable concentrations of Ca, Na, and F. The leachability of rare earth elements was tested using normalized kinetic testing (humidity cells with 64 weekly cycles). The geochemical results obtained indicate that the highest sum of light rare earth leached is recorded in the ferrocarbonatite (HG) (42 µg/l), while the lowest sum (8.8 µg/l) is from in the ferrocarbonatite (LG). For heavy rare earths, the leaching is between 0.27 and 1.5 µg/l with the maximum in the breccia and the minimum in the ferrocarbonatites (HG).

Keywords. Rare earth element, carbonatite deposit, distribution of REE, leaching

Introduction

The group of rare earth elements (REE) is composed of seventeen chemical elements (fifteen lanthanides, La to Lu, as well as Y and Sc). These elements are often classified in two main categories: light (LREE) and heavy (HREE) rare earth elements, with different uses and market demand (Andrade et al., 1999; Goonan, 2011; Humphries, 2013). According to the USGS (United

States Geological Survey), the 2008 world production of REE was higher than demand. The situation was completely reversed in 2010 with the increase in demand and restrictions on exports from China (USGS, 2013). Furthermore, Industrial Minerals Company of Australia (IMCOA) estimates that the global demand for REE can reach 160 000 tons in 2016. It is also estimated that the annual China demand may increase from 70 000 tons to 105,000 tons between 2011 and 2016 (Humphries, 2013; Yang et al., 2013). As a consequence, REE exploitation projects rapidly grow around the world. REE are omnipresent, not only in nature, but also in our daily lives. Thanks to their unique physical and chemical properties, REE are found in the most common applications like hybrid vehicles, rechargeable batteries, cell phones, LCD monitors, laptops, certain medical imaging equipment, radar systems, catalytic convertors, alloys, etc. (Calas, 2012; Chen, 2011; Goonan, 2011; Marcoux, 2013).

The LREE are the most abundant in the crust (10-100 ppm), whereas HREE are less abundant (1-10 ppm) (Gibert, 2012). The Promethium (Pm) element is not mentioned in these groups because it a synthetic element. All REE (expect promethium) are generally found in REE deposits, but their distribution and concentrations vary depending on the geological context. Within deposits, REE are mainly concentrated in the magmatic processes (Chakhmouradian and Wall, 2012; Orris and Grauch, 2002). During magma cooling, these elements are slightly integrated in the first formed minerals. Therefore, they are mainly collected at the end of the crystallization process (Chakhmouradian et Wall, 2012). The main and frequent REE deposits are: alkaline and hyperalkaline magmatism, carbonatites, and cationic clays. The main REE-bearing phases are silicates, carbonates, fluo¬carbonates, oxides, phosphates, and sulfates (Chakhmouradian and Zaitsev, 2012; Kanazawa and Kamitani, 2006; Verplanck and Gosen, 2011; Zaitsev et al., 2014).

The leaching of REE from geologic material depends on various parameters such as composition of the raw material, leaching agent used, concentration of the solvent, temperature, leaching time, and particle size distribution, (Baral et al., 2014; Bian et al., 2011). All these parameters may play a role in the prediction of the geochemical behaviour of REE-bearing mine wastes.

LREE and HREE exhibit different geochemical behaviours in terms of affinity, fractionation, sorption, and mobility (Genna et al., 2014; Pourret and Davranche, 2013; Steinmann and Stille, 1998). However, further research is necessary in order to fill important gaps on REE knowledge, especially on the reactivity of REE-bearing phases, as well as on REE leaching and toxicity

(Gonzalez et al., 2014). Therefore, the aims of this study are: (1) to evaluate the REE distribution in five different REE-bearing lithologies and (2) to study their leaching behaviour using kinetic tests (humidity cell). The samples that will be studied in this paper come from a carbonatite LREE deposit in Canada.

Material and methods

Humidity cell (ASTM D5744-13) tests were used to study the REE leaching rates using five samples coming from a carbonatite deposit (exploration cores). The following describe the materials and methods used in more details.

Sampling

Approximately 5 kg of three waste rock lithologies (described as breccia, calciocarbonatite, and silicocarbonatite) and two ore grades (ferrocarbonatites low grade LG and high-grade HG) were sampled from drill cores. These samples were crushed to <¼ inch and homogenized separately.

Analytical methods

The chemical compositions of the samples were analyzed by Inductively Coupled Plasma (ICP-AES) after a multi-acid digestion (HCl, HNO3, Br2, HF). Leachates from testing were analysed with the ICP-AES and ICP-MS following acidification of a filtered (0.45 µm) aliquot to about 2 % HNO3.

The mineralogical study was performed on polished sections of the five samples by optical (Zeiss Axio imager.M2m) and scanning electron microscope (SEM–Hitachi S-3500N), equipped with a microanalysis system (energy dispersive spectroscopy INCA XMax 20 mm2 SDD). The polished sections were prepared using a method developed for samples containing heavy minerals in order to avoid their preferential sedimentation. The OM observations mainly focused on sulfide minerals, while the analysis of the REE-bearing minerals was made using the SEM-EDS system.

Humidity cell tests

Humidity cell tests were performed in a Plexiglass chamber that provided air input and output. Five cells were filled with 1 kg of each sample placed on a geotextile lying on a perforated grid. The experiments lasted 64 weekly cycles. Dry air was passed through the sample container for the first three days, followed by humidified air for the next three days, and leaching on the 7th

day with 500 ml of deionized water (pH ≈6) (Benzaazoua et al., 2004; Plante et al., 2010). Dry and humid air flows as well as the temperature were maintained stable for the length of the test. The leached solutions were analysed for pH and REE contents.

Results and discussion

Mineralogical characterization

Optical microscopy observations show that pyrite (FeS_2) is the most abundant sulfide mineral in the five samples observed, whereas sphalerite (ZnS), galena (PbS), pyrrhotite ($Fe_{(1-X)}S$), chalcopyrite ($CuFeS_2$), and pentlandite $(Fe,Ni)_9S_8$ occurs as minor sulfides. The weight percentages of the various sulfides observed were estimated using reconciliation with the chemical analyses, assuming all Zn within sphalerite, all Pb within galena, all Cu within chalcopyrite, and Ni within pentlandite. The results are summarized in Table 1.

Table 1: Proportions of sulfide minerals obtained by mineralogical calculations in the five samples.

Sample	FeS_2	$CuFeS_2$	ZnS	PbS	$Fe_{(1-X)}S$
Breccia	1.54	0.02	0.13	0.03	0.04
Calcio	0.63	0.01	0.19	0.02	0.02
Ferro(1)	0.32	0.01	0.13	0.01	0.01
Ferro(2)	1.48	0.01	0.09	0.01	0.04
Silico	0.58	0.02	0.08	0.01	0.02

Calcio =Calciocarbonatite (LG), Ferro (1)=Ferrocarbonatite (LG), Ferro(2)=Ferrocarbonatite (HG), and Silico=Silicocarbonatite (LG).

The following results were obtained with the SEM-EDS: (i) the REE are associated with carbonates; (ii) all analysed minerals contain mostly LREE (La, Ce, Pr, Nd, Sm, and Eu); (iii) the sum of LREE in each analysed mineral varies between ~ 3 and 10 wt %; (iv) the only HREE identified are Gd and Yb with less than 0.4 % in all REE-bearing minerals; (v) three groups of REE-bearing carbonate minerals were observed with variable concentrations of Ca, Na, and F, which are illustrated within Figure 1.

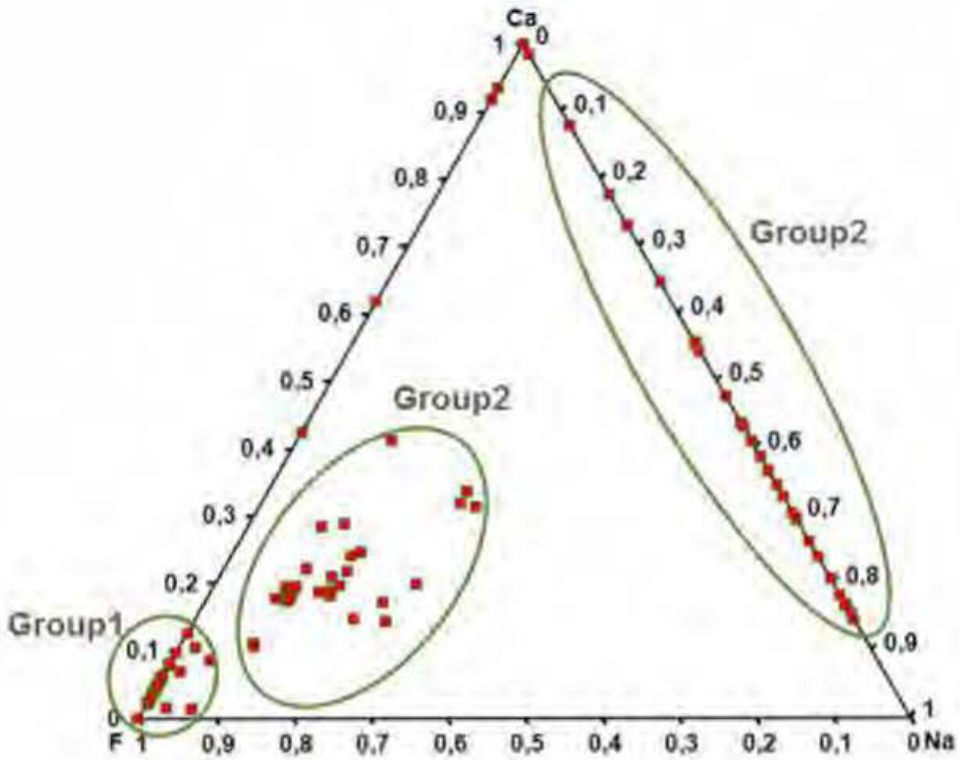

Figure 1: distribution of Ca, F, and Na in the analysed Minerals.

Chemical characterization

The REE contents of the samples are shown in Figure 2 and Table 2. Cerium is the most abundant element in all samples (Figure 2), with a maximum content within the silicocarbonatite (LG) and the minimum content in the breccia sample.

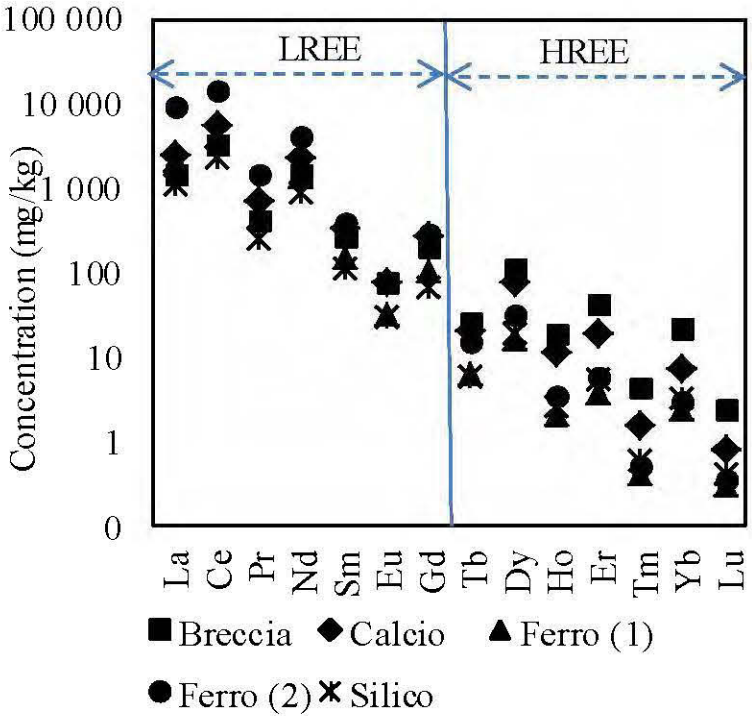

Figure 2 : Graphical representation of REE contents in samples; Calcio=Calicocarbonatite (LG), Ferro (1) =Ferrocarbonatite (LG), Ferro (2) =Ferrocarbonatite (HG), and Silico=Silicocarbonatite (LG).

The LREE content varies between 4604 mg/l (Silicocarbonatite) and 29158 mg/l (Ferrocarbonatite HG), while the HREE content is below 600 mg/l in all samples (Table 2).

Table 2 REE assays of the samples

Sample	Breccia	Calcio	Ferro(1)	Ferro(2)	Silico
∑LREE (mg/l)	7 145	11 457	8 330	29 158	4 604
∑HREE (mg/l)	596.1	305.95	76.08	109.64	87.14

Calcio=Calicocarbonatite (LG), Ferro (1)=Ferrocarbonatite (LG), Ferro (2)=Ferrocarbonatite (HG), and Silico=Silicocarbonatite (LG); LREE (La to Gd), and HRE E(Tb to Lu, plus Y and Sc).

Calcio=Calicocarbonatite (LG), Ferro (1)=Ferrocarbonatite (LG), Ferro (2)=Ferrocarbonatite (HG), and Silico=Silicocarbonatite (LG); LREE (La to Gd), and HRE E(Tb to Lu, plus Y and Sc).

Kinetic testing results

Humidity cells were used to evaluate the geochemical behavior of the ores and lithologies. The results of the leachate analyzes are presented in the following. The highest sum of LREE leached is recorded in the ferrocarbonatite (HG) (42 µg/l), while the lowest sum is found in the ferrocarbonatite (LG) (8.8 µg/l). The leaching of LREE is higher than HREE regardless of the sample (Figure 3). For HREE, the leached concentrations are between 0.27 µg/l (ferrocarbonatite HG) and 1.5 µg/l (breccia). It can be noticed that even though the HREE occurs in very small quantities in the solid samples, they are found to be leached during the humidity cell tests. This suggests a high mobility of HREE in comparison to LREE. This behavior may be explained by the following phenomena: (i) the higher ionic radius of HREE ions relative to LREE ions, which makes them less stable in the crystal matrix; (ii) the geochemical affinity of the leached LREE to carbonates, iron oxyhydroxides, and phosphates, which may mobilize the LREE upon their leaching into the drainage waters; (iii) the geochemical speciation, which drives the precipitation of secondary REE-bearing minerals (Bau, 1999; Kawabe 1999; Millero, 1992). All these hypotheses will need to be verified in further research.

During humidity cell tests, the dissolution of the REE-bearing carbonates depicted in Figure 1 produces fluoride, calcium, sodium, and REE ions. Figures 4, 5, and 6 respectively show the normalised cumulative masses of REE vs fluorine (F), REE vs calcium (Ca), and REE vs sodium (Na) leached out of all materials. F and REE release seem to be correlated almost linearly. On the other hand, Ca and REE exhibit a relationship involving an inflexion point (figure 5) between a rapid initial release of REE vs Ca, followed by a slower stabilized REE release vs Ca, for all materials but the silicocarbonatite, in which the relationship is closer to a straight line.

Although these results still need to be interpreted further, they suggest that REE release is associated to fluorine-bearing and Ca-bearing carbonates, in all materials of this carbonatite complex. Advanced mineralogical characterization needs to be performed in order to better understand the REE release mechanism from the crystal lattices. Detailed sorption studies should also be performed in order to verify the hypothesis that the carbonates or other phases may sorb the leached REE within these materials. Sequential extractions performed before and after the humidity cell tests will enable to appreciate possible changes in REE speciation. Thermodynamical

equilibrium calculations will also be performed to verify if REE secondary minerals might be oversaturated within the leachates of the humidity cells.

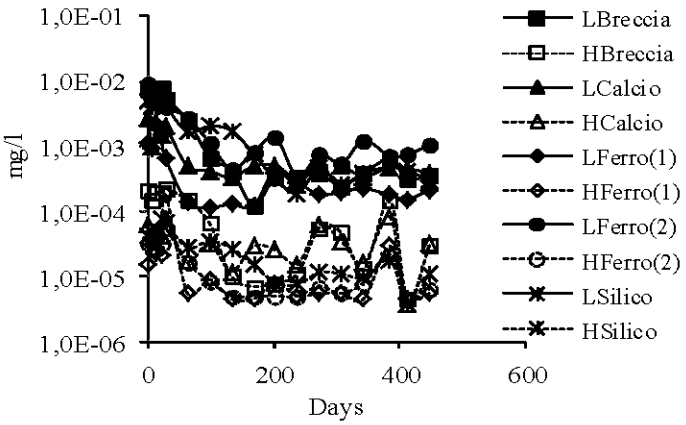

Figure 3 : Evolution of the sum of LREE and HREE with time in the five studied lithologies (L and H refer to LREE and HREE, respectively).

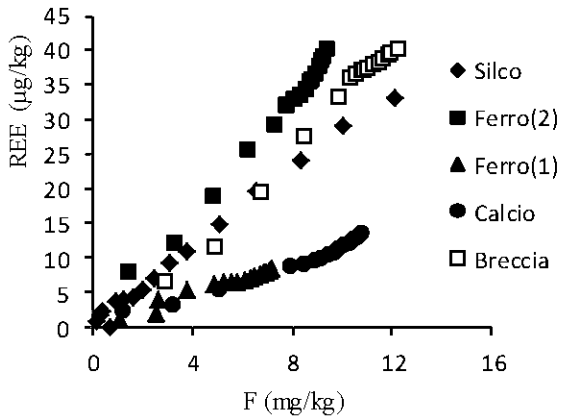

Figure 4 : Cumulative masses of REE and F leached out of the kinetic tests on the five samples studied; (the legend is the same as the other figures).

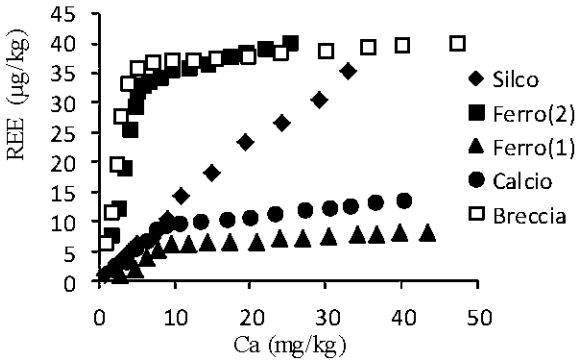

Figure 5 : Cumulative masses of REE and Ca leached out of the kinetic tests on the five samples studied; (the legend is the same as the other figures).

Finally, it is clear that a better understanding of the geochemical behaviour of REE passes by the study of sorption, complexation, speciation and mobility of REE. In order to address these issues, future work will include the following techniques: batch adsorption in controlled conditions, sequential chemical extractions, and XPS studies.

Conclusion and perspectives

The two main objectives of this study are: (1) to evaluate the REE distribution in solid samples, and (2) to predict their leaching behavior using kinetic tests (humidity cells). Five samples chosen to represent the heterogeneity of the deposit were tested for up to 64 weeks. Geochemical results from kinetic tests show that the highest sum of LREE leached is recorded in the ferrocarbonatite (HG) (42 µg/l), while the lowest sum is found in the ferrocarbonatite (LG) (8.8 µg/l). For HREE, the leached concentrations are between 0.27 µg/l from the ferrocarbonatite HG, and 1.5 µg/l from the breccia. Mineralogical results show that REE are mostly associated with carbonates enriched in LREE (La, Ce, Pr, Nd, Sm and Eu).

For a better understanding of the geochemical behavior of REE, further research is needed in the following areas: (i) advanced chemical and physical characterizations, (ii) comparison of column tests results with those of humidity cell, (iii) sorption studies, and (iv) determination of the various REE-bearing secondary minerals that can form during kinetic tests.

Acknowledgements

The authors thank the URSTM, staff for their support with laboratory work and NSERC for funding of this study.

References

Andrade, F. R. D., P. Möller, V. Lüders, P. Dulski et H. A. Gilg. 1999. «Hydrothermal rare earth elements mineralization in the Barra do Itapirapuã carbonatite, southern Brazil: behaviour of selected trace elements and stable isotopes (C, O)». Chemical Geology, vol. 155, no 1–2, p. 91-113.

Baral, S. S., K. Raja Shekar, Megha Sharma et P. V. Rao. 2014. «Optimization of leaching parameters for the extraction of rare earth metal using decision making method». Hydrometallurgy, vol. 143, p. 60-67.

Bau, Michael. 1999. «Scavenging of dissolved yttrium and rare earths by precipitating iron oxyhydroxide: experimental evidence for Ce oxidation, Y-Ho fractionation, and lanthanide tetrad effect». Geochimica et Cosmochimica Acta, vol. 63, no 1, p. 67-77.

Benzaazoua, M., B. Bussiére, A. M. Dagenais et M. Archambault. 2004. «Kinetic tests comparison and interpretation for prediction of the Joutel tailings acid generation potential». Environmental Geology, vol. 46, no 8, p. 1086-1101.

Bian, Xue, Shao-hua Yin, Yao Luo et Wen-yuan Wu. 2011. «Leaching kinetics of bastnaesite concentrate in HCl solution». Transactions of Nonferrous Metals Society of China, vol. 21, no 10, p. 2306-2310.

Calas, G. 2012. «Elements ». International Magazine of Mineralogy, Geochemistry, and Petrology, vol. 8, no ISSN: 1811-5209.

Chakhmouradian, A. R., et F. Wall. 2012. «Rare Earth Elements: Minerals, Mines, Magnets (and More)». Elements, vol. 8, no 5, p. 333-340.

Chakhmouradian, A. R., et A. N. Zaitsev. 2012. «Rare Earth Mineralization in Igneous Rocks: Sources and Processes». Elements, vol. 8, no 5, p. 347-353.

Chen, Zhanheng. 2011. «Global rare earth resources and scenarios of future rare earth industry». Journal of Rare Earths, vol. 29, no 1, p. 1-6.

Genna, Dominique, Damien Gaboury et Gilles Roy. 2014. «Evolution of a volcanogenic hydrothermal system recorded by the behavior of LREE and Eu: Case study of the Key Tuffite at

Bracemac–McLeod deposits, Matagami, Canada». Ore Geology Reviews, vol. 63, no 0, p. 160-177.

Gibert, Benoit. 2012. «Ressources minérales et matériaux pour l'énergie». Laboratoire Géosciences Montpellier-Bât.22 - 2eme étage, France.

Gonzalez, Veronica, Davide A. L. Vignati, Corinne Leyval et Laure Giamberini. 2014. «Environmental fate and ecotoxicity of lanthanides: Are they a uniform group beyond chemistry?». Environment International, vol. 71, no 0, p. 148-157.

Goonan, Thomas G. 2011. «Rare Earth Elements—End Use and Recyclability». USGC (Science for a changing world).

Gupta, C.K., et N. Krishnamurthy. 1992. «Extractive metallurgy of rare earths». International Materials Review, vol. 37, no 5, p. 197–248.

Humphries, Marc. 2013. «Rare Earth Elements: The Global Supply Chain». Congressional Research Service, 7-5700 (http://www.fas. org/sgp/crs/natsec/R41347.pdf)

Kanazawa, Yasuo, et Masaharu Kamitani. 2006. «Rare earth minerals and resources in the world». Journal of Alloys and Compounds, vol. 408–412, no 0, p. 1339-1343.

Kawabe, IWAO. 1999. «Hydration change of aqueous lanthanide ions and tetrad effects in lanthanide(III)-carbonate complexation». Geochemical journal, vol. 33, p. 267-275.

Lipin, B.R, Mckay, G.A. «Geochemistry and mineralogy of rare earth elements». Mineralogical society of america, reviews in mineralogy, Volume 21,1989.

Marcoux, Eric. 2013. «Métallogénie des gisements épithermaux et porphyriques et des terres rares : guide d'exploration». Formation organisée par le comité d'éducation continue de l'ICM de Rouyn-Noranda , Quebec, Canada.

Millero, Frank J. 1992. «Stability constants for the formation of rare earth-inorganic complexes as a function of ionic strength». Geochimica et Cosmochimica Acta, vol. 56, no 8, p. 3123-3132.

Morin KA, Hutt NM (1997) Environmental Geochemistry of Minesite Drainage: Practical Theory and Case Studies. MDAG Publishing, Vancouver.

Orris, Greta J., et Richard I. Grauch. 2002. «Rare Earth Element Mine,Deposits, and Occurences». USGS (Science for a changing world).

Plante, B., M. Benzaazoua et B. Bussière. 2010. «Predicting Geochemical Behaviour of Waste Rock with Low Acid Generating Potential Using Laboratory Kinetic Tests». Mine Water and the Environment, vol. 30, no 1, p. 2-21.

Pourret, Olivier, et Mélanie Davranche. 2013. «Rare earth element sorption onto hydrous manganese oxide: A modeling study». Journal of Colloid and Interface Science, vol. 395, no 0, p. 18-23.

Steinmann, Marc, et Peter Stille. 1998. «Strongly fractionated REE patterns in salts and their implications for REE migration in chloride-rich brines at elevated temperatures and pressures». Comptes Rendus de l'Académie des Sciences - Series IIA - Earth and Planetary Science, vol. 327, no 3, p. 173-180.

Verplanck, Philip L., et Bradley S. Van Gosen. 2011. «Carbonatite and alkaline intrusion-related rare earth element deposits-a deposit model ». USGS.

Yang, X. Jin, A. Lin, Xiao-Liang Li, Yiding Wuc, W. Zhoud et Z.Chene. 2013. «China's ion-adsorption rare earth resources, mining consequences and preservation». Environmental Development, vol. 8, no 0, p. 131-136.

Zaitsev, Anatoly N., C. Terry Williams, Teresa E. Jeffries, Stanislav Strekopytov, Jacques Moutte, Olga V. Ivashchenkova, John Spratt, Sergey V. Petrov, Frances Wall, Reimar Seltmann et Alexey P. Borozdin. 2014. «Rare earth elements in phoscorites and carbonatites of the Devonian Kola Alkaline Province, Russia: Examples from Kovdor, Khibina, Vuoriyarvi and Turiy Mys complexes». Ore Geology Reviews, vol. 61, no 0, p. 204-225.

ANNEXE B- ARTICLE 7 - MINERALOGICAL AND GEOCHEMICAL STUDY OF RARE EARTH ELEMENTS FROM A SILICATE DEPOSIT : CASE OF KIPAWA ORE

Cet article est présenté à la conférence Process Mineralogy '17. Cape Town, South Africa en 2017

M. Edahbi [a] ; B. Plante [a] ; M. Benzaazoua [a]; L.Kormos[d]; S.Doire[C]

[a] Université du Québec en Abitibi-Témiscamingue (UQAT), 445 boul de l'Université, Rouyn-Noranda J9X 5E4, QC, Canada.

[c] Matamec Explorations Inc, Canada

[d] XPS consulting and testwork services, SudBury, Canada

Abstract

The leachability of the rare earth elements (REE) from the Kipawa deposit, a Heavy REE (HREE) mine project of Matamec resources, was investigated in order to predict their geochemical behavior and to evaluate the factors controlling the REE mobility in ambient conditions. All lithologies of the deposit, including ore and waste rocks, were sampled, characterized using automated SEM-EDS mineralogy, and submitted to kinetic testing using weathering cells in order to investigate their REE leaching potential.

All leachates showed a neutral to alkaline pH (7.0 to 9.5) and alkalinity values between 10 and 173 mg $CaCO_3$/l. The REE concentrations leached from the materials are all below 15 µg/l. Works are underway (i.e. thermodynamic equilibrium calculations) to determine the control factors of the REE release in the leachates.

Keywords: Rare earth elements; mineralogy; geochemical behavior; leachability; weathering cells

1. Introduction

The rare earths industry is of big importance to the world economy. For example, the North American REE industry directly contributes to the economy strength with $795 million in shipments, employing nearly 1,050 workers with a payroll of $116 million (Rare Earth technology Alliance, 2014). Rare earth elements are used in hybrid vehicles, rechargeable batteries, clean energy (renewable energy), mobile (cell) phones, flat screen display panels, compact fluorescent light bulbs, laptop computers, disk drives, catalytic converters, etc. For the moment, China fills

94 % of the global REE market (Lema et al., 2016). As a circumvention strategy, the exploitation of REE deposits constitutes a high economic potential, in order to reduce this dependence to the Chinese REE industry (Biennemas et al., 2013; Edahbi et al., 2015).

The group of rare earth elements (REE), called also lanthanides, is composed of seventeen chemical elements (fifteen lanthanides, La to Lu, as well as Y and Sc). These REE are found in various geological settings such as magmatism, sedimentary deposits, and metamorphism, and show an affinity with several mineral phases such as apatite (Calas, 2012). The lanthanides exhibit similar chemical and physical properties and differ only in the number of electrons in the 4f shell. Moreover, the size difference of REE ions promotes their cationic exchange with other elements in different minerals and geological formations (Jia, 1991; Lipin and Mckay., 1989).

Refining and mining REE are known to generate large amounts of liquid and solid wastes which could present disastrous effects on the environment. In Canada, the legislation forces mining companies to manage their wastes in order to minimize environmental impacts. The mine waste rocks and tailings are generally stored at the surface and exposed to ambient conditions. The reaction between water, oxygen, and some reactive minerals such as sulfides (i.e. pyrite, pyrrhotite, chalcopyrite, sphalerite, etc.) can generate contaminated mine drainage. Furthermore, the REE deposits are known to be associated to several radioactive elements such as thorium (Th), niobium (Nb), and uranium (U) (Dai et al., 2013; Hao et al., 2015). The release of REE and associated elements must be predicted in order to define appropriate management scenarios and thus avoid significant adverse environmental effects.

The purpose of this paper is to study the geochemical behavior of REE-bearing minerals from the Kipawa deposit (Canada). This knowledge will enable to predict the water quality of future REE wastes and contribute to minimize their environmental impacts.

2. Materials and methods

Automated mineralogy (QEMSCAN) and weathering cell tests were used to characterize and study the REE leaching potential using six lithologies coming from the Kipawa deposit. The following describe the materials and methods used in more details.

2.1. Methodology and Sampling

Approximately 10 kg of five waste rock lithologies, described as syenite waste (SW), calcite-poor waste (WCCP), calcite-rich waste (WCR), peralcalin gneiss (PG), and monzonitic basement gneiss (MBG), were sampled from drill cores (waste rock, while a magnetic concentrate (MC) was provided by Matamec explorations. These samples were crushed to <¼ inch and homogenized separately (Figure 1). The REE are associated to silicate minerals within the Kipawa deposit: mainly eudialyte (a sodic silicate), yttro-titanite/mosandrite (titanite silicate), and britholite (calcic silico-phosphate) (Roche et al., 2012).

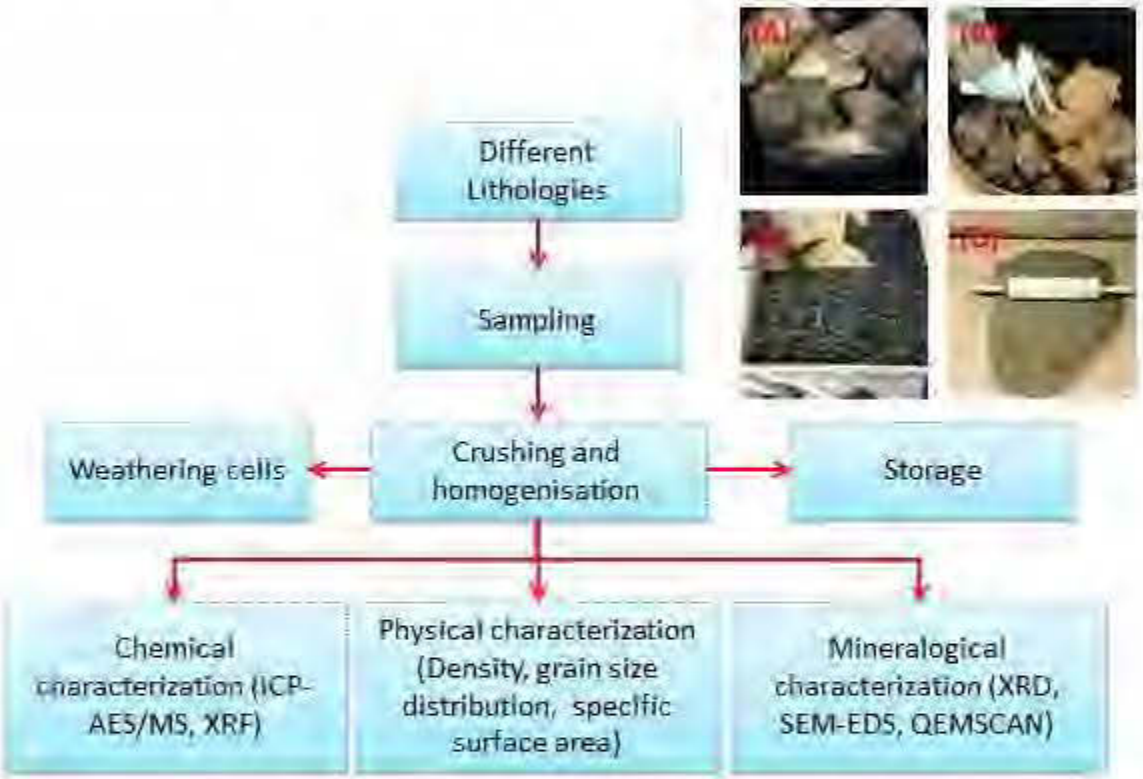

Figure 1: Methodology used for preparing samples.

2.2. Physical, chemical, and mineralogical characterizations

○ Physical and chemical characterization

The grain size distribution was measured using a laser analyzer (Malvern Mastersizer). The specific gravity (Gs) was analyzed with a helium gas pycnometer (Micromeritics Accupyc 1330). The specific surface area was determined by helium adsorption using a BET interpretation (Brunauer et al. 1938).

The major and trace elements of the materials were determined by Inductively Coupled Plasma (ICP-AES/MS) analysis after a multi-acid digestion (HCl, HNO_3, Br_2, HF). The sulfide sulfur in the solids was determined by subtraction of the sulfate sulfur (determined by a 40 % HCl extraction; method adapted from Sobek et al., 1978) from the total sulfur (ICP-AES analysis). The S and C content were determined using an ELTRA CS-2000 induction furnace. The REE in the leachates were analyzed with an ICP-MS, while an ICP- AES was used to analyze other elements such as S, Ca, Mg, Mn, Fe, Sr, F, P, K , Zn, Pb, Si, and Na. The leachates were filtered (0.45 µm) and acidified (2 % HNO_3) for ICP analyses.

Pore water, pH, Eh, and electrical conductivity measurements were determined immediately with a pH/mV meter and an electrical conductivity meter (EC meter).

- **Mineralogical characterization**

The crystalline minerals in all samples (waste rocks and magnetic concentrate) were determined by the X-ray diffraction (Bruker AXS Advance D8), using a copper cathode (K_α radiation). The DiffracPlus EVA software was used to identify the detected minerals and the TOPAS software was used to quantify their abundance using Rietveld refinement (Johnson et al. 1985).

A scanning electron microscope (SEM–Hitachi S-3500N), equipped with a microanalysis system (energy dispersive spectroscopy, or EDS) was used in order to confirm the presence of the phases detected by XRD, to analyze the elemental composition of the REE-bearing minerals present in samples, as well as to detect minerals in concentrations lower than the XRD detection limit. The analyses were performed on polished sections of the six samples, prepared using a method developed to avoid the preferential sedimentation (Bouzahzah et al. 2015).

The QEMSCAN (quantitative evaluation of minerals by scanning electron microscopy) automated mineralogical analysis tool enables quantitative chemical analysis of materials and generation of high-resolution mineral maps and images. It was used to evaluate the distribution and deportment of REE in all samples. Electron microprobe mineralogical analyses (EPMA) were also performed on selected minerals in order to define the REE content of minerals with more accuracy. This knowledge is crucial to understand the geochemical behavior of the REE-bearing minerals (Peelman et al., 2016).

- **Weathering cell tests**

Weathering cell tests are used to predict the geochemical behavior of mine wastes under leaching conditions. A Buchner-type funnel containing 67 g of samples arranged uniformly on a filter paper is used, and then the sample is subjected to bi-weekly 50 ml leaching cycles (Benzaazoua et al., 2004, 2014; Plante et al., 2010).

3. Results and discussion

3.1. Sample properties

-Physical characterization

The determination of particles distribution has a great importance in the interpretation of kinetic test results (Erguler et al., 2015), since fine particles are more reactive than coarse particles. The particle size distributions of the materials are shown in Table 1. The materials were prepared in order to show a particle size distribution similar to that of the magnetic concentrate (MC); the D_{50} values vary between 18 and 30 μm (Table 1) for all samples.

The other physical properties are summarized in Table 1. The specific gravity was practically similar in all samples (2.8-3.16 $g.cm^{-3}$). The specific surface area of MC (5.17 $m^2.g^{-1}$) was higher than for the waste rocks (1.75-3.14 $m^2.g^{-1}$).

-Chemical characterization

The chemical compositions of the samples are shown in Table 1. The whole-rock analyses of the waste rocks samples (WS, WCCP and MC) show similar concentrations of SiO_2 (52–54 %), Al_2O_3 (6–7 %), Fe_2O_3 (8–9 %), Na_2O (4–6 wt.%), and K_2O (1.78–3 %), and higher differences in MgO (6–14 %) and CaO (6.64–11.99 %) (Table 1).

The whole-rock analyses of the PG and MBG samples show similar concentrations of SiO_2 (60–70 %), Al_2O_3 (11–13 %), Fe_2O_3 (6–9 %), and Na_2O (4.65–7.8 %) (Table 1). In comparison with these samples, WCCR presented a higher concentration of CaO (29.5 %) and a lower concentration of SiO_2 (19.02 %). The WCCR material is the only one with significant carbonate content, therefore it shows the highest carbon concentration (6.36 %) in comparison to the other samples (less than 0.14 %). The sulfur content is less than 0.07 % in all samples. The chemical composition of all samples is highlighted in Table 1.

The results in Table 1 show that all samples are richer in LREE (412-6117 mg/l) than in HREE (106-5595 mg/l). The MC has the highest concentration of LREE, while the MBG contains the lowest concentration. Yttrium is the most abundant element in all samples, with a maximum in the MC (11 712 mg/l) and a minimum in the MBG sample (524 mg/l).

Table 1 Physical and chemical compositions of WS, WCCP, WCCR, MC, PG and MBG samples.

		WS	WCCP	WCCR	MC	PG	MBG
Physical properties							
Specific gravity	$g.cm^{-3}$	3.01	3.12	2.96	3.16	2.91	2.8
Specific surface area	$m^2.g^{-1}$	2.28	2.25	3.14	5.17	2.49	1.75
D_{90}	µm	110	115	60	60	110	60
D_{80}	µm	70	80	50	50	70	42
D_{50}	µm	25	30	20	20	25	18
Chemical composition							
C total	%	0.07	0.06	6.36	0.14	0.06	0.03
S total	%	0.02	0.02	0.02	0.04	0.07	0.01
SiO_2	%	55.98	52.92	19.02	54.3	60.42	70.18
Al_2O_3	%	6.89	5.93	0.66	7.06	13.76	11.18
Fe_2O_3	%	6.29	4.26	0.5	7.95	8.99	6.09
MgO	%	10.5	14.2	24.78	6.88	0.84	0.15
CaO	%	6.64	11.19	29.5	9.38	2.31	0.61
Na_2O	%	6.1	4.43	0.18	6.19	7.85	4.64
K_2O	%	2.99	1.78	0.36	2.15	3.05	5.03
TiO_2	%	0.33	0.26	0.02	0.84	0.96	0.39
P_2O_5	%	0.21	0.42	0.01	0.45	0.28	0.05
MnO	%	0.31	0.27	0.03	0.51	0.19	0.13
Cr_2O_3	%	0.04	0.04	0.05	0.08	0.04	0.1
V_2O_5	%	< 0.01	< 0.01	< 0.01	0.01	< 0.01	< 0.01
LOI	%	0.92	0.94	23.28	1.39	0.52	0.19
Rare earth elements							
Sc	mg/l	37.25	21.64	1.09	37.91	9.09	2.65
Y	mg/l	450.35	413.99	218.17	4497.99	409.94	83.06
La	mg/l	201.39	166.24	116.5	1208.74	146.17	103.76
Ce	mg/l	393.09	360.13	188.15	2687.22	300.66	190.72
Pr	mg/l	44.07	42.6	18.66	320.19	36.53	21.82
Nd	mg/l	163.5	163.96	64.62	1287.3	144.84	80.03

Sm	mg/l	31.2	33.81	12.06	297.47	29.95	12.34
Eu	mg/l	3.73	4.08	1.42	37.51	3.83	0.98
Gd	mg/l	27.83	29.27	10.51	278.41	27.75	8.35
Tb	mg/l	5.14	5.18	1.88	51.56	5.01	1.13
Dy	mg/l	35.01	36.2	13.21	368.84	35.94	6.7
Ho	mg/l	7.81	7.79	2.95	78.03	7.6	1.28
Er	mg/l	29.27	28.87	10.62	267.38	25.87	4.06
Tm	mg/l	4.91	4.93	1.52	38.73	3.63	0.65
Yb	mg/l	43.09	43.97	10.3	254.93	24.34	6.32

3.2. Mineralogical characterization

The mineralogical composition of the materials determined by XRD is shown in Figure 2. All studied samples are generally composed of the same mineralogical phases; quartz (SiO_2), biotite $K(Mg,Fe)_3(AlSi_3O_{10}(OH,F)_2)$, diopside ($CaMgSi_2O_6$), aegirine-augite, actinolite ($Ca_2(Mg,Fe)_5Si_8O_{22}(OH)_2$), calcite ($CaCO_3$), and microcline ($KAlSi_3O_8$). Other minerals include zircon, magnesio/ferri-katophorite, dolomite, and titanite.

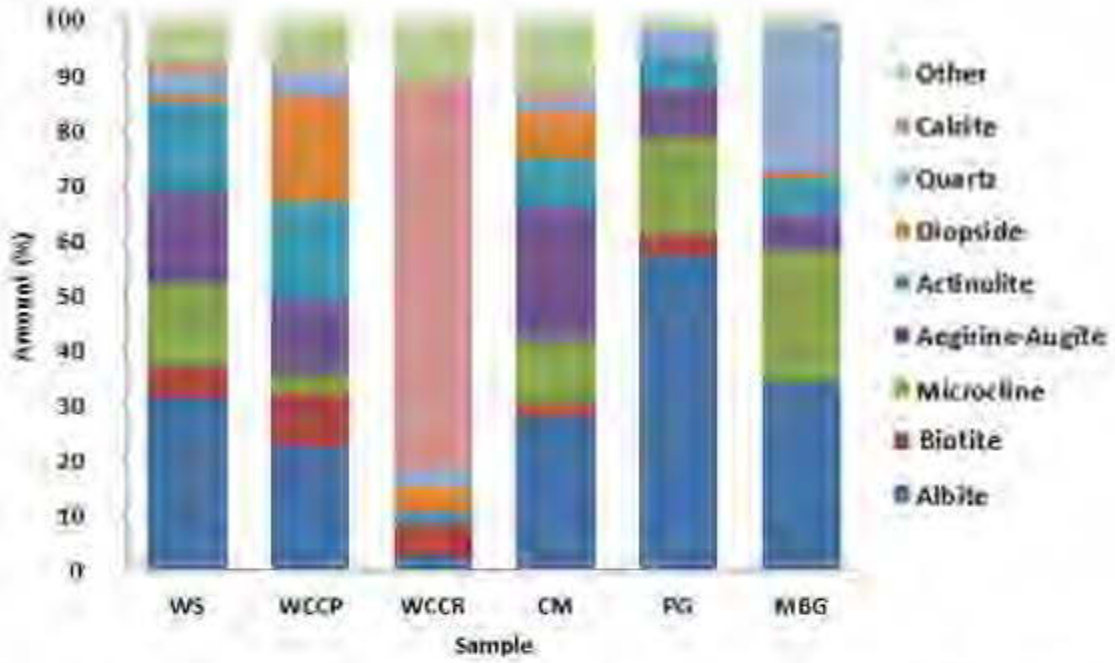

Figure 2: Quantification of crystalline phase minerals in WS, WCCP, WCCR, CM, PG and MBG samples.

The Figure 3 illustrates the different forms in which the REE-bearing minerals are found in the samples: practically liberated particles (more than 80%), associated to other minerals, and included within gangue minerals. The results obtained with the SEM-EDS show that: (i) the REE are associated with magnesiokatophorite/katophorite, apatite, zircon (Figure 3); (ii) all analysed minerals contain mostly LREE (La, Ce, Pr, Nd, Sm, and Y); (iii) three groups of silicate minerals were detected with variable concentrations of Y. Sulfide particles (pyrite, pyrrhotite, galena, and sphalerite) were identified in all samples. The QEMSCAN results show that the REE distribution is more concentrated in finer fractions.

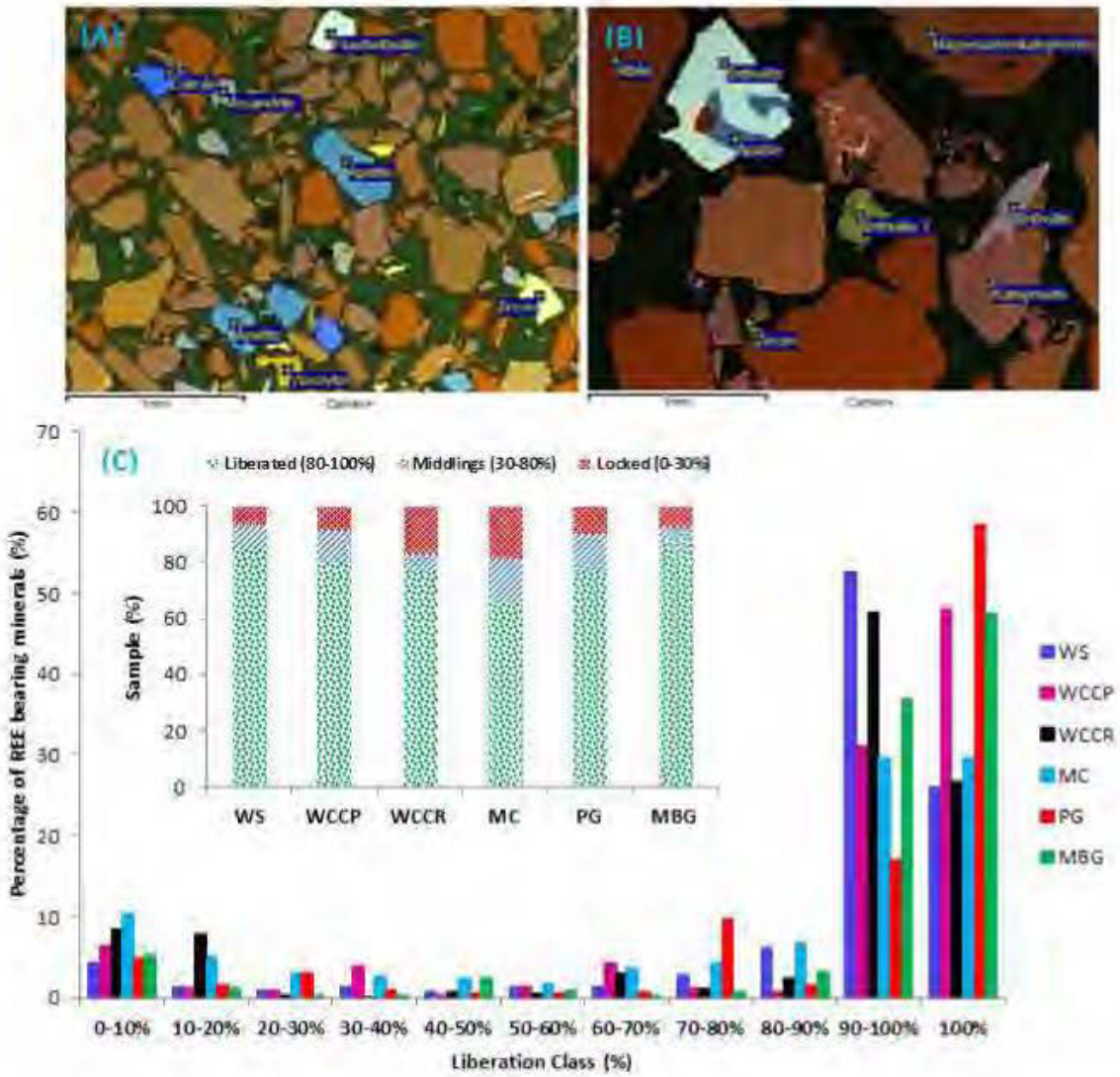

Figure 3: Scanning Electron Microscope (SEM) electron micrograph showing gangue minerals, REE-bearing minerals (A), and their mineralogical associations (B) and liberation of the REE-bearing minerals (C).

The correlation of elemental analysis by QEMSCAN and chemical analyses by ICP is shown in Figure 3 for La, Ce, Nd, Pr, Sm, and Y. These concentrations obtained by both methods are generally of the same order. The discrepancies observed are probably due mainly to the dissemination of the REE mineralization at low concentrations in the gangue minerals, which is challenging to quantification by QEMSCAN.

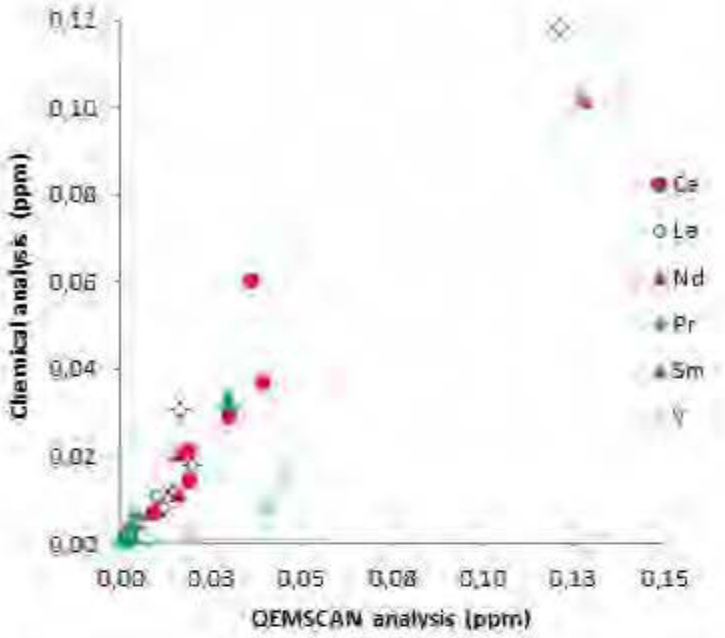

Figure 4 : Comparison of La, Ce, Nd, Pr, Sm, and Y determined by QEMSCAN and ICP

3.3. Geochemical behavior

The geochemical behavior of the materials was evaluated using weathering cells. The pH, electrical conductivity, Eh, and alkalinity values of the weathering cells are presented in Figures 4a, 4b, 4c, and 4d, respectively.

The leachates of all samples had a relatively stable pH, varying between 7 and 9.78. The leachates of the WCCR and WCCP showed a higher pH, varying between 8.5 and 9.78 while the MC, PG, and MBG samples showed a pH varying between 7.01 and 9.44. The electrical conductivity of the samples varies between 30 and 168 µS/cm. The redox potential varied from 428 to 816 mV, while the alkalinity values stabilize below 100 mg/l.

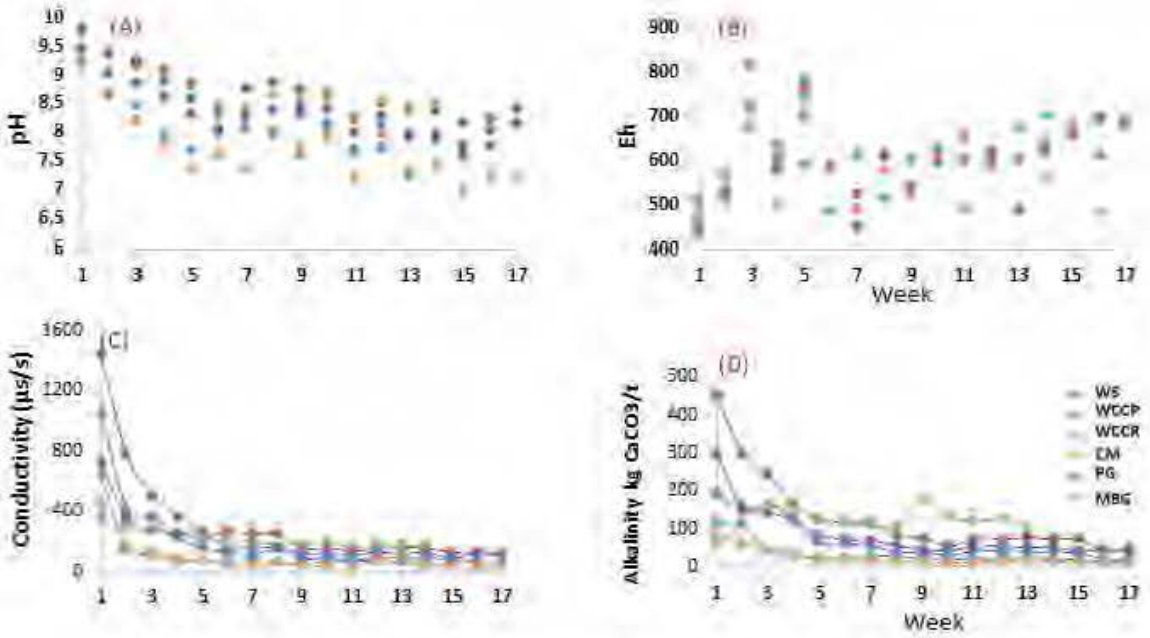

Figure 5: pH (a), electrical conductivity (µS/cm) (b), Eh (mV) (c), and alkalinity values (d) of the weathering cell leachates

The concentrations of dissolved elements (sulfates, metals, and REE are shown in Figures 5a to 5f. The concentrations of S (47.7 mg.L^{-1}), Ca (22.5 mg.L^{-1}), Zn (0.084 mg.L^{-1}), and Mn (0.31 mg.L^{-1}) in the MC were higher than in other samples (SW, WCCP, WCCR, PG, and MBG). The concentrations were often higher in the first flushes due to a combination of the leaching of oxidized products formed prior to the kinetic test, the rapid reaction and of the finer particles and their depletion, and the surface passivation of the minerals (Benzaazoua et al. 2004). The highest sum of LREE leached (figure 5f) is recorded in sample MC (31 mg/l), while the lowest sum is found in the WCCR (4 mg/l). The leaching of LREE is higher than HREE regardless of the sample nature (Figure 5). The leached concentrations of HREE are between 70 and 3.5 mg/l, with the maximum in the MC and the minimum in the WCCR. Despite the abundance of LREE relative to HREE in all samples, the HREE are higher in the leachates compared to the LREE. This suggests a higher mobility of the HREE in comparison to LREE. This behavior may be explained by: (i) ionic radius; (HREE have a high ionic radius relative to LREE, which makes them less stable in the crystal matrix, (ii) geochemical affinity of the LREE to carbonates, iron oxyhydroxides, and phosphates (iii) their geochemical speciation in the leachates.

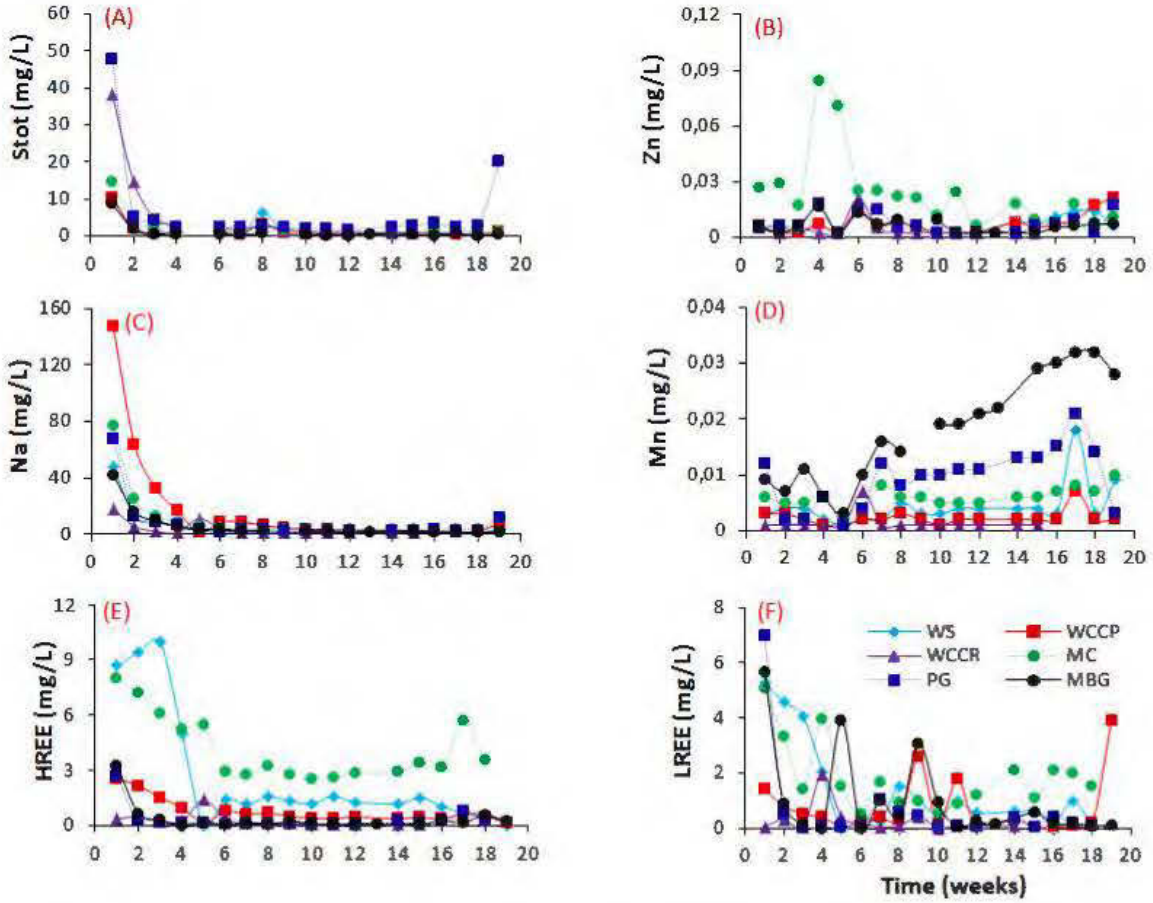

Figure 6: Leachates punctual concentrations of studied samples: total sulfur (A), Zn (B), Na (C), Mn (D), HREE (E) and LREE (F).

Conclusion

The mineralogical characterization and the geochemical behavior of REE-bearing minerals from different lithologies and a REE concentrate was investigated in this study. A thorough characterization of these samples showed that the REE-bearing minerals are either liberated, associated to gangue minerals, or included in other gangue minerals. The main REE-bearing minerals are fluobritholite, mosandrite, and eudialyte. The present study confirms that REE-bearing mineral dissolution occurs when they are in contact with water and oxygen. The leachability of LREE is lower than that of HREE.-This behavior may be explained by: (i) ionic

radius (HREE have a high ionic radius relative to LREE, which makes them less stable in the crystal matrix), and (ii) geochemical affinity of the LREE to carbonates, iron oxyhydroxides etc.

In order to better understand the geochemical behavior of REE, further research is needed: (i) advanced chemical and physical characterizations using EXAFS and XPS techniques, (ii) comparison of field tests results with those of laboratory tests, and (iii) determination of the various REE-bearing secondary minerals that can form during kinetic tests and control REE leaching from the materials.

Acknowledgements

The authors thank the URSTM, staff for their support with laboratory work and NSERC for funding of this study.

References

Benzaazoua, M., Bussière, B., Dagenais, A.M., Archambault, M., 2004. Kinetic tests comparison and interpretation for prediction of the Joutel tailings acid generation potential. Environmental Geology 46, 1086-1101.

Biennemas, K., Jones, P.T., Blanpain, B., Gerven, T.V., Yang, Y., Walton, A., Buchert, M., 2013. Recycling of rare earth earths: a critical review. Journal of cleaner production 51, 1-22.

Bouzahzah H., Benzaazoua M., Bussière B., 2014. Prediction of Acid Mine Drainage: Importance of Mineralogy and the Test Protocols for Static and Kinetic Tests Mine Water and the Environment. Mine Water and the Environment", Mine Water and the Environment, 33:54–65.

Calas, G. 2012. «Elements ». International Magazine of Mineralogy, Geochemistry, and Petrology, vol. 8, no ISSN: 1811-5209.

Chen, Zhanheng. 2011. «Global rare earth resources and scenarios of future rare earth industry». Journal of Rare Earths, vol. 29, no 1, p. 1.

Chakhmouradian, A. R., et F. Wall. 2012. «Rare Earth Elements: Minerals, Mines, Magnets (and More)». Elements, vol. 8, no 5, p. 333-340.

Chen, Zhanheng. 2011. «Global rare earth resources and scenarios of future rare earth industry». Journal of Rare Earths, vol. 29, no 1, p. 1-6.

Cheng, Zhen, Jingkun Jiang, Oscar Fajardo, Shuxiao Wang et Jiming Hao. 2013. «Characteristics and health impacts of particulate matter pollution in China (2001–2011)». Atmospheric Environment, vol. 65, no 0, p. 186-194.

Dai, Shifeng, Panpan Xie, Shaohui Jia, Colin R. Ward, James C. Hower, Xiaoyun Yan et David French. 2017. «Enrichment of U-Re-V-Cr-Se and rare earth elements in the Late Permian coals of the Moxinpo Coalfield, Chongqing, China: Genetic implications from geochemical and mineralogical data». Ore Geology Reviews, vol. 80, p. 1-17.

Davris, P., S. Stopic, E. Balomenos, D. Panias, I. Paspaliaris et B. Friedrich. «Leaching of rare earth elements from eudialyte concentrate by suppressing silica gel formation». Minerals Engineering.

Edahbi, M., Plante, B., Bouzahzah, H., Benzaazoua, M. 2015. Mineralogical and geochemical study of rare earth elements from a carbonatite deposit. Proceedings of the 13th SGA biennial meeting, Nancy, France, 24-27 août 2015.

Elzinga, E. J., R. J. Reeder, S. H. Withers, R. E. Peale, R. A. Mason, K. M. Beck et W. P. Hess. 2002. «EXAFS study of rare-earth element coordination in calcite». Geochimica et Cosmochimica Acta, vol. 66, no 16, p. 2875-2885.

Erguler, Zeynal Abiddin, et Güzide Kalyoncu Erguler. 2015. «The effect of particle size on acid mine drainage generation: Kinetic column tests». Minerals Engineering, vol. 76, p. 154-167.

Hong, Feng. 2006. «Rare Earth: Production, Trade and Demand». Journal of Iron and Steel Research, International, vol. 13, p. 33-38.

Gupta, C., Krishnamurthy, N., 1992. Extractive metallurgy of rare earths. Int. Mater. Rev. 37, 197–248.

Hao, Zhe, Yonghua Li, Hairong Li, Binggan Wei, Xiaoyong Liao, Tao Liang et Jiangping Yu. 2015. «Levels of rare earth elements, heavy metals and uranium in a population living in Baiyun Obo, Inner Mongolia, China: A pilot study». Chemosphere, vol. 128, p. 161-170.

Humphries, Marc. 2013. «Rare Earth Elements: The Global Supply Chain». Congressional Research Service, 7-5700 (http://www.fas. org/sgp/crs/natsec/R41347.pdf).

Jia, Y. Q. 1991. «Crystal radii and effective ionic radii of the rare earth ions». Journal of Solid State Chemistry, vol. 95, no 1, p. 184-187.

Lema. I.B., Leal Filho.w., 2016. "Rare earth industry, Technological, Economic, and environnemental Implications".

Lipin, B.R, Mackay, G.A., 1989. Geochemistry and mineralogy of rare earth elements. Mineralogical society of America, volume 21.

Peelman, Sebastiaan, Zhi H. I. Sun, Jilt Sietsma et Yongxiang Yang. 2016. «Chapter 21 - Leaching of Rare Earth Elements: Review of Past and Present Technologies A2 - Lima, Ismar Borges De». In Rare Earths Industry, Walter Leal Filho, p. 319-334. Boston: Elsevier.

Plante, B., M. Benzaazoua, and B. Bussière. 2010b. “Kinetic Testing and Sorption Studies by Modified Weathering Cells to Characterize the Potential to Generate Contaminated Neutral Drainage.” Mine Water and the Environment 30 (1) (December 19): 22–37.

Plante, B., Bussière, B., Benzaazoua, M., 2014. Lab to field scale effects on contaminated neutral drainage prediction from the Tio mine waste rocks. Journal of Geochemical Exploration 137, 37-47.

Sapsford, D. J., R. J. Bowell, J. N. Geroni, K. M. Penman et M. Dey. 2012. «Factors influencing the release rate of uranium, thorium, yttrium and rare earth elements from a low grade ore». Minerals Engineering, vol. 39, p. 165-172.

Technical Report prepared by Roche in collaboration with SGS, Golder and Genivar, 2012. " Feasibility study for Kipawa project, Temescamingue Area, Québec, Canada". Le PDF est accessible par le lien suivant: http://www.matamec.com/vns-site/uploads/ documents/ matamecfs2013sedar.pdf.

ANNEXE C - ARTICLE 8 - MINERALOGICAL CHARACTERIZATION AND GEOCHEMICAL BEHAVIOR OF RARE EARTH ELEMENTS FROM A CARBONATITE DEPOSIT

Cet article est présenté à la conférence Process Mineralogy '17. Cape Town, South Africa en 2017

M. Edahbi [a]; B. Plante [a]; M. Benzaazoua [a]; L. Kormos[b] ; M. Pelletier [C]

[a] Université du Québec en Abitibi-Témiscamingue (UQAT), 445 boul de l'Université, Rouyn-Noranda J9X 5E4, QC, Canada.

[b]XPS consulting and testwork services, SudBury, Canada

[C]Ressources Géoméga, St-Lambert, Canada

Abstract

The paper will focus on the geochemical characterization of the Montviel carbonatite deposit, located in Quebec (Canada). The five main lithologies of the deposit (ore and waste rocks) were sampled, characterized, and submitted to kinetic testing in order to investigate their REE leaching potential. A REE concentrate was also prepared from the ore sample using a combination of gravimetric and magnetic methods. All samples were submitted to a Qemscan analysis coupled to EPMA (electron probe microanalysis). These results indicate that the main REE-bearing minerals are burbankite, Kukharenkoite-Ce, monazite, and apatite.

The geochemical behavior of the waste rocks and ore samples was studied using humidity cells while a weathering cell (small-scale humidity cell) was used for the REE concentrate. The kinetic testing results show that low concentrations of light REE are leached (8.8-139.6 µg/l total light REE) from the materials. These results are explained by a low reactivity of the REE-bearing carbonates in the kinetic testing conditions, and by precipitation of secondary REE minerals.

Keywords: Carbonatite, rare earth elements, Qemscan mineralogy, geochemical behavior

1. Introduction

During the last decades, rare earth elements (REE), also called lanthanides (La to Lu, Sc, and Y), are considered as strategic metals, as they are a key component of modern technologies. REE are subject to high supply risk. China currently produces 99 % of heavy rare earth elements (HREE)

and 87 % of light rare earth elements (LREE) (European Commission, 2014). The REE prices are significantly affected by the Chinese monopoly. As a circumvention strategy; mining companies have decided to develop new mining projects in other countries such as Australia, USA, and Canada. Carbonatites are known for their REE potential due to the favourable geological context for REE-bearing minerals crystallization and formation.

Several carbonatite deposits in Canada have emerged as a possible resource for the REE, such as the Montviel deposit (Quebec, Canada). The REE-bearing minerals within the Montviel deposit are contained mainly in ferrocarbonatites, breccia, and calcio/silicocarbonatites (Edahbi et al., 2015).

Water-rock interaction within mine wastes influences the mine drainage quality. The release of REE and other associated elements is controlled by the mineralogical composition of the rocks and by pH, temperature, degree of saturation, secondary precipitation, and the presence of impurities within the reactive minerals, etc.

In order to anticipate potential environmental impacts of mining, the prediction of REE leaching from mine wastes is required. The determination of the geochemical behavior of REE mine wastes requires an extensive mineralogical characterization of the materials and kinetic testing of the different lithologies of the deposit. This work aims to understand the geochemical behavior of the Montviel mine wastes in order to predict its water drainage quality.

2. Materials and methods

2.1. Material sampling

The materials used in this work were supplied by Geomega Resources. Approximately 5 kg of the different lithologies were sampled from drill cores: low-grade and high-grade ferrocarbonatites (FeC-LG and FeC-HG, respectively), silicocarbonatite (SiC), calciocarbonatite (CaC), and breccia (BreC). The REE concentrate (REE-ConC) was prepared using a Mozley table and a Knelson concentrator from a finely ground aliquote of the FeC-HG sample (Bunge et al., 1991; Burt, 1984; Jordens et al., 2016). The samples were dried at low temperature (<60°C), crushed, homogenized, and stored in sealed plastic bags.

2.2. Physical and chemical analysis

The specific gravity (Gs) was determined with a Micromeritics Helium Pycnometer. The grain size distributions were analyzed using a laser analyzer (Malvern Mastersizer S). The specific surface area (S.S.A.) was determined by using a Micromeritics Surface Area Analyser using the B.E.T. method (Brunauer et al., 1938).

The whole-rock analyses were performed using an X-ray Fluorescence (Bruker, Tiger Model), analyzer on a powdered aliquot of the samples. Chemical analyses were carried out by Inductively Coupled Plasma (ICP-AES/MS) after a multi-acid digestion (HCl, HNO_3, Br_2, and HF). The total sulfur and carbon contents were measured using an induction furnace analyzer (ELTRA CS-2000). The acid-base accounting (AP: acid-generating potential; NP: neutralization potential; NNP=NP-AP: net neutralization potential) was determined using the modified Sobek procedure (MEND, 1997).

The physico-chemical parameters of the weathering cell leachates (pH, conductivity, Eh) were determined using a pH/Eh/electrical conductivity meter. The ICP-MS was used to analyze the REE concentrations in the weathering cell leachates, while the other elements were measured using the ICP-AES on an acidified (2 % HNO_3) and filtered (<0.45 μm) aliquot.

2.3. Mineralogical analyses

The crystalline minerals were identified by X-ray diffraction (XRD; Brucker D8 Advance, with a detection limit and precision of approximately 0.1 to 0.5 %, operating with a copper cathode, K_α radiation) using the DIFFRACT.EVA program, and quantified using the TOPAS 4.2 program based on a Rietveld (1993) interpretation. The acid base accounting (ABA) were determined by using the protocol prescribed by Lawrence and 128 Wang (1996). The acid-generation potential (AP) and neutralization potential (NP) were calculated using the percentage of sulfur and carbon respectively. The net neutralization potential (NNP) was calculated (NNP=NP-AP).

Mineralogical observations and local X-ray microanalysis were realized on a Hitachi S-3500N scanning electron microscope (SEM), equipped with an Energy-Dispersive X-ray Spectroscopy (EDS) probe (Oxford Instruments 20 mm^2 X-Max Silicon Drift Detector (SDD)). The polished section observations were determined using Backscattered electrons imaging mode (BSE). Electron probe microanalyses (EPMA), which have lower limits of detections than the EDS-SEM system, were also used to analyze the trace metal composition of certain accessory minerals known for their affinity to REE, such as apatite.

In order to understand the effect of mineralogy, particle size, and degree of liberation on the geochemical behavior of REE-bearing minerals, a QEMSCAN (quantitative evaluation of materials by scanning electron microscopy) analysis was performed. QEMSCAN is a system based on image analysis which allows to measure mineralogical variability at the micrometer-scale (Jordens et al., 2016; Pascoe et al., 2007; Smythe et al., 2013).

2.4. Weathering cells

A weathering cell test was used to evaluate the geochemistry of the REE concentrate (Bouzahzah et al. 2014; Plante et al., 2010; Villeneuve et al., 2004). The weathering cells consist of bi-weekly flushes by 50ml of deionized water on 67g of a sample. The sample is left to dry under ambient air between flushes. The bi-weekly leachates are combined and analyzed for their pH, Eh, electrical conductivity, and dissolved constituents.

3. Results and discussion

3.1. Physical properties

The physical properties of the samples studied are summarized in Table 1. The Gs of the samples range from 3 to 3.60. The specific gravity of the REE-ConC (3.60) is greater than that of all samples (3.00-3.36) due to its higher content in sulfides and REE-bearing minerals. The FeC required to be finely ground in order to ensure a high recovery of REE-bearing minerals in the REE concentrate.

The D_{50} and D_{90} values respectively represent the grain size for 50, and 90 % passing on the cumulative grain size distribution curve. The D_{50} and D_{90} values (the grain size passing 50 and 90 % on the cumulative grain size distribution curve, respectively) also highlight the grain size differences between the waste rocks samples and REE-ConC sample. The D_{50} and D_{90} values of the REE-ConC are significantly lower (124-209 μm) than for the waste rock samples (D_{50}: 2075-2775 μm and D_{90}: 5000-5500 μm).

Table 2 Physical properties of the studied samples

	Unit	REE-ConC	BreC	CaC	FeC-LG	FeC-HG	SiC
Carbon	(%)	6.98	5.69	9.31	9.77	8.73	6.79
Sulfur	(%)	2.77	0.9	0.4	0.2	0.8	0.4
D_{50}	(μm)	124	2250	2075	2775	2250	2250

D_{90}	(µm)	209	5100	5000	5500	5200	5000
Specific gravity		3.60	3.00	3.10	3.36	3.30	3.26

3.2. Chemical composition

The chemical characteristics of the samples studied are summarized in Table 2. The chemical characterizations show that the REE-ConC sampe contains higher concentrations of REE, Fe, Ca, Mg, Mn, Zn, Na, K, Ba, and Pb compared to the other samples. Indeed, the highest sum of LREE is recorded in the REE-ConC (36226 mg/l), while the lowest sum is found in the BreC (LG) (4400 mg/l). The samples are rich in LREE compared to HREE. Lanthanum (La), cerium (Ce), and neodymium (Nd) are the most abundant elements in all samples, with a maximum content in the REE-ConC and a minimum content in the breccia sample.

The acid-base accounting results show that the AP values are all lower ($4.1<AP<86.5$ kg $CaCO_3$/t) than the NP values ($44<NP<602$ kg $CaCO_3$/t), leading to NNP values within the non-acid generating zone (>20 kg $CaCO_3$/t).

Table 3 Chemical and ABA characterization of the samples studied (elements in mg/l; AP, NP and NNP in kg $CaCO_3$/t)

	REE-ConC	Brec	CaC-LG	FeC- LG	FeC-HG	SiC- LG
Chemical composition						
Fe	155700	6800	12000	20000	16000	12000
Ca	70130	19000	19000	11000	9200	11000
Mg	26990	2600	2300	4200	3300	3800
Mn	11570	550	1300	2100	1700	1300
Zn	1186	67	62	81	29	49
Na	11900	320	450	120	900	460
K	3240	1500	910	750	960	1600
Ba	35000	510	1800	1400	1900	2600
Pb	6363	26	12	8	8	8
Rare earth elements						
La	10881	500	2 500	2 100	8 900	1 100

Ce	19302	3 200	5 400	4 200	14 000	2 200
Pr	1414	400	680	450	1400	250
Nd	4629	1 500	2 200	1 300	4 100	850
Sm	420	270	330	150	390	110
Eu	80	75	77	31	78	28
Gd	156	200	270	99	290	66
Tb	0,9	24	20	6.2	15	5.5
Dy	28	110	74	16	31	18
Ho	2,9	18	11	2	3.3	2.5
Er	6,4	42	18	3.7	5.5	5.1
Tm	0,3	4,3	1.5	0.39	0.49	0.56
Yb	2,7	21	6.9	2.3	2.9	3.1
Lu	0,3	2.3	0.75	0.29	0.35	0.38
ΣLREE	36226	5600	10780	8050	28400	4400
ΣHREE	698	764	800	298	804	222
AP	86.5	16.2	7.8	4.1	20.3	4.4
NP	581.3	472	602	542	493	442
NNP	494.9	455.8	594.2	537.9	472.7	437.6

3.3. Mineralogical characterization

The mineralogy of REE-ConC, determined by XRD analysis, is dominated by carbonates (i.e. ankerite, 34-43wt. %; siderite, 12-16wt. %; calcite, 8-11wt. %), bassanite (3-5wt. %), ilmenite (1wt. %),, biotite (7-16wt. %), sulfides, and hematite (0-10wt. %),. Two types of REE-bearing minerals are present: carbonates (burbankite, Kukharenkoite, synchysite) and phosphates (monazite). However, the concentration of the possible Nb/Th-bearing minerals is too low to be detected by XRD. The mineralogical composition of the REE-ConC is given in Table 3. It is important to note that a significant proportion of the REE are distributed in the <106 μm size fraction. The mineralogical data shows that carbonernaite, ancylite, barytocalcite, and apatite minerals are undetectable by XRD.

Table 4 mineralogical composition of the FeC-HG before and after concentration.

Mineral	Formula	Phase (%)	
		Before concentration	After concentration
Ankerite	$Ca(Fe,Mg,Mn)(CO_3)_2$	43.74	34.47
Siderite	$FeCO_3$	11.68	16
Monazite	$(La,Ce,Nd)PO_4$	0.92	3.4
Biotite	$K(Fe, Mg)_3(AlSi_3)O_{10}(F,OH)_2$	16.22	6.65
Burbankite	$(Na,Ca)_3(Sr,Ba,Ce)_3(CO3)_5$	5.31	1.3
Strontianite	$SrCO_3$	1.1	0.23
Kukharenkoite	$Ba_2Ce(CO_3)_3F$	4.03	1.56
Calcite	$CaCO_3$	7.9	11.44
Pyrrhotite	Fe(1-x)S	-	3.21
Pyrite	FeS_2	0.78	2.1
Quartz	SiO_2	2.33	3.25
Synchysite-Ce	$CaCe(CO_3)_2F$	0.9	0.26
Ilmenite	$FeTiO_3$	3.18	5.23
Bassanite	$2CaSO_4•(H_2O)$	-	9.62
Hematite	Fe_2O_3	1.41	1.12
Pyrochlore	$(Na,Ca)_2Nb_2O_6(OH,F)$	0.45	-
	Total	100	100

These XRD results are confirmed through the other mineralogical investigations performed. The SEM-EDS results show that: (i) REE are associated with the minerals barytocalcite, apatite, and a Ba-Sr-REE carbonate; (ii) all analysed minerals mostly contain LREE (La, Ce, Pr, Nd, Sm); (iii) two groups of REE-bearing minerals (carbonates and phosphates) were detected with variable concentrations of REE.

The QEMSCAN observations summarized in figure 1 show that sulfides and oxides are more abundant in the REE-ConC in comparison with other lithologies, pyrite being the most abundant. The main REE-bearing minerals are ancylite, burbankite, carbonernaite, kukharenkoite, qaqarssukite, monazite, and apatite, while the gangue minerals are mainly other carbonates, oxides,

and sulfides. All REE-bearing minerals are liberated (more than 70 %), especially in the REE-ConC. The results are summarized in Figure 2.

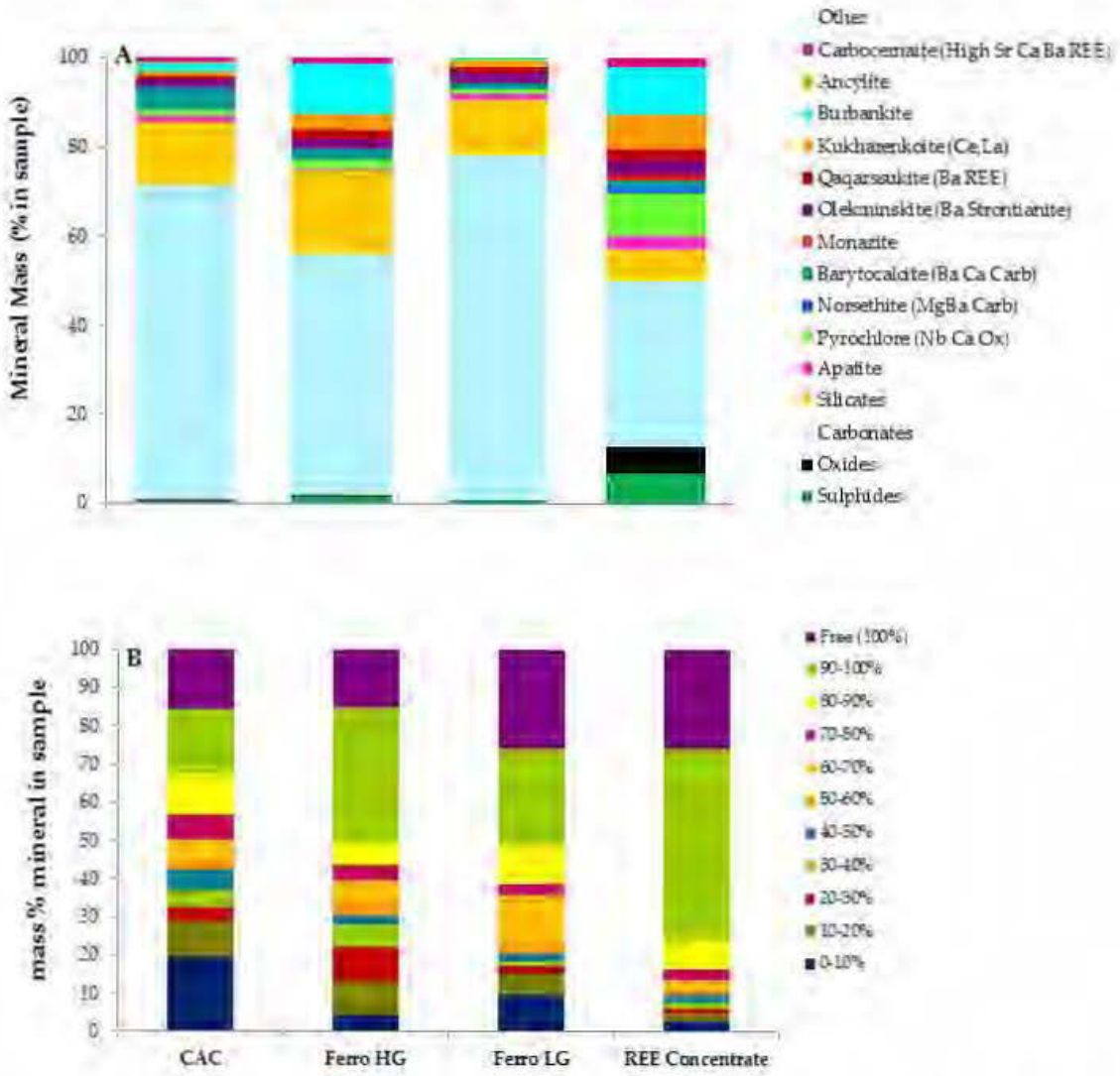

Figure 1 : Mineralogical composition (A) and liberation of REE-bearing minerals (B) within the REE concentrate and waste rocks samples.

3.4. Distribution of the REE within the REE concentrate

The LREE, Nb, and Th display a similar trend, with their concentrations increasing with decreasing particle size (Figure 2). In general, 41 % of LREE, 36 % of Nb, and 19 % of Th are present in the size fraction below 106 µm. This distribution of the LREE in the fine fractions could be explained by a higher grindability of REE-bearing minerals in comparison with other gangue minerals.

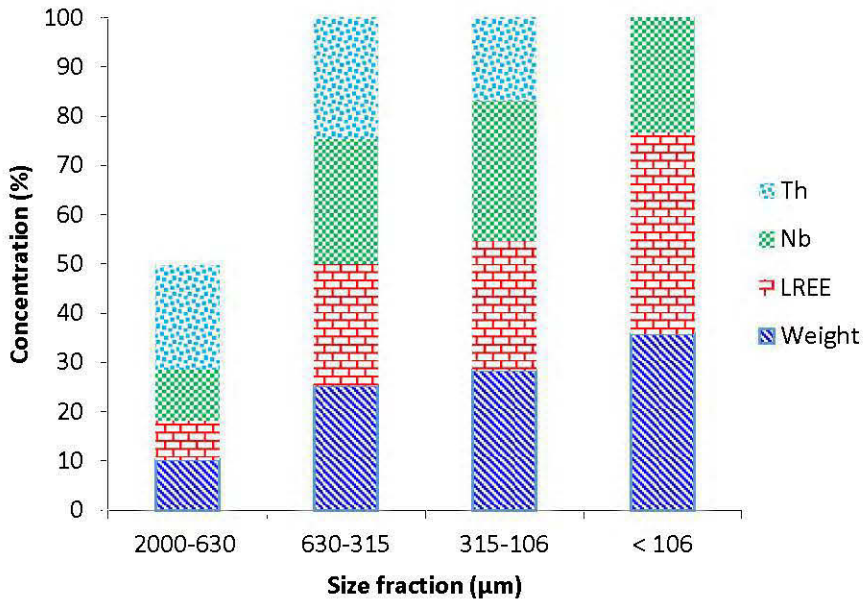

Figure 2 : Distribution of mass, LREE and rare metals by size-fractions in the REE-ConC.

3.5. Geochemical behavior

The weathering cell test results are shown in Figure 3. The pH of all the cell leachates remains alkaline (7.27-8.95) during the test. The electric conductivities of the leachates stabilize rapidly between 117 and 169 µS/cm. The redox potential (Eh) varied from 228 to 553 mV. The alkalinity values stabilize between 37 and 110 mg $CaCO_3$/l, while the acidity is always below 5 mg $CaCO_3$/l. All these parameters stabilize after the first 60 days approximately.

The LREE concentrations are higher in the leachates from the REE-ConC (1-133 µg/l) compared to those of HREE (0.03-61 µg/l). The HREE are in lower concentrations in the solid samples relative to the LREE (Table 2). However, the proportion of HREE to LREE leached during the weathering cell tests are higher than their relative contents in the solids. This suggests that the LREE have a lower mobility than the HREE. This could be explained by the fact that the LREE have larger ionic radii and higher valences than the HREE, which probably favors their precipitation as secondary minerals.

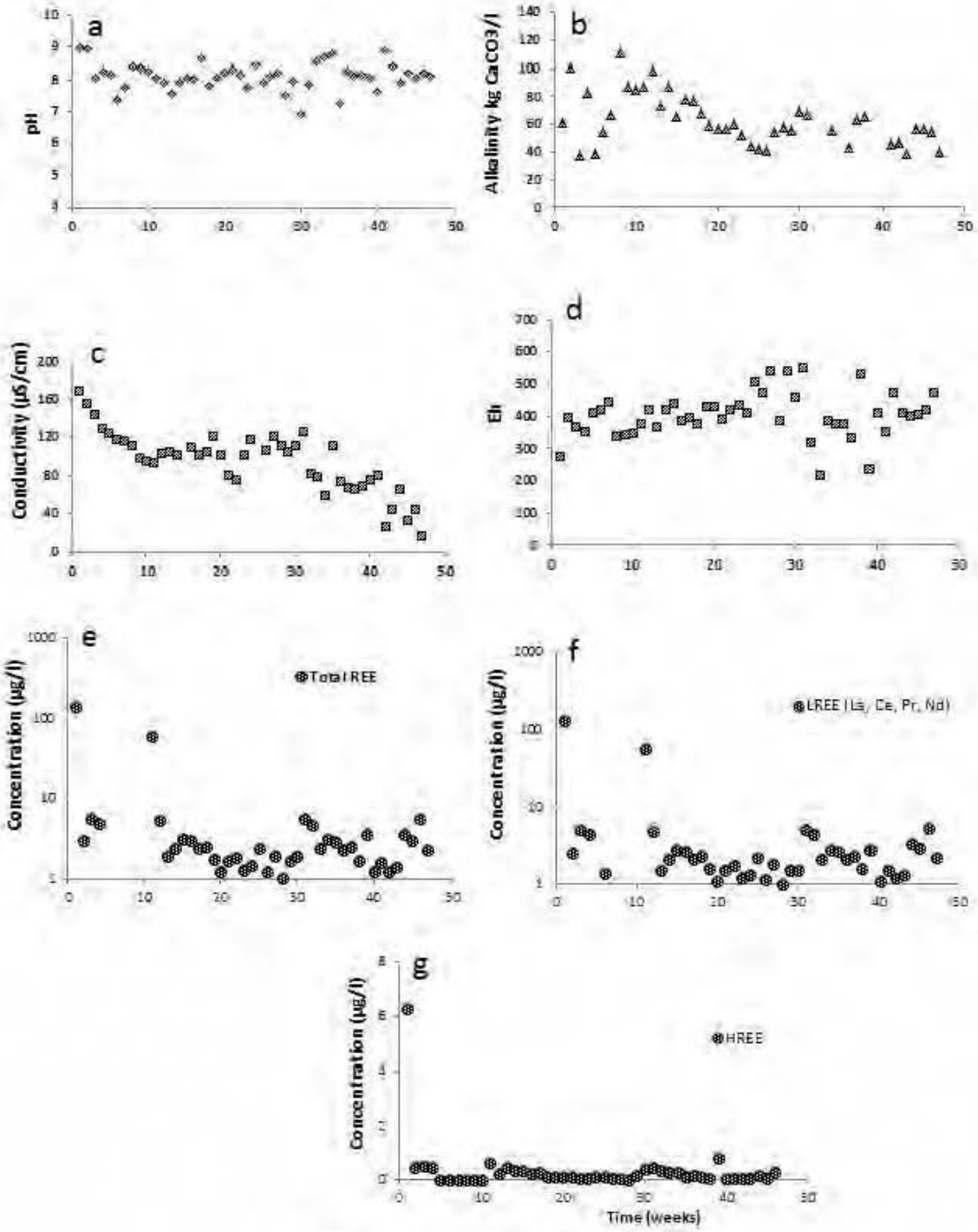

Figure 3 : Weathering cell results on REE-ConC.

Conclusion

This work examined the geochemical behavior of REE from a carbonatite deposit. The conclusions are as follows:

- The combination of the Mozley table and the knelson concentrator is a good technique for concentrating REE-bearing minerals;
- The REE, Nb, and Th are more concentrated in the finer fractions, and mostly associated with carbonates;
- Several accessory minerals contain REE, such as apatite and pyrochlore;
- The leachability of REE from the studied carbonatite deposit is low in weathering cell conditions;
- The mobility of LREE is lower compared to HREE in the weathering cell test conditions.

Acknowledgements

The authors thank the URSTM, staff for their support with laboratory work and NSERC/Geomega Resources for funding of this study.

References

Alderton, D.H.M., Pearce, J.A., Potts, P.J., 1980. Rare earth element mobility during granite alteration: evidence from southwest England. Earth Planet. Sci. Lett. 49, 149–165.

Benzaazoua, M., Marion, P., Liouville-Bourgeois, L., Joussemet, R., Houot, R., Franco, A., Pinto, A., 2002. Mineralogical distribution of some minor and trace elements during a laboratory flotation processing of Neves-Corvo ore (Portugal). Int. J.Miner. Process. 66, 163–181.

Bunge, R.C., Fuerstenau, D.W., 1991. Separation characteristics of a magnetogravimetric separator. In: Proceeding of the XV11th International Mineral Processing Congress, Dresden, vol. 3, pp. 31–42.

Burt, R.O., 1984. Gravity Separation Technology. Elsevier Science Publishers, Amsterdam.

Censi, P., F. Saiano, A. Pisciotta et N. Tuzzolino. 2014. «Geochemical behaviour of rare earths in Vitis vinifera grafted onto different rootstocks and growing on several soils». Science of The Total Environment, vol. 473–474, p. 597-608.

Edahbi, M., Plante, B., Bouzahzah, H., Benzaazoua, M. 2015. Mineralogical and geochemical study of rare earth elements from a carbonatite deposit. Proceedings of the 13th SGA biennial meeting, Nancy, France, 24-27 août 2015.

Falconer, A., 2003. Gravity separation: old technique/new methods. Phys. Separat. Sci. Eng. 12, 31–48.

Grammatikopoulos, T., Mercer, W., Gunning, C., 2013. Mineralogical characterization using QEMSCAN of the Nechalacho heavy rare earth metal deposit, Northwest Territories, Canada. Can. Metall. Quart. 52 (3), 265–277.

Jordens, A., C. Marion, T. Grammatikopoulos et K. E. Waters. 2016. «Understanding the effect of mineralogy on muscovite flotation using QEMSCAN». International Journal of Mineral Processing, vol. 155, p. 6-12.

Jordens, Adam, Chris Marion, Ray Langlois, Tassos Grammatikopoulos, Richard S. Sheridan, Chaoyi Teng, Hendrix Demers, Raynald Gauvin, Neil A. Rowson et Kristian E. Waters. 2016. «Beneficiation of the Nechalacho rare earth deposit. Part 2: Characterisation of products from gravity and magnetic separation». Minerals Engineering, vol. 99, p. 96-110.

Liu, Haiyan, Huaming Guo, Lina Xing, Yanhong Zhan, Fulan Li, Jingli Shao, Hong Niu, Xing Liang et Changqing Li. 2016. «Geochemical behaviors of rare earth elements in groundwater along a flow path in the North China Plain». Journal of Asian Earth Sciences, vol. 117, p. 33-51.

MEND, 1996. Determination of neutralization potential for acid rock drainage prediction. MEND Report 1.16.3. Author: Lawrence, R.W., Wang, Y., Canada.

Pascoe et al., 2007 R.D. Pascoe, M.R. Power, B. Simpson:QEMSCAN analysis as a tool for improved understanding of gravity separator performance, Miner. Eng., 20 (2007), pp. 487–495.

Richards, R.G., Mc Hunter, D.M., Gates, P.J., Palmer, M.K., 2000. Gravity separation of ultra-fine (0.1 mm) minerals using spiral separators. Minerals Engineering 13 (1), 65–77.

Smythe, Duncan M., Annegret Lombard et Louis L. Coetzee. 2013. «Rare Earth Element deportment studies utilising QEMSCAN technology». Minerals Engineering, vol. 52, p. 52-61.

Zhou, J., et Y. Gu. 2016. «Chapter 6 - Geometallurgical Characterization and Automated Mineralogy of Gold Ores A2 - Adams, Mike D». In Gold Ore Processing (Second Edition), p. 95-111: Elsevier.

Zhu, Zhaozhou, Cong-Qiang Liu, Zhong-Liang Wang, Xiaolong Liu et Jun Li. 2016. «Rare earth elements concentrations and speciation in rainwater from Guiyang, an acid rain impacted zone of Southwest China». Chemical Geology, vol. 442, p. 23-34.

ANNEXE D - ARTICLE 9 - CIL GOLD LOSS CHARACTERIZATION IN A DOUBLE REFRACTORY ORE: CREATING A SYNERGISTIC APPROACH BETWEEN MINERALOGICAL CHARACTERIZATION, DIAGNOSTIC LEACH TESTS AND PREG-ROBBING TESTS

Cet article est accepté dans la revue Hydrometallurgy, 2018

Edahbi M[a]; Mermillod-Blondin.R[b]; Plante B[a]; Benzaazoua M[a]

[a] Université du Québec en Abitibi-Témiscamingue (UQAT), 445 boul de l'Université, Rouyn-Noranda J9X 5E4, QC, Canada.

[b] Technical Services, Agnico Eagles Mines, QC, Canada

Abstract

A double refractory gold ore contains gold in solid-solution in both sulphides and carbonaceous matter. The diagnostic leach test (DLT) and preg-robbing (PR) approaches are widely used to investigate the occurrence and the distribution of refractory gold. The DLT serves to qualitatively evaluate the gold occurrences within the ore. Preg-robbing, or the ore's capacity to fix dissolved gold, is evaluated to determine physical surface interactions (preg-borrowing) and chemical interactions (preg-robbing). The objective of this project is to characterize the refractory gold in AEM's Kittilä ore using DLT and PRT approaches coupled with mineralogical analyses to confirm testing.

The studied material was sampled at the outlet of the autoclave and cyanidation processes. Different reagents were used in the DLT procedure: sodium carbonate (Na_2CO_3), sodium hydroxide (NaOH), hydrochloric acid (HCl), and nitric acid (HNO_3). The final residue was roasted at a temperature of around 900°C. These reagents were selected based on the mineralogical composition of the studied samples. After each leaching test/roasting, cyanide leaching with activated carbon was required to recover gold cyanide. The results show that gold is present in two forms: to a small extent in its native form and in association with sulfide minerals (i.e. arsenopyrite, pyrite) and autoclave secondary minerals such as calcium sulfate, iron sulfates and iron oxides (i.e. hematite), along with carbonaceous matter. The results of PR tests indicate that 1 % of the gold is non-recoverable applying only cyanidation.

Keywords: Refractory gold; characterization; diagnostic leaching tests; preg-robbing tests; cyanide leaching.

1. Introduction

The gold from the Kittilä mine is in a refractory form, where gold atoms are associated with the crystal lattice of arsenopyrite and pyrite (Daniel et al., 2009; Kojonen et al., 1999). Only 10-20% of the ore is in its native form. It is also reported that refractory gold-bearing sulphides are commonly associated with native carbon (i.e. amorphous and graphite) (Radtke et al., 1970; Schmitz et al., 2001a; Stenebråten et al., 2000; Wyche et al., 2015). Moreover, the gold ore from the Kittilä mine is also associated with carbonaceous matter which could reduce the gold recovery by the high potential adsorption capacity of the carbonaceous material (preg-robbing phenomena) (Wadnerkar et al., 2015). Physical and mineralogical characterization of the native carbon could affect the extractive metallurgy of the refractory gold (Abotsi et al., 1986).

The metallurgical treatment of gold is generally performed, to recover gold from primary and secondary minerals, in two stages (Cui and Zhang, 2008): gold extraction and refining of the metal. The extraction process is carried out using cyanidation (Bas et al., 2017; Botz et al., 2016). The pregnant leach solution was purified using activated carbon adsorption. However, the extraction of refractory gold is generally difficult to accomplish due to encapsulated/locked gold within gangue minerals, solid-solution gold in pyrite and arsenopyrite, and cyanide consumption due to high amounts of sulfide minerals (Dunn and Chamberlain, 1997; Fraser and Wells, 1991; Fleming et al., 2011). Consequently, the performance of reagents is highly limited, despite the use of various reagents at different conditions (i.e. acidic and/or basic) (Abruzzese et al., 1995; Aylmore et al., 2001; Gönen et al., 2007). In such cases, pre-treatments are required to improve gold recovery at economically viable levels (Climo et al., 2000; Zadehfini et al., 2011). Gravity separation, ionic flotation, roasting, high pressure oxidation and biological oxidation are the most common techniques used in the gold industry to extract refractory gold (Fraser and Wells, 1991; Marsden and House, 2006; La Brooy et al., 1994; Syed, 2012). The hydrometallurgical process is the most used during the gold recovery compared to other processes such pyrometallurgical process (Dunn et al., 1997). However, all these methods are costly and require a major long-term investment. Mineralogical and surface characterization techniques (ICP-MS, SIMS, QEMSCAN, and EPMA)

are recommended to improve the metallurgical efficiency as they allow the refractory gold-bearing minerals and their degree of liberation to be determined (Derycke et al., 2013; Goodall et al., 2005).

Diagnostic leach tests (DLT) and preg-robbing tests (PRT) are widely used to investigate the occurrence and distribution of refractory gold (Dimov and Hart, 2014; Dunne et al., 2012; Hausen et al., 1984; Lorenzen, 1995; Menne et al., 1992; Miller et al., 2016; Simmons, 1995). The DLT serves to qualitatively evaluate the gold occurrences within the ore. The PRT indicates the ore's capacity to fix dissolved gold. It evaluates the physical surface interactions (preg-borrowing), and chemical interactions (preg-robbing). Gold recovery at the Kittilä mine is highly dependent on the carbonaceous matter (Figure 1). A high carbon content in the tailing leads to high gold losses. The estimation of the ore's sorption capacity was initially evaluated by cyanidation tests using activated carbon. Recently, high gold losses were observed. The typical relationship between the total organic carbon (TOC) content and the sorption capacity was not observed. A preliminary hypothesis was that the carbon preg-robbing capacities may vary within the deposit. The present study aims to test this hypothesis.

Currently, further research is necessary to fill in important gaps regarding refractory gold recovery. The challenges are to determine the link between the gold in the tailings and the total TOC, and the relationship between reactivity and carbon maturity. The specific aims of this study are: (1) to evaluate the gold distribution in four different samples by DLT in alkaline and acid conditions and (2) to estimate the PR capacity of the carbonaceous materials using different adsorption tests (with and without activated carbon).

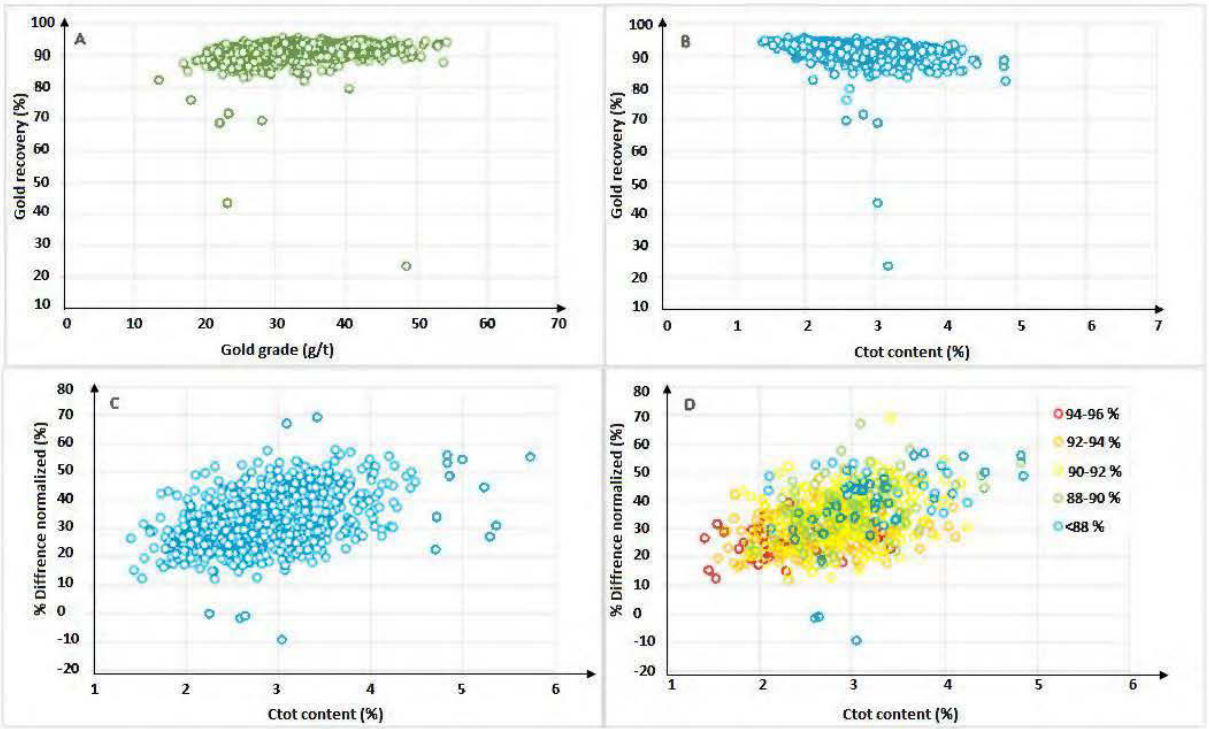

Figure 1: Gold Recovery as a function of Au grade and C_{tot} Content (A and B), and Gold Recovery as a function of TOC Content and TOC Reactivity (calculation via bottle roll tests with/without activated carbon).

2. Material and Methods

Mineralogical characterization, DLT and adsorption tests were performed to study the gold distribution and preg-robbing, using four samples taken from the mill CIL tailings at the Kittilä Mine in Finland (oxidized tailings). The following section describes the materials and methods used in more detail.

2.1. Sampling

Approximately 10 kg of four CIL tailings (identified as Tail-17, Tail-19, Tail-22, and Tail-25 respectively taken September 17, 19, 22, and 25, 2016) were sampled from the metallurgical circuit following CIL treatment (Figure 2). These samples were dried, de-agglomerated and homogenized separately.

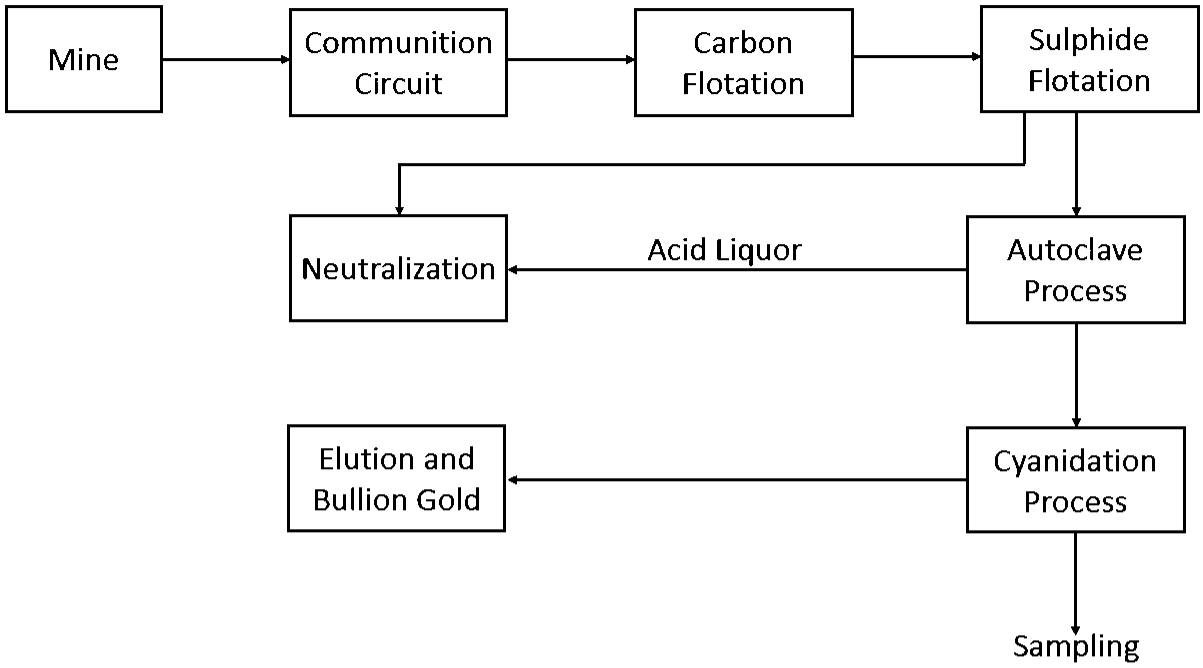

Figure 2: Au processing flow chart for Kittilä Mine and sampling locations

The main characteristics of the studied samples are depicted in Table 1. Tail-17 and Tail-19 are characterized by low carbon content (2.74 to 2.87%) compared to Tail-22 and Tail-25. In terms of TOC reactivity, Tail-17 and Tail-22 are far more reactive than Tail-19 and Tail-25. In terms of gold recovery, Tail-17, Tail-19, and Tail-25 present similar grade recovery (91-93%) contrary to Tail-22 which is characterized by high carbon and high reactivity (Figure 3).

Table1. Metallurgical Characteristics, Ctot Content, and TOC Reactivity of Samples

Sample	**TOC Content**	**Ctot (%)**	**TOC Reactivity**	**% Difference**	**Recovery (%)**
Tail-17	Low carbon	2.74	Highly reactive	41	93
Tail-19	Low carbon	2.87	Low reactivity	32	91
Tail-22	High carbon	3.40	Highly reactive	45	89
Tail-25	High carbon	3.07	Low reactivity	27	92

% Difference= 1-(Recovery with activated carbon / Recovery without activated carbon)

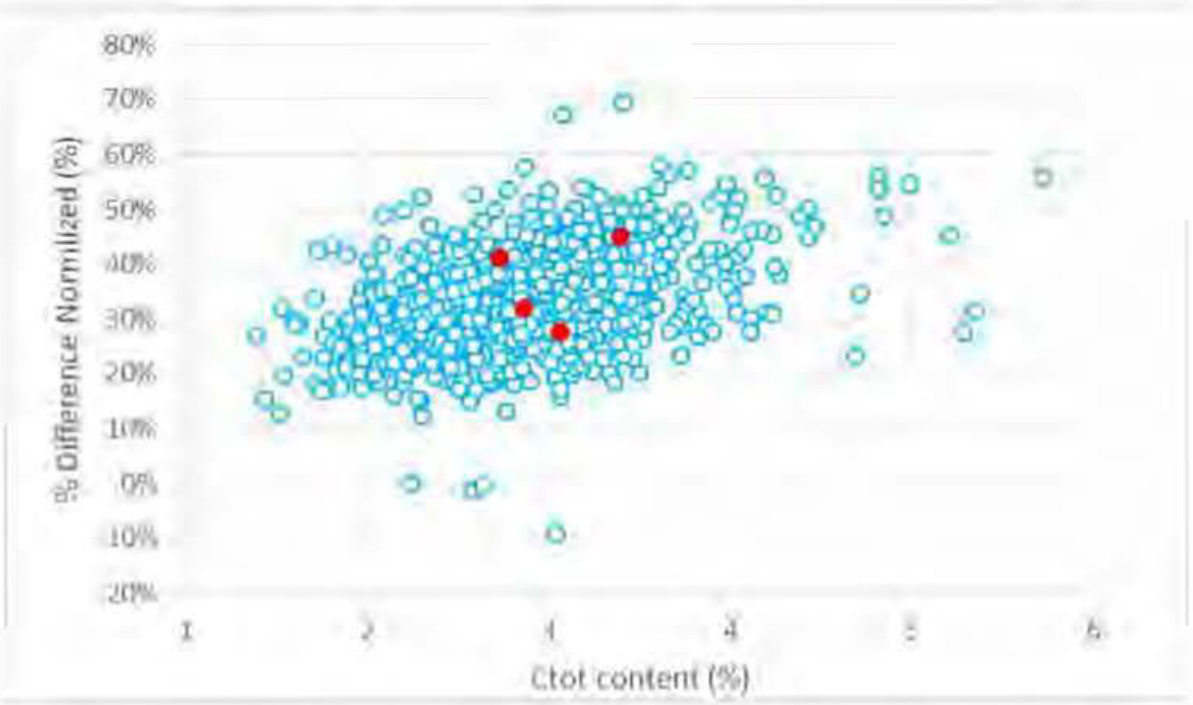

Figure 3: Gold Recovery as a Function of C_{tot} Content in Studied Samples (in red).

2.2. Analytical Methods

The grain size distributions were analyzed using a laser analyzer (Malvern Mastersizer S). The chemical compositions of the samples were analyzed by Inductively Coupled Plasma (ICP-AES) after a multi-acid digestion (HCl, HNO_3, Br_2, and HF) of a 500-mg aliquot. Leachates from testing were analyzed with the ICP-AES following acidification of a filtered (0.45 µm) aliquot to about 2% HNO_3. The S and C content were determined using an ELTRA CS-2000 induction furnace.

The mineralogical study was performed on polished sections of the four samples by optical microscope (OM – Zeiss Axio imager.M2m) and scanning electron microscope (SEM – Hitachi S-3500N), equipped with a microanalysis system (energy dispersive spectroscopy INCA XMax 20 mm^2 SDD). The OM observations mainly focused on sulfide minerals, while the analyses of other minerals were done using the SEM-EDS system.

The crystalline minerals were identified by X-ray diffraction (XRD; Brucker D8 Advance, with a detection limit and precision of approximately 0.1 to 0.5%, operating with a copper cathode, Kα radiation) using the DIFFRACT.EVA program, and quantified using the TOPAS 4.2 program based on a Rietveld (1993) interpretation.

The D-SIMS technique is a benchmark technique for analyzing submicroscopic (invisible) gold in minerals. The submicroscopic gold detected and quantified by the D-SIMS instrument is refractory gold, i.e. it is locked within the crystalline structure of the mineral phase (most often in sulfide minerals) and cannot be directly released by the cyanide leach process. This type of gold may be present as finely disseminated, colloidal-size gold particles (< 0.5μm) or as a solid solution within the sulfide mineral matrix. During the D-SIMS analysis, an ion beam removes consecutive layers of material from the surface of the polished mineral grains and generates depth profiles of the distribution of the chosen elements of interest. Examples of D-SIMS depth profiles show the distribution of the basic matrix elements (S, Fe) as well as the trace elements (Au and As). The spikes in the gold signal intensity in the depth profiles represent colloidal gold, and the yellow-coloured areas represent the approximate size of this colloidal-type, submicroscopic gold. The typical size is in the range of 100 – 200 nm. Dynamic SIMS depth profiles for solid solution, submicroscopic gold show a steady (flat) Au signal similar to the matrix elements, but with different levels of intensity depending on the concentration of submicroscopic gold present in the mineral phase.

The marked mineral particles of interest were analyzed using the Cameca IMS-3f SIMS instrument, and concentration depth profiles for Au, As, S and Fe were produced. The quantification of the gold and arsenic in pyrite, hematite and jarosite was established using internal mineral specific standards.

2.3. Diagnostic Leach Tests

Selective alkaline reagents ($NaCO_3$, NaOH), acid reagents (HCl, and HNO_3), and roasting were used to evaluate the gold distribution within samples during gold DLTs. To improve the dissolution of gold-bearing minerals, all pulps were heated to temperatures of 80°C. After each oxidation test, cyanide leaching with activated carbon was used to extract the dissolved gold. The methodology followed for the diagnostic leach procedure is described in Figure 4, as developed by Kalonji Kabambi (2015). Five stages can be distinguished:

- Stage 1: Leach sample reacts with sodium carbonate to dissolve labile gypsum and free gold;
- Stage 2: Leach sample reacts with sodium hydroxide to dissolve labile jarosite;

- Stage 3: Leach sample reacts with hydrochloric acid to dissolve iron oxide, especially hematite;
- Stage 4: Leach sample reacts with nitric acid to dissolve sulfide minerals, especially pyrite.
- Roasting at 900°C to burn native carbon into volatile CO_2.

After each stage, the material is cyanide loaded in a tank for 16 hours with activated carbon (500 g/t), 5 g/t of NaCN, 50 g/t of carbon, 0.3 g/t of $Pb(NO_3)$, 8 ppm of O_2, and 50% of solid.

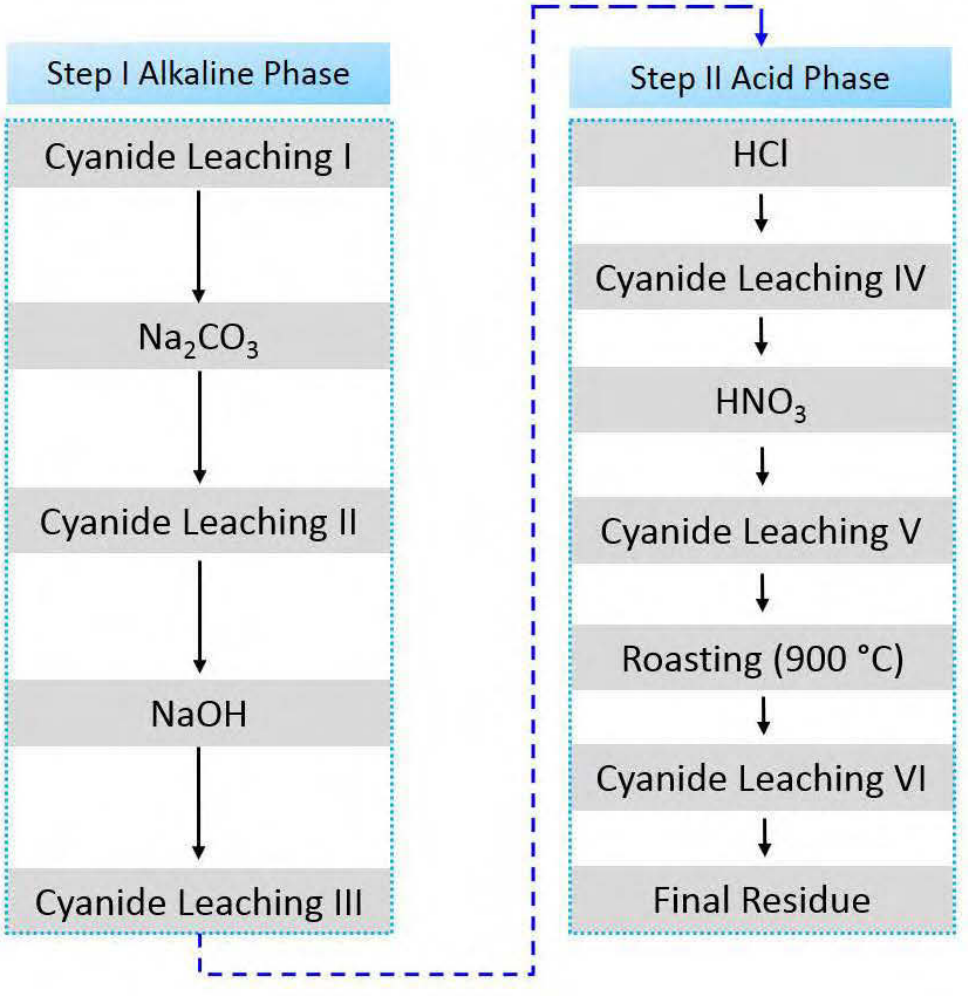

Figure 4: Diagnostic Leach Tests for Refractory Gold Ores

2.4. Preg-Robbing Tests

To determine the preg-robbing value, the material must be conditioned with an amount of gold cyanide solution. The method is based on a comparative procedure using five parallel cyanide leaching tests. The details of the conditions are as follows:

- Normal Test (N): Leaching with only a cyanide solution in contact with the material;
- Gold Test (G): Leaching with a standard solution of gold cyanide in contact with the material;
- Normal Carbon Test (NC): Leaching with a solution of cyanide in contact with the material and activated carbon;
- Gold Carbon Test (GC): Leaching with a standard solution of gold cyanide in contact with the material and activated carbon;
- Carbon Test (C): Contact of a standard gold cyanide solution with the activated carbon, without material.

The concentration of standard gold cyanide used in this study was determined through a series of kinetic tests. The objective was to determine which concentration to use without saturating the adsorption sites of the carbonaceous matter within the ore.

The standard gold solution concentration is around 100 mg/L obtained with $KAu(CN)_2$ salt. At this concentration, the 50, 100, 200, 400, 600, and 800 mL of Au standard correspond to 5, 10, 20, 40, 60, and 80 mg/L respectively.

3. Results and Discussion

3.1. *Physical and Chemical Analysis*

The particle size distribution is of great importance in the assessment of diagnostic leach and preg-robbing tests. Fine particles are known to be more reactive than coarse particles. The particle size distributions of the material are shown in Figure 5. The samples were de-agglomerated to obtain a similar particle size distribution in order to ensure equivalent experimental conditions. The D_{50} and D_{90} values varied between 7-7.5 μm and 40-45 μm respectively for all samples.

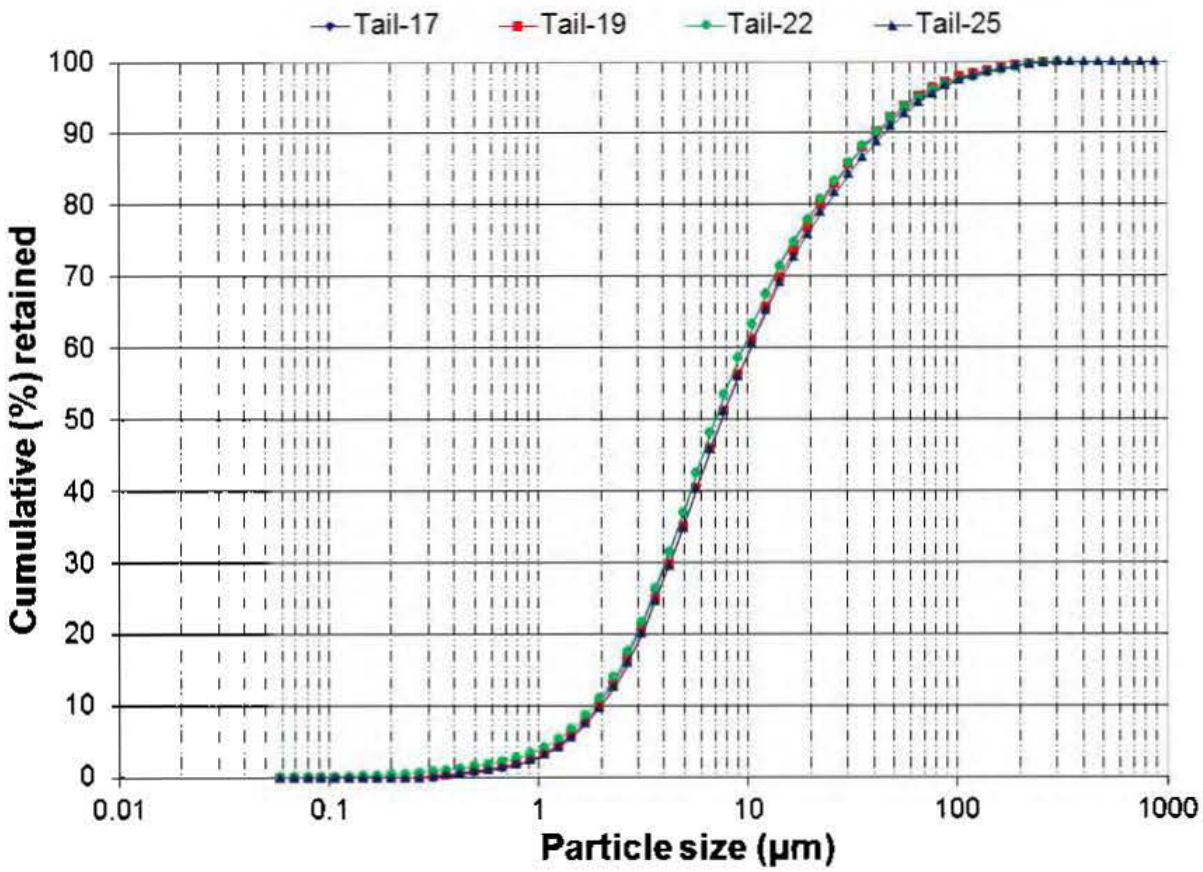

Figure 5: Particle Size Distribution of the Four Mill Tailings Samples Collected

The Kittilä CIL tailings have a sulfur content ranging from 4.3 to 4.8 wt. %. However, a part of the analyzed sulfur is in the sulfate form (e.g. gypsum and anhydrite). Small amounts of carbon are recorded in all samples. Carbon is significantly important in Tail-19, Tail-22, and Tail-25 (2.86-3.38%) compared to Tail-17 (1.83%). Tail-17 and Tail-19 are characterized by significant quantities of gold (2.1-2.23 g/t) in comparison to Tail-22 and Tail-25 (1.63-1.77 g/t). The tailings also contain important contents of silver (11.1-16.5 g/t), iron (14.03-16.02%), and arsenic (4.3-5.05%). The Si, Al, K, and Na analysis results indicate the presence of silicates and aluminosilicates in the tailings. Note that the sulfur sulfide content is primarily in arsenopyrite and pyrite. Other sulfide minerals (i.e. galena, sphalerite, and chalcopyrite) are present in negligible amounts as demonstrated by the Pb, Zn, and Cu contents. The results also show that all samples contain small quantities of Sb (400-700 g/t), Ni (90-100 g/t), and Co (15-40 g/t). Fe is the most abundant element in the samples, with a maximum in Tail-25 (16.2 %) and a minimum in Tail-22 (14.03 %). The chemical compositions of the samples are presented in Table 2.

Table 2. Chemical Composition of Samples Tail-17, Tail-19, Tail-22 and Tail-25

	Au (g/t)	Ag (ppm)	Cu (%)	Zn (%)	Pb (%)	Fe (%)	As (%)	Sb (g/t)	Ni (g/t)	Co (g/t)	C_{total} (%)	S_{total} (%)
Tail-17	2.1	11.1	0.025	0.011	0.007	15.18	4.78	700	90	30	1.83	4.28
Tail-19	2.23	13.6	0.026	0.021	0.007	15.77	4.3	740	110	15	2.86	5.67
Tail-22	1.77	16.5	0.027	0.015	0.005	14.03	5.05	410	90	30	3.38	5.68
Tail-25	1.63	12.20	0.028	0.021	0.008	16.2	4.64	420	140	40	3.02	5.8

3.2. *Mineralogical Analysis*

3.2.1. *XRD Analysis*

The mineralogical composition of the tailings determined by XRD is summarized in Figure 6. All samples show similar mineralogical phases but in different proportions: quartz (SiO_2), biotite ($K(Mg,Fe)_3(AlSi_3O_{10}(OH,F)_2$), gypsum ($CaSO_4.2H_2O$), orthoclase ($KAlSi_3O_8$), rutile ($TiO_2$), pyrite ($FeS_2$), jarosite ($KFe_3(SO_4)_2(OH)_6$), muscovite ($KAl_2(Si_3Al)O_{10}(OH,F)_2$), and anhydrite ($CaSO_4$) (Figure 6). Quartz represents more than 24 % of the samples and the remaining phases are mainly silicate and sulfate minerals (i.e., albite, muscovite, jarosite, anhydrite, and gypsum) (Figure 6).

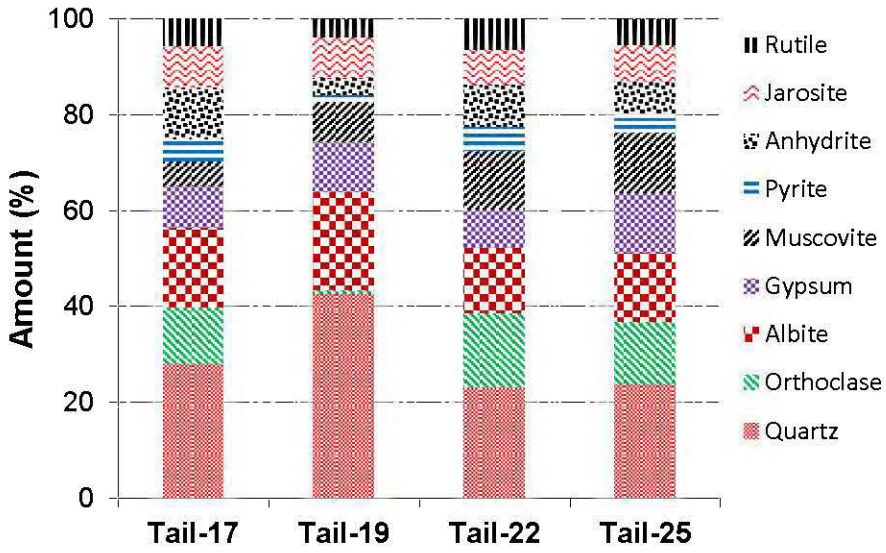

Figure 6: Quantification of Crystalline Phase Minerals in Samples Tail-17, Tail-19, Tail-22 and Tail-25

3.2.2. SIMS Analysis

One objective of this study was to quantify and establish the distribution of the submicroscopic gold content in the following minerals: pyrite, hematite and jarosite. The description of the sample analyzed by D-SIMS is provided in Table 3. In total, 100 analyses are performed.

The hematite and jarosite phases very often exhibit complex structures: disseminated in quartz phases, present as intergrowth or forming rims around other particles such as gypsum, rutile and other gangue minerals. Examples of backscattered electron (BSE) images and SEM/EDX compositional analyses of hematite and jarosite phases are shown in Figure 7.

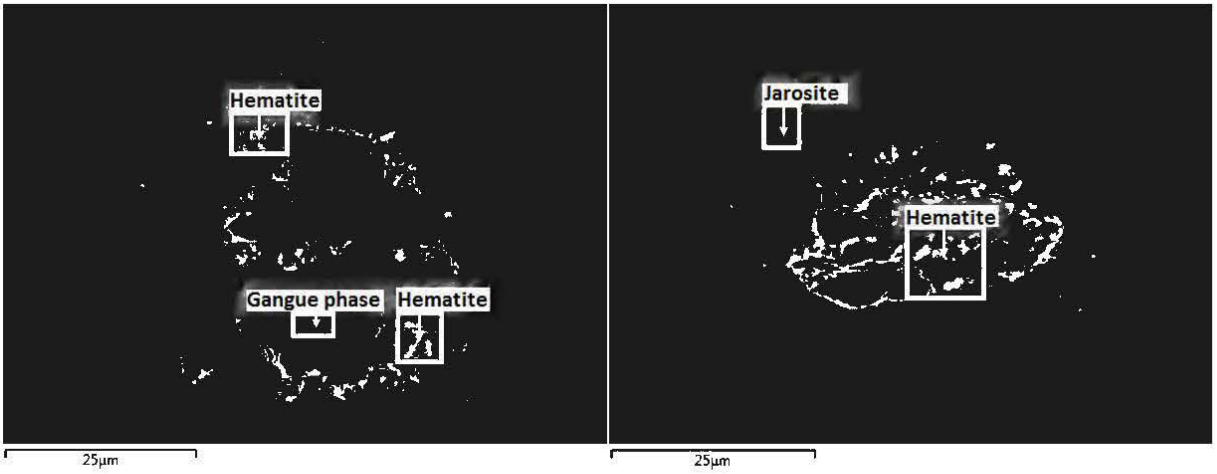

Figure 7: Backscattered Electron (BSE) Image of Leach Tails Sample and EDX Compositional Analyses of Hematite and Jarosite.

- *Identified Gold Carriers*

The main gold-bearing minerals are pyrite, hematite and jarosite. Different morphological types of pyrite were identified: coarse (Au 29.09 ppm), porous (Au 11.13 ppm), microcrystalline (Au 15.09 ppm) and disseminated (Au 6.31 ppm) (Figure 8). The pyrite mineral phase is rich in arsenic. There is a strong positive correlation between the measured Au and As contents in the pyrite mineral phase, as shown in Figure 9. The estimated average gold concentration in the hematite

mineral phase is Au = 5.13 ppm, while the estimated average gold concentration in the jarosite mineral phase is Au = 15.43 ppm (Table 3).

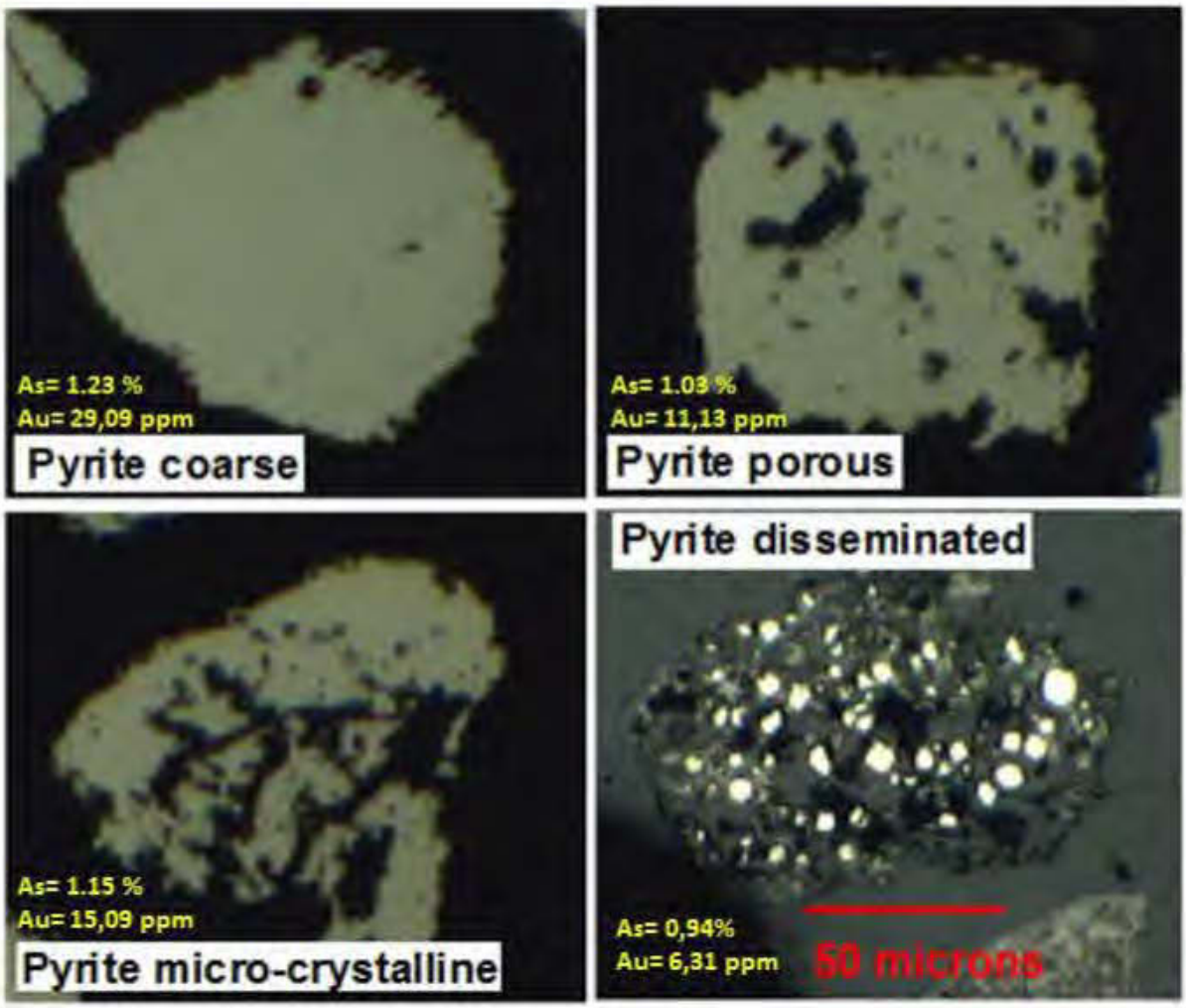

Figure 8: Examples of Mineral Phases Analyzed by D-SIMS.

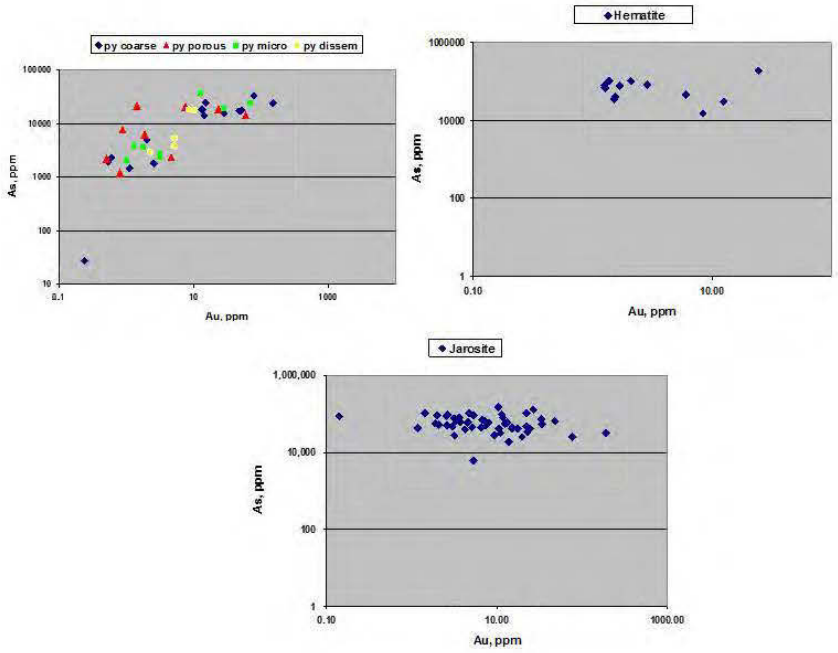

Figure 9: Correlation between Measured Concentrations of Submicroscopic Gold and Arsenic in Pyrite, Hematite, and Jarosite.

- *Submicroscopic Gold Content as Part of the Gold Deportment Balance*

The gold deportment balance for the leach tails sample studied is summarized in Table 3 and depicted in the deportment balance diagram in Figure 10. The combined submicroscopic gold contained in the pyrite, hematite and jarosite mineral phases accounts for 73.9% of the total assayed gold in the sample. The jarosite mineral phase is the major gold carrier of submicroscopic gold in the sample (58.8%), followed by the pyrite (11.7%) and hematite (3.5%) phases.

Table 3. Gold Deportment in the Leach Tails Sample.

Sample	Leach Tails	
Gold assayed in the sample	2.23 g/t	
Forms and Carriers of Gold	Au g/t	% in sample assay
Other forms of gold: visible gold, surface gold preg-robbed on carbonaceous matter, soluble gold salts[2]	0.581	26.06
Submicroscopic gold[3]		
Pyrite	0.260	11.68
Hematite	0.077	3.45
Jarosite	1.312	58.81
Subtotal submicroscopic gold	1.649	73.94
Total	2.23	100.00

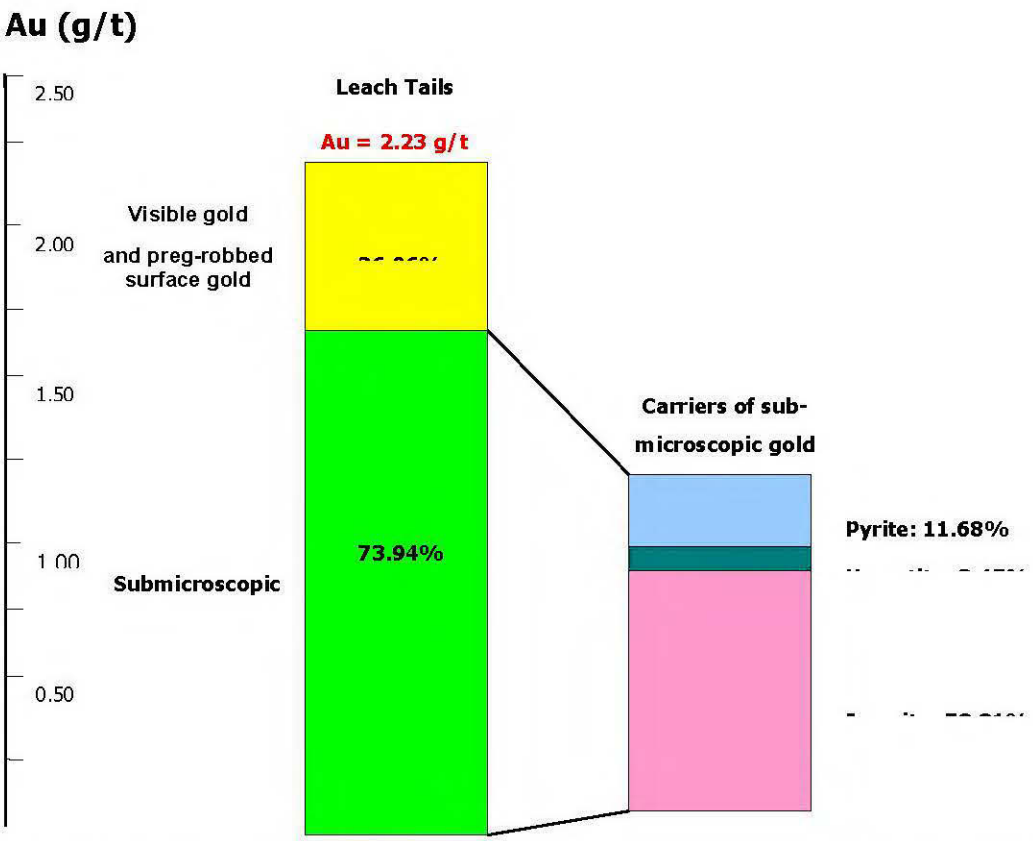

Figure 10: Gold Deportment Diagram, representing all major forms and carriers of gold in the Leach Tails sample. The relative distribution of gold per carrier is given in % of the total assayed value for gold in the sample.

3.3. Diagnostic Leach Tests

Diagnostic leach testing is used to evaluate the distribution of gold in different minerals via an oxidative process during leaching phases. The results indicate that about 24.7% of the gold content occurs as free cyanidable gold in all the tailings (Table 4). There was less than 19 % free cyanidable gold in Tail-19 and Tail-22. An average of 47.4 % is locked within digestible minerals (i.e. hematite, jarosite, pyrite, gypsum, and carbonaceous matter). The remaining portion, approximately 27.74 %, is locked in gangue minerals (i.e. silicates). Tail-17 and Tail-19 have low TOC contents compared to Tail-22 and Tail-25. However, the TOC reactivity of Tail-17, Tail-22 and Tail-25 is high in comparison to Tail-19. Tail-19 corresponds to the Kittilä ore with significant gold content, where refractoriness is induced by the dissemination and encapsulation of very fine

particles of gold, primarily in oxides, sulphides, carbonaceous matter and silicates in lesser proportion (Table 4). All the results are summarized in Table 4.

Table 4. Results of the Diagnostic Leach Test

Description**	Gold Distribution (%)			
	Tail-17	**Tail-19**	**Tail-22**	**Tail-25**
Free cyanidable	28	18.9	19	33
Digestible mineral-locked gold content	47	47.8	56.9	38
Silicate-locked gold content	25	33	24	29

** Only autoclave products (jarosite and hematite) that were analyzed using D-SIMS to confirm DLT values

The calculation of the gold distribution within the different minerals was performed using a mass-balance approach. The distribution of total gold content (2 g/t) is shown in Figure 10. The gold distribution exhibits a similar trend in all the samples except in Tail-25 where the gold content is less than 0.04 g/t within gypsum. In fact, the cyanidable gold varies between 0.32 and 0.56 g/t. The most gold-bearing minerals within the samples are jarosite-trapped (0.23-0.60 g/t), silicates (0.41-0.49 g/t), hematite (0.03-0.09 g/t), and pyrite (0.12-0.26 g/t). However, the gold content associated with carbon does not exceed 0.01 g/t with a maximum in Tail-19 (0.01 g/t). The comparison between the analyzed gold and the calculated gold shows an excellent correlation, with less than a 1.2% error (Figure 11).

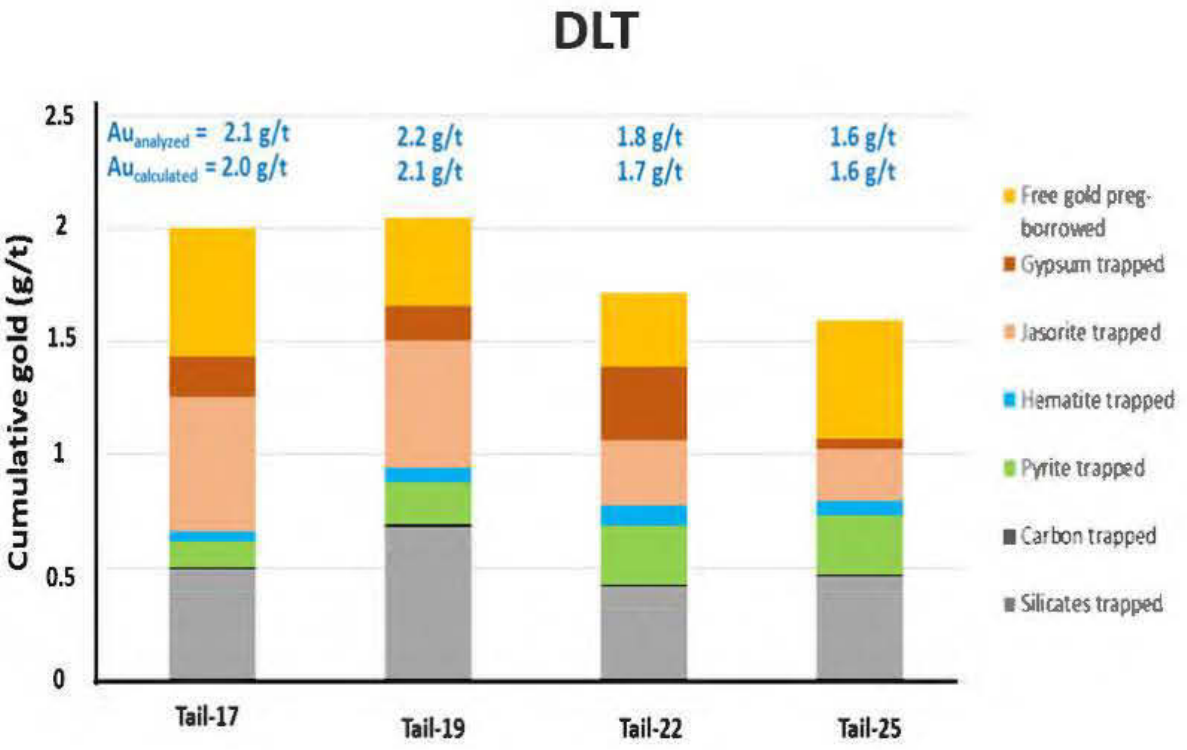

Figure 11: Diagnostic Leach Test Results

3.4. Absorption Tests

The purpose of these tests is to assess the efficiency of tailings adsorption. The results obtained using kinetic tests show a linearity of adsorption by C-matter. The lowest dopingconcentration is selected in order to closely match the real gold concentration in the mill (Figure 12).

The adsorption under a static regime is expressed in terms of percentage (R) of gold removed by adsorbents (tailings) and is calculated as follows:

$$R = \frac{(\mathrm{Ci} - \mathrm{C})}{\mathrm{C}} * 100$$

Ci: initial concentration of gold (mg/L)

C: residual concentration of gold (mg/L)

The adsorption test used to estimate the adsorption behaviour of gold on tailings shows that when the gold concentration is increased, the amount adsorbed decreases. An increase in the percentage of adsorption (R) as a direct function of the gold concentration is observed until a maximum value of 20 mg/L, for the four adsorbents. In all samples except Tail-17, the percentage of adsorption (R)

decreases with the gold concentration until a value of 20 mg/L and then remains stable at all other concentrations. For Tail-19, Tail-22, and Tail-25, the equilibrium is reached following the addition of 20 mg/L of gold, while for Tail-17, the saturation is achieved after the addition of 60 mg/L of gold. This can be explained by the saturation of the tailings adsorption sites with the increase in gold concentration (Figure 13). In this case, a concentration of 5 mg/L was chosen for the preg-robbing tests.

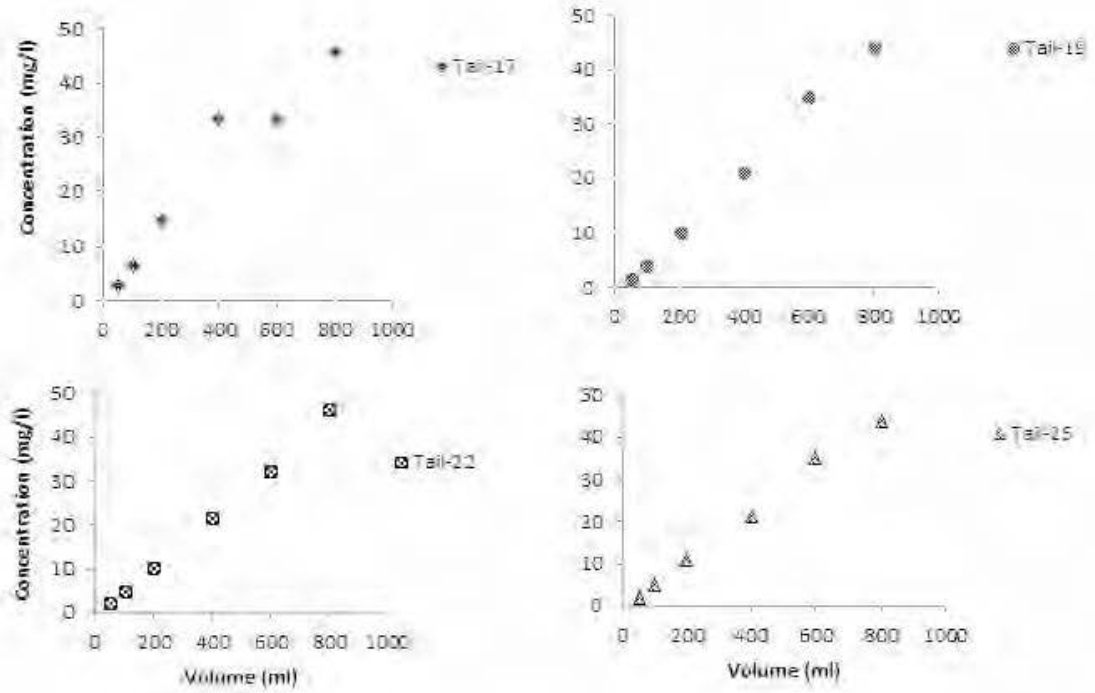

Figure 12: Results of Adsorption Tests

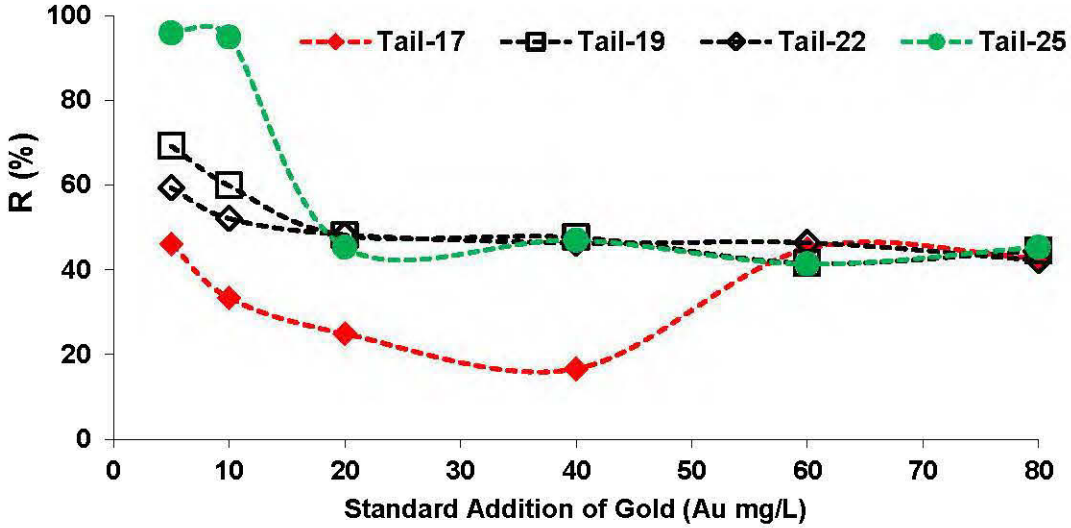

Figure 13: Evolution of the Gold Concentration with the Coefficient of Percentage (R) in the Adsorption Process at pH = 10.5 and for a Tailings Mass of 100 g.

3.5. Preg-Robbing Tests

The preg-robbing test is conducted using a known amount of standard cyanided gold in contact with samples. After 16 hours of cyanidation, the gold concentration is measured in order to quantify the amount of gold adsorbed by the samples. Indeed, standard additions of gold are used in duplicate for two reasons: to characterize the preg-robbing potential of the studied tailings and to evaluate the repeatability of the laboratory results. The preg-robbing potential of the CIL was highlighted by the strong deviation between two linearities (line with a 1:1 slope which reflect the absence of adsorption and the trend line of the results). Results show that there is a strong deviation with respect to linearity which suggests that gold was greatly adsorbed by the samples (Figure 14). It is important to note that all samples present the same behaviour. The addition of 4% (w/w) of activated carbon is used to evaluate the strong preg-robbing potential. The results show that all amounts of residual soluble gold are adsorbed by the activated carbon (residual concentration of gold is less than 0.005 mg/L). The four tailings are mostly composed of silicate, iron oxides (hematite), sulfate minerals and carbonaceous matter. The latter is supposed to exhibit significant preg-robbing potential. The results presented in Table 5 indicate that only preg-borrowing has an important influence on the leaching process of the gold. The PRT values (around 10%) in all

samples indicate that the preg-borrowing (PB) phenomenon was dominant compared to the preg-robbing (PR) (Table 5). Further characterization using secondary ion mass spectrometry (SIMS) is needed to identify Au-bearing minerals, both Au-liberated and refractory, and to confirm the results of initial characterization of the leaching behaviour. In this type of experiment, a representative sample in terms of grain size is always required.

Analysis of the preg-robbing potential for all samples is summarized in Table 5. The results show a low preg-robbing potential (less than 1% of the residual gold in CIL tailings). This geochemical behaviour is probably caused by a low adsorption and/or precipitation of aurodicyanide within carbonaceous matter. The results obtained for preg-robbing potential are similar to the results found in other sulfide ores where the preg-robbing was driven by sulfide minerals in the presence of free cyanide (Goodall et al., 2005; Rees et al., 2000). In order to achieve good recovery, the refractory fraction of the gold must be leached prior to any cyanidation.

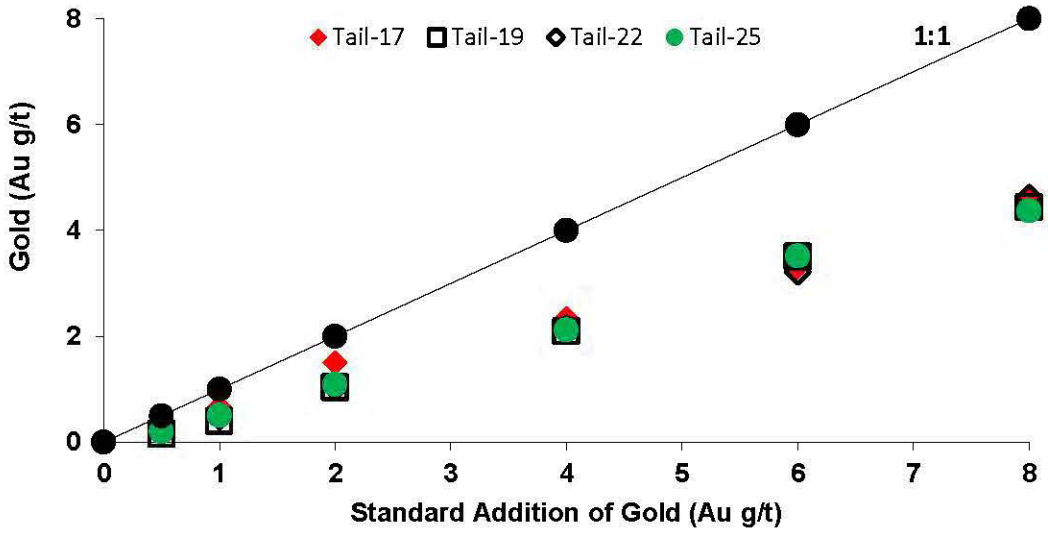

Figure 14: Results of Preg-Robbing Potential for Studied Samples

Table 5. Results of Preg-Robbing Tests for Studied Samples

	Tail-17	Tail-19	Tail-22	Tail-25	Test Conditions
TOC Content	Low	Low	High	High	
TOC Reactivity	High	Low	High	Low	
Head Gold Grade	2.10	2.23	1.78	1.71	-
Tails for Test N	2.23	2.28	1.93	1.85	No activated carbon
Tails for Test G	12.95	12.71	10.94	10.46	With gold doping
Tails for Test NC	1.71	1.9	1.49	1.54	With activated carbon
Tails for Test GC	2.84	2.92	2.58	2.49	With gold doping, and activated carbon
Interpreted Data					
PR+PB doped gold	10.73	10.43	9.01	8.61	Test G - N
PR doped gold	1.14	1.03	1.09	0.95	Test GC - NC
% of PR in PR+PB	11%	10%	12%	11%	PR / (PR+PB)
PB in LT	0.52	0.38	0.44	0.31	Test NC - N
PR in LT	0.06	0.04	0.06	0.04	Calculated with % of PR

Conclusions

The main conclusions that can be drawn from this study are:

- Free / preg-borrowed gold accounts for 20-35 % of the residual gold (0.5 g/t opportunity);
- Gold trapped in autoclave products represents 20 to 40 % (0.5 g/t opportunity);
- Pyrite-trapped / preg-robbed gold accounts for around 5-20 % (mainly pyrite);
- There is a high association of gold with silicates; 25-35 % (approx. 1 g/t);
- There is little irreversible association of gold with carbonaceous matter (< 0.1 g/t) = low preg-robbing.

For a better understanding of the geochemical behaviour of gold under leaching conditions, further research is needed in the following areas: (i) Confirm opportunities from free / preg-borrowed gold, via mineralogy of gold deportment, (ii) Test autoclave operating parameters with SIMS analysis

(partial gold deportment), (iii) Conduct partial DLT (CYA-HCl-CYA-Roasting-CYA), (iv) Add recyanidation (bottle roll test) of the DLT (longer contact time, more reagent concentrations or cleaner water), and (v) Confirm silicate locking (grinding and cyanidation tests and roasting simulation with gold doped carbon and pure quartz (or DLT tails or similar minerals).

Acknowledgements

The authors thank gratefully the mining company Kittilä for the great help, especially in the sampling steps.

References

Abotsi et al., 1986. Surface chemistry of carbonaceous gold ores. I. Characterization of the carbonaceous matter and adsorption behavior in aurocyanide solution. Int. J. Miner. Process. 18, 217-236.

Abruzzese et al., 1995. Thiosulfate leaching for gold hydrometallurgy. Hydrometallurgy 39, 265-276. Acar, S., Ball, B., 1989.

Aylmore et al., 2001. Thiosulfate leaching of gold—A review. Minerals Engineering, Vol. 14, No. 2, p. 135-174.

Bas et al., 2017. A review on electrochemical dissolution and passivation of gold during cyanidation in presence of sulphides and oxides. Hydrometallurgy, vol. 172, p. 30-44.

Botz et al., 2005. Cyanide treatment: physical, chemical and biological processes. Advances in gold ore processing, 672-700.

Climo et al., 2000. Biooxidation as pre-treatment for a telluriderich refractory gold concentrate. Miner. Eng. 13 (12), 1219–1229.

Cui and Zhang, 2008. Metallurgical recovery of metals from electronic waste: a review. J. Hazard. Mater., 158 (2008), pp. 228-256;

Daniel et al., 2009. Technical Report on the December 31, 2009, Mineral Resource and Mineral Reserve Estimate and the Suuri Extension Project, Kittila Mine, Finland. Agnico-Eagle Mines Limited 145 King Street East, Suite 400 Toronto, Ontario, Canada M5C 2Y7.

Derycke et al., 2013. Surface chemical characterization of different pyrite size fractions for flotation purposes. International Journal of Mineral Processing, Vol. 118, p. 1-14.

Dimov, S., Hart, B., 2014. Quantitive analysis of sub-microscopic and surface preg-robbed gold in gold deportment studies. in: Proceesings of XXVII International Mineral Processing Congress, IMPC 2014, Santiago, Chile. Paper #1408.

Dunn and Chamberlain, 1997. The recovery of gold from refractory arsenopyrite concentrates by pyrolysis-oxidation. Minerals Engineering, Vol. 10, No. 9, p. 919-928.

Dunne et al., 2012. Assessment of options for economic processing of preg-robbing gold ores. World Gold 2007, Vol. 121, pp. 217-223.

Fleming et al., 2011. Factors influencing the rate of gold cyanide leaching and adsorption on activated carbon, and their impact on the design of CIL and CIP circuits. Minerals Engineering, Vol. 24, No. 6, p. 484-494.

Fraser and Wells, 1991. Processing of refractory gold ores. Minerals Engineering, 4(7), 1029-1041.

Gönen et al., 2007. Leaching and CIL processes in gold recovery from refractory ore with thiourea solutions. Minerals Engineering, Vol. 20, No. 6, p. 559-565.

Goodall et al., 2005. A new method for determination of preg-robbing in gold ores. Minerals Engineering, Vol. 18, No. 12, p. 1135-1141.

Hausen et al., 1984. Study of preg-robbing in the cyanidation of carbonaceous gold ores from carlin, Nevada. In: The Second International Congress on Applied Mineralogy in the Minerals Industry, Los Angeles, California, Metallurgical Society of AIME.

Kalonji Kabambi et al., 2015. Diagnostic Leach Procedure for Refractory Gold Ores. Canadian Mineral Processors section Nord-Ouest Québécois.

Kojonen et al., 1999. Determination of refractory gold distribution by microanalysis, diagnostic leaching and image analysis. Mineralogy and Petrology, 67(1), 1-19.

La Brooy et al., 1994. Review of gold extraction from ores. Minerals Engineering, 7(10), 1213-1241.

Lorenzen, L., 1995. Some guidelines to the design of a diagnostic leaching experiment. Minerals Engineering, 8(3): 247–256.

Marsden and House, 2006. The chemistry of gold extraction. SME.

Menne et al., 1992. Assaying Cyanide Extractable Gold within an Hour, and Addressing Effects of Preg- and Assay-Robbing. Extractive Metallurgy of Gold and Base Metals, Kalgoorlie WA, AusIMM.

Miller et al., 2016. Chapter 49 - Preg-Robbing Gold Ores A2 - Adams, Mike D. In Gold Ore Processing (Second Edition), p. 885-907.

Osseo-Asare et al., 1984. Carbonaceous matter in gold ores: isolation, characterization and adsorption behaviour in aurocyanide solutions. In: Kudryk, V., Corrigan,

Quach et al., 1993. Adsorption of Gold Cyanide on Gangue Minerals. APCChE and Chemeca 93, Melbourne, Australia.

Radtke et al., 1970. Studies of hydrothermal gold deposition (I). Carlin gold deposit, Nevada: The role of carbonaceous materials in gold deposition. Economic Geology 65 (2), 87–102.

Rees et al., 2000. Preg-robbing phenomena in the cyanidation of sulphide gold ores. Hydrometallurgy 58, 61–80.

Schmitz et al., 2001a. Adsorption of aurocyanide complexes onto carbonaceous matter from preg-robbing Goldstrike ore. Hydrometallurgy 61, 121–135.

Simmons, G.L., 1995. Pressure oxidation process development for treatment refractory carbonaceous ores at Twin Creeks. In SME Annual Meeting, Denver, Colorado.

Stenebråten et al., 2000. Characterization of Goldstrike ore carbonaceous material. Part 2: physical characteristics. Miner. Metall. Proc. 17 (1), 7-15.

Syed et al., 2012. Recovery of gold from secondary sources—a review. Hydrometallurgy, 115, 30-51.

Wadnerkar et al., 2015. Modeling and Optimization of Carbon in Leach (CIL) Circuit for Gold Recovery. Minerals Engineering, Vol. 83, p. 136-148.

Wyche et al., 2015.The Suurikuusikko Gold Deposit (KittilÄ Mine), Northern Finland A2 - O'Brien, Wolfgang D. MaierRaimo LahtinenHugh. In Mineral Deposits of Finland, p. 411-433.

Zadehfini et al., 2011. Effect of mechanical activation on thiosulphate leaching of gold from complex sulfide concentrate. Trans. Nonferrous Metals Soc. China 21, 2744–2751.